



University of  
Massachusetts  
Amherst

## **Fabrication, Characterization and Utilization of Filled Hydrogel Particles as Food Grade Delivery Systems**

Item Type	Dissertation (Open Access)
Authors	Matalanis, Alison M.
DOI	<a href="https://doi.org/10.7275/1kmy-n756">10.7275/1kmy-n756</a>
Download date	2026-03-10 12:37:10
Link to Item	<a href="https://hdl.handle.net/20.500.14394/39098">https://hdl.handle.net/20.500.14394/39098</a>

**FABRICATION, CHARACTERIZATION AND UTILIZATION OF FILLED  
HYDROGEL PARTICLES AS FOOD GRADE DELIVERY SYSTEMS**

A Dissertation Presented

by

ALISON M. MATALANIS

Submitted to the Graduate School of the  
University of Massachusetts Amherst in partial fulfillment  
of the requirements for the degree of

DOCTOR OF PHILOSOPHY

September 2012

The Department of Food Science

© Copyright by Alison M. Matalanis 2012

All Rights Reserved

**FABRICATION, CHARACTERIZATION AND UTILIZATION OF FILLED  
HYDROGEL PARTICLES AS FOOD GRADE DELIVERY SYSTEMS**

A Dissertation Presented

by

ALISON M. MATALANIS

Approved as to style and content by:

---

D. Julian McClements, Chair

---

Eric A. Decker, Member

---

Julie M. Goddard, Member

---

Anthony D. Dinsmore, Member

---

Eric A. Decker, Department Head  
Department of Food Science

## DEDICATION

To my daughter, husband, and parents who made this goal a reality.

## ACKNOWLEDGMENTS

First, I would like to thank my advisor, Dr. Julian McClements, for his assistance and guidance during my tenure in his laboratory. I am extremely grateful for both the financial and academic support he has provided me over the last four years. I would also like to thank my committee members: Dr. Decker, Dr. Goddard, and Dr. Dinsmore, for serving on my committee and for their helpful suggestions. In particular, I would like to thank Dr. Decker for his advice and guidance with the oxidation studies I conducted for this work.

There have been many wonderful people that I have met and worked with during my time at UMass. In particular, I would like to thank Jean Alamed for all of her support and friendship. Throughout my time at UMass, Jean was the one person I could always go to for help, advice, and most importantly, compassion. I would also like to express my appreciation to all of the current and former members of the McClements laboratory especially Jia Jia, Bingcan, Tanu, Sandra, Owen, Yong-Hee, Tang, Dao, Seung Jun, and Thora.

Lastly, I would like to express my sincere appreciation to my family especially my daughter, Nicole, my husband, Claude, my mom, Elizabeth, and my stepfather, Emile. Throughout the entire process of returning back to school, my husband has been amazingly supportive and for this I am forever grateful. I am also greatly indebted to my mom for taking care of my daughter while I finished my degree at UMass. Completing this degree would have been impossible without her. I am also very grateful to God for all of the wonderful gifts He gives me each and every day.

## ABSTRACT

### FABRICATION, CHARACTERIZATION AND UTILIZATION OF FILLED HYDROGEL PARTICLES AS FOOD GRADE DELIVERY SYSTEMS

SEPTEMBER 2012

ALISON M. MATALANIS, B.S., CORNELL UNIVERSITY

M.S., PURDUE UNIVERSITY

Ph.D., UNIVERSITY OF MASSACHUSETTS AMHERST

Directed by: Professor D. Julian McClements

Filled hydrogel particles consisting of emulsified oil droplets encapsulated within a hydrogel matrix were fabricated based on the phase separation of proteins and polysaccharides through aggregative and segregative mechanisms. A 3% (wt/wt) pectin and 3% (wt/wt) caseinate mixture at pH 7 separated into an upper pectin-rich phase and a lower casein-rich phase. Casein-coated lipid droplets added to this mixture partitioned into the lower casein-rich phase. When shear was applied, an oil-in-water-in-water ( $O/W_1/W_2$ ) emulsion consisting of oil droplets (O) contained within a casein-rich dispersed phase ( $W_1$ ) suspended in a pectin-rich continuous phase ( $W_2$ ) was formed.

Acidification from pH 7 to 5 promoted adsorption of pectin onto casein-rich  $W_1$  droplets, forming filled hydrogel particles. Particles were then cross-linked using transglutaminase.

Particles were assessed for stability to changes in pH, increasing levels of salts (sodium chloride and calcium chloride), and susceptibility to lipid oxidation. Both cross-linked and not cross-linked particles were stable at low pH (pH 2-5). At high pH, cross-

linked particles maintained their integrity while not cross-linked particles disintegrated. Particles were stable to sodium chloride (0-500 mM). Calcium chloride levels above 4 mM resulted in system gelation.

The rate of lipid oxidation for 1% (vol/vol) fish oil encapsulated within filled hydrogel particles was compared to that of oil-in-water emulsions stabilized by either Tween 20 or casein. Emulsions stabilized by Tween 20 oxidized faster than either filled hydrogel particles or casein stabilized emulsions, while filled hydrogel particles and casein stabilized emulsions showed similar oxidation rates. Using an in-vitro digestion model, the digestion of lipid encapsulated within filled hydrogel particles was compared to that of a casein stabilized oil-in-water emulsion. Results showed similar rates of digestion for both hydrogel and emulsion samples.

Attempts to fabricate particles using free oil (rather than emulsified oil) were unsuccessful and resulted in the formation of large non-encapsulated oil droplets ( $d \sim 10 \mu\text{m}$ ). By controlling particle concentrations of biopolymer, water, and oil, it was possible to fabricate particles that were highly resistant to gravitational separation which was attributed to the equivalent density of the continuous and particle phases. Results highlight the potential applications and versatility of this delivery system.

## TABLE OF CONTENTS

	Page
ACKNOWLEDGMENTS .....	v
ABSTRACT.....	vi
LIST OF TABLES .....	xiv
LIST OF FIGURES .....	xv
CHAPTER	
1. INTRODUCTION.....	1
1.1 Introduction.....	1
1.2 Objectives .....	3
2. LITERATURE REVIEW .....	5
2.1 Emulsion-Based Delivery Systems for Lipophilic Bioactives .....	5
2.2 Biopolymer Phase Separation .....	5
2.2.1 Basis for Phase Separation.....	7
2.2.2 Phase Composition and the Phase Diagram.....	8
2.2.3 Water-in-Water Emulsions .....	10
2.3 Filled Hydrogel Particles .....	11
2.3.1 Macroscopic Gel Disruption Method.....	13
2.3.2 Simple Coacervation Method .....	13
2.3.3 Injection Method.....	14
2.3.4 Emulsion Methods .....	14
2.3.5 Gelation Methods.....	18
2.3.5.1 Protein Gelation .....	18
2.3.5.2 Polysaccharide Gelation.....	20
2.4 Applications of Emulsion-Based Delivery Systems for Lipophilic Bioactives.....	23
2.4.1 Modification of Physical Properties Using Filled Hydrogel Particles.....	24
2.4.2 Modification Chemical Properties Using Filled Hydrogel Particles.....	31

2.4.2.1 Lipid Oxidation.....	32
2.4.2.2 Factors Influencing Oxidative Stability of Food .....	34
2.4.2.3 Antioxidants.....	35
2.4.3 Modification of Biological Response Using Filled Hydrogel Particles .....	37
2.4.3.1 Lipid Digestion in Humans.....	37
2.4.3.2 Controlling Lipid Digestion and Bioavailability .....	39
<b>3. FABRICATION AND CHARACTERIZATION OF FILLED HYDROGEL PARTICLES BASED ON SEQUENTIAL SEGREGATIVE AND AGGREGATIVE BIOPOLYMER PHASE SEPARATION .....</b>	<b>42</b>
3.1 Abstract.....	42
3.2 Introduction.....	43
3.3 Materials .....	47
3.4 Methods.....	48
3.4.1 Solution Preparation.....	48
3.4.2 Emulsion Preparation.....	49
3.4.3 Formation and Characterization of Phase Separated Biopolymer Mixtures .....	49
3.4.4 Characterization of Lipid Droplet Partitioning in Phase Separated Biopolymer Mixtures .....	51
3.4.5 Laser Vertical Profiling.....	51
3.4.6 Confocal Fluorescence Microscopy.....	52
3.4.7 Quantification of Depletion Interactions in Phase Separated Systems .....	53
3.4.8 Formation, Characterization, and Stability of Hydrogel Particles.....	54
3.4.9 Formation, Characterization and Stability of Filled Hydrogel Particles.....	58
3.5. Results & Discussion.....	59
3.5.1 Formation and Characterization of Phase Separated Biopolymer Mixtures.....	59
3.5.2 Characterization of Lipid Droplet Partitioning in Phase Separated Systems .....	63
3.5.3 Formation, Characterization and Stability of Hydrogel Particles.....	72
3.5.4 Formation, Characterization and Stability of Filled Hydrogel Particles.....	78
3.6 Conclusions.....	79

4. FACTORS INFLUENCING THE FORMATION AND STABILITY OF FILLED HYDROGEL PARTICLES FABRICATED BY PROTEIN/POLYSACCHARIDE PHASE SEPARATION AND ENZYMATIC CROSS-LINKING.....	82
4.1 Abstract.....	82
4.2 Introduction.....	83
4.3. Materials and Methods.....	86
4.3.1 Materials .....	86
4.3.2 Methods.....	87
4.3.2.1 Solution Preparation.....	87
4.3.2.2 Emulsion Preparation.....	88
4.3.2.3 Formation of Phase Separated Biopolymer Mixtures.....	88
4.3.2.4 Formation of Filled Hydrogel Particles .....	89
4.3.2.5 Analysis of Filled Hydrogel Particles .....	91
4.3.2.6 Stability Testing of Filled Hydrogel Particles .....	93
4.3.2.7 Statistical Analysis.....	95
4.4. Results and Discussion .....	95
4.4.1 Influence of Mixing Conditions on the Size of Filled Hydrogel Particles.....	95
4.4.2 Influence of pH on the Stability of Cross-Linked and Control (Not Cross-Linked) Filled Hydrogel Particles.....	102
4.4.3 Influence of Sodium Chloride on the Stability of Filled Hydrogel Particles.....	108
4.4.4 Influence of Calcium Chloride on the Stability of Filled Hydrogel Particle .....	111
4.4.5 Influence of Heating on the Stability of Filled Hydrogel Particles.....	114
4.5 Conclusions.....	115
5. INHIBITION OF LIPID OXIDATION BY ENCAPSULATION OF EMULSION DROPLETS WITHIN HYDROGEL MICROSPHERES .....	117
5.1 Abstract.....	117
5.2 Introduction.....	117
5.3 Materials and Methods.....	121
5.3.1 Materials .....	121
5.3.2 Methods.....	122
5.3.2.1 Solution Preparation.....	122
5.3.2.2 Emulsion Preparation.....	122

5.3.2.3 Formation of Filled Hydrogel Microspheres .....	123
5.3.2.4 Sample Preparation and Storage Conditions.....	125
5.3.2.5 Evaluation of Physical Properties of Emulsions and Filled Hydrogel Microspheres.....	125
5.3.2.6 Determination of Lipid Oxidation .....	126
5.4 Results & Discussion .....	129
5.4.1 Evaluation of Physical Properties of Emulsions and Filled Hydrogel Microspheres.....	129
5.4.2 Lipid Oxidation in Filled Hydrogel Microspheres and Emulsions.....	131
5.5 Conclusions.....	135
<b>6. INFLUENCE OF LIPID DROPLET ENCAPSULATION WITHIN BIOPOLYMER HYDROGEL MICROSPHERES ON THEIR DIGESTION: AN IN VITRO STUDY.....</b>	<b>137</b>
6.1 Abstract.....	137
6.2 Introduction.....	138
6.3 Materials and Methods.....	140
6.3.1 Materials .....	140
6.3.2 Methods.....	141
6.3.2.1 Formation and Characterization of Phase Separated Biopolymer Mixtures .....	141
6.3.2.2 Emulsion Preparation.....	142
6.3.2.3 Formation of Filled Hydrogel Microspheres .....	143
6.3.2.4 Fat Extraction and Analysis of Filled Hydrogel Microspheres and Emulsion.....	144
6.3.2.5 Simulated Gastrointestinal Digestion Model .....	145
6.3.2.6 Evaluation of the Physical Properties of Emulsions and Filled Hydrogel Microspheres During Digestion .....	146
6.3.2.7 Statistical Analysis.....	149
6.4 Results and Discussion .....	149
6.4.1 Characterization of Emulsions and Filled Hydrogel Microspheres During Digestion.....	149
6.4.1.1 Particle Size and Electrical Charge.....	149
6.4.1.2 Microstructure.....	152
6.4.1.3 Macrostructure .....	157

6.4.2 In Vitro Lipid Digestion of Emulsion and Filled Hydrogel Microspheres.....	157
6.5 Conclusions.....	160
<b>7. HYDROGEL MICROSPHERES FOR ENCAPSULATION OF LIPOPHILIC COMPONENTS: OPTIMIZATION OF FABRICATION &amp; PERFORMANCE .....</b>	<b>162</b>
7.1 Abstract.....	162
7.2 Introduction.....	163
7.3 Materials and Methods.....	165
7.3.1 Materials .....	165
7.3.2 Methods.....	166
7.3.2.1 Formation and Characterization of Phase Separated Biopolymer Mixtures .....	166
7.3.2.2 Emulsion Preparation.....	168
7.3.2.3 Influence of Order of Addition on Lipid Loading Capacity .....	168
7.3.2.4 Fat Extraction and Analysis of Filled Hydrogel Microspheres.....	170
7.3.2.5 Simplification of Fabrication Method.....	170
7.3.2.6 Evaluation of Physical Characteristics of Filled Hydrogel Microspheres.....	172
7.3.2.7 Influence of Volume Ratio on Filled Hydrogel Microsphere Formation.....	174
7.3.2.8 Fabrication of Density Matched Filled Hydrogel Microspheres.....	174
7.3.2.9 Statistical Analysis.....	176
7.4 Results and Discussion .....	176
7.4.1 Influence of Order of Addition on Lipid Loading Capacity .....	176
7.4.2 Simplification of Fabrication Method.....	177
7.4.3 Influence of Volume Ratio on Filled Hydrogel Microsphere Formation and Microstructure .....	180
7.4.4 Fabrication of Density Matched Filled Hydrogel Microspheres.....	184
7.4.4.1 Structural and Physicochemical Properties.....	184
7.4.4.2 Stability to Gravitational Separation.....	190
7.5 Conclusions.....	196
<b>8. CONCLUSIONS.....</b>	<b>199</b>

APPENDIX: PARTITIONING OF EMULSION DROPLETS IN PHASE SEPARATED  
BIOPOLYMER MIXTURES .....203

BIBLIOGRAPHY.....207

## LIST OF TABLES

Table	Page
3.1. Physical and Chemical Properties of Phase Separated Layers of 3% Pectin/3% Caseinate at pH 7.....	59
5.1. Particle size diameter and zeta potential of tween stabilized emulsion, casein stabilized emulsion, and cross-linked filled hydrogel particles .....	130
7.1. Apparent viscosity for continuous and dispersed phase and viscosity ratio for microsphere with increasing oil levels (0-27.3% oil) .....	188
7.2. Apparent Viscosity, n, K, zeta potential, and LAB readings for particles with increasing oil levels (0-27.3% oil).....	189
7.3. Physical properties associated with calculating creaming velocity (U) for filled hydrogel particles with increasing concentrations of oil (0-27.3% w/w) .....	190

## LIST OF FIGURES

Figure	Page
2.1. Possible outcomes of mixing a ternary biopolymer system consisting of biopolymer A, biopolymer B, and a solvent .....	6
2.2. Typical phase diagram for a mixture of a protein and polysaccharide .....	9
2.3. Picture of a typical filled hydrogel particle consisting of a lipid droplets surrounded by a biopolymer matrix .....	12
2.4. General mechanism for the acyl transfer reaction between the $\gamma$ -carboxy amide group of glutamine and the $\epsilon$ -amino group of lysine catalyzed by transglutaminase .....	19
2.5. Schematic diagram of the gelation of carrageenan according to the domain model. Adapted from (Dea, 1989) .....	22
2.6. Schematic drawing depicting the “egg-box” model for the gelation of low methoxy pectin and alginate by calcium ions ( $\bullet$ ). Adapted from (Morris, 2007) .....	23
2.7. Mechanism of lipid autoxidation .....	33
2.8. Mechanism of type I and type II sensitizers in photooxidation process .....	34
2.9. Schematic of the human digestion system .....	38
3.1. Example of a typical laser vertical profile for a creamed sample .....	55
3.2. Picture of phase separated 3% pectin/3% caseinate system at pH 7 with casein-rich phase shown dyed in pink with Rhodamine B .....	61
3.3. Apparent viscosity versus shear rate for upper, lower, and 83% upper/17% lower phase at 25°C .....	61
3.4. Percent back scattering versus height of test tube (mm) following storage at room temperature for 1% oil in 3% pectin/3% caseinate mixtures at pH 7 .....	64
3.5. Confocal image of 3% pectin/3% caseinate mixture with 1% (wt.) emulsified corn oil at pH 7, oil is shown in red and caseinate is shown in green .....	66

3.6.	Area under the creaming curve for increasing concentrations of upper/lower phase from 3% pectin/3% caseinate phase separated mixtures (pH 7) added to 1% (wt.) emulsified corn oil at pH 7 after 1 day of storage at room temperature .....	67
3.7A.	Photograph of 1% (wt.) emulsified corn oil with increasing proportions of upper phase after 1 day of storage at room temperature .....	69
3.7B.	Photograph of 1% (wt.) emulsified corn oil with increasing proportions of lower phase after 1 day of storage at room temperature .....	69
3.8A.	Confocal image of 1% (wt.) emulsified corn oil with 0.2:8.8 proportion of upper phase:buffer after 1 day of storage at room temperature, oil droplets are dyed in red.....	71
3.8B.	Confocal image of 1% (wt.) emulsified corn oil with 2.0:7.0 proportion upper phase:buffer after 1 day of storage at room temperature, oil droplets are dyed in red.....	71
3.8C.	Confocal image of 1% emulsified corn oil with 0.2:8.8 proportion of lower phase:buffer after 1 day of storage at room temperature, oil droplets are dyed in red.....	71
3.8D.	Confocal image of 1% emulsified corn oil with 2.0:7.0 proportion of lower phase:buffer after 1 day of storage at room temperature, oil droplets are dyed in red.....	71
3.9.	Apparent viscosity versus pH for 3% pectin/3% caseinate mixture, upper phase of 3% pectin/3% caseinate mixture and lower phase of 3% pectin/3% caseinate acidified from pH 7 to pH 5 at a shear rate of 1 (1/s) at 25° C .....	76
3.10.	Confocal image of pectin/caseinate biopolymer particles encapsulating emulsified corn oil, corn oil is dyed in green and casein is dyed in red .....	78
4.1.	Particle diameter determined by image analysis (Equivalent D(0.1), D(0.5), and D(0.9)) (µm) for hydrogel particles created under different mixing conditions at pH 5 .....	96
4.2.	Particle diameter determined by static light scattering (D(0.1) and D(0.5) (µm) for hydrogel particles created under different mixing conditions at pH 5.....	97
4.3A.	Representative DIC microscopy image of hydrogel particles subjected to no mixing (0 rpm) at pH 5 .....	98

4.3B.	Representative DIC microscopy image of hydrogel particles subjected to 100 rpm mixing treatment at pH 5 .....	98
4.3C.	Representative DIC microscopy image of hydrogel particles subjected to 1000 rpm mixing treatment at pH 5 .....	98
4.4.	Particle diameter (D <sub>3,2</sub> (μm)) determined by static light scattering versus pH for filled hydrogel particles treated with TGase and filled hydrogel particles not treated with TGase .....	102
4.5.	Particle diameter (Equiv. D(0.5)) for filled hydrogel particles treated and not treated with TGase at pH 3, pH5, and pH 7.....	104
4.6A.	Representative DIC microscopy image of filled hydrogel particles not treated with TGase at pH 5 previously diluted by a factor of 10 in pH 5 adjusted buffer .....	106
4.6B.	Representative DIC microscopy image of filled hydrogel particles treated with TGase at pH 5 previously diluted by a factor of 10 in pH 5 adjusted buffer .....	106
4.6C.	Representative DIC microscopy image of filled hydrogel particles not treated with TGase at pH 7 previously diluted by a factor of 10 in pH 7 buffer.....	106
4.6D.	Representative DIC microscopy image of filled hydrogel particles treated with TGase at pH 7 previously diluted by a factor of 10 in pH 7 buffer .....	106
4.7.	Zeta potential versus pH for filled hydrogel particles treated and not treated with TGase .....	107
4.8.	Zeta potential versus sodium chloride concentration for filled hydrogel particles treated and not treated with TGase.....	110
4.9.	Particle size (D <sub>3,2</sub> ) (μm) versus calcium chloride concentration for filled hydrogel particles treated and not treated with TGase.....	112
4.10.	Photograph of filled hydrogel particles with increasing concentrations of calcium chloride (0-8 mM) .....	112
4.11.	Zeta potential versus calcium chloride concentration for filled hydrogel particles treated and not treated with TGase.....	113
5.1.	Formation of filled hydrogel microspheres by a multiple step process.....	120
5.2.	Particle size distribution of casein stabilized emulsion, Tween stabilized emulsion, and filled hydrogel microspheres. ....	129

5.3.	Microstructure of filled hydrogel microspheres determined by optical microscopy with differential interference contrast (DIC).....	131
5.4.	Concentration of primary reaction products (hydroperoxides) formed during storage at 55 °C detected in casein stabilized emulsions, Tween stabilized emulsions, and filled hydrogel microspheres. ....	132
5.5.	Concentration of secondary reaction products (propanal) formed during storage at 55 °C detected in casein stabilized emulsions, Tween stabilized emulsions, and filled hydrogel microspheres .....	133
6.1.	Particle size (D 3,2) (um) for emulsion and hydrogel samples prior to digestion and following simulated digestion in the mouth, stomach, and small intestine.....	150
6.2	Zeta potential measurements for emulsion and hydrogel microspheres prior to digestion and following simulated digestion in the mouth, stomach, and small intestine .....	150
6.3A.	Confocal micrograph of filled hydrogel microspheres prior to digestion at pH 7, oil is shown in green and protein is shown in red.....	153
6.3B.	Confocal micrograph of filled hydrogel microspheres following simulated mouth conditions at pH 6.8, oil is shown in green and protein is shown in red .....	153
6.3C.	Confocal micrograph of filled hydrogel microspheres following simulated gastric conditions at pH 2.5, oil is shown in green and protein is shown in red .....	153
6.3D.	Confocal micrograph of filled hydrogel microspheres following in vitro lipid digestion at pH 7, oil is shown in green and protein is shown in red .....	153
6.4A.	Confocal micrograph of casein stabilized emulsion prior to digestion at pH 7, oil is shown in green .....	154
6.4B.	Confocal micrograph of casein stabilized emulsion following simulated gastric conditions at pH 2.5, oil is shown in green .....	154
6.4C.	Confocal micrograph of casein stabilized emulsion following simulated mouth conditions at pH 6.8, oil is shown in green.....	154
6.4D.	Confocal micrograph of casein stabilized emulsion following in vitro lipid digestion at pH 7, oil is shown in green.....	154

6.5A.	Photograph of filled hydrogel microspheres prior to digestion (I), following simulated mouth conditions (II), following simulated gastric conditions (III), and following in vitro lipid digestion (IV), oil dyed in red .....	158
6.5B.	Photograph of emulsion sample prior to digestion (I), following simulated mouth conditions (II), following simulated gastric conditions (III), and following in vitro lipid digestion (IV), oil dyed in red .....	158
6.6.	% Free fatty acids (FFA) released versus time (minutes) for filled hydrogel microsphere and emulsion samples during in vitro lipid digestion at pH 7 .....	160
7.1.	Confocal micrograph images of structures formed from oil, caseinate, and pectin (pH 5) using three different methods. ....	178
7.2	Particle size distribution of particles formed by the Free Oil-Simple Method., the Free Oil-Complex Method, and the Emulsion Method. ....	179
7.3A.	Optical micrographs of filled hydrogel particles formed from 1% (vol/vol) particle phase (oil droplets + lower phase) and 99% (vol/vol) upper phase .....	182
7.3B	Optical micrographs of filled hydrogel particles formed from 40% (vol/vol)particle phase (oil droplets + lower phase) and 60% (vol/vol) upper phase .....	182
7.4.	Photograph and micrograph of filled hydrogel particles formed from 30% (vol/vol) lower phase and emulsion and 70% (vol/vol) upper phase after centrifugation at 1,000 g for ten minutes. Note coagulated protein on surface of mixture, and coagulated protein (left) and free particles (right) in micrograph.....	183
7.5A.	Confocal micrographs of filled hydrogel particles containing 0% (w/w) oil. The protein appears red, and the scale bars represent 10 $\mu\text{m}$ .....	186
7.5B.	Confocal micrographs of filled hydrogel particles containing 9.1% (w/w) oil. The oil appears in green while the protein appears red, and the scale bars represent 10 $\mu\text{m}$ .....	186
7.5C.	Confocal micrographs of filled hydrogel particles containing 18.2% (w/w) oil. The oil appears in green while the protein appears red, and the scale bars represent 10 $\mu\text{m}$ .....	186
7.5D.	Confocal micrographs of filled hydrogel particles containing 27.3% (w/w) oil. The oil appears in green while the protein appears red, and the scale bars represent 10 $\mu\text{m}$ .....	186

7.6.	Mean particle diameter ( $D_{32}$ ) for filled hydrogel particles fabricated with increasing concentrations of emulsified oil in the disperse phase .....	188
7.7.	Photographs of filled hydrogel particles with increasing oil content (0, 9.1, 18.2, and 27.3% oil) diluted 1:100 in buffer at pH 5 after 0 (A) and 7 (B) days storage at ambient temperature .....	193
7.8.	Comparison of vertical laser profiles of % transmission versus sample height for filled hydrogel particles diluted 1:100 in buffer (pH 5) containing 0% oil and 27.3% oil after 7 days of storage at room temperature .....	194
7.9.	Predicted and experimental sedimentation indices versus oil content of filled hydrogel particles diluted 1:100 in buffer at pH 5 after 7 days of storage at room temperature.....	195
7.10.	Sedimentation index versus oil content of filled hydrogel particles diluted 1:100 in buffer at pH 5 after centrifugation at $150 \times g$ for 1 hour .....	197
A1.1.	Schematic drawing depicting the formation of filled hydrogel particles by sequential segregative and aggregative phase separation of pectin and casein.....	204

# CHAPTER 1

## INTRODUCTION

### 1.1 Introduction

Chronic disease prevention is an important public health issue for developed countries. Factors such as an aging population and increasing health care costs highlight the need for chronic disease prevention in the developed world. Nutritional therapies such as functional foods and dietary supplements represent one approach towards the prevention of chronic disease (Heurtault, Saulnier, Pech, Proust, & Benoit, 2003; Eussen, et al., 2011). Although there are many definitions of functional foods, one common theme is that functional foods may provide health benefits “beyond basic nutrition” (Henry, 2010). These health benefits are usually associated with the incorporation of one or more bioactive compounds (Eussen, et al., 2011). Most bioactive compounds fall under one of three classifications, namely lipids, proteins, or carbohydrates. Of these three categories, lipophilic bioactives pose several challenges regarding their incorporation into foods. In particular, these hydrophobic compounds are difficult to incorporate into aqueous foods, and they are often highly susceptible to oxidative deterioration (McClements, Decker, & Park, 2009a; de Vos, Faas, Spasojevic, & Sikkema, 2010). Thus, there is a great need to develop food grade delivery systems that can be used to encapsulate and protect lipophilic bioactives.

Food grade delivery systems for lipophilic bioactives must possess a number of important attributes. One essential quality of these systems is that they are compatible with both the lipophilic bioactive as well as the product that they will be incorporated into to create a functional food or beverage. Other desirable attributes may include

enhanced stability or controlled release of the desired lipophilic bioactive. For these reasons, emulsion-based delivery systems are especially well suited for creating delivery systems for bioactive lipids (McClements, Decker, & Weiss, 2007) .

Conventional oil-in-water (O/W) emulsions are the most common type of emulsion-based delivery systems. The popularity of O/W emulsion-based delivery systems can be attributed to their low production costs and to their ease of manufacture. Despite these advantages, conventional emulsion-based delivery systems have limited potential in terms of their ability for bioactive protection and controlled bioactive release. Thus, more sophisticated emulsion-based delivery systems such as filled hydrogel particles may be appropriate for certain applications where chemical stability or bioactive release is critical (McClements, Decker, Park, & Weiss 2009b; McClements, et al., 2007).

Hydrogel particles can broadly be defined as hydrophilic gelled particles formed from biopolymers such as polysaccharides and proteins. Filled hydrogel particles are hydrogel particles where emulsified oil has been incorporated inside the particle prior to gelation such that these droplets become encapsulated inside the hydrogel matrix. Thus, these particles can be thought of as a type of oil-in-water-in-water emulsion (O/W<sub>1</sub>/W<sub>2</sub>) (McClements, et al., 2007). There are a number of techniques to form hydrogel particles. Most of these techniques are based on either the breakup of a continuous gel matrix to form discrete hydrogel particles or the formation of dispersed droplets that are then gelled by the addition of a gelling agent (Burey, Bhsndari, Howes, & Gidley, 2008).

As stated previously, it may be possible to create food grade delivery systems with enhanced stability, targeted release, or improved bioaccessibility using sophisticated

emulsion-based systems. Filled hydrogel particles are one example of this type of delivery system as these particles can be fabricated from food grade proteins, polysaccharides, and lipids. Thus, the overall objective of this work is to develop a method for fabricating filled hydrogel particles and to examine the chemical and physical properties of this novel delivery system.

## **1.2 Objectives**

The overall goal of this project is to encapsulate beneficial lipophilic food constituents inside a novel delivery system composed of proteins and polysaccharides known as filled hydrogel particles. Following fabrication, this system will be evaluated for its physical properties, its chemical and environmental stability, and its bioaccessibility.

### **Specific Project Objectives:**

**1. Fabrication and Characterization of Filled Hydrogel Particles:** Mixtures of proteins and polysaccharides that exhibit thermodynamic incompatibility will be used to construct a two phase system consisting of a protein-rich phase and a polysaccharide-rich phase. Upon mixing, this system will form a water-in-water emulsion. Once this protein and polysaccharide mixture is identified and characterized, emulsified oil will be incorporated into this system, and upon mixing, this system should form an oil-in-water-in-water emulsion. To trap this structure, a gelling agent such as an enzyme or a chemical will be added to form stable particles.

### **2. Influence of Environmental Stress on Filled Hydrogel Particle Stability:**

Following fabrication, it is essential that these particles are evaluated under various

environmental stresses such as oxygen and salt as well as various temperature and pH ranges. It is essential that these particles are evaluated against conventional oil-in-water emulsions for their susceptibility to lipid oxidation since enhanced stability against oxidation was one of the main justifications for developing this system. These particles will also need to be evaluated for their stability to high salt and high acid conditions, especially those conditions commonly seen in foods.

### **3. Influence of Lipid Encapsulation within Filled Hydrogel Particles on Lipid**

**Digestion:** To create a successful delivery systems for foods, it is important that the bioactive targeted for delivery can be digested by the human body. For this reason, an in-vitro model for lipid digestion will be used to assess the bioavailability of the lipid encapsulated within these particles.

### **4. Optimization of the Fabrication and Performance of Filled Hydrogel**

**Particles:** As with any process, it is essential that the method to fabricate filled hydrogel particles is both simple and efficient. In an effort to optimize this process, experiments will be conducted to reduce the number of processing steps associated with particle fabrication and to increase the lipid loading capacity of these particles. Additionally, studies will be conducted on the fabrication of particles that resist gravitation separation during storage (i.e. density matched particles).

## **CHAPTER 2**

### **LITERATURE REVIEW**

#### **2.1 Emulsion-Based Delivery Systems for Lipophilic Bioactives**

There is a great need in the food industry to develop novel delivery systems for bioactive compounds. Many of these beneficial constituents such as  $\omega$ -3 fatty acids, carotenoids, fat-soluble vitamins, and phytosterols are lipophilic, making the incorporation of these compounds into aqueous foods and beverages challenging. In addition to incorporation problems, many of these lipophilic compounds are chemically unstable and tend to degrade during storage when incorporated into foods (McClements, et al., 2007; Belitz, Grosch, & Schieberle, 2009a). Traditionally, oil-in-water emulsion (O/W) which consist of small oil droplets dispersed in a continuous watery phase have been used by the food industry to incorporate lipids into aqueous foods and beverages. There are, however, other possible emulsion-based delivery systems for these compounds including multilayer ( $O_M/W$ ), water-in-oil-in-water (W/O/W), oil-in-water-in-water (O/W/W) emulsions (McClements, et al., 2007; McClements, 2005). Depending on the application, these novel delivery systems may have significant advantages over conventional O/W emulsions such as enhanced stability or controlled bioactive release.

#### **2.2 Biopolymer Phase Separation**

When a biopolymer system consisting of two biopolymers and a solvent are mixed together, there are three possible outcomes: miscibility, association or segregation

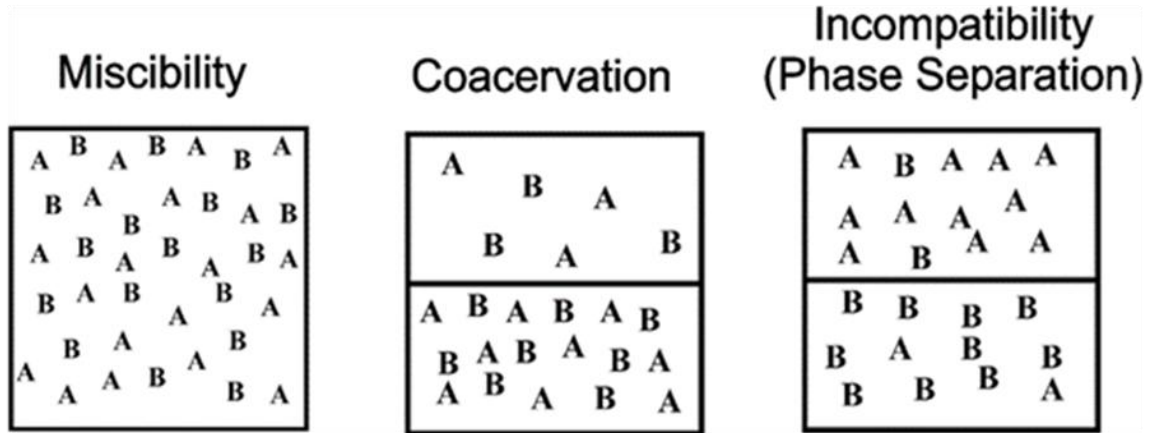


**Figure 2.1:** Possible outcomes of mixing a ternary biopolymer system consisting of biopolymer A, biopolymer B, and a solvent

(Syrbe, Bauer, & Klostermeyer, et al., 1998; de Kruif & Tuinier, 2001) (Figure 2.1). For

miscibility to occur, interactions between different biopolymer molecules must be the same as interactions between identical molecules, that is another molecule of itself.

Miscibility is typically quite uncommon for high molecular biopolymer mixtures as slight charges on subunits repeated many times across the length of the biopolymer chain result in significant attractive or repulsive forces that prevent spontaneous mixing (Syrbe, et al., 1998).

Association tends to occur when there is a sufficiently strong attraction between biopolymer molecules, *e.g.*, an electrostatic attraction between oppositely charged biopolymers (Tolstoguzov, 2003). Biopolymer association leads to the formation of a two phase system consisting of one aqueous phase rich in both biopolymers, and another aqueous phase depleted in both biopolymers. Segregation tends to occur when there is a net repulsion between biopolymer molecules, which is usually the result of an entropy of mixing (excluded volume) effect (de Kruif & Tuinier, 2001; Grinberg & Tolstoguzov,

1997). If left undisturbed, ternary biopolymer systems experiencing segregation will, over time, separate into two distinct phases (Norton & Frith, 2001). Each of these phases will consist of high amounts of one biopolymer along with small amounts of the other biopolymer (Syrbe, et al., 1998; de Kruif & Tuinier et al., 2001; Norton & Frith, 2001).

### 2.2.1 Basis for Phase Separation

The change in free energy associated with the mixing of two biopolymers in a solvent can generally be described by the following Gibbs free energy equation (Equation 2.1):

$$\Delta G_{mix} = \Delta E_{mix} - T \Delta S_{mix} \quad (2.1)$$

In Equation 1,  $\Delta G_{mix}$  is the change in free energy due to mixing,  $\Delta E_{mix}$  is the change in molecular interaction energy due to mixing,  $T$  is temperature, and  $\Delta S_{mix}$  is the change in entropy due to mixing. Based on this equation, one would predict that the two biopolymers would phase separate when  $\Delta G_{mix}$  is highly positive but remain miscible (mixed) when  $\Delta G_{mix}$  is highly negative. Although this equation is a simplistic view of the thermodynamics of mixing, it does highlight the importance of molecular interactions, mixing entropy, and temperature in determining whether two biopolymer will mix or phase separate (McClements, 2005).

For an extremely dilute solution of biopolymers, the entropic gains of the mixed state are able to overcome any unfavorable molecular interactions between biopolymers. At high concentrations of biopolymers, separation can proceed by two different mechanisms depending on the structural similarities of the two biopolymers. For expanded biopolymers of similar structures, separation is attributed to unfavorable

interactions between polymer segments. In the case of polymers with dissimilar size and shape, it is the loss in conformational entropy at the interface of two dissimilar biopolymers that drives separation (de Kruif & Tuinier, 2001). In general, most macromolecules in mixed solution prefer to be surrounded by macromolecules identical to themselves (Norton & Frith, 2001; Tolstoguzov, 2003). Temperature is another parameter that can influence the mixing behavior of biopolymers. Lowering the temperature of a mixed biopolymer solution tends to encourage phase separation as many biopolymers at lower temperatures interact with themselves to form ordered structures (Norton & Frith, 2001). Conversely, increasing the temperature tends to encourage solubility and mixing (de Kruif & Tuinier, 2001).

### **2.2.2 Phase Composition and the Phase Diagram**

As mentioned previously, biopolymer phase separation leads to the formation of two distinct phases where each phase is rich in one biopolymer and poor in the other biopolymer. To model the behavior and composition of biopolymer mixtures in solution, a phase diagram such as the one shown in Figure 2.2 can be used. On the x and y axes are the percent concentrations of each biopolymer (typically a protein and a polysaccharide). The binodal curve located on the diagram separates it into two regions. All mixtures of protein and polysaccharide at concentrations to the left of the binodal are miscible while mixtures at concentrations to the right of the binodal will phase separate. In addition to delineating the phase diagram into regions of compatibility and incompatibility, the phase after separation. A tie line can be thought of as a connecting line between the overall composition of the biopolymer mixture prior to separation and the biopolymer

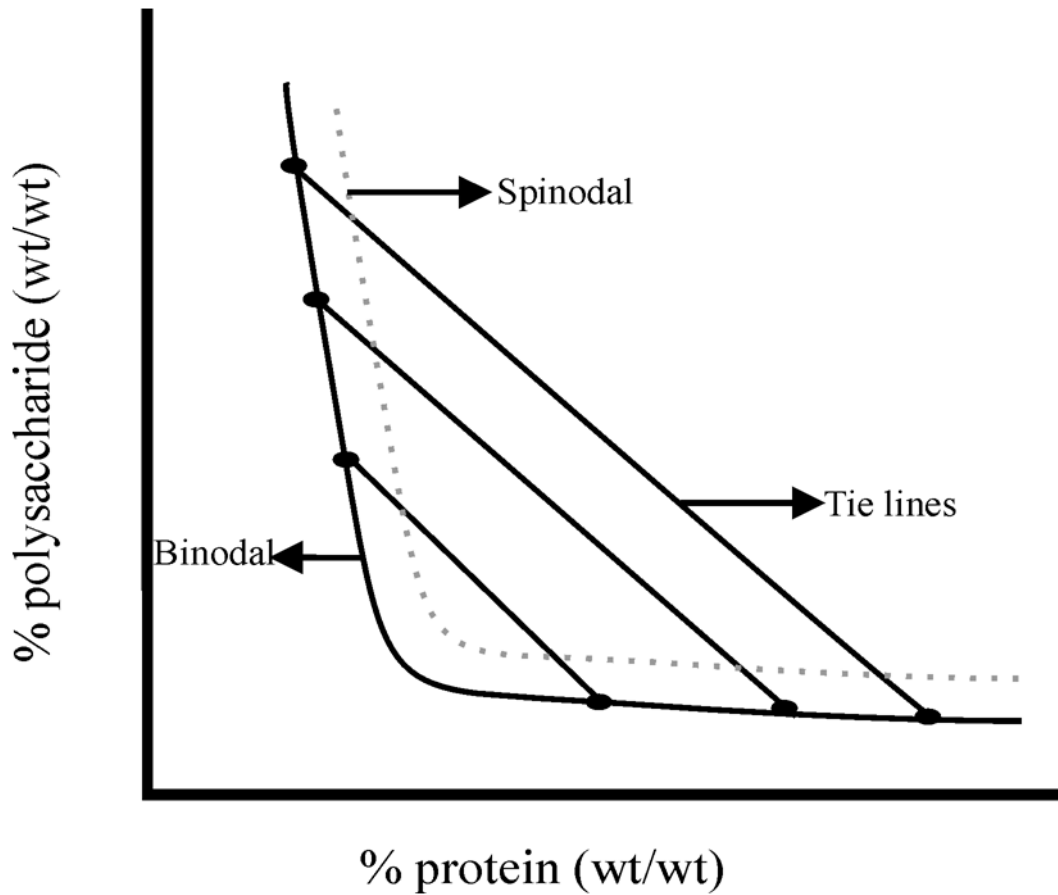


**Figure 2.2:** Typical phase diagram for a mixture of a protein and polysaccharide

concentration in each phase after separation. All mixtures of biopolymers that lie on the same tie line will separate into phases with the same concentration of each biopolymer. The relative volumes of each phase, however, will be different as this is calculated as the distance of the tie line from the overall composition of the mixture to the opposite phase binodal divided by the total length of the tie line.

In addition to the binodal, there is also the spinodal curve. The spinodal curve separates biopolymer mixtures that phase separate (mixtures to the right of the binodal curve) into two classification according to their mode of phase separation. Mixtures

located between the spinodal and the binodal will phase separate by way of a nucleation mechanism, a process that can take an extremely long time. Thus, mixture located between this region may not show phase separation during normal experimental time scales. Mixtures located to the right of the spinodal phase will spontaneously phase separate, and thus, these mixtures will rapidly phase separate. As the phase diagram clearly illustrates, the binodal curve remains close to the x and y axis, reaffirming the fact that each phase consists mostly of only one biopolymer (Frith, 2010).

### **2.2.3 Water-in-Water Emulsions**

When a phase separated system is mixed together, it tends to form a water-in-water (W/W) emulsion where each biopolymer phase forms either the dispersed or continuous phase. Typically, the phase that occupies the greater volume will become the continuous phase while the phase that occupies less volume will become the dispersed phase (Norton & Frith, 2001; Tolstoguzov, 2003). Water-in-water emulsions are unstable systems. If a water-in-water emulsion is left undisturbed, the dispersed phase of W/W emulsion will begin to ripen, coalesce, and over time, completely separate from the continuous phase (Norton & Frith, 2001).

The interfacial tension of W/W emulsions is quite low, usually three to four orders of magnitude below conventional oil-in-water and water-in-oil emulsions (Norton & Frith, 2001; Erni, Cramer, Marti, Windhab, & Fischer, 2009). The low interfacial tension of W/W emulsions can be attributed to the highly similar composition of the dispersed and continuous phases as both phases are mostly water along with proteins and polysaccharides that are soluble in either phases. Because of the low interfacial tension of W/W emulsions, even mild shear forces can result in substantial deformation and break

up of droplets of the dispersed phase (Tolstoguzov, 2002). As a result of shearing, various anisotropic structures including elliptical shaped droplets and even thread-like structures can be formed (Erni, et al., 2009). Upon the removal of shear flow, surface instabilities will have a tendency to break up these elongated structures into smaller droplets (Mewis, Yang, Van Puyvelde, Moldenaers, & Walker, 1998). Since the time scale for the growth of these instabilities is dependent on the interfacial tension of the system among other parameters, the time required for these structures to break up can be much longer compared to systems with relatively high interfacial tension (Erni, et al., 2009). If the unique structure of these particles is trapped by gelling the dispersed phase of a W/W emulsion, the rheological properties of the entire system can be dramatically altered. For example, Marti, Höfler, Fischer, & Windhab (2005) demonstrated that in concentrated suspensions the partial replacement of spherical particles with fiber-like particles resulted in a large increase in the viscosity of the system.

### **2.3 Filled Hydrogel Particles**

A hydrogel can broadly be defined as a water-swollen matrix formed by cross-linked hydrophilic polymers. Hydrogels can hold large quantities of water while still maintaining structural integrity. Although synthetic polymers are often used to create hydrogels for pharmaceutical and biomedical applications, most of these polymers are not allowed in foods and beverages (Chen, Remondetto, & Subirade, 2006). In place of synthetic polymers, polysaccharides and some food proteins can be used to create food grade hydrogels. Using one of the processing methods discussed below, proteins, polysaccharides, or a mixture of both proteins and polysaccharides can be used to form discrete hydrogel particles. Filled hydrogel particles as shown in Figure 2.3 are hydrogel

particles where emulsified oil has been incorporated inside the particle prior to gelation such that these droplets become encapsulated inside the hydrogel matrix. Typically, these particles are formed from biopolymers that are capable of both phase separation and hydrogel particle formation (Burey, et al., 2008; McClements, 2010a).

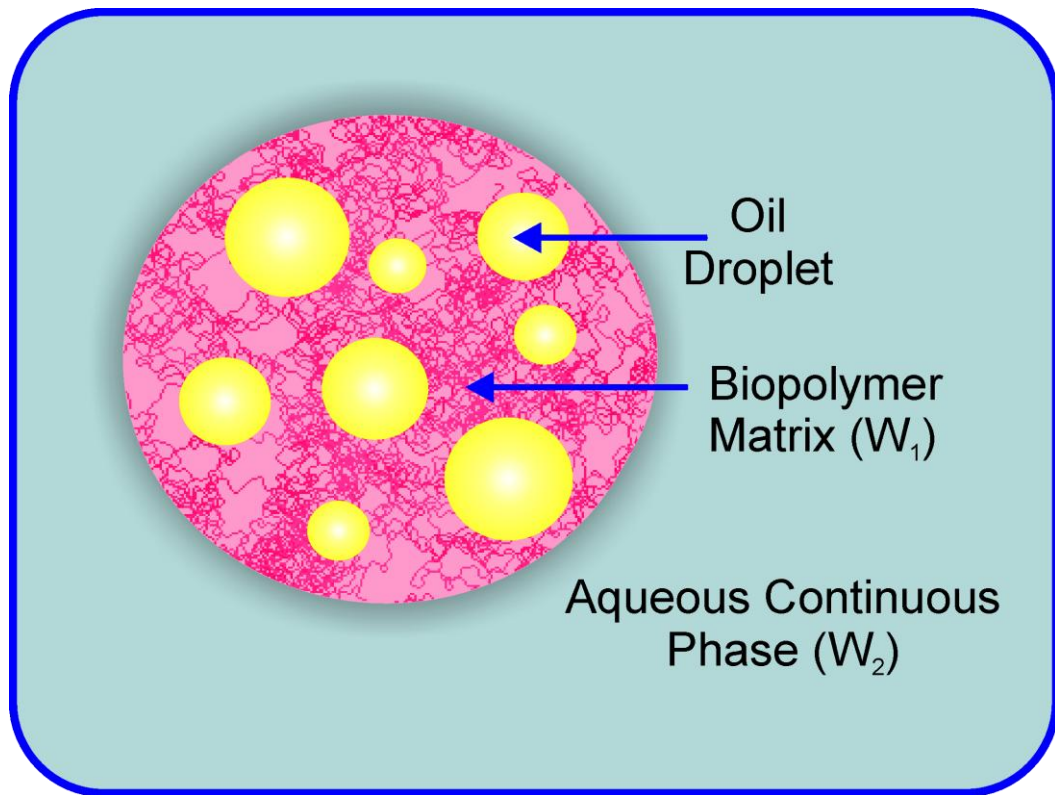


**Figure 2.3:** Picture of a typical filled hydrogel particle consisting of a lipid droplets surrounded by a biopolymer matrix

There are a number of techniques to form hydrogel particles. Most of these techniques are based on either the breakup of a continuous gel matrix to form discrete hydrogel particles or the formation of dispersed droplets that are then gelled by a specific mechanism such as a change in temperature (heat or cold gelation) or the addition of an enzyme or ions such as calcium (Burey, et al., 2008; McClements, 2010a). According to

McClements (2010a), the main methods for creating filled hydrogel particles are as follows: macroscopic gel disruption, simple coacervation, injection, and emulsion methods.

### **2.3.1 Macroscopic Gel Disruption Method**

Macroscopic gel disruption involves the formation of a continuous gel network that is subsequently broken up by the application of force such as shear (McClements, 2010a). This method is commonly executed by bring a hydrocolloid solution close to gelation and then applying shear to break the gel into discrete particles before a cohesive gel has formed (Burey, et al., 2008). To create filled hydrogel particles, a filled macroscopic gel would be formed prior to break up (McClements, 2010a).

### **2.3.2 Simple Coacervation Method**

Coacervation is the separation of a colloidal liquid system into two phases, a phase rich in colloid particles along with a phase rich in the equilibrium solution (de Kruif, Weinbreck, & de Vries, 2004). Unlike complex coacervation which involves the interaction between two biopolymers, simple coacervation involves the self-association and subsequent separation of one biopolymer into the colloid-rich phase of the system (Madene, Jacquot, M., Scher, J., & Desobry, 2006; Burey, et al., 2008). To promote self-association, environmental conditions such as ionic strength, temperature, or dielectric constant are adjusted as these changes impact solvent quality. To create filled hydrogel particles by this method, lipid droplets would be incorporated into the biopolymer system prior to adjusting solution conditions. Once solution conditions are

adjusted, the newly formed filled hydrogel particles may require an additional treatment to gel their final structure (McClements, Decker, Park, & Weiss, 2008; McClements, 2010a).

### **2.3.3 Injection Method**

The injection method relies on the use of an aqueous bath that is capable of gelling a specific biopolymer. In this method, small droplets of a biopolymer solution are introduced into this aqueous bath where they quickly gel into discrete biopolymer particles (McClements, 2010a). The way in which the droplets are injected into the bath can have a major impact on final particle size. Particles formed by syringe needles are typically quite large with a size range of 0.5-6 mm while atomization of the biopolymer solution into the aqueous gelation bath can produce smaller particles with an approximate size of several hundred microns (Burey, et al., 2008). To form filled hydrogel particles, lipid droplets would be incorporated into the biopolymer mixture prior to its addition to the gelling bath (McClements, 2010a).

### **2.3.4 Emulsion Methods**

Among the four major techniques for forming filled hydrogel particles, emulsion-based methods are probably the most versatile and practical for producing small (micron-sized) particles. One way to form particles using this method is to create an oil-in-water-in-oil (O/W/O) emulsion where the inner oil phase contains the bioactive component, the water phase contains a biopolymer capable of gelation, and the outer oil phase acts as a lipophilic solvent. To form this multiple emulsion, an emulsified oil-in-water (O/W) emulsion is homogenized into a separate oil phase that also contains a lipophilic

emulsifier. Next, the biopolymer located inside the water phase of the multiple emulsion is gelled by enzymatic, thermal, or chemical treatments (McClements, et al., 2007; McClements, 2010a). Factors such as the viscosity of the outer oil phase, the type of lipophilic surfactant used, and the mixing/emulsification conditions for the incorporation of the initial O/W emulsion into the outer oil phase can have a major impact on the final size of these biopolymer particles. Depending on these conditions, the size of these particles can vary significantly from nanometers to millimeters. Following the formation of these biopolymer particles, the outer phase of oil can be removed by a combination of washing and filtration (Reis, Neufeld, Vilela, Ribeiro, & Veiga, 2006). The process of separating the outer oil phase from the newly formed biopolymer particles is a major drawback to this method as this process can be difficult and messy. Moreover, this step adds to the complexity of this method (Burey, et al., 2008).

Another emulsion-based method for forming filled hydrogel particles involves the entrapment of emulsified oil inside biopolymer coacervates (McClements, 2010). Complex coacervation involves the separation of a solution composed of at least two macromolecules into two immiscible phases, a phase rich in both macromolecules and another phase consisting of the equilibrium solution. The two macromolecules involved in complex coacervation are usually oppositely charged and often consist of a protein and an anionic polysaccharide. Depending on the strength of the interaction between the two oppositely charged macromolecules, either coacervation or precipitation may occur. Precipitation typically occurs when strong polyelectrolytes (polymers with a high charge

density such as sulfated carrageenan) interact (de Kruif et al., 2004). Precipitates are fairly dense complexes that tend to separate from solution as a solid (Cooper, Dubin, & Kayitmazer, 2005).

Unlike precipitates, coacervates tend to form between weak polyelectrolytes as interactions between these macromolecules are short range, soft attractions (de Kruif et al., 2004). Coacervates are less dense than solid precipitates but more dense and less hydrated than soluble complexes. In general, coacervates are composed of 20-30% protein and polymer. Compared to precipitates, coacervates tend to have a more regular structure and are less prone to aggregation and sedimentation. For these reasons, coacervation is usually preferred over precipitation for encapsulation (McClements, et al., 2007; McClements, 2010a). To encapsulate oil inside coacervates and form filled hydrogel particles, first the oil is dispersed into a solution of two polyelectrolyte that are capable of forming coacervates. Solution conditions are then adjusted such that coacervation is favored, and the dispersed oil is encapsulated inside the newly formed complexes. Maximum encapsulation typically occurs when the pH of the solution is adjusted such that maximum coacervation is achieved (Cooper et al., 2005). Coacervates often dissociate and break up when solution conditions such as the pH or ionic strength are adjusted; coacervates are also susceptible to coalescence. To improve the stability of coacervates used for encapsulation, one or both of the polyelectrolytes present in the coacervates can be cross-linked by chemical, enzymatic, or thermal treatments (Cooper et al., 2005; McClements, et al., 2007; McClements, 2010a).

The incorporation of emulsified oil into the dispersed phase ( $W_1$ ) of a water-in-water ( $W_1/W_2$ ) emulsion is yet another emulsion-based method for forming filled

hydrogel particles. As discussed in previous sections, two biopolymers will tend to phase separate when both macromolecules are present at sufficient concentrations and forces between the two biopolymers are repulsive. In general, these forces tend to be the result of either electrostatic repulsion or steric exclusion (McClements, 2010a). When a biopolymer mixture that experiences phase separation is mixed together, this mixture will form a water-in-water emulsion consisting of droplets of an aqueous immiscible phase with a certain biopolymer composition dispersed in a continuous aqueous phase with a different biopolymer composition (Tolstoguzov, 2003). Incorporating emulsified oil into the dispersed phase of a W/W emulsion can occur by one of two ways. Either emulsified oil can be mixed with a biopolymer mixture prior to phase separation, or the O/W emulsion can be incorporated into the dispersed phase of a phase separated biopolymer mixture and then this mixture is introduced to the continuous phase to form an O/W/W emulsion (McClements, et al., 2007; McClements, 2010a).

As discussed previously, W/W emulsions are unstable systems that over time will separate into two phases, a dispersed phase and a continuous phase (Norton & Frith, 2001). To halt this separation process and preserve the structure of the O/W/W emulsion, solution conditions can be adjusted such that one of the two aqueous phases of the W/W emulsion forms a gel (McClements, et al., 2007; McClements, 2010a). For example, an O/W/W emulsion that contained a biopolymer capable of cold-set gelation could be gelled by reducing the temperature of mixture. In another case, the O/W/W emulsion could be gelled by the addition of ions if the emulsion contained a biopolymer capable of ionotropic gelation.

### **2.3.5 Gelation Methods**

To trap the structure of filled hydrogel particles, a number of different gelation methods can be used. Gelation can proceed by one of two ways, either by forming chemical or physical gels. Chemical gels are formed by covalent interactions between polymers while physical gels, the most common form of gels in food, are formed by physical interactions between polymers. Both proteins and polysaccharides are capable of gelation although the gelation mechanism and properties of these two types of gels are often quite different (Renard, van de Velde, & Visschers, 2006).

#### **2.3.5.1 Protein Gelation**

In the case of food proteins, globular protein gels are probably the most common form of food protein gels. These gels are usually formed by heating globular proteins which causes them to unfold followed by the association and aggregation of the denatured protein to form a gel. The addition of certain ions such as calcium from various salts with or without heating can also cause protein gels to form. These ions help to shield the electrostatic repulsive forces present in the system, and thus, protein-protein associations can occur and a gel can form. Acids are another way to gel food proteins. The addition of acid will promote protein denaturation which will in turn encourage gelation (Totosaus, Montejano, Salazar, & Guerrero, 2002).

With the recent advances in enzyme technology, enzymes designed to gel proteins such as the enzyme transglutaminase are now readily available for commercial use. Enzymatic protein gelation involves the formation of chemical cross-links between protein chains to form a gel. The most popular and widely available enzyme for protein gelation is the enzyme transglutaminase (Protein-Glutamine:Amine-Glutamyl-

transferase, E.C. 2.3.2.13). This enzyme is capable of forming inter- and intra-molecular cross-links between the  $\gamma$ -carboxy amide group on glutamine and the  $\epsilon$ -amino group on lysine on proteins (Figure 2.4) (Ha & Iuchi, 2003).

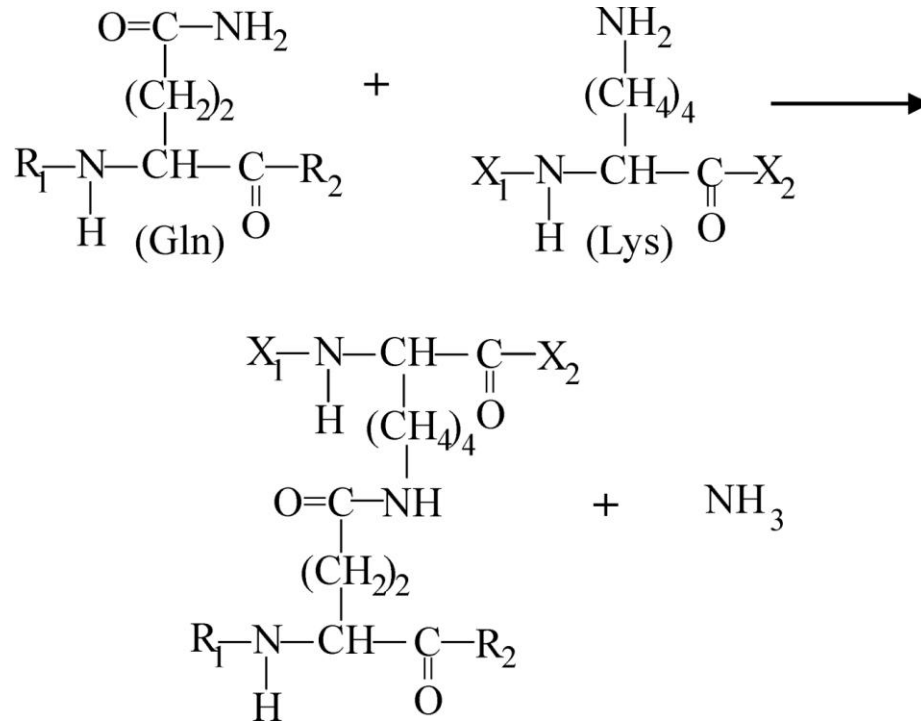


**Figure 2.4:** General mechanism for the acyl transfer reaction between the  $\gamma$ -carboxy amide group of glutamine and the  $\epsilon$ -amino group of lysine catalyzed by transglutaminase

Transglutaminase is a ubiquitous enzyme in nature as it has been found in mammals, plants, fish, and bacteria (DeJong, et al., 2002). Although transglutaminase can be isolated from mammalian blood and tissue, the commercial form of this enzyme is derived from the bacteria *Streptomyces mobaraensis*. The microbial form is preferred over the mammalian form as bacterial transglutaminase can be produced in large quantities using industrial scale culturing methods. Another advantage of using bacterial transglutaminase as opposed to mammalian transglutaminase is that calcium is required

as co-factor for mammalian transglutaminase but not for bacterial transglutaminase. Since the addition of calcium is known to cause changes in the texture and appearance of some foods, it would be desirable to use transglutaminase derived from bacteria rather than mammals (Dickinson, 1997a; Dube, Schäfer, Neidhart, & Carle, 2007).

The ability of transglutaminase to cross-link a protein strongly depends on the accessibility of the glutamine and lysine residues on the protein. For this reason, proteins with flexible structures such as casein and gelatin are good substrates for cross-linking with transglutaminase while proteins with more rigid structures such as native  $\alpha$ -lactalbumin are poor substrates for transglutaminase (DeJong & Koppelman, 2002). Reaction conditions are also important for achieving sufficient protein cross-linking using transglutaminase. In the case of transglutaminase sourced from *Streptomyces mobaraensis*, the optimum pH and temperature for this enzyme is between pH 6-7 at 50°C although 90-100% of enzyme activity is retained from pH 5-9 (Dube, et al., 2007). To inactivate transglutaminase, the most common method is thermal inactivation. This enzyme can also be deactivated by adjusting pH outside of the range of high enzyme activity or by adding certain chemical inhibitors such as N-ethylmaleimide (NEM) (DeJong & Koppelman et al., 2002; Dube, et al., 2007).

#### **2.3.5.2 Polysaccharide Gelation**

With the exception of starch-based polysaccharides and cellulose derivatives, most gelling polysaccharides are composed of more than one type of sugar unit and are thus heteropolysaccharides. The combination of multiple sugar units along with various side chains for many polysaccharides means that gelation methods can vary widely among different polysaccharides. Some of the most common gelation methods for

polysaccharides include cold-setting gels and heat-setting gels (Morris, 2007). Ionotropic gelation is also another important gelling mechanism for polysaccharides (Burey, et al., 2008).

In the case of cold-set polysaccharide gels, typically a hydrocolloid powder is dissolved into hot or boil water and then the solution is cooled and allowed to gel (Burey, et al., 2008). From a structural prospective, many of these polysaccharides in solution form ordered helical structure that transition to less ordered coils upon heating. As the solution is cooled, the helices reform and then aggregate to form a gel. Common examples of this type of gel include gellan and agar (Morris, 2007). For some polysaccharides such as iota or kappa carrageenan, a combination of heating along with the addition of monovalent cations such as potassium is required for gelation. In this case, these cations act as bridges to connect and cross-link the helices formed during cooling to promote gel formation (Oakenfull & Glicksman, 1987). The gelation of carrageenan, an example of a polysaccharide that requires both heating/cooling and ion addition, is depicted in the schematic diagram of the domain model of gelation in Figure 2.5.

Heat-set polysaccharide gels rely on the application of heat to gel. One of the best examples of this type of gel is gelatinized starch. During the heating process, native starch granules swell and release amylose, a linear biopolymer that is primarily responsible for starch gelation. Following solubilization, the entanglement of amylose is believed to be responsible for the formation of starch gels (Oakenfull & Glicksman, 1987). As is the case for most gels formed by heating, gelation occurs when the native structure of the polysaccharide unfolds and forms an expanded gel network (Burey, et al., 2008).

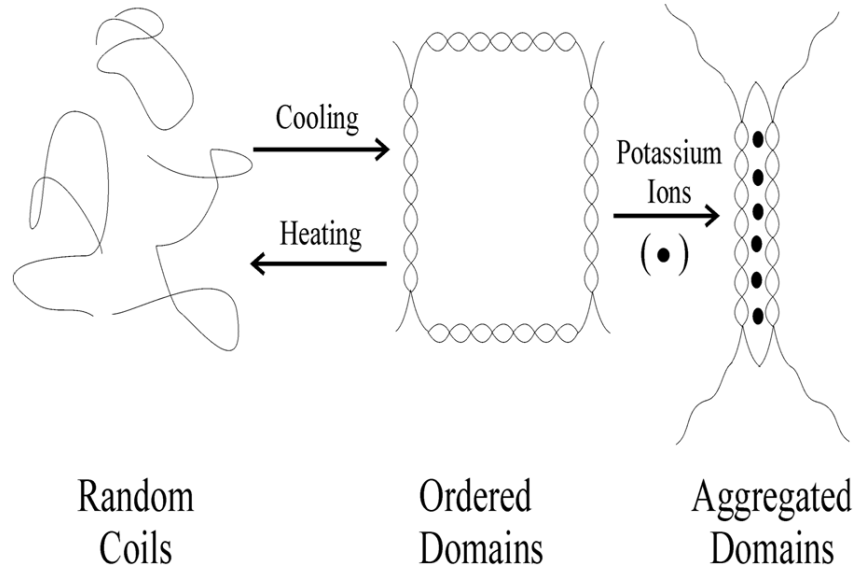


**Figure 2.5:** Schematic diagram of the gelation of carrageenan according to the domain model. Adapted from (Dea, 1989)

Ionotropic gelation involves the use of ions to form a network gelled structure from a polysaccharide. Often times, this type of gelation is associated with a negatively charged polysaccharide interacting with a specific cation (Burey, et al., 2008). For many of the polysaccharides that require specific ions to gel, network development is associated with the aggregation of block structures between separate polymer chains. For example in the case of the gelation of alginate and low-methoxy pectin by calcium salts, the negatively charged side chains located on each polymer block can be neutralized by positively charged cations such as calcium. This charge neutralization allows two or more blocks to aggregate with the cations acting as a bridge between negatively charged blocks. This type of gelation is commonly depicted as shown in Figure 2.6 and is known as the “egg-box” model (Oakenfull & Glicksman, 1987).

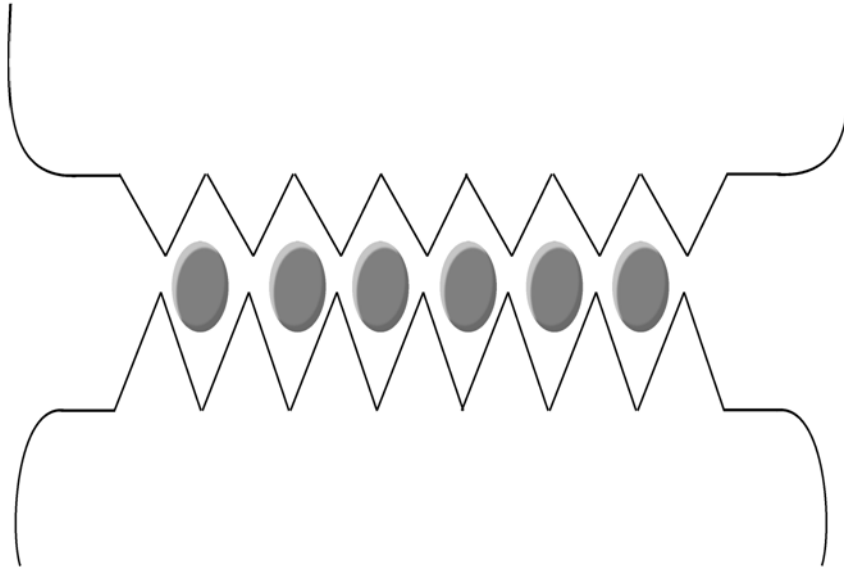


**Figure 2.6:** Schematic drawing depicting the “egg-box” model for the gelation of low methoxy pectin and alginate by calcium ions (●). Adapted from (Morris, 2007)

#### **2.4 Applications of Emulsion-Based Delivery Systems for Lipophilic Bioactives**

When designing an emulsion-based delivery systems, it is crucial that the delivery system does not negatively impact the physiochemical properties of the target food or beverage. Conversely, delivery systems could be designed such that they improve the physical, chemical, or biological properties of either the bioactive or the target food or beverage. Hydrogel particles have found many applications in the pharmaceutical industry to protect and deliver drugs to specific locations in the body. Based on this success in the drug industry, there is great potential to develop filled hydrogel particles with desirable attributes and traits for application in foods and beverages (McClements,

et al., 2007). In the following section, we discuss how these particles could be used to modify either the physical and chemical properties of the bioactive or the target food or the biological response of the bioactive in the body.

#### **2.4.1 Modification of Physical Properties Using Filled Hydrogel Particles**

*Optical Properties:* The optical properties of a food or beverage can generally be defined by two properties, namely opacity and color. Using tristimulus color coordinates such as the CIELAB  $L^*a^*b^*$  system to quantify the optical properties of food,  $L^*$  measures the lightness of a system while  $a^*$  and  $b^*$  indicate the color of the system (McClements, 2010a). For this coordinate system,  $L^*$  is measured on a scale of 0 to 100 with 0 being black and 100 being white. For the coordinate  $a^*$ ,  $a(+)$  is for red and  $a(-)$  is for green while for the coordinate  $b^*$ ,  $b(+)$  is for yellow and  $b(-)$  is for blue. The range for both of these coordinates is from approximately -80 to +80 (Wrolstad & Smith, 2010).

The opacity of a food or beverage is based on the light scattering properties of the system (McClements, 2002). In general, opaque foods reflect light, transparent foods transmit light, and translucent foods both reflect and transmit light (Wrolstad & Smith, 2010). The influence of the addition of filled hydrogel particles on the optical properties of a food or beverage is dependent on the size, refractive index, and concentration of these particles. According to Mie theory, emulsions with appreciably small particles sizes (below 50 nm) will appear transparent while emulsions with larger particles (500 nm-2000 nm) will appear as opaque (Jones & McClements, 2010). In practice, the entire particle size distribution of the emulsion must be below 80 nm to achieve optical transparency (Wooster, Golding, & Sanguansri, 2008). An increase in the difference between the refractive index of the particle and its surrounding medium will also increase

turbidity (McClements, 2010a). The influence of filled hydrogel particles on the turbidity of a system would be partially important for their incorporation into transparent beverages such as fortified waters or fruit juices. To maintain the transparency of these products, it would be necessary to fabricate nanosized filled hydrogel particles.

The color of a food or beverage is determined by the absorption of select wavelengths of light by the system. Using the coordinates  $a^*$  and  $b^*$  from the  $L^*a^*b^*$  coordinate system, the parameter chroma ( $C^*$ ) can be calculated as follows:

$$C^* = (a^{*2} + b^{*2})^{1/2} \quad (2.2)$$

In addition to chroma, the parameter hue angle ( $H^*$ ) calculated as follows:

$$H^* = \arctan^{b^*/a^*} \quad (2.3)$$

is also used to define color. It is important to measure and include the parameter  $L^*$  when evaluating food color as samples with the same values for chroma and hue but differing values for  $L^*$  may appear quite different (Wrolstad & Smith, 2010). The lightness of an emulsion increases dramatically as the percentage of lipid droplets increases from 0% wt to 5% wt followed by a more gradual increase at higher droplet percentages. Thus, the addition of filled hydrogel particles to a food or beverage could result in a decrease in the color intensity of the final product (McClements, 2010a).

*Rheological Properties:* The rheology or texture of foods may also be positively or negatively affected by the incorporation of filled hydrogel particles. In general, the rheology of a colloidal suspension depends on the effective particle concentration, the

shape of these particles and any interactions between particles. The behavior of a flowing dispersion is controlled by three forces, namely hydrodynamic, Brownian, and colloidal forces. For dispersions consisting of large particles ( $> 10 \mu\text{m}$ ) hydrodynamic forces (forces associated with the motion of particles to the surrounding fluid) dominate. For dispersion consisting of particles between 1nm-10  $\mu\text{m}$  (typically referred to as colloidal dispersions), Brownian motion and interparticle forces dominate at low shear rates while at high shear rates hydrodynamic forces are most important (Genovese, Lozano, & Rao, 2007).

The impact of filled hydrogel particles on the viscosity of fluid foods can be described by Equation 2.4:

$$\frac{\eta}{\eta_0} = \left( 1 - \frac{\phi_{eff}}{\phi_c} \right)^{-2} \quad (2.4)$$

Here,  $\eta_0$  is the shear viscosity of the liquid surrounding the particles,  $\phi_{eff}$  ( $= R\phi$ ) is the *effective* volume fraction of the biopolymer particles,  $\phi$  is the actual volume fraction of the biopolymer molecules that make up the particles,  $R$  is the effective volume ratio (the total effective volume occupied by the biopolymer particle divided by the total volume occupied of the actual biopolymer chains) and  $\phi_c$  is the critical packing parameter ( $\approx 0.6$ ) where spherical particles become close packed (Jones & McClements, 2010). The effective volume of a biopolymer particle may be much greater than the actual volume of the biopolymer molecules for a number of reasons: (i) *solvation* –biopolymer particles may trap solvent molecules such as water; (ii) *flocculation* – flocculated particles trap

solvent molecules between them; (iii) *non-sphericity* – non-spherical particles have a greater effective volume than an equivalent mass of spherical particles.

Filled hydrogel particles may be designed to provide desirable rheological attributes to a product such as thickness or creaminess, or they may be designed to have negligible impact on the textural attributes of a product. Factors including the concentration, size and shape, and composition of these particles all play an important role in how the rheology of the target food or beverage is affected. Particle-particle interactions are also important as the addition of flocculated or aggregated systems will tend to increase solution viscosity.

*Stability:* For any delivery system, it is essential that the system remain stable throughout the entire life cycle of the product. Furthermore, the filled hydrogel particles should not adversely impact the normal shelf-life of the product itself. Filled hydrogel particles may become unstable in a food product through a variety of mechanisms, including gravitational separation (creaming or sedimentation), aggregation (flocculation or coalescence), volumetric changes (swelling or shrinking), and dissociation (erosion or disintegration). It is imperative that the major physicochemical mechanism that promotes particle instability be identified so that it can be successfully inhibited or prevented. The dominant instability mechanism will depend on the composition and structure of the particles, the characteristics of the particles themselves and environmental conditions.

The creaming rate of non-interacting rigid spherical particles in a dilute Newtonian liquid is given by Equation 2.5:

$$U = -\frac{2gr^2(\rho_2 - \rho_1)}{9\eta_1} \quad (2.5)$$

Here, U is the creaming velocity (positive U for creaming; negative U for sedimentation), g is the acceleration due to gravity, r is the radius of the particle,  $\rho$  is the density,  $\eta$  is the shear viscosity, and the subscripts 1 and 2 refer to the continuous phase and particles, respectively (Jones & McClements, 2010). The density of filled hydrogel particles ( $\rho_2$ ) can be estimated using Equation 2.6:

$$\rho_2 = \phi_B \rho_B + \phi_L \rho_L + (1 - \phi_B - \phi_L) \rho_w \quad (2.6)$$

Here the subscripts B, W and L refer to the biopolymer, water and oil phases, respectively, and  $\phi$  is the volume fraction while  $\rho$  is the density. According to equation 5, sedimentation will increase as both particle size and density increases. On the other hand, creaming will tend to occur when high levels of lipid are incorporated into these particles as the density of the particles ( $\rho_2$ ) will be less than that of the continuous phase ( $\rho_1$ ). Depending on the concentration of each component, it may be possible to fabricate density matched filled hydrogel particles. The use of density matched particles for low viscosity products may be imperative to prevent particle sedimentation during shelf-life. Particle sedimentation would be less of a concern for highly viscous products such as desserts or sauces.

Mathematical models may also be useful in predicting the impact of other types of instabilities on the shelf-life of biopolymer particles. For example, the tendency for particle aggregation to occur can be predicted by calculating the relative strength of the

various attractive and repulsive colloidal interactions operating between them. These interactions include van der Waals, steric, electrostatic and hydrophobic forces (McClements, 2005). When attractive forces dominate, particles have a tendency to aggregate, but when repulsive forces dominate, particles resist aggregation. The tendency for swelling, shrinking, erosion or dissociation to occur is highly system specific and will depend on the type of bonds holding the biopolymer molecules together in the particles.

*Controlled Release:* The properties of filled hydrogel particles can be modified to control the release of a specific functional food component, such as a flavor, antimicrobial, antioxidant, or bioactive nutrient. Controlled release may be particularly important for delivery systems designed to release an active component at a particular site in the body. Four main mechanisms, which primarily differ in the role the carrier particle plays in controlling release, have been described:

*Diffusion:* In this mechanism, the active component simply diffuses into the surrounding medium through the biopolymer particle matrix, which remains intact. The main factors that influence diffusion rate are the permeability of the active component through the biopolymer matrix and the solubility of this component in the matrix (Gibbs & Kermasha, 1999; Madene, et al., 2006). For biopolymer networks, the diffusion rate may depend on the pore size of the biopolymer network compared to the size of the diffusing active component. Cross-linking of the biopolymer matrix may influence diffusion rates as a high degree of cross-linking has been shown to decrease release rates (Gibbs & Kermasha, 1999). Colloidal interactions such as electrostatic or hydrophobic attractions between the biopolymer network and the active component will also influence release rates.

*Erosion:* In the case of erosion, the active component is released by either degradation at the surface of the biopolymer matrix (heterogeneous erosion) or throughout the biopolymer matrix (homogeneous erosion) (Madene, et al., 2006; Pothakamury & Barbosa-Cánovas, 1995). Matrix erosion may be due to physical, chemical or enzymatic degradation processes, such as dissociation of physical bonds or the hydrolysis of chemical or enzymatic covalent bonds. Studies involving the disintegration of food in a gastric model system have shown that solvent absorption plays an important role in promoting surface erosion in solid foods (Kong & Singh, 2009). Since the most common form of release is activation by solvents (Gibbs & Kermasha, 1999), erosion is an important mechanism in controlling the release of active components from many food encapsulation systems.

*Fragmentation:* Fragmentation occurs when the active component is released as a result of fracture of the biopolymer matrix. Fragmentation occurs when the applied stress is greater than the critical stress (Kong & Singh, 2009). The bioactive will still diffuse out of the particles, but the rate of release will be much faster due to the increased surface area and decreased diffusion path.

*Swelling:* For systems where release is controlled by swelling, the active component is distributed inside an impermeable biopolymer matrix. When the particles in this system are exposed to solvent, the biopolymer matrix swells, and the active components can then diffuse out. Various solvents such as glycerin can be used to control swelling which ultimately controls active release (Gibbs & Kermasha, 1999; Madene, et al., 2006).

Mathematical theories have been developed to model different types of release mechanisms involving particulate systems (Pothakamury & Barbosa-Canovas 1995; Siepmann & Siepmann, 2008). To select an appropriate model of release, one must first know the origin of the release mechanism as either diffusion, erosion, swelling, or fragmentation. For many systems, more than one mechanism may be important for modeling active release. Once the mechanism of release is determined, a wide range of parameters such as the shape and size of biopolymer particles or the initial concentration of active component can be modeled in an effort to minimize experimental trials. Environmental conditions at the point of controlled release must also be considered.

#### **2.4.2 Modification Chemical Properties Using Filled Hydrogel Particles**

One of the primary reasons for fabricating filled hydrogel particles is to encapsulate and protect bioactive lipids. Among the various types of bioactive lipids, omega-3 fatty acids have been shown to be effective agents at reducing the risk of developing chronic diseases such as heart disease, arthritis, and some types of cancer (Ruxton, Reed, Simpson, Millington, & Ruxton, 2007; Riediger, Othman, Suh, & Moghadasian, 2009; Yashodhara, et al., 2009). Unfortunately because omega-3 fatty acids are highly unsaturated, lipids rich in these fatty acids are readily susceptible to oxidative deterioration and to the production of objectionable off-flavors such as metallic, fishy, and rancid aromas (Jacobsen, Let, Nielsen, & Meyer, 2008). Since food proteins are known to be effective natural antioxidants, incorporating omega-3 fatty acid enriched lipids into protein-rich hydrogel particles would be one strategy to enhance the stability of omega-3 rich lipids.

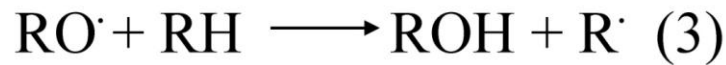
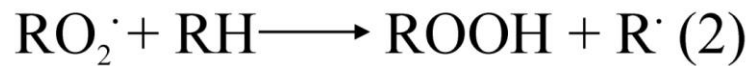
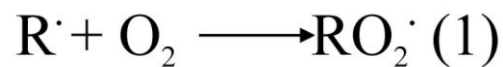
### 2.4.2.1 Lipid Oxidation

The process of lipid oxidation is of great concern to food scientists. As lipids present in foods react with oxygen-active species, there can be profound changes in the nutritional and sensory qualities of foods. In the case of edible oils, both autoxidation and photosensitized oxidation are responsible for oil degradation. In the case of autoxidation, ground state triplet oxygen ( $^3\text{O}_2$ ) reacts with lipid radicals to produce lipid hydroperoxides. Photosensitized oxidation, on the other hand, involves the direct interaction between singlet oxygen ( $^1\text{O}_2$ ) and the double bonds of unsaturated fatty acids to form lipid hydroperoxides. The lipid hydroperoxides formed from both of these reactions decompose into volatile low molecular compounds by a similar mechanism (Choe & Min, 2006).

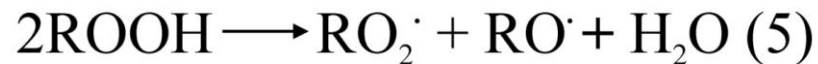
Autoxidation can be divided into four stages: initiation, propagation, branching, and termination. During the initiation stage, free radical species including peroxy ( $\text{RO}_2\cdot$ ), alkoxy ( $\text{RO}\cdot$ ), and alkyl ( $\text{R}\cdot$ ) are formed by a series of reactions believed to be catalyzed by light and transition metals. These radicals then react with unsaturated fatty acids or oxygen to form a number of reactive compounds including alkyl radicals and hydroperoxides during the propagation stage (Figure 2.7, equations 1-3). Lipid hydroperoxides are commonly referred to as the primary products of lipid oxidation. Although these compounds are associated with lipid oxidation, a process usually associated with undesirable off flavors, monohydroperoxides are odorless and tasteless (Belitz, et al., 2009a). The stage of lipid oxidation known as branching involves the homolytic cleavage of lipid hydroperoxides to form an alkoxy radical and an alkyl radical. Alkoxy radicals can then undergo homolytic  $\beta$ -scission which ultimately results

in the formation of the secondary products of lipid oxidation, namely low molecular weight aldehydes, ketones, alcohols, and hydrocarbons (McClements & Decker, 2000; Choe & Min, 2006). It is the volatile secondary products of lipid oxidation that are primarily responsible for off-flavor development in foods (Jacobsen, 1999).

### Propagation:



### Branching:



### Termination:



**Figure 2.7:** Mechanism of lipid autoxidation

Sensitizers are compounds in foods such as chlorophylls, pheophytins, and riboflavin that can convert to an excited state by absorbing light. The energy from the excited sensitizer is then used to generate either directly or indirectly lipid hydroperoxides. In the case of type I sensitizers, the excited sensitizer reacts directly with lipid substrates to generate alkyl radicals that then follow the autoxidation pathway (Figure 2.8). Alternatively, type II sensitizers react instead with triplet oxygen to form singlet oxygen. Because of its high energy state, singlet oxygen can react directly with the double bonds of unsaturated fatty acids and form lipid hydroperoxides (Choe & Min, 2006; Belitz, et al., 2009a).

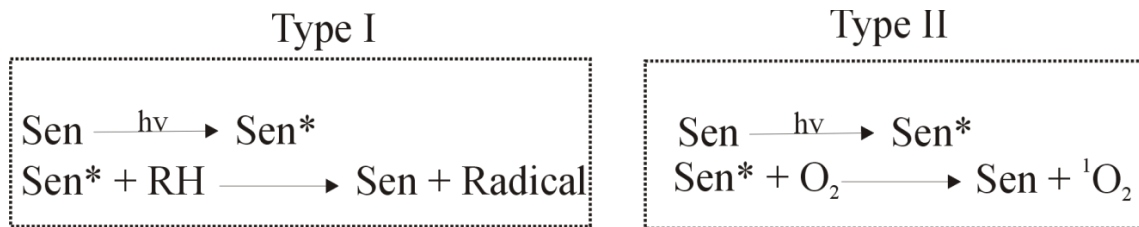


**Figure 2.8:** Mechanism of type I and type II sensitizers in photooxidation process

#### 2.4.2.2 Factors Influencing Oxidative Stability of Food

There are a wide range of factors that can either accelerate or retard lipid oxidation in foods. In terms of extrinsic factors, environmental conditions including temperature, light, and oxygen concentration play an important role in determining lipid oxidation rates. As a general rule, autoxidation of oil increases as the temperature increases. Furthermore, elevated temperatures tend to accelerate the decomposition of lipid hydroperoxides into various secondary products (Frankel., 1980). As for the influence of light on lipid oxidation, exposure to light in the presence of sensitizers such as chlorophyll can result in increased levels of singlet oxygen. These excited sensitizers

can also react directly on fatty acids to generate free radicals or to form superoxide anions from triplet oxygen (Decker, 1998). Depending on the concentration, oxygen levels may influence the rate of lipid oxidation. Above a certain concentration, oxygen levels do not impact lipid oxidation; however at low levels of oxygen, oxidation rates are highly dependent on oxygen levels (Coupland & McClements, 1996; McClements & Decker, 2000; Choe & Min, 2006).

In addition to environmental factors, oil composition as well as minor contaminants present in food oils can have profound effects on lipid oxidation. As the degree of unsaturation increases, the susceptibility of oil to oxidation also increases. This phenomenon can partially be attributed to the 1,4 pentadiene structure of unsaturated fatty acids and the subsequent reduced energy requirement for hydrogen abstraction from this chemical structure (Belitz, et al., 2009a). Other minor components in food oils that may either accelerate or inhibit lipid oxidation include free fatty acids, metals, phospholipids, carotenoids, chlorophyll, phenolic compounds, and tocopherols (Choe & Min, 2006; Chen, McClements, & Decker, 2011). Transition metals such as copper and iron are known accelerate lipid oxidation by reacting with lipid hydroperoxides (ROOH) to form highly reactive peroxy (ROO<sup>•</sup>) and alkoxy (RO<sup>•</sup>) radicals (McClements & Decker, 2000) as well as form other reactive species such as singlet oxygen and hydrogen peroxide (Choe & Min, 2006).

### **2.4.2.3 Antioxidants**

Antioxidants are substances in foods that are designed to inhibit or retard lipid oxidation in foods. Antioxidants prevent lipid oxidation by a number of different mechanisms including scavenging free radicals, chelating metals, quenching singlet

oxygen and photosensitizers, and inactivating lipoxygenase. Depending on their mechanism of action, antioxidants can be divided into two categories (Choe & Min, 2009). The first type known as primary antioxidants work by directly accepting free radicals to convert them into more stable products. Examples of this type of antioxidant include synthetic BHT and BHA as well as natural antioxidants such as tocopherols. Secondary antioxidants, on the other hand, are unable to react directly with free radicals and convert them into more stable compounds. Instead, these antioxidants inhibit oxidation indirectly by mechanisms such as chelating transition metals, regenerating antioxidants, and scavenging oxygen. Examples of secondary antioxidants include EDTA and citric acid (McClements & Decker, 2000).

There is a strong demand in the food industry to develop natural products that do not include synthetic antioxidants. Thus, the development and incorporation of natural antioxidants into foods has been a major area of research for the food industry. Major classes of natural food antioxidants include carotenoids, phenolic compounds, ascorbic acid, proteins and their derivatives, Maillard reaction products, phospholipids, and sterols (Choe & Min, 2009). Recent research has also shown that polysaccharides are capable of inhibiting oxidation in oil-in-water emulsions (Waraho, McClements, & Decker, 2011). Since filled hydrogel particles are fabricated from proteins and polysaccharides, it may be possible to take advantage of the natural antioxidant properties of these biopolymers to protect bioactive lipids. For example, research on the oxidation of lipids in food emulsions has shown that both interfacial proteins as well as protein in the continuous phase of an emulsion can enhance oxidative stability (Faraji, McClements, & Decker, 2004; Waraho, et al., 2011). Embedding emulsified lipid droplets inside a protein-rich

hydrogel particle would be one way to create a concentrated protein-rich environment for emulsified lipid that would in theory retard lipid oxidation.

### **2.4.3 Modification of Biological Response Using Filled Hydrogel Particles**

Targeted drug release is an important area of research for the pharmaceutical industry. In the case of oral medicines, substantial efforts have been made to formulate drugs that release in the mouth, stomach, small intestine, and especially the colon (Hao & Heng, 2003; Arora, Ali, Ahuja, Khar, & Baboota, 2005; Streubel, Siepmann, & Bodmeier, 2006; Van & Kinget 1995; Yang, Chu, & Fix, 2002). Many of the approaches for targeted drug release in the pharmaceutical industry can be applied to the food industry to develop functional foods and dietary supplements with superior properties such as enhanced release and absorption (McClements, et al., 2008).

#### **2.4.3.1 Lipid Digestion in Humans**

The overall process of lipid digestion in humans is shown below in Figure 2.9. The first step of digestion is ingestion and mastication of food. Inside the mouth, food is exposed to a high pH (6-7) and experiences high shear. Saliva composed of approximately 99% water along with small amounts of proteins, minerals, and enzymes mixes with the food during chewing. After mastication and swallowing, the partially digested food is now referred to as bolus. During swallowing, bolus moves from the mouth to the stomach by way of the esophagus (Wildman & Medeiros, 2000; McClements, et al., 2009a; Chen, 2009).

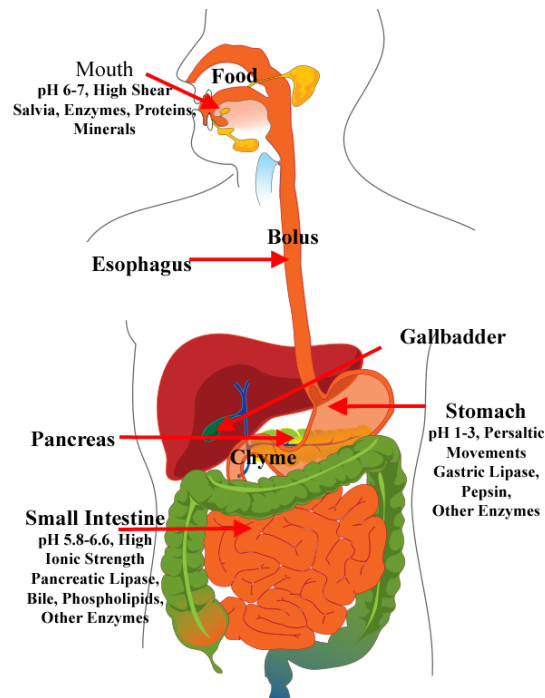


**Figure 2.9:** Schematic of the human digestion system

The environment of the stomach is highly acidic (pH 1-3), and there are a large number of enzymes present including gastric lipase and pepsin. Peristaltic movements in the stomach help to disperse lipids into droplets and move the bolus towards the small intestine. Fat soluble vitamins are typically located in the inner core of these lipid droplets. Gastric lipase present in stomach binds to the surface of lipid droplets and partially digests triacylglycerols (TAG) into diacylglycerols (DAG), monoacylglycerols (MAG), and free fatty acids (FFA). The activity of gastric lipase stops when 10-30% of the free fatty acids from TAG have been released (McClements, et al., 2008; McClements, et al., 2009a; Singh, Ye, & Horne, 2009).

Digested food from the stomach (now referred to as chyme) is transported into the duodenum of the small intestine. Sodium bicarbonate is secreted into the small intestine

to neutralize chyme to a pH of 5.8-6.6. The ionic strength of the small intestine is relatively high (~140 mM). This is due to the mixture of bile salts, pancreatic lipase/colipase, phospholipids, and other enzymes that are incorporated into chyme to aid in digestion and absorption. Pancreatic lipase along with the co-enzyme colipase bind to the surface of lipid droplets and digest TAG and DAG to MAG (sn-2 position) and FFA. At low concentrations, bile salts present in the small intestine act to remove sn-2 MAG and FFA from the surface of lipid droplets (McClements, et al., 2008; McClements, et al., 2009a; Singh, et al., 2009). Bile salts aid in the formation of micelles composed of mostly sn-2 MAG, FFA, and phospholipids. Both bile salt micelles and vesicles transport these products of digestion to the intestinal mucosa (Carey, Small, and Bliss, 1983).

#### **2.4.3.2 Controlling Lipid Digestion and Bioavailability**

Bioavailability refers to the portion or percentage of an ingested component that ends up in the systemic circulation. The bioavailability of lipids in foods depends on several factors including the accessibility of lipids to digestion, the transport of lipids across the intestinal mucosa, and the metabolism of lipids in the liver (McClements, et al., 2008; McClements, et al., 2009a). For example, the carrier solvent for a lipophilic compound can determine how this component is broken down in the body. Long chain fatty acids (FA) from TAG present in common food oils usually bypass metabolism by the liver and are instead repackaged into lipoproteins that are then transported by the intestinal lymph system to the circulatory system for systemic circulation. Unlike long chain FA, medium and short chain FA are transported to the liver by way of the portal vein for possible metabolism before systemic circulation (Porter, Trevaskis, & Charman, 2007; Dahan & Hoffman, 2008). Other factors that can influence bioavailability include

the size of lipid droplets with smaller droplets tending to be digested faster than larger droplets, the type of surfactants used to form lipid-based emulsion, and the physical form of the lipid (solid versus liquid). Ingredients in foods such as fiber may also affect lipid digestion (McClements, et al., 2009a; McClements & Li, 2010).

A number of different strategies can be used to control the digestion of emulsified lipids. Most of these approaches involve controlling the access of the enzyme lipase to TAGs and DAGs. According to McClements and Li (2010), there are five main strategies for altering lipid digestion, namely lipase inactivation, ingredient interactions, mass transport barriers, physical barriers, and accumulation of reaction products.

*Lipase Inactivation:* In this strategy, the active site of lipase is blocked by a specially designed ligand such as the active compound in a pharmaceutical.

*Ingredient Interactions:* This strategy involves nonspecific binding interactions that occur between different components of the digestion medium. These interactions can then retard lipid digestion by inactivating lipase or preventing the transport of digestion products. For example, pectin has been shown to bind bile salts under physiological conditions (Koseki, et al., 1987; Dongowski, 1997).

*Mass Transport Barriers:* In this approach, the rate of lipid digestion is dependent on the diffusion of lipase across a gel network such as lipids encapsulated inside hydrogel particles.

*Physical Barrier:* In this case, a physical barrier such as a coating is placed on the droplet surface to prevent lipase from binding. For example, research has shown that components including small molecule surfactants, phospholipids, and proteins can prevent lipase from coming in contact with the surface of emulsified oil droplets (Gargouri, Julien, Bois,

Verger, & Sarda, 1983; Ivanova, Panaiotov, Bois, Gargouri, & Verger, 1990; Wickham, Garrod, Leney, Wilson, & Fillery-Travis, 1998).

*Accumulation of Reaction Products:* The digestion of lipids by lipase can be reduced if the products of digestion (FFAs and MAGs) remain on the surface of lipid droplets as these products can prevent lipase from binding to the surface of lipid droplets. In a study conducted by Reis et al (2008), the addition of sn-2 monopalmitin to a model gastrointestinal system resulted in a reduction of lipid digestion. This reduction in lipid digestion was attributed to the ability of monopalmitin to deabsorb lipase and to exclude triglycerides (the substrate) from the water-oil droplet interface.

Among the strategies mentioned previously, barrier-based approaches would likely be the best way to design filled hydrogel particles with modified lipid digestion. In a recent study involving calcium alginate beads, in vitro digestion was substantially lowered for emulsified lipids encapsulated inside calcium alginate beads compared to the same amount of free emulsified lipids. Moreover, lipid digestion was not inhibited by the addition of calcium alginate beads not containing emulsified lipids to the system. The authors of this study attributed this reduction in lipid digestion to the diffusion of lipase through the gel network of the alginate beads. In this same study, the digestion of encapsulated lipids could be increased as the degree of cross-linking (i.e. the permeability of the mass transport barrier) for the calcium-alginate gel decreased (Li, Hu, Du, Xiao, & McClements, 2011).

## CHAPTER 3

### FABRICATION AND CHARACTERIZATION OF FILLED HYDROGEL PARTICLES BASED ON SEQUENTIAL SEGREGATIVE AND AGGREGATIVE BIOPOLYMER PHASE SEPARATION

#### 3.1 Abstract

In this work, filled hydrogel particles were created based on the ability of proteins and ionic polysaccharides to phase separate through both aggregative (complexation) and segregative (incompatibility) mechanisms. At pH 7, a mixture of 3% (w/w) high-methoxy pectin and 3% (w/w) sodium caseinate phase separated through a segregative mechanism. Following centrifugation, the phase separated system consisted of an upper pectin-rich phase and a lower casein-rich phase. Casein-coated lipid droplets added to the phase separated pectin/caseinate system partitioned into the lower casein-rich phase. This was attributed to a reduction in the unfavorable osmotic stress in this phase associated with biopolymer depletion. When shear was applied this system formed an oil-in-water-in-water ( $O/W_1/W_2$ ) emulsion consisting of oil droplets (O) contained within a casein-rich watery dispersed phase ( $W_1$ ) suspended in a pectin-rich watery continuous phase ( $W_2$ ). Acidification of the  $O/W_1/W_2$  system from pH 7 to 5 promoted adsorption of pectin around the casein-rich  $W_1$  droplets, resulting in the formation of filled hydrogel particles ( $d = 3$  to  $4 \mu\text{m}$ ) that remained stable to aggregation or dissociation when stored for 24 hours at ambient temperature. These particles may be useful as encapsulation and delivery systems for lipophilic components in the food, cosmetics and pharmaceutical industries.

### 3.2 Introduction

In recent years, the potential health benefits associated with regular consumption of certain lipophilic food constituents has been demonstrated, *e.g.*,  $\omega$ -3 fatty acids, carotenoids, fat-soluble vitamins, and phytosterols (Mozafari, et al., 2006; McClements, et al., 2007). Advances in lipid nutrition pose opportunities and challenges as consumer demand for functional foods containing these lipid-soluble constituents increase. Many of these components are chemically unstable and tend to degrade during storage when incorporated into foods (Chaiyasit, Elias, McClements, & Decker, 2007; Belitz, et al., 2009a). Most of these lipophilic components also have a low-water solubility, which means it is difficult to incorporate them directly into aqueous-based foods and beverages. There is therefore a growing need in the food industry to develop delivery systems to encapsulate, protect and release these beneficial lipophilic compounds.

Emulsion-based delivery systems are particularly suitable for incorporating lipophilic constituents into aqueous foods and beverages (McClements, et al., 2007). Unlike delivery systems based on microencapsulation, which are limited to solid food applications, emulsion-based delivery systems can easily be incorporated into liquid foods and beverages (Palzer, 2009). Most emulsion-based delivery systems currently used in the food industry are conventional oil-in-water emulsions (O/W) consisting of oil droplets dispersed within a watery continuous phase, *e.g.*, milk, cream, ice cream, sauces, dips, salad dressings, mayonnaise, and soft drinks. Nevertheless, a number of other kinds of structured emulsions can be fabricated from food-grade ingredients, including multilayer ( $O_M/W$ ), water-in-oil-in-water (W/O/W), water-in-water (W/W) and oil-in-water-in-water (O/W/W) emulsions (McClements, 2005; McClements, et al., 2007).

These structured emulsions may have advantages over conventional emulsions as delivery systems for certain applications within the food industry. In this study, we focused on the development of filled hydrogel particles based on the formation and stabilization of O/W/W emulsions.

Filled hydrogel particles can be assembled from mixed biopolymer systems that are capable of phase separating. When a ternary biopolymer system consisting of two biopolymers and a solvent are mixed together, there are three possible outcomes: miscibility, association or segregation (Sybbe, et al., 1998; de Kruif & Tuinier, 2001). Association tends to occur when there is a sufficiently strong attraction between biopolymer molecules, *e.g.*, an electrostatic attraction between oppositely charged biopolymers (Tolstoguzov, 2003). Biopolymer association leads to the formation of a two phase system consisting of one aqueous phase rich in both biopolymers, and another aqueous phase depleted in both biopolymers. Segregation tends to occur when there is a net repulsion between biopolymer molecules, which is usually the result of an entropy of mixing (excluded volume) effect (Grinberg & Tolstoguzov, 1997; de Kruif & Tuinier, 2001). Biopolymer segregation leads to the formation of a two phase system consisting of one aqueous phase rich in one of the biopolymers, and another aqueous phase rich in the other biopolymer. The type of phase behavior exhibited by a particular combination of biopolymer molecules depends on system composition (*e.g.*, biopolymer concentrations), biopolymer characteristics (*e.g.*, molecular weight, electrical charge, conformation) and solution conditions (*e.g.*, pH, ionic strength, temperature, applied mechanical forces).

It is possible to prepare W/W emulsions with different structures by carefully controlling these parameters to control the thermodynamics and kinetics of biopolymer phase separation (Norton & Frith, 2001). A number of studies have shown that W/W emulsions can be used to create lipid filled hydrogel particles (Malone & Appelqvist, 2003; Lian, Malone, Homan, & Norton, 2004; Kim, Decker, & McClements, 2006). In these systems, an O/W emulsion is mixed with a W/W emulsion under conditions where the oil droplets preferentially partition into the biopolymer phase that eventually forms the dispersed aqueous phase. The resulting system is an O/W/W emulsion consisting of oil droplets dispersed within a watery phase, which is itself dispersed within another watery phase.

In this study, we examined the possibility of using both segregative and associative phase separation of mixed biopolymer solutions to form filled hydrogel particles from O/W/W emulsions. Initially, a W/W emulsion is formed based on thermodynamic incompatibility of a mixed protein and anionic polysaccharide system under conditions where they are both negatively charged (pH 7). The nature of the dispersed phase in this type of system depends on the relative volume fractions of the two biopolymer-rich phases (Tolstoguzov, 2003). Typically, the biopolymer phase with the lower volume fraction tends to form the dispersed phase. In our study, we wanted the dispersed phase to be protein-rich since many proteins are known to have good antioxidant properties and may therefore be able to protect encapsulated lipids against chemical degradation. In addition, we wanted the lipid droplets to preferentially partition into the protein-rich dispersed phase, since this structural arrangement is required to form

O/W/W emulsions. We therefore aimed to establish the factors that influence the partitioning of lipid droplets between the dispersed and continuous phases.

O/W/W emulsions formed by segregative biopolymer phase separation are typically unstable because of the tendency for the dispersed aqueous phase to settle, ripen and coalesce, eventually resulting in complete phase separation (Norton & Frith, 2001). To halt this separation, one or both of the biopolymer phases can be gelled to create either a gel network (continuous phase gelation) or hydrogel particles (dispersed phase gelation) (Norton & Frith, 2001; Turgeon, Beaulieu, Schmitt, & Sanchez, 2003). Alternatively, it is possible to stabilize the dispersed biopolymer phase by altering the pH so that the proteins change from negative to positive, thereby promoting the formation of a layer of anionic polysaccharides around the protein-rich droplets (Rediguieri, de Freitas, Lettinga & Tuinier, 2007).

To achieve the above objective we used a protein-polysaccharide system that has previously been shown to form W/W emulsions at neutral pH due to a segregative phase separation mechanism: 3 wt% sodium caseinate and 3 wt% high methoxy pectin (Rediguieri et al., 2007). At pH 7, this system consists of anionic protein-rich watery droplets dispersed within an anionic polysaccharide-rich continuous phase. This system could be stabilized by acidifying the solution to pH 5 to promote adsorption of anionic polysaccharide molecules around the surfaces of the cationic protein-rich watery droplets through electrostatic attraction (Rediguieri et al., 2007). In our study, we incorporated casein-stabilized lipid droplets into this phase separated system in order to form filled hydrogel particles that consisted of lipid droplets trapped within casein-rich watery droplets.

These filled hydrogel particles could be used as delivery systems to encapsulate, protect and release lipophilic bioactive components. The lipophilic constituents would be dissolved in the oil phase prior to formation of the initial oil-in-water emulsion. This type of delivery system may have several advantages over conventional emulsions, including protection against oxidation and targeted release inside the human body (McClements, et al., 2007).

### **3.3 Materials**

Commercial sodium caseinate was kindly donated by American Casein Company (Burlington, NJ) and was used without further purification. The percentage of protein and moisture for this material were 91.4% and 5.0% respectively as provided by the manufacturer. A commercial high methoxy pectin (Genu Pectin (Citrus), USP/100) was kindly donated by CP Kelco (Lille Skensved, Denmark) and was used without further purification. The composition of this material as provided by the manufacturer was 8.2% moisture, 89.3% galacturonic acid and 8.9% methoxy groups, which corresponds to a degree of esterification (DE) of approximately 62%. Glucono-delta-Lactone (F5010) was kindly donated from Jungbunzlauer (Newton, MA). Mazola corn oil (ACH Food Companies, Memphis, TN) was purchased at a local supermarket and used as received.

For confocal microscopy work, technical grade Nile red dye (CAS #7385-67-3) was purchased from Sigma-Aldrich (St. Louis, MO). A commercial protein labeling kit for Alexa Fluor 488 and the non-polar dye Bodipy 493/503 were purchased from Invitrogen (Carlsbad, CA). The protein dye Rhodamine B (CAS #81-88-9) was

purchased from Sigma-Aldrich (St. Louis, MO). All other chemicals used in this research were purchased from Sigma-Aldrich (St Louis, MO). Double distilled water was used to make all solutions.

### **3.4 Methods**

This study was divided into four sets of experiments. Firstly, the physicochemical properties of the two biopolymer phases formed after segregative phase separation at pH 7 were characterized to determine their volume fractions, compositions, densities, refractive indices and rheological properties. Secondly, the partitioning of the lipid droplets between these two different biopolymer phases was determined, and the influence of depletion interactions on partitioning was examined. Thirdly, W/W emulsions were formed by blending protein and anionic polysaccharide mixtures at pH 7 to form protein-rich particles followed by acidification to pH 5 to form a polysaccharide coating around the protein-rich particles, and the properties of these W/W emulsions were characterized. Fourthly, O/W/W emulsions were formed by blending lipid droplets, proteins and anionic polysaccharide mixtures at pH 7 followed by acidification to pH 5 to form polysaccharide-coated protein-rich filled hydrogel particles.

#### **3.4.1 Solution Preparation**

Sodium caseinate stock solutions (6% and 12% w/w, dry weight basis) and pectin stock solutions (6% w/w, dry weight basis) were prepared in buffer solutions containing an antimicrobial to prevent microbial growth (0.04% sodium azide, 10 mM phosphate buffer, pH 7). Stock solutions were mixed for 30 min using a mechanical stirrer (speed 7, Stedfast Stirrer Model SL 1200, Thermo Fisher Scientific, Waltham, MA). Initially, the

sodium caseinate stock solution had a pH of ~6.8 and the pectin stock solution had a pH of ~3.8. Both solutions were then adjusted to pH 7.0 by adding 4 M sodium hydroxide. The stock solutions were then centrifuged for 2 hours at 10,000 g to sediment and remove any insoluble matter.

### **3.4.2 Emulsion Preparation**

Caseinate stabilized oil-in-water emulsions (10% oil w/w) were formed from corn oil, sodium caseinate, and buffer solution (0.04% sodium azide, 10 mM phosphate buffer, pH 7). A coarse emulsion was formed first by blending this mixture at medium speed for 2 minutes with a high speed blender (Tissue Tearor Model 985370-395, Biospec Products Inc., Bartlesville, OK). The coarse emulsion was then homogenized with a high pressure homogenizer (Microfluidizer Model 110 L, Microfluidics, Newton, MA) for 3 passes at a chamber pressure of 11,000 psi. Emulsions formed by this method had an average volume-weighted mean diameter ( $D_{4,3}$ ) of 0.37  $\mu\text{m}$  and an average surface-weighted mean diameter ( $D_{3,2}$ ) of 0.32  $\mu\text{m}$  as measured by static light scattering (Mastersizer 2000, Malvern, Worcestershire, UK).

### **3.4.3 Formation and Characterization of Phase Separated Biopolymer Mixtures**

Equal weights of 6% w/w sodium caseinate and 6% w/w pectin stock solutions were mixed together, the pH was checked and adjusted to pH 7 if necessary with 4 M sodium hydroxide, and the mixture was then stirred for 30 min (Stedfast Stirrer Model SL 1200, Thermo Fisher Scientific, Waltham, MA) at speed 7. Following stirring, 25 grams of this mixture was transferred into 8-50 ml centrifuge tubes (Nalgene Oak Ridge High Speed Polypropylene Copolymer Conical Centrifuge Tubes, Thermo Fisher Scientific,

Rochester, NY) and centrifuged at 10,000 g for 2 hours at 20°C. Longer centrifugation times did not change the height of the phase separated layers, indicating that 2 hours of centrifugation was sufficient for complete phase separation. After removal from the centrifuge the centrifuged samples were allowed to settle until distinct upper and lower phases were visible. The heights of each phase phases were measured for each tube using a metric ruler. To determine the volume fraction of each phase, a calibration curve using water was created to relate the height of each phase to its corresponding volume. In a separate experiment, a protein dye (Rhodamine B) was used to identify the two phases of this system following centrifugation. The dye was dissolved in double distilled water at a concentration of 0.05% w/v. This solution was then added to a mixture of 3% w/w pectin /3% w/w caseinate at a concentration of 5µl/gram of mixture, and the mixture was mixed, centrifuged and photographed.

After volume measurements were taken, the upper and lower phases were carefully separated. The density of each phase and the density of corn oil were measured using an oscillating glass U-tube densitometer at 20°C (Mettler Toledo, Columbus, OH). The refractive indices of the upper and lower phases were determined using a bench top refractometer (Bausch & Lomb, Cat. No. 33.46.10, Rochester, NY). The concentration of protein in the upper and lower phases was determined by the Bradford protein assay (Bradford, 1976) A standard curve of absorbance *versus* concentration of sodium caseinate was constructed to determine the protein concentration of the two phases. The concentration of carbohydrate in the upper and lower phases was determined using the phenol-sulfuric acid method (Dubois, Gilles, Hamilton, Rebers, & Smith, 1956). A

standard curve of absorbance *versus* concentration of pectin was constructed to determine the carbohydrate concentration of the two phases.

Rheological measurements of the upper and lower phases, as well as of a blended mixture of 83% (by volume) upper phase and 17% lower phase, were carried out using a dynamic shear rheometer (Kinexus, Malvern, Worcestershire, UK) at 25°C. A cup and bob geometry consisting of a bob with a diameter of 25 mm and a cup with a diameter of 27.5 mm was used to create an equilibrium flow curve for shear rates from 0.1 s<sup>-1</sup> to 100 s<sup>-1</sup>. To account for thixotropic behavior, samples were sheared at each rate until steady state was achieved.

#### **3.4.4 Characterization of Lipid Droplet Partitioning in Phase Separated Biopolymer Mixtures**

The location of the lipid droplets within phase separated biopolymer mixtures was determined using laser vertical profiling and confocal fluorescence microscopy. An estimate of the relative magnitude of the depletion interactions in the system were determined from creaming stability measurements.

#### **3.4.5 Laser Vertical Profiling**

A series of samples were prepared with different concentrations of lipid droplets (0.1%, 1%, 2.5% and 5% (w/w)), but the same biopolymer composition (3% caseinate/3% pectin) by mixing different ratios of stock emulsion, stock pectin solution, stock caseinate solution and buffer solution (10 mM phosphate buffer, pH 7). Six grams of each mixture were transferred to flat bottomed glass test tubes (15 mm × 140 mm). Triplicate samples were made for each oil concentration. Samples were periodically

scanned during storage at room temperature using a laser vertical profiling system (Turbiscan Classic MA 2000, Formulacion, Wynnewood PA).

### **3.4.6 Confocal Fluorescence Microscopy**

In order to visualize the location of the oil in this system by confocal microscopy, the oil phase was dyed with 0.1 mg of Nile red per ml of oil. The mixture was covered with aluminum foil to prevent photobleaching and allowed to stir overnight to completely dissolve the dye into the oil. In addition to dyeing the oil phase, the fluorescent dye Alexa Fluor 488 (Invitrogen, Carlsbad, CA) was used to visualize the protein in this system. The procedures for forming a conjugate between casein and Alexa Fluor 488 were followed as described in the manufacturer's instructions. Emulsion (10% corn oil, 1% caseinate w/w), pectin stock solution, caseinate stock solution and buffer were mixed together to form a mixed system that consisted of: 1 % corn oil, 3% caseinate and 3% pectin (0.04 % sodium azide, 10 mM phosphate buffer, pH 7). This mixture was gently stirred with a glass stirring rod to form a homogenous mixture without forming air bubbles. After stirring, a small amount of this mixture was transferred to a glass microscope slide and covered with a glass cover slip (Number #1). The cover slip was fixed to the slide using nail polish. A small amount of Type A immersion oil (Nikon, Melville, NY) was placed on top of the cover slip, and the specimen was viewed with a microscope (Nikon D-Eclipse C1 80i, Nikon, Melville, NY) using an oil immersion objective lens (60 $\times$ , 1.40 NA). After the image was focused, an air cooled argon ion laser Model IMA1010 BOS (Melles Griot, Carlsbad, CA) was used to excite the specimen at 488 nm. Emission spectra for Alexa Fluor 488 were detected in the 515 nm channel equipped with a narrow pass filter (HQ 515/30m); emission spectra for Nile red were

detected in the 605 nm channel equipped with a long pass (LP) filter (HQ 605LP/75m). The pinhole size was set at 61.5  $\mu\text{m}$ . To minimize cross talk between detector channels, gain settings were manipulated such that these settings showed little to no cross talk in samples labeled individually with either Nile red or Alexa Fluor 488. All images were taken and processed using the instruments software program (EZ- CS1 version 3.8, Nikon, Melville, NY).

### **3.4.7 Quantification of Depletion Interactions in Phase Separated Systems**

To better understand the forces driving the partitioning of oil droplets in the phase separated biopolymer systems, the CFC (critical flocculation concentration) of the lipid droplets in both the upper and lower phases were determined. Sufficient quantities of upper and lower phases were obtained by centrifugation and careful separation as described previously. A 10% (w/w) corn oil, 1% (w/w) caseinate stabilized emulsion was also prepared as described previously. A series of samples were then prepared that contained a constant weight (1%, w/w) of emulsified oil but increasing amounts of either the upper phase or the lower phase. Buffer solution (10 mM phosphate, pH 7) was used to adjust the concentration of upper and lower phases added to these samples. The samples were poured into flat bottom test tubes (15 mm  $\times$  140 mm), and then carefully mixed to ensure they were homogeneous without introducing air bubbles.

Samples were stored at room temperature and were periodically measured by laser vertical scanning to monitor changes in droplet location (Turbiscan Classic MA 2000, Formulacion, Wynnewood PA). Initial experiments confirmed that 1 day was sufficient to distinguish samples where depletion flocculation occurred (high levels of biopolymer) from those that were stable to depletion flocculation (low levels of

biopolymer). Transmission (T%) and back-scattering (B%) profiles as a function of sample height were collected and analyzed using the instruments software program (Turbisoft version 1.21). Changes due to creaming were determined by subtracting the profiles measured after 1 day storage from those measured after 0 hours ( $\Delta B\%(h) = B\%(h, 1 \text{ day}) - B\%(h, 0 \text{ day})$ ). The CFC was defined as the lowest concentration of either biopolymer phase that resulted in the formation of a creamed layer after one day storage. The formation of a creamed layer was defined as an increase of greater than 20% in the back scattering signal at the top of the test tube relative to the initial value (Fig. 3.1). To quantify differences in degree of creaming among samples, the area under the creaming curve was calculated by integration. Digital photographs were also taken of all samples both before and after storage. Selected samples were also studied using confocal microscopy as described above with slight modifications: the pin hole was set to 33.3  $\mu\text{m}$ , and only the 488 nm laser and the 605 nm detector channel was used to excite and detect Nile red. All images were magnified by a factor of 2 $\times$  using the digital zoom feature.

### **3.4.8 Formation, Characterization, and Stability of Hydrogel Particles**

Equal weights of 6% (w/w) pectin and 6% (w/w) caseinate stock solutions were mixed together (300 rpm, Stedfast Stirrer Model SL 1200, Thermo Fisher Scientific, Waltham, MA). The pH of this mixture was adjusted to 7 using 4 M sodium hydroxide. While maintaining the stirring speed at 7, this mixture was acidified to pH 5 with 1 M citric acid at a rate of 1 drop of acid per 10 seconds. After the mixture reached pH 5, the newly formed particles were transferred to glass storage bottles at room temperature for

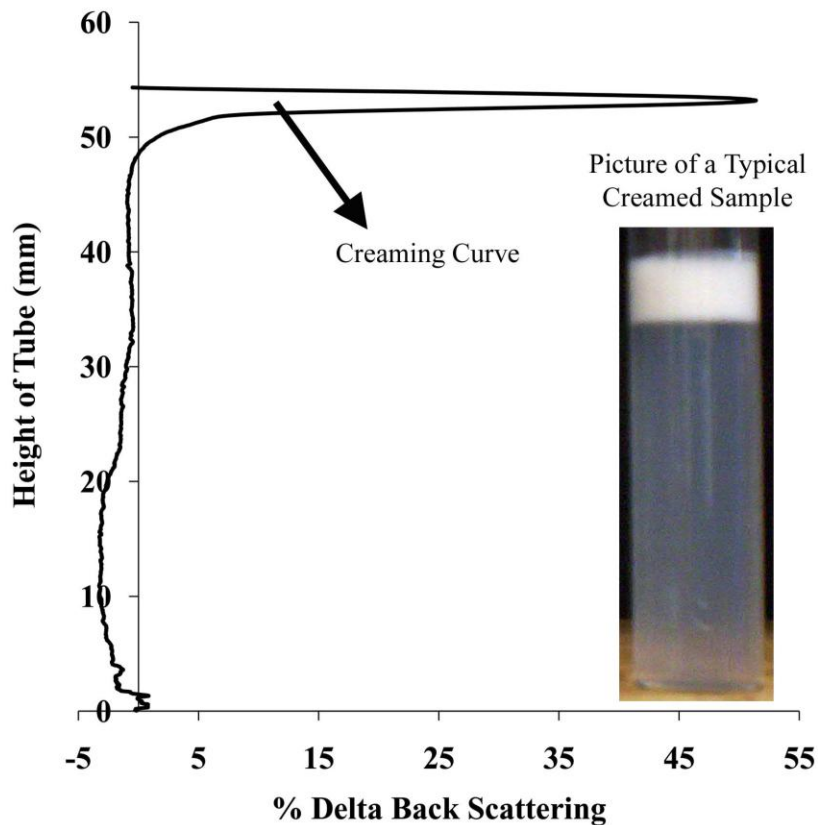


**Figure 3.1:** Example of a typical laser vertical profile for a creamed sample

stability testing. The mean particle size and  $\zeta$ -potential of the samples were analyzed after 0, 1, 3, 5, 7, 14, 21, and 29 days of storage at ambient temperature.

Mean particle size was measured using static light scattering (Mastersizer 2000 Mastersizer 2000 with a small volume sample dispersion unit (Hydro 2000 SM) (Malvern, Worcestershire, UK) with a small volume sample dispersion unit (Malvern, Worcestershire, UK), and the Fraunhofer approximation was used for the dispersed phase (hydrogel). 10 mM phosphate buffer adjusted to pH 5 was used to dilute the W/W emulsions for particle size analysis. The samples were stirred at 1250 rpm throughout

particle size measurements. The parameter  $D_{3,2}$  was used to compare the average particle size of the measured samples.  $D_{3,2}$  is commonly referred to as the average-volume mean diameter. This parameter is calculated as follows:

$$D_{3,2} = \frac{\sum_{i=1} n_i d_i^3}{\sum_{i=1} n_i d_i^2} \quad (3.1)$$

where  $n_i$  is the number of particles in each size class per unit volume of emulsion and  $d_i$  is the diameter of the particles in each size class (McClements, 2005). The stability of these particles to dilution was also examined. For this set of experiments, the pectin/caseinate particles were diluted and dispersed in the measurement chamber of the light scattering instrument as described previously. Particle size measurements were taken at 20 minute intervals from 0 to 2 hours.

Particle charge measurements were made using a particle electrophoresis instrument (Malvern Nano ZS, Model ZEN 3500 with a folded capillary cell). For this measurement, 1.357 was used as the refractive index of the dispersed phase, and 1.330 was used as the refractive index of the continuous phase. The viscosity and relative dielectric constant of the continuous phase were 1.0120 mPa s and 80.4 respectively. Two consecutive 1:10 dilutions in buffer (pH 5) were used to dilute the sample prior to analysis (total dilution = 1:100). The formation of biopolymer particles during acidification was examined under controlled shear conditions using a dynamic shear rheometer (Kinexus rheometer, Malvern, Worcestershire, UK). A cup and bob geometry consisting of a bob with a diameter of 25 mm and a cup with a diameter of 27.5 mm were

used for all of these experiments. Glucono-delta-lactone (GDL) was used to slowly acidify the biopolymer mixtures from pH 7 to 5 at 25 °C while subsequently monitoring sample viscosity. GDL was stirred into a solution containing 3% pectin / 3% caseinate (pH 7) at a ratio of 0.36 GDL:1 caseinate (Braga, Menossi, & Cunha, 2006). This ratio of GDL to caseinate resulted in a consistent decline from pH 7 to pH 5 within 140 minutes. To further solubilize GDL, this mixture was blended with a high speed blender for 30 seconds before an aliquot (approximately 20 ml) of the mixture was added to the rheometer while the remaining mixture was used to monitor changes in pH using a pH meter. Two different shear rates were examined, a “low” shear rate of  $1 \text{ s}^{-1}$  and a “high” shear rate of  $100 \text{ s}^{-1}$ . A sampling rate of one measurement per minute was used to construct a viscosity *versus* time curve during acidification. There was a delay of approximately 2 minutes between when GDL was added to the sample and when rheological measurements were started.

In addition to the phase separated mixture, the upper and lower phases of this system were examined individually for changes in viscosity *versus* time during slow acidification. The same ratio of 0.36 GDL:1 caseinate was used to acidify these phases; caseinate concentrations were calculated based on results from protein determination experiments. The same procedure as described above was used to prepare and test these samples; however these phases were only tested at a shear rate of  $1 \text{ s}^{-1}$  due to the difficulty in obtaining large quantities of the lower phase for testing. In the case of the individual upper and lower phases, the time to achieve pH 5 was approximately 70 minutes and 25 minutes for the upper and lower phases, respectively.

Since pH measurements were not recorded as frequently as rheological measurements (20 minute intervals versus one minute intervals), a graph of pH *versus* time was constructed for each sample, and a polynomial trend line fitted to this data was used to calculate sample pH for each corresponding rheological measurement.

### **3.4.9 Formation, Characterization and Stability of Filled Hydrogel Particles**

Large hydrogel particles containing lipid droplets were formed under mild shear conditions so that they could be viewed by confocal microscopy. In this set of experiments, the lipid droplets were dyed with Bodipy 493 while the protein phase was dyed with rhodamine B. Bodipy 493 dye (0.1 mg/mL) was added to corn oil, and this mixture was covered and stirred overnight to ensure the dye was completely solubilized in the oil. A 10% (w/w) corn oil, 1% caseinate stabilized emulsion was prepared with Bodipy dyed oil using the same procedure described previously. A mixture of Bodipy dyed emulsion and 12% (w/w) caseinate stock was weighed out such that the mixture consisted of 2% oil and 6% caseinate. This mixture was stirred with a magnetic stir bar for 30 min. Next, 6% pectin (w/w) stock was added to this beaker such that the final concentration by weight was 1% corn oil, 3% pectin, and 3% caseinate. The mixture was adjusted from approximately pH 6.8 to pH 7 using 4 N sodium hydroxide. A magnetic stir bar was used to stir the mixture as it was slowly acidified (1 drop of 1M citric acid per 10 seconds) to pH 5. Samples of these biopolymer particles were fixed and then scanned as described previously with the following modifications. Bodipy 493 was excited with the 488 nm laser and detected in the 515 channel (HQ 515/30m). Rhodamine B was excited with a 543 nm Melles Griot helium-neon laser Model 05-LGP-193 (Melles Griot, Carlsbad, CA) and detected in the 605 nm channel (HQ 605LP/75m).

The pinhole setting was small (33.3  $\mu\text{m}$ ), and the image was magnified by a factor of 4 $\times$  using the digital zoom feature.

### 3.5. Results & Discussion

#### 3.5.1 Formation and Characterization of Phase Separated Biopolymer Mixtures

The purpose of this set of experiments was to characterize the composition and physicochemical properties of the upper and lower phases formed after segregative phase separation of 3% pectin/3% caseinate mixtures (pH 7). The separation of the two phases was enhanced using centrifugation. The protein concentration, carbohydrate concentration, refractive index, density, and phase volume of the upper and lower phases are summarized in Table 3.1.

**Table 3.1:** Physical and Chemical Properties of Phase Separated Layers of 3% Pectin/3% Caseinate at pH 7

Physical/ Chemical Property	Upper Phase (After Separation by Centrifugation)	Lower Phase (After Separation by Centrifugation)
Density (@ 20°C)	1.0195 +/- 0.0004 g/cm <sup>3</sup>	1.0389 +/- 0.0004 g/cm <sup>3</sup>
Phase Volume	83% (CV 1%)	17% (CV 3%)
Protein Concentration	18.4 +/- 0.5 mg/ml	206.3 +/- 7.5 mg/ml
Carbohydrate Concentration	52.9 +/- 0.5 mg/ml	4.5 +/- 0.3 mg/ml
Refractive Index	1.341	1.358

The volume of the upper phase of the biopolymer mixture following centrifugation was significantly larger (83%) than the lower phase (17%). Chemical analysis of the two phases revealed that the upper phase was richer in carbohydrate ( $52.9 \pm 0.5$  mg/mL) than the lower phase ( $4.5 \pm 0.3$  mg/mL), while the lower phase was richer in protein ( $206.3 \pm 7.5$  mg/mL) than the upper phase ( $18.4 \pm 0.1$  mg/mL). The formation of two phases rich in different biopolymers is clear evidence of segregative phase separation. A digital photograph of the phase separated system after centrifugation provides additional evidence of the relative location of the biopolymers in the phase separated system (Figure 3.2). A red protein dye (Rhodamine B) incorporated into the mixed biopolymer system clearly showed that there was a higher protein concentration (casein) in the lower phase than in the upper phase. These results are in good agreement with those of others who examined a similar phase separated system (Rediguieri, et al., 2007). As expected, the density of the upper phase was less ( $1.0194$  g/cm<sup>3</sup>) than the lower phase ( $1.0403$  g/cm<sup>3</sup>), and both biopolymer phases were more dense than corn oil ( $0.9198$  g/cm<sup>3</sup>).

The kinetics of phase separation depends on the rheological properties of the biopolymer phases, and hence we determined the apparent viscosities of the upper and lower phases (Figure 3.3). We also measured the apparent viscosity of a blended mixture of 83% upper phase and 17% lower phase (by volume). The upper and lower biopolymer phases both demonstrated slight shear thinning, especially at shear rates exceeding  $1$  s<sup>-1</sup>.

The apparent viscosity of the lower phase was higher than that of the upper phase at all ( $> 20\%$  w/w) leads to the high viscosity of this phase. The mixed system, containing 83% upper phase and 17% lower phase, behaved differently at lower and

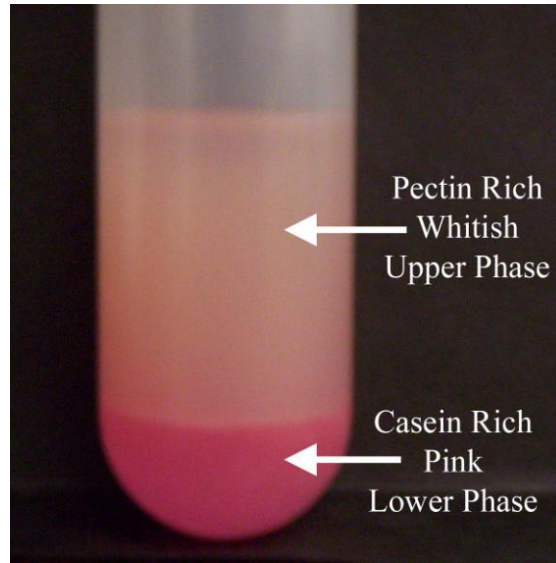


**Figure 3.2:** Picture of phase separated 3% pectin/3% caseinate system at pH 7 with casein-rich phase shown dyed in pink with Rhodamine B

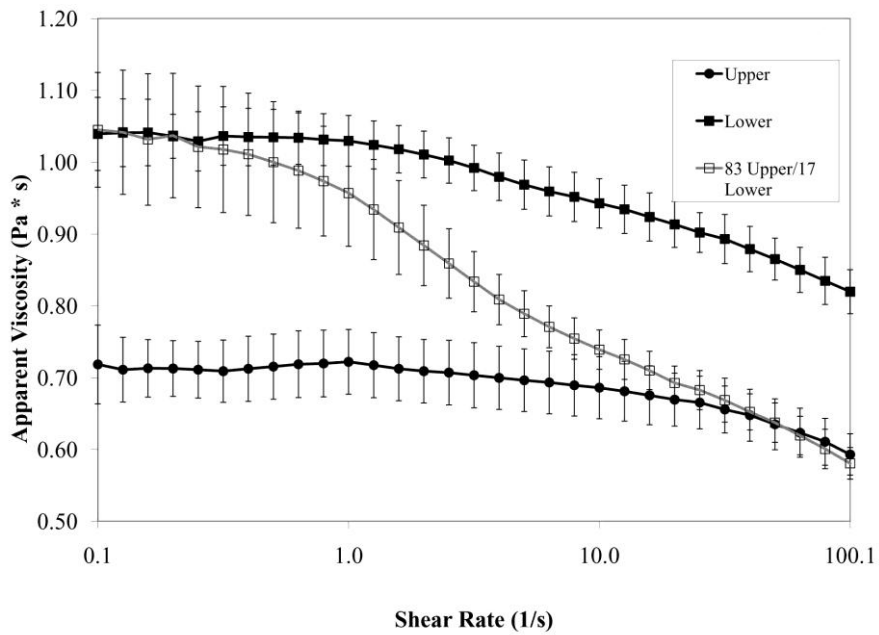


**Figure 3.3:** Apparent viscosity versus shear rate for upper, lower, and 83% upper/17% lower phase at 25°C

higher shear rates (Figure 3.3). At relatively low shear rates (0.1 to 1.0 s<sup>-1</sup>), the viscosity behavior was similar to that of the lower phase, while at higher shear rates (10.0 to 100.1 s<sup>-1</sup>) it was similar to the upper phase. This result suggests that the mixed system may have undergone a phase inversion or some other structural rearrangement during shearing. The overall viscosity of a colloidal dispersion is determined by the viscosity of the continuous phase, as well as the effective particle concentration (McClements, 2005; Genovese, et al., 2007). At low shear rates, our microscopy studies indicated that the continuous phase was the pectin-rich phase (see later). Hence, the fact that the apparent viscosity of the mixed system was considerably higher than that of the pectin-rich upper phase, suggests that the hydrogel particles ( $\phi = 17\%$ ) made a strong contribution to the overall viscosity. When the shear rate was increased it is likely that the hydrogel particles became deformed and disrupted, which would account for the observed steep decrease in apparent viscosity of the mixed system (Figure. 3.3).

Previous studies have shown that the rheological properties of phase-separated biopolymer mixtures (gelatin and dextran) behave differently when exposed to increasing shear rates (Van Puyvelde, Antonov & Moldenaers, 2003). At low shear rates, either droplet coalescence or breakup dominated the structure of the phase separated system, while above a critical shear rate a steady state condition is reached between droplet breakup and droplet coalescence, resulting in a unique consistent structure. This observation supports our findings that at lower shear rates the presence of the dispersed phase droplets dominate the overall rheological properties of our system, but at higher shear rates droplet breakup increases and the rheological properties of the continuous pectin-rich dominate (Van Puyvelde, et al., 2003).

### 3.5.2 Characterization of Lipid Droplet Partitioning in Phase Separated Systems

This set of experiments addressed the preference of lipid droplets for either the upper pectin-rich phase or the lower caseinate-rich phase. A series of 3% pectin/3% caseinate mixtures were prepared containing different levels of casein-coated lipid droplets (0.1 to 5 w/w% corn oil). Initially, all of the mixed systems were optically opaque and homogenous in appearance, but their appearance changed during storage due to structural rearrangements within the system. The change in appearance was characterized by taking digital photographs and by laser vertical profiling of changes in the back scattering along the height of the tubes. In our experiments involving laser vertical profiling, a change in the back scatter profile of a sample over the course of storage indicates the migration of emulsified oil droplets as these oil droplets are strong scatters of light.

After 3 weeks storage at ambient temperature, the vertical profiles of the samples containing 1% (w/w) oil showed an increase in the % backscatter towards the lower end of the tube and a decrease in the % backscatter towards the upper end of the tube. This trend continued throughout the remaining 3 weeks of storage (Figure 3.4). By the sixth week of storage, two distinct phases, an upper semi-transparent layer and a lower opaque layer, were clearly visible. A similar trend was observed for the mixture containing 0.1% (w/w) oil (not shown) although the increase in % backscatter was, as expected, less than for 1% oil. These observations show that the emulsified oil droplets preferentially migrate to the lower, caseinate-rich phase of this system.

Tolstoguzov (2003) also found that the addition of lipid droplets to a thermodynamically incompatible protein/polysaccharide mixed system resulted in the

migration of lipid droplets to the lower protein-rich phase. In addition, previous experiments in our laboratory using phase separated systems containing whey protein-coated lipid droplets, heat-denatured whey protein and pectin showed that the oil droplets partitioned into the protein-rich phase (Kim, et al., 2006).

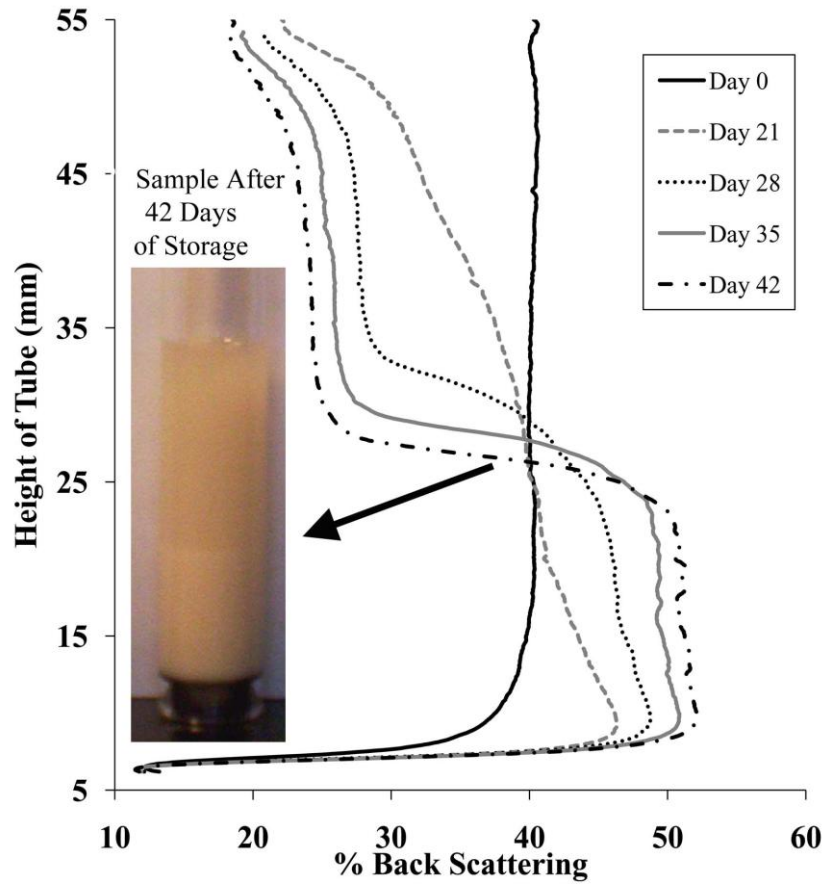


**Figure 3.4:** Percent back scattering versus height of test tube (mm) following storage at room temperature for 1% oil in 3% pectin/3% caseinate mixtures at pH 7

Lipid droplets have a lower density than either the upper or lower biopolymer phases (Table 3.1), and therefore one would have expected them to move upwards rather than downwards. There must therefore be another driving force that favors the partitioning of

the lipid droplets into the lower caesinate-rich phase, rather than the upper pectin-rich phase. We postulate that this driving force for droplet partitioning is a depletion interaction, associated with differences in the exclusion of biopolymers from the immediate vicinity of lipid droplet surfaces (Dickinson, 2003). Since pectin is a much larger molecule than casein, the excluded volume surrounding a droplet in the upper pectin-rich phase would be much greater compared to that in the lower casein-rich phase. This difference in excluded volume may explain the partitioning of lipid droplets in this phase separated biopolymer mixture (see below for further discussion of depletion forces). An analysis of the major factors (entropy of mixing, gravity, depletion) affecting the partitioning of lipid droplets in phase separated biopolymer mixtures is given in Appendix. Predictions of the relative magnitude of these three factors demonstrate that the depletion force (favoring accumulation of the droplets in the lower casein-rich phase) is much stronger than either the entropy of mixing (favoring random distribution of the droplets through the system) or gravitational (favoring accumulation of the droplets in the upper pectin-rich phase) contributions (Appendix).

Interestingly, we did not observe a clear phase separation of the mixed biopolymer systems containing higher droplet concentrations (2.5 w/w% oil and 5 w/w% oil) after 3 weeks storage. This may have been because at higher droplet concentrations a network structure of flocculated droplets was formed, which inhibited their migration into the lower phase. Alternatively, the flocs formed may have been too large to move easily through the biopolymer network.

The location of the lipid droplets in the water-in-water emulsions was visualized more directly using confocal microscopy. The relative locations of the protein (Alexa

Fluor 488) and oil phase (Nile Red) were determined using fluorescent dyes. The lipid droplets (shown in red) are clearly located inside large caseinate-rich droplets (shown in green) (Figure 3.5). These images confirm that the lipid droplets partition into the caseinate-rich phase rather than the pectin-rich phase. Furthermore, they confirm that the lower caseinate-rich phase is the dispersed phase while the upper pectin-rich phase is the continuous phase of the water-in-water emulsion. The relatively large size of the droplets

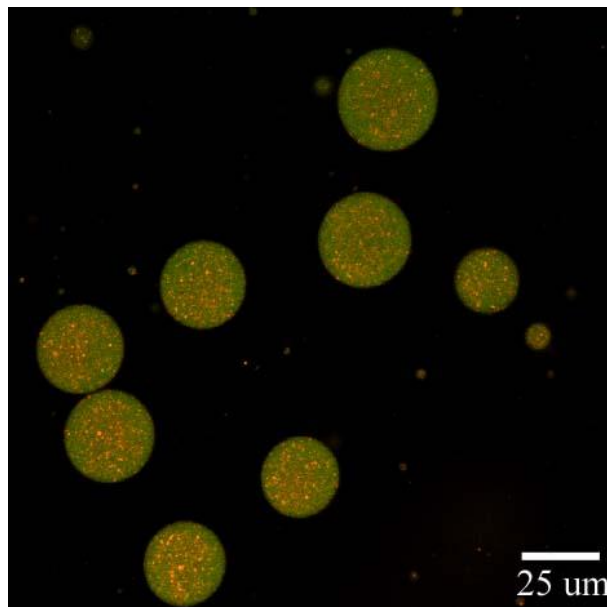


**Figure 3.5:** Confocal image of 3% pectin/3% caseinate mixture with 1% (wt.) emulsified corn oil at pH 7, oil is shown in red and caseinate is shown in green

in these images ( $d > 15 \mu\text{m}$ ) is due to the mild shearing conditions applied to the biopolymer mixture prior to being observed under the microscope.

As mentioned above, we postulate that the major driving force for migration of the lipid droplets into the caseinate-rich phase rather than the pectin-rich phase is differences between the depletion interactions in the two biopolymer phases. We

hypothesize that the unfavorable depletion interaction (due to the osmotic pressure gradient generated by biopolymer exclusion from the droplet surfaces) is greater in the pectin-rich phase than in the caseinate-rich phase, thereby favoring movement of the droplets into the caseinate-rich phase. To obtain some indication of the difference in strength of the depletion interactions in the two biopolymer phases (Figure 3.6), we carried out a series of experiments to calculate the critical flocculation concentration

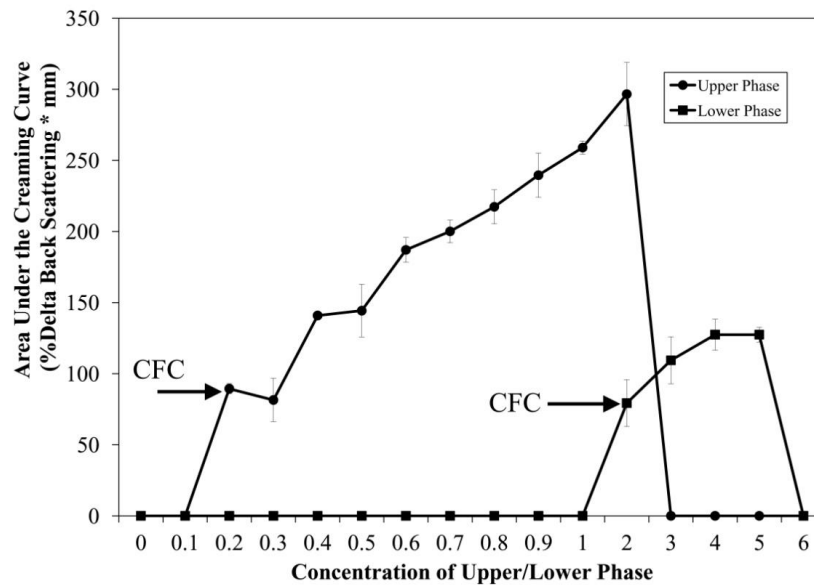


**Figure 3.6:** Area under the creaming curve for increasing concentrations of upper/lower phase from 3% pectin/3% caseinate phase separated mixtures (pH 7) added to 1% (wt.) emulsified corn oil at pH 7 after 1 day of storage at room temperature

(CFC). The CFC is the biopolymer concentration where the strength of the depletion attraction between droplets becomes strong enough to overcome the repulsive

interactions (such as electrostatic or steric). It is therefore a measure of the strength of the depletion interactions in a system, and thus, the lower the CFC, the stronger the depletion interactions.

To determine the CFC for both the upper and lower phases of our 3% pectin, 3% caseinate phase separated mixture, large quantities of upper and lower phases were carefully separated from each other following centrifugation. After these two phases were separated, a series of samples were prepared that contained a constant weight of emulsified oil (1 wt%) along with increasing amounts of either the upper biopolymer phase (pectin-rich) or the lower biopolymer phase (caseinate-rich). These systems were formed by mixing different mass ratios of emulsion (E), biopolymer phase (U or L for upper or lower phase), and buffer (B) solution. The emulsions all contained 1 part emulsion and 9 parts biopolymer phase (biopolymer + buffer phase). The emulsions were then stored for 1 day and the creaming stability of the lipid droplets in the systems was determined.

The emulsions to which the upper phase was added were relatively stable to creaming at  $\leq 0.1U$ , but exhibited creaming at  $\geq 0.2U$ , hence the CFC was defined as 0.2U (Figures 3.6, 3.7A). Based on previous chemical analysis of the undiluted upper phase, 0.2U corresponds to about 0.12 w/w% pectin and 0.04 w/w% caseinate. On the other hand, the emulsions to which the lower phase was added were stable to creaming up until much higher concentrations of lower phase, with the CFC being around 2L (Figures 3.6, 3.7B). According to chemical analysis, the amount of biopolymer present in 2L would be about 0.10 w/w% pectin and 4.6 w/w% caseinate. Several other researchers have also reported that pectin or caseinate can induce depletion flocculation in caseinate

stabilized oil-in-water emulsions at neutral pH 7, with the levels of pectin required being appreciably less than the levels of caseinate (Dickinson, Semenova, Antipova, & Pelan, 1998; Surh, Decker, & McClements 2006; Liu, Corredig, & Alexander, 2007). At high

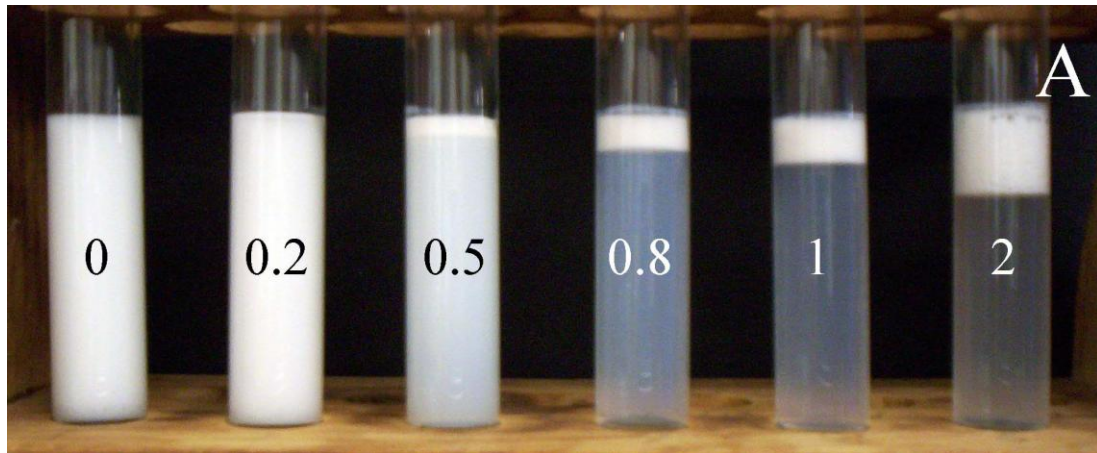


**Figure 3.7A:** Photograph of 1% (wt.) emulsified corn oil with increasing proportions of upper phase after 1 day of storage at room temperature

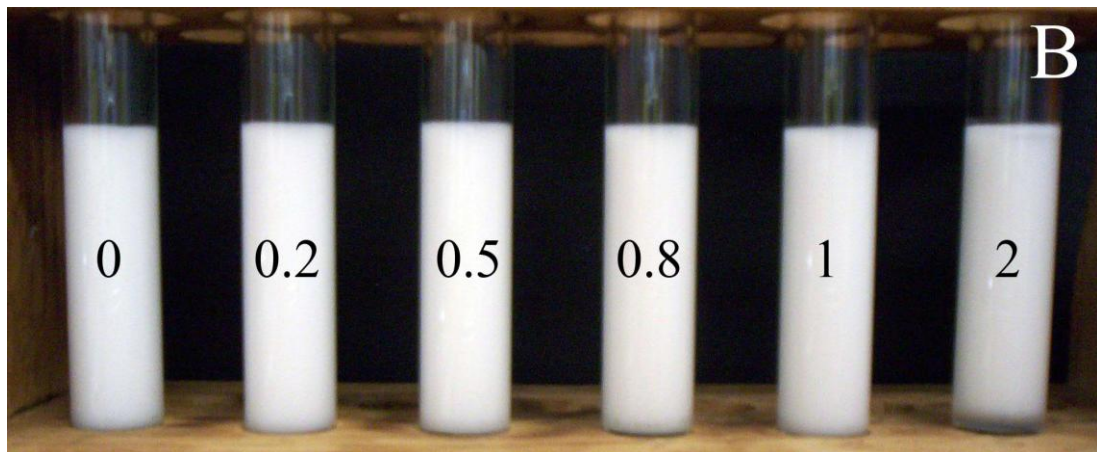


**Figure 3.7B:** Photograph of 1% (wt.) emulsified corn oil with increasing proportions of lower phase after 1 day of storage at room temperature

concentrations of upper and lower phases, the high viscosity of these samples prevented the migration of emulsified oil droplets to the surface. Thus, no creaming was observed for concentrations of upper phase above 2U and for concentrations of lower phase above 5L (Figure 3.6).

Confocal images of specific samples with different proportions of upper phase or lower phase were taken to visualize microstructural changes in these samples. Figure 3.8A is a confocal image of an emulsion with 0.2U:8.8B after 1 day of storage. This image shows that the oil droplets in this system (shown in red) have aggregated into small clusters of droplets. This image can be directly compared to Figure 3.8C, a confocal image of an emulsion with 0.2L:8.8B after 1 day of storage, which shows no flocculation or aggregation of emulsion droplets, indicating that this concentration of lower phase had no noticeable effect on emulsion stability. At the higher level of 2.0U:7.0B, it is clear that this sample is completely unstable as its microstructure consists of mostly large aggregates (Figure 3.8B). Figure 3.8B can be compared with Figure 3.8D, a confocal image of the sample with 2.0L:7.0B after 1 day of storage. Although some flocculation is seen in Figure 3.8D, its microstructure is considerably more uniform and less aggregated when compared with the emulsion containing the same proportion (2.0U) of upper phase (Figure 3.8B). Based on these findings, the CFC for the upper phase (0.2U:8.8B) was considerably less than that of the lower phase (2.0L:7.0B), which supports our hypothesis that the depletion interactions are stronger in the upper pectin-rich phase than in the lower caseinate-rich phase.

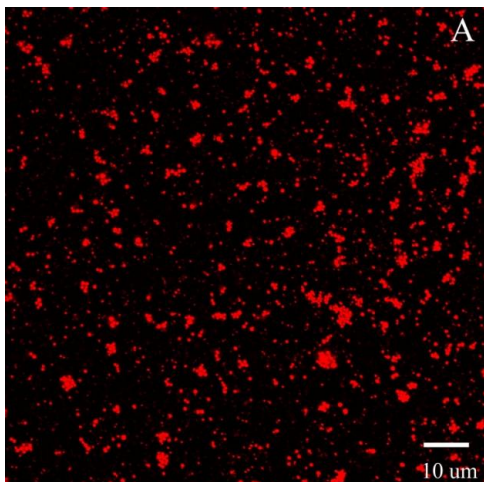


**Figure 3.8A:** Confocal image of 1% (wt.) emulsified corn oil with 0.2:8.8 proportion of upper phase:buffer after 1 day of storage at room temperature, oil droplets are dyed in red

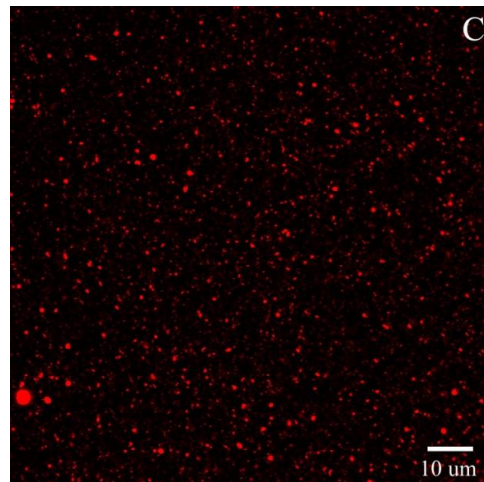


**Figure 3.8C:** Confocal image of 1% emulsified corn oil with 0.2:8.8 proportion of lower phase:buffer after 1 day of storage at room temperature, oil droplets are dyed in red

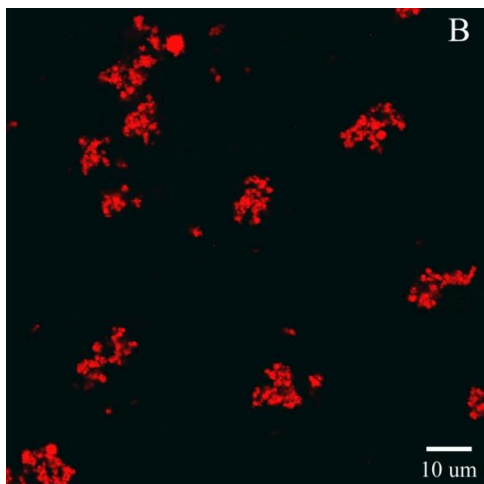


**Figure 3.8B:** Confocal image of 1% (wt.) emulsified corn oil with 2.0:7.0 proportion upper phase:buffer after 1 day of storage at room temperature, oil droplets are dyed in red

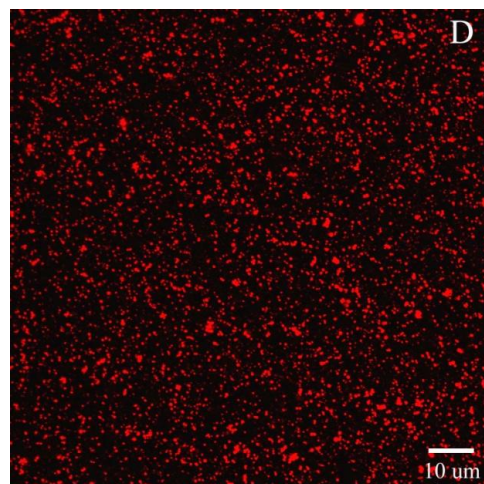


**Figure 3.8D:** Confocal image of 1% emulsified corn oil with 2.0:7.0 proportion of lower phase:buffer after 1 day of storage at room temperature, oil droplets are dyed in red

### 3.5.3 Formation, Characterization and Stability of Hydrogel Particles

Knowledge of the physicochemical properties of hydrogel particles, such as their size, charge and stability, are important for their practical applications. For this reason, we measured the initial particle size,  $\zeta$ -potential and storage stability of the hydrogel particles present in W/W emulsions formed at pH 7 and then adjusted to pH 5 to promote pectin adsorption around the protein-rich particles. The initial surface-weighted mean diameter ( $D_{3,2}$ ) was  $4.98 \pm 0.15 \mu\text{m}$ . After 29 days of storage,  $D_{3,2}$  was  $4.83 \pm 0.06 \mu\text{m}$ , indicating that the particles were stable during storage. The initial  $\zeta$ -potential of the hydrogel particles was  $-31.3 \text{ mV} \pm 0.2 \text{ mV}$  and remained unchanged after 29 days storage ( $-31.0 \pm 0.5 \text{ mV}$ ). The relatively small particle size of our particles is likely to be due to the intense shearing this mixture received during acidification. Intense shearing would induce droplet break up, ultimately resulting in smaller biopolymer particles.

Rheological studies conducted on phase separated systems have shown that a wide range of sizes and morphologies of the dispersed phase can be obtained depending on shear conditions. In most of these studies, the morphology and size of these droplets of dispersed phase can be measured by microscopy or small angle light scattering after the system is subjected to shear. The low interfacial tension of aqueous phase separated systems (typically  $10^{-7}$  to  $10^{-5} \text{ N/m}$ ) means that it is relatively easy to deform and disrupt the dispersed phase by shearing (Erni, et al., 2009). For example in the rheological study conducted by Van Puyvelde et al (2003), the application of increasing shear rates (1 to  $30 \text{ s}^{-1}$ ) on a phase separated mixture of gelatin and dextran resulted in a substantial decrease in the diameter of the dispersed phase droplets. A recent study published on the formation of whey protein microgels from a phase separated mixture of  $\kappa$ -carrageenan and whey

protein also showed that increasing shear rate during gelation reduced the size of these microgels (Gaaloul, Corredig, M., & Turgeon, 2009) During the acidification of our 3% pectin/3% caseinate mixture from pH 7 to 5, no precipitation of caseinate was observed. This observation suggests that electrostatic interactions between positive portions of casein aggregates and negatively charged pectin molecules prevented casein from precipitating. The negative  $\zeta$ -potential measured on both initial and stored particles suggests that pectin molecules have adsorbed onto the surface of caseinate-rich droplets when the system was acidified.

It is informative to compare the behavior of our system containing caseinate-rich droplets with the behavior of caseinate dispersions. Caseinate dispersions consist of small aggregates of casein molecules stabilized by repulsive forces at neutral pH. As the pH of a caseinate dispersion is reduced towards its isoelectric point (pH 4.6), these repulsive forces decrease, resulting in aggregation and precipitation at approximately pH 5 (Ruis, Venema, & van der Linden, 2007). Compared to caseinate, pectin is stable to aggregation in aqueous solutions across a wide pH range (Sila, et al., 2009). Several researchers have previously examined the stabilizing effects of high methoxy pectin on sodium caseinate dispersions (Pedersen & Jorgensen, 1991; Pereyra, Schmidt, & Wicker, 1997; Pereyra, Schmidt & Wicker, 1997). In these studies, pure sodium caseinate dispersions were unstable around pH 5, but the addition of high methoxy pectin resulted in a system that was stable to approximately pH 4. Furthermore, interactions between high methoxy pectin and caseinate were clearly detected above pH 5. Thus, it is reasonable to suggest that pectin and caseinate interact in our system during acidification from pH 7 to 5.

When our hydrogel particles were diluted in buffer (same pH and ionic strength as undiluted sample), the particles became unstable. After being diluted and stirred in the chamber of the light scattering instrument the concentration of large particles in the sample (10-1000  $\mu\text{m}$ ) steadily increased over the course of 2 hours. A decline in the % obscuration of the sample was also observed during this time, which was further evidence that the diluted particles were unstable. The adsorption of high-methoxy pectin to caseinate particles under acidic conditions is thought to be a relatively weak association (Syrbe, et al., 1998). Several researchers have suggested that the stabilizing effect of pectin on acidified casein micelles or aggregates is concentration dependent. At low concentrations of pectin, there is not enough pectin to completely cover the casein micelle or aggregate, resulting in bridging flocculation between pectin chains on adjacent micelles or aggregates. As the concentration of pectin is increased such that full coverage is achieved, the system is stabilized, and casein aggregation is prevented. At even higher concentrations of pectin, the system is further stabilized by the formation of a gel network (Syrbe, et al., 1998; Dickinson, 1998; Marozziene & de Kruif, 2000). Analysis of the continuous phase of this system at pH 7 showed that the concentration of pectin present in this phase is approximately 5% (wt/wt), an amount that should be sufficient to form a gel network. When our concentrated system is diluted to a concentration suitable for particle size analysis by static light scattering, the amount of pectin present is substantially reduced. This reduction ultimately leads to particle aggregation as a result of the loss of network structure and the loss of pectin coverage.

To better understand the interaction between pectin and caseinate during acidification, a mixture of 3% pectin/3% caseinate was acidified with glucono-delta-

lactone from pH 7 to 5 under controlled shear conditions using a rheometer. Figure 3.9 shows the change in apparent viscosity *versus* pH for the 3% pectin/3% caseinate mixture, the pectin-rich upper phase, and the casein-rich lower phase at a shear rate of  $1 \text{ s}^{-1}$ . Results for the 3% pectin/3% caseinate mixture sheared at a rate of  $100 \text{ s}^{-1}$  are not included since there was little difference in final particle size at this increased shear rate and the upper and lower phases were not examined at this higher shear due to constraints on sample quantities.

There are significantly fewer apparent viscosity measurements for the lower phase compared to either the mixture or the upper phase because acidification of the lower phase occurred over a much shorter time. Also, the pH range at which measurements were taken is narrower for the lower phase because acidification was rapid (*i.e.* pH at first viscosity measurement was  $\sim 6.5$ ) and viscosity measurements became unstable at approximately pH 5.2 as the protein gel structure formed during acidification started to breakdown. For the mixture of pectin and caseinate, the apparent viscosity started to decrease at approximately pH 6.2, and this decrease continued until the mixture reached around pH 5.2. The decline in apparent viscosity during the acidification of our pectin/caseinate mixtures suggests that pectin from the continuous phase is interacting with the caseinate-rich dispersed phase. As pectin from the continuous phase is attracted to the caseinate-rich dispersed phase, the amount of free pectin in the continuous phase will decrease, resulting in a lower apparent viscosity. Rediguieri et al (2007) also noted a decrease in the apparent viscosity of a 3% pectin/3% caseinate at pH 5 compared to pH 7.

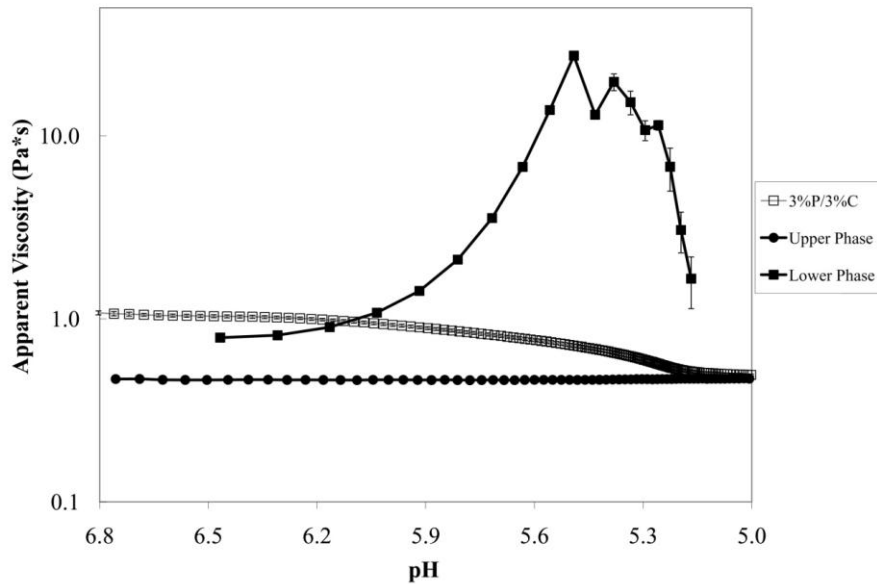


**Figure 3.9:** Apparent viscosity versus pH for 3% pectin/3% caseinate mixture, upper phase of 3% pectin/3% caseinate mixture and lower phase of 3% pectin/3% caseinate acidified from pH 7 to pH 5 at a shear rate of 1 (1/s) at 25° C

To confirm that the decline in apparent viscosity was due to an interaction between the two phases, both the upper and lower phases were acidified separately under a constant shear of  $1 \text{ s}^{-1}$  inside the rheometer. Figure 3.9 shows the change in apparent viscosity of the upper phase during acidification. Throughout testing, the apparent viscosity of the upper phase remained constant with almost no variation between replicates as noted by the very small error bars. This result clearly demonstrated that pectin alone was not responsible for the decline in apparent viscosity seen in the pectin/caseinate mixture. Acidification of the lower caseinate-rich phase resulted in a dramatic and steep increase in apparent viscosity followed by a sharp unstable breakdown (Figure 3.9). This rapid increase in apparent viscosity can be attributed to the formation

of a casein gel and the subsequent break down of this gel due to continued shearing. The formation of sodium caseinate gels by way of slow acidification of sodium caseinate dispersions using GDL is well established in the literature (Chen, Dickinson, & Edwards, 1999; Braga, et al., 2006). Since the apparent viscosity of the pectin/caseinate mixture gradually decreased rather than increased during acidification, it is clear that this decline was not due to the caseinate phase alone.

In our phase separated system, pectin and caseinate begin to interact at about pH 6, a pH that is well above the isoelectric point of sodium caseinate. This observation is different from the findings of other studies where strong interactions between pectin and casein occurred only at approximately pH 5 and below (Pereyra, et al., 1997; Tuinier, Rolin, & de Kruif, 2002). However, there are two major differences between our research and research previously performed on pectin-casein interactions, namely the concentrations of pectin and casein and the use of casein in a micellar *versus* non-micellar form. Much of the research conducted on the interaction between pectin and caseinate or casein micelles has involved dilute systems of pectin and casein. For example, Pedersen & Jorgensen (1991) examined the interaction between high methoxy pectin and sodium caseinate both at concentrations of less than 0.1%. At this low concentration, pectin and caseinate do not display thermodynamic incompatibility (Einhorn-Stoll, Salazar, Jaafar, & Kunzek, 2001; Rediguieri, et al., 2007). This difference in concentration and in biopolymer structure (miscibility *versus* incompatibility) could explain why pectin and casein interacted at a higher pH in our system. Since the dispersed phase contains high concentrations of casein, slight changes in the electrical

charge of these proteins during acidification would result in rapid migration of negatively charged pectins to the dispersed phase.

### 3.5.4 Formation, Characterization and Stability of Filled Hydrogel Particles

Finally, we examined the structure of mixed biopolymer systems containing lipid droplets at pH 5. Only mild shear conditions were used during the formation of these systems so that the particles formed were large enough to be viewed using optical microscopy. Figure 3.10 shows a confocal image of our mixed systems with casein dyed

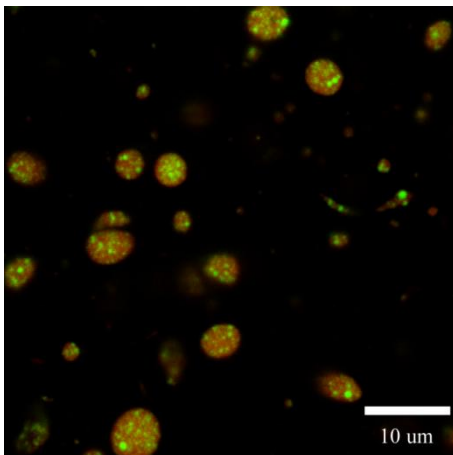


**Figure 3.10:** Confocal image of pectin/caseinate biopolymer particles encapsulating emulsified corn oil, corn oil is dyed in green and casein is dyed in red

in red and corn oil dyed in green. The size of these filled hydrogel particles is approximately 3 to 4  $\mu\text{m}$  in diameter, which is similar to the diameter of the unfilled hydrogel particles prepared in Section 3.5.3. This image confirms that biopolymer

particles are formed at pH 5 and that emulsified oil can be encapsulated inside these particles. These particles remained stable following 24 hours of storage at ambient temperature at pH 5.

Preliminary experiments on the stability of these particles to different pH conditions indicated that they retained their integrity when adjusted to pH 3, but that they dissociated when they were adjusted to pH 7 (data not shown). This might be expected since there would be electrostatic attraction between the positively charged protein and negatively charged pectin at pH 3 ( $\text{pH} < \text{pI}$ ), but electrostatic repulsion between the negatively charged protein and negatively charged pectin at pH 7 ( $\text{pH} > \text{pI}$ ).

For many commercial applications of filled hydrogel particles it is important that they maintain their physical integrity over a wide range of solution and environmental conditions. It would therefore be useful to examine different methods of cross-linking the biopolymer molecules within the hydrogel particles in order to improve their stability. This could be achieved using physical, chemical or enzymatic methods.

### **3.6 Conclusions**

The objective of this study was to develop delivery systems for lipophilic constituents based on combined segregative and aggregative phase separation processes in mixed biopolymer systems. A pectin and caseinate system previously described in the literature was used to encapsulate lipid droplets within hydrogel particles. We were able to show that the lipid droplets preferentially accumulated into the dispersed caseinate-rich phase as opposed to the pectin-rich continuous phase when they are added to our mixed pectin/caseinate system at pH7. The origin of this effect was attributed to the reduction

in the depletion interactions in the system when the droplets moved from the pectin-rich to the casein-rich phase.

Acidification of our pectin/caseinate system from pH 7 to 5 resulted in the formation of biopolymer particles that were stable in a concentrated form for at least one month of storage. This stability represents a significant deviation from the aggregation and precipitation that occurs in caseinate dispersions without pectin. Rheological measurements confirmed that particle formation involved an interaction between the pectin-rich continuous phase and the casein-rich dispersed phase and that this interaction started at approximately pH 6. Lastly, we were able to show that emulsified oil can be encapsulated within the biopolymer particles by acidifying our phase separated system with emulsified oil present in the dispersed phase.

This study confirms that the phenomena of biopolymer phase separation can be exploited to create delivery systems for lipophilic food bioactives. The great potential of this technique also raises questions on how to optimize this method. The influence of shear during particle formation is one important area that requires further investigation. Our initial results clearly show that different shear conditions influence the final particle size of this system. From a practical standpoint, it would be important to investigate how mixing speed can influence particle size and morphology. The use of more sophisticated processing equipment (such as colloid mills or homogenizers) to form these particles may be another way to effectively control their size and shape. Methods to form biopolymer particles other than acidification should also be investigated to determine if enzymatic or ionic gelation would produce more stable and versatile delivery systems. Unlike our current method of gelation which is pH dependent, forming more permanent cross-links

such as those created by enzyme treatments or ionic gelation should enhance the stability of this delivery system to changes in pH and dilution. In summary, this work demonstrates the ability of phase separated protein/polysaccharide systems to be successfully used as food-grade bioactive delivery systems.

## CHAPTER 4

### FACTORS INFLUENCING THE FORMATION AND STABILITY OF FILLED HYDROGEL PARTICLES FABRICATED BY PROTEIN/POLYSACCHARIDE PHASE SEPARATION AND ENZYMATIC CROSS-LINKING

#### 4.1 Abstract

Filled hydrogel particles can be used to encapsulate, protect, and deliver lipophilic components. In this study, we investigated the influence of preparation conditions on the size of filled hydrogel particles created using biopolymer phase separation and enzymatic cross-linking. We then investigated the stability of these particles to external stresses: pH (pH 2-8); heat (40°-90°C, 20 minutes); sodium chloride (0-500 mM); and calcium chloride (0-8 mM). Filled hydrogel particles were fabricated as follows: (i) high methoxy pectin, sodium caseinate, and caseinate-coated lipid droplets were mixed at pH 7 under conditions where phase separation due to thermodynamic incompatibility occurred; (ii) this mixture was acidified (pH 5) to induce adsorption of anionic pectin molecules around lipid-filled caseinate-rich particles; (iii) the caseinate within the particles was enzymatically cross-linked using transglutaminase. Three mixing conditions (0, 100, and 1000 rpm) were tested during particle acidification. Particle size measurements indicated that larger particles were formed at 0 and 100 rpm than at 1000 rpm. Under high pH conditions (pH 7-8), particles cross-linked with transglutaminase remained intact while control particles (not cross-linked) disintegrated. The addition of calcium to both control and cross-linked particles resulted in system gelation above 4 mM calcium chloride.

Control and cross-linked particles remained stable to heating and to the addition of sodium chloride. Results from this study demonstrate the versatility and robustness of this delivery system for lipophilic bioactives.

## **4.2 Introduction**

There is a great need in the food industry to develop novel delivery systems for bioactive compounds. Many of these beneficial constituents such as  $\omega$ -3 fatty acids, carotenoids, fat-soluble vitamins, and phytosterols are lipophilic, making their incorporation into aqueous foods and beverages challenging. In addition, many of these lipophilic compounds are chemically unstable and tend to degrade during storage when incorporated into foods (McClements, et al., 2007; Belitz, et al., 2009a). Traditionally, oil-in-water (O/W) emulsions, which consist of small oil droplets dispersed in a continuous watery phase, have been used by the food industry to incorporate lipids into aqueous foods and beverages. There are, however, other possible emulsion-based delivery systems for these compounds including multilayer ( $O_M/W$ ), water-in-oil-in-water (W/O/W), and oil-in-water-in-water (O/W/W) emulsions (McClements, 2005; McClements, et al., 2007). Depending on the application, these novel delivery systems may have significant advantages over conventional O/W emulsions such as enhanced stability or controlled bioactive release.

In this study, a delivery system based on the formation of an O/W/W emulsion was developed to form filled hydrogel particles. This technique of forming O/W/W emulsions to encapsulate lipids has been used previously by a number of researchers (Malone & Appelqvist, 2003; Lian, et al., 2004; Kim, et al., 2006). To create this emulsion, two biopolymers, a protein and a polysaccharide, that exhibit phase separation

were used. Phase separation is a common phenomenon for mixtures of biopolymers especially proteins and polysaccharides. A biopolymer system that experiences phase separation or incompatibility will separate into two distinct phases with each phase rich in one biopolymer and poor in the other (Grinberg & Tolstoguzov, 1997; Syrbe, et al., 1998). In general, phase separation is favored at relatively high biopolymer concentrations (typically above 2%) and when the charge on both biopolymers is either the same or neutral (Grinberg & Tolstoguzov, 1997; Tolstoguzov, 2003). When a phase separated system is mixed together, it tends to form a water-in-water (W/W) emulsion where each biopolymer phase forms either the dispersed or continuous phase. Typically, the phase that occupies the greater volume will become the continuous phase while the phase that occupies less volume will become the dispersed phase (Norton & Frith, 2001; Tolstoguzov, 2003).

In this work, a mixture of high methoxy pectin and sodium caseinate was used to create a phase separated protein/polysaccharide system. A similar system was previously investigated by Rediguieri et al (2007). Biopolymer concentrations and external conditions for this system were controlled such that the continuous phase was the phase rich in polysaccharide while the dispersed phase was the phase rich in protein. Previous work confirmed that emulsified oil droplets added to this phase separated system preferentially partition into the protein rich dispersed phase, forming an O/W/W emulsion (Matalanis, Lesmes, Decker, & McClements, 2010). Since food proteins have been shown to have good antioxidant properties (McClements & Decker, 2000; Kellerby, McClements, & Decker, 2006), incorporating emulsified oil into the dispersed protein-rich phase should help protect against lipid oxidation.

Water-in-water emulsions are unstable systems. Over time, the dispersed phase of W/W emulsions will begin to ripen, coalesce, and ultimately separate from the continuous phase (Norton & Frith, 2001). Instability is a common problem for particles formed from W/W emulsions. For example, Kim et al (2006) was able to form an O/W/W emulsion from a mixture of heat denatured whey protein and pectin; however this emulsion rapidly separated after mixing (Kim, et al., 2006). Rediguieri et al (2007) showed that microparticles created from a phase separated mixture of pectin and sodium caseinate at pH 5 disintegrated when the pH was increased to pH 7. This loss in structure was attributed to the reversible pH dependent complexation of pectin and caseinate. The process of separation can be arrested by gelling either the continuous phase to form a continuous gel network or by gelling the dispersed phase to form discrete gelled particles (Burey, et al., 2008). Shear conditions prior to gelation can have a major impact on the final structure of gelled W/W emulsions. In the absence of applied shear, the dispersed phase of a W/W emulsion will typically form spherical droplets ranging in size from approximately 2-20  $\mu\text{m}$ . By applying shear to a non-gelled W/W emulsion, the most obvious effect is a reduction in the size of the dispersed droplets (Norton & Frith, 2001). In addition to a reduction in droplet size, anisotropic particles can be formed as the low interfacial tension and high viscosities of W/W emulsions allows for substantial droplet deformation in response to modest shear flows (Erni, et al., 2009).

To prevent phase separation in a W/W emulsion, the dispersed or continuous phase of the emulsion can be gelled by several different means including changes in temperature (*e.g.*, cold-set or heat-set gelation), the addition of ions (*e.g.*, such as calcium or potassium), or the addition of protein cross-linking agents (such as the enzyme

transglutaminase). In this study, the protein-rich dispersed phase was gelled in two stages. First, the pH of the phase separated high methoxy pectin/sodium caseinate mixture was decreased from pH 7 to pH 5 to promote the complexation of pectin from the continuous phase with sodium caseinate from the dispersed phase to form discrete filled hydrogel particles. Following acidification, this system was incubated with transglutaminase, an enzyme capable of forming inter- and intra-molecular cross-links between the  $\gamma$ -carboxy amide group on glutamine and the  $\epsilon$ -amino group on lysine of proteins (DeJong & Koppelman, 2002). Cross-linking caseinate present in the dispersed phase of this system would aid in the formation of stable filled hydrogel particles. To assess the stability of our filled hydrogel particles both before and after cross-linking, we subjected these particles to changes in pH, temperature, and ionic strength (sodium chloride and calcium chloride). Information on the stability of these particles to common external stresses is essential before their application to real food products. Thus, the objectives of this study were to examine factors such as mixing conditions and enzyme cross-linking that influence the initial formation of filled hydrogel particles and to evaluate the stability of these particles to external stresses such as changes in pH, ionic strength, and temperature.

## **4.3 Materials and Methods**

### **4.3.1 Materials**

Commercial sodium caseinate was kindly donated by American Casein Company (Burlington, NJ) and was used without further purification. The percentage of protein

and moisture for this material were 91.3% and 5.3% respectively as provided by the manufacturer. High methoxy pectin (Genu Pectin (Citrus), USP/100) was kindly donated by CP Kelco (Lille Skensved, Denmark). The composition of this material as provided by the manufacturer was 6.9% moisture, 89.0% galacturonic acid and 8.6% methoxy groups, which corresponds to a degree of esterification (DE) of approximately 62%. Glucono-delta-Lactone (F5010) was kindly donated from Jungbunzlauer (Newton, MA). Mazola corn oil (ACH Food Companies, Memphis, TN) was purchased at a local supermarket. The enzyme transglutaminase (Activa® TI) was kindly donated by Ajinomoto Food Ingredients (Chicago, Illinois). According to the manufacturer, the activity of this enzyme preparation is 100 units of activity per gram of powdered preparation. All other chemicals used in this research were purchased from Sigma-Aldrich (St Louis, MO). Double distilled water was used to make all solutions.

#### **4.3.2 Methods**

This study was divided into two separate sets of experiments. The first set of experiments was designed to evaluate the effect of different mixing conditions on the size of filled hydrogel particles. In the second set of experiments, the enzyme transglutaminase was used to create cross-linked filled hydrogel particles. Cross-linked and control (not-cross-linked) particles were then evaluated for their stability to changes in pH, ionic strength, and temperature.

##### **4.3.2.1 Solution Preparation**

Sodium caseinate stock solutions (6% w/w, dry weight basis) and pectin stock solutions (6% w/w, dry weight basis) were prepared in buffer solutions containing an

antimicrobial (0.04% sodium azide, 10 mM phosphate buffer, pH 7). Stock solutions were mixed for 30 min using a mechanical stirrer (Stedfast Stirrer Model SL 1200, Thermo Fisher Scientific, Waltham, MA). Initially, the sodium caseinate solution had a pH of ~6.8 and the pectin stock solution had a pH of ~3.8. Both solutions were adjusted to pH 7.0 by adding 4 M sodium hydroxide. The solutions were centrifuged for 2 hours at 10,000 g to remove any insoluble matter.

#### **4.3.2.2 Emulsion Preparation**

Oil-in-water emulsions (20% oil vol/vol) stabilized with 2% (w/w) sodium caseinate were formed from corn oil, sodium caseinate, and buffer solution (0.04% sodium azide, 10 mM phosphate buffer, pH 7). A coarse emulsion was formed first by blending this mixture at a speed of 20,000 rpm for 2 minutes with a high speed blender (Tissue Tearor Model 985370-395, Biospec Products Inc., Bartlesville, OK). The coarse emulsion was then homogenized with a high pressure homogenizer (Microfluidizer Model 110 L, Microfluidics, Newton, MA) for 3 passes at a chamber pressure of 11,000 psi. Emulsions formed by this method had an average volume-weighted mean diameter (D<sub>4,3</sub>) of 0.37 μm and an average surface-weighted mean diameter (D<sub>3,2</sub>) of 0.32 μm as measured by static light scattering (Mastersizer 2000, Malvern, Worcestershire, UK).

#### **4.3.2.3 Formation of Phase Separated Biopolymer Mixtures**

Previous experiments have shown that an equal weight mixture of 6% pectin and 6% caseinate (final concentration 3% pectin, 3% caseinate) at pH 7 will phase separate into an upper phase rich in pectin and a lower phase rich in caseinate<sup>11</sup>. The relative location of these two layers can be attributed to a difference in density with the upper

phase having a lower density (~1.02 g/ml) than the lower phase (~1.04 g/ml)(Matalanis, et al., 2010) . Thus, equal weights of 6% w/w sodium caseinate and 6% w/w pectin stock solutions were mixed together, the pH was checked and adjusted to pH 7 if necessary with 4 M sodium hydroxide, and the mixture was then stirred for 30 min (Stedfast Stirrer Model SL 1200, Thermo Fisher Scientific, Waltham, MA). Thus, the concentration of pectin and caseinate in this mixture was 3% pectin/3% caseinate. Following stirring, this mixture was centrifuged at 10,000 g for 2 hours at 20°C. Previous experiments confirmed that 2 hours of centrifugation was sufficient for complete phase separation. Following centrifugation, the samples were allowed to settle until distinct upper and lower phases were visible. The upper and lower phases were separated and stored for further use.

#### **4.3.2.4 Formation of Filled Hydrogel Particles**

A water-in-water (W/W) emulsion is formed when proportions of the isolated upper and lower phases described in section 4.3.2.3 are mixed together. When the proportion of upper phase is much greater (above ~80% vol/vol) than the proportion of lower phase, the lower phase will form the dispersed phase of the W/W emulsion, and the upper phase will form the continuous phase. The addition of emulsified oil to this W/W emulsion results in the emulsified oil droplets partitioning into the dispersed phase.

For the first set of experiments, filled hydrogel particles were formed from a mixture of 5% (vol/vol) lower phase, 90% (vol/vol) continuous phase and 5% (vol/vol) of a 20% (vol/vol) corn oil-in-water emulsion. Thus, the final mixture contained 1% (vol/vol) corn oil. This mixture was then stirred with an overhead stirrer at 300 rpm for 30 minutes. The pH of the mixture was measured and adjusted to pH 7 with 4M sodium hydroxide if necessary. After this initial premixing, mixtures were subjected to the

different mixing conditions during acidification. For samples stirred at 100 and 1000 rpm, the speed of the overhead mixer was first adjusted and a pH probe was inserted to monitor pH. One drop of 1 M citric acid was added every 10 seconds until the mixture reached pH 5. For the no mixing sample, glucono-delta-lactone (GDL) was added to the premixed sample at a ratio of 0.11 GDL:1 protein and allowed to mix for 2 minutes at 300 rpm. This sample was then stored overnight without any additional mixing such that the final pH of the sample was  $5.0 \pm 0.2$ . After overnight storage, the pH of the sample was checked and adjusted to pH 5 if necessary with either 1 M citric acid or 1 M sodium hydroxide.

For the second set of experiments, filled hydrogel particles were fabricated following the procedure described for the no mix (0 rpm) sample using GDL as an acidulant. Initially, it was thought that the acidification process was unnecessary since the desired structure (O/W/W emulsion), although unstable, is formed at pH 7. To stabilize this system at pH 7, the enzyme transglutaminase would be used to cross-link caseinate, forming stable filled hydrogel particles. Unfortunately, this approach was unsuccessful at creating filled hydrogel particles as the caseinate present in the system formed such extensive cross-links that large aggregates of caseinate were formed during incubation with transglutaminase.

To form cross-linked filled hydrogel particles, fabricated particles were transferred to a 40°C water bath, and a solution of transglutaminase (0.1 g transglutaminase/ ml of 10 mM phosphate buffer pH 5) was added at a level of 10 Units of enzyme activity/ per gram of protein using an overhead stirrer at 300 rpm. This

mixture was incubated with constant agitation at 300 rpm for 2 hours. To inactivate transglutaminase, the mixture was heated in a 85°C water bath for 5 minutes with constant agitation at 300 rpm. The mixture was then cooled on ice for 20 mins. Control (not cross-linked) particles were exposed to the same incubation and inactivation conditions as enzyme treated particles.

#### **4.3.2.5 Analysis of Filled Hydrogel Particles**

To assess the influence of mixing conditions on the size of filled hydrogel particles, samples were evaluated by static light scattering and optical microscopy. For static light scattering measurements, particles were measured using a Mastersizer 2000 with a small volume sample dispersion unit (Hydro 2000 SM) (Malvern, Worcestershire, UK), and the Fraunhofer approximation was used for the dispersed phase (hydrogel). All samples were diluted in 10 mM phosphate buffer adjusted to pH 5, and the stirrer speed was set to 1250 rpm. Since the sample was difficult to disperse inside the dispersion unit, all samples were pre-diluted at a ratio of 1 part sample:1 part buffer prior to measuring. Each sample was measured in duplicate. The parameter  $D_{3,2}$  often referred to as the average volume mean diameter was used to assess particle size. A definition of this parameter can be found on page 56.

For the determination of particle dimensions by optical microscopy, a total of five slides were prepared for each image. Because of the significant number of small particles in the samples mixed at 1000 rpm, it was necessary to dilute these samples at a ratio of 1 part sample:3 parts buffer (10 mM phosphate buffer, pH 5) so that individual particles could be resolved and measured. Fixed slides were magnified using a microscope (Nikon D-Eclipse C1 80i, Nikon, Melville, NY) with an oil immersion objective lens (60×, 1.40

NA) along with a 1.8x camera zoom. For each slide preparation, 5 fields of view were captured for a total of 25 images per sample. The software program Nikon Elements BR version 3.0 (Nikon, Melville, NY) was used to capture all images, and the software program ImageJ (NIH, Bethesda, MD) was then used for image analysis. Using ImageJ, images were first converted to binary images, and particles with a circularity of less than 0.5 were excluded as this significantly reduced the number of overlapping particles that were measured. Circularity,  $C$ , was calculated using the following equation:

$$C = 4\pi \times \frac{A}{(P^2)} \quad (4.1)$$

where  $A$ = area of the particle calculated after thresholding and  $P$ = perimeter of the particle calculated as the outlined area of each thresholded particle.

Particles with a calculated surface area below  $0.02 \mu\text{m}^2$  were not included in microscopy analysis. Following analysis, the area of each particle was used to calculate equivalent diameter,  $ED$ , using the following equation:

$$ED = 2 \times \sqrt{\left(\frac{A}{\pi}\right)} \quad (4.2)$$

The equivalent diameter was then used to calculate the equivalent spherical volume (ESV) of each particle using the following equation:

$$ESV = \frac{\pi ED^3}{6} \quad (4.3)$$

$D(0.1)$ ,  $D(0.5)$  and  $D(0.9)$  were calculated as the diameter of the particle with an equivalent spherical volume at 10%, 50%, and 90% of the cumulative volume of all analyzed particle. In addition to optical microscopy, representative images of each sample were taken using differential interference contrast (DIC) microscopy. DIC images

were taken with the same microscope, magnification and camera zoom settings as previously listed.

#### **4.3.2.6 Stability Testing of Filled Hydrogel Particles**

In this set of experiments, the stability of cross-linked filled hydrogel particles under various external conditions was compared to control (not cross-linked) filled hydrogel particles. Following adjustment to external conditions, all samples were stored overnight prior to analysis the following day using static light scattering,  $\zeta$ - potential, and microscopy.

To assess the stability of the hydrogel particles to changes in pH, 1 M hydrochloric acid and 1 M sodium hydroxide were used to adjust the pH of these particles from pH 2 to 8 in one unit increments. For sodium chloride experiments, a 4 M sodium chloride solution was made by dissolving sodium chloride into 10 mM phosphate buffer followed by adjusting this solution to pH 5 using 1 M hydrochloric acid. This salt solution along with 10 mM phosphate buffer adjusted to pH 5 was used in different ratios (same total volume) to adjust the ionic strength of aliquots of particles to the following concentrations: 0, 50, 100, 150, 200, 250, and 500 mM sodium chloride. For calcium chloride experiments, phosphate buffer could not be used to make a 50mM calcium chloride stock solution as this solution remained cloudy due to the formation of calcium phosphate. Therefore, 50 mM calcium chloride was dissolved in double distilled water and adjusted to pH 5. This stock solution along with 10 mM phosphate buffer adjusted to pH 5 was used in different ratios (same total volume) to adjust the concentration of calcium in these samples to the following levels: 0, 2, 4, 6, and 8 mM calcium chloride.

To assess the effects of heating on particle stability, aliquots of particles were heated for

20 minutes in a water bath set to the following temperatures: 40, 50, 60, 70, 80, and 90 °C. Following heating, all samples were immediately transferred to a 25°C water bath to rapidly cool to room temperature.

The particle size of all samples was measured by static light scattering using the procedure described in section 4.3.2.5, with the exception that 10 mM phosphate buffer adjusted to the same pH and ionic strength as the analyzed sample was used as the dispersant. The zeta potential of all samples was measured by laser doppler electrophoresis (Zetamaster, Malvern, Worcestershire, UK). Prior to measuring, samples were diluted with 10 mM phosphate buffer adjusted to the same pH and ionic strength as the analyzed sample. Initial experiments confirmed that a dilution factor of 1:1000 resulted in satisfactory count rates. Preliminary experiments confirmed that the zeta potential remained negative from pH 2 to 8, from 0 to 200 mM sodium chloride, and from 0 to 8 mM calcium chloride which allowed for the use of a lower modulation frequency of 250 Hz. Five zeta potential measurements were taken per sample injected, and each sample was measured in duplicate for a total of ten zeta potential readings per sample. For samples adjusted with increasing concentrations of sodium chloride, zeta potential measurements could not be performed on samples adjusted to 250 or 500 mM sodium chloride as measurements were unstable. This instability can be attributed to the high electrical conductivity of high ionic strength solutions which can result in electrode polarization and thermally-induced convective flow inside the sample cell (Miller, Yalamanchili, & Kellar, 1992).

DIC microscopy images were taken of all adjusted samples using the same microscopy, objective, and camera zoom setting listed in Section 4.2.2.5. To distinguish

filled hydrogel particles from a system undergoing phase separation (i.e. a water-in-water emulsion), all samples were diluted in 10 mM phosphate buffer adjusted to the same pH as the sample by a factor of 1:10. Since phase separation is concentration dependent, sample dilution would prevent water-in-water emulsion formation while retaining the structure of stable filled hydrogel particles.

#### **4.3.2.7 Statistical Analysis**

All experiments were carried out in triplicate using freshly prepared samples. One-way ANOVA tests were used to test significance of parameter means.

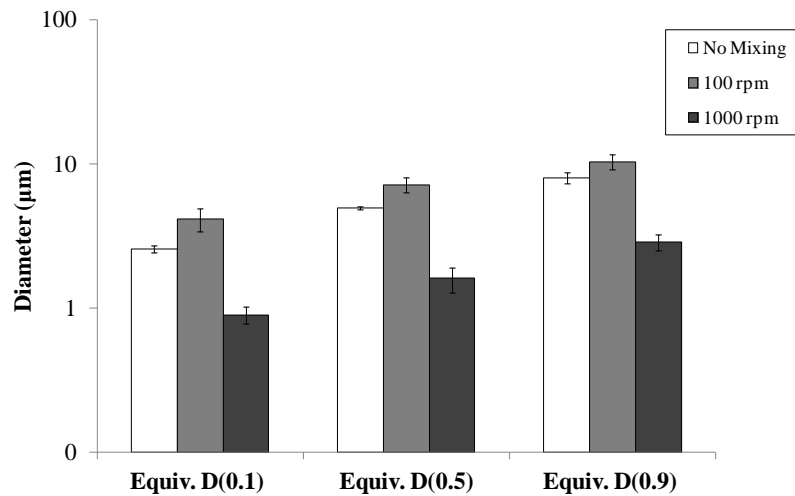
### **4.4. Results and Discussion**

#### **4.4.1 Influence of Mixing Conditions on the Size of Filled Hydrogel Particles**

The purpose of this set of experiments was to determine the effect of different mixing conditions during particle formation on the size of filled hydrogel particles. A mixture of 5% dispersed and 90% continuous phase previously isolated from a phase separated 3% pectin/3% caseinate mixture along with 5% of a 20% oil-in-water emulsion was premixed at pH 7. This mixture was then acidified to pH 5 while it was subjected to one of three following mixing conditions: no mixing, mixing at 100 rpm, and mixing at 1000 rpm.

Image analysis of filled hydrogel particles indicated that mixing conditions impacted final particle size (Figure 4.1). One-way ANOVA tests showed that mixing conditions had a statistically significant impact on average particle diameter for all size

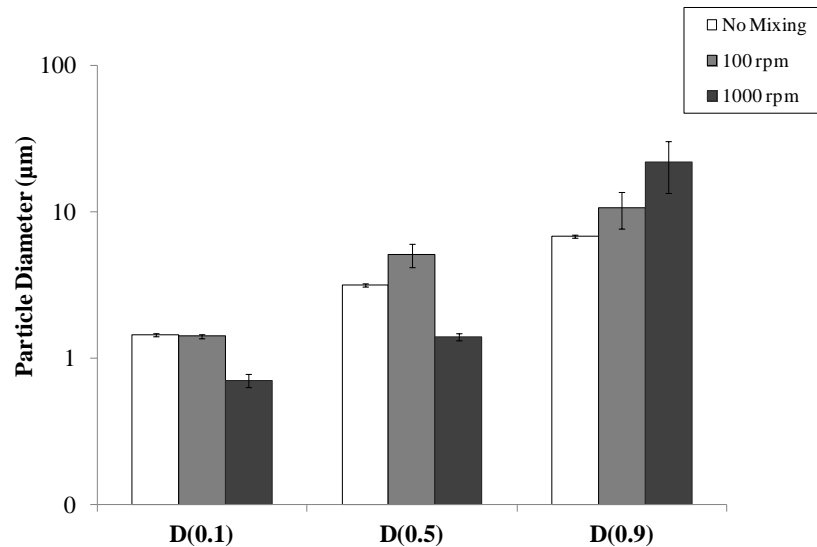
classes. As expected, the most intense mixing conditions (1000 rpm with an overhead stirrer) resulted in the formation of filled hydrogel particles with the smallest diameters for all three size classes, that is D(0.1), D(0.5) and D (0.9). Surprisingly, diameters for particles subjected to no mixing were smaller than those subjected to stirring at 100 rpm although this difference was substantially less than the difference between either of these treatments and mixing at 1000 rpm.



**Figure 4.1:** Particle diameter determined by image analysis (Equivalent D(0.1), D(0.5), and D(0.9)) (µm) for hydrogel particles created under different mixing conditions at pH 5

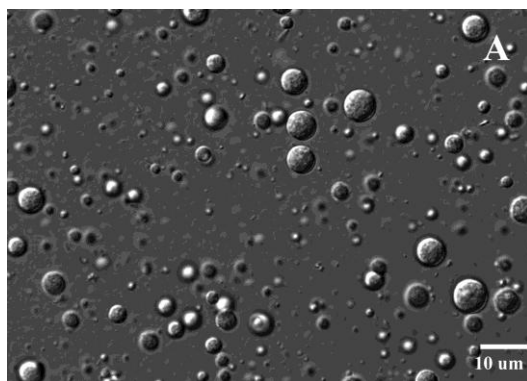
Particle size was also determined by static light scattering (Figure 4.2). Compared to image analysis, the diameters obtained by light scattering were similar in size for the parameters D(0.1) and D(0.5). For the parameter D(0.9), particle diameters obtained by light scattering were both higher and did not follow the same trend as those obtained by

image analysis. One-way ANOVA tests performed on light scattering results showed that mixing conditions have a statistically significant effect on D(0.1) and D(0.5) at  $\alpha = 0.05$ . Mixing conditions also affected the parameter D(0.9) although this effect was less pronounced than its effect on the other two size classes ( $p = 0.049$ ). A representative DIC microscopy image of a sample mixed at 1000 rpm (Figure 4.3C) can be directly



**Figure 4.2:** Particle diameter determined by static light scattering (D(0.1) and D(0.5) ( $\mu\text{m}$ ) for hydrogel particles created under different mixing conditions at pH 5

compared to a DIC microscopy images of a sample that received no mixing (Figure 4.3A) and a sample that was mixed at 100 rpm (Figure 4.3B). It is clear that the particles present in the sample mixed at 1000 rpm are substantially smaller and more uniform compared to the particles present in either of the other two samples.



**Figure 4.3A:** Representative DIC microscopy image of hydrogel particles subjected to no mixing (0 rpm) at pH 5

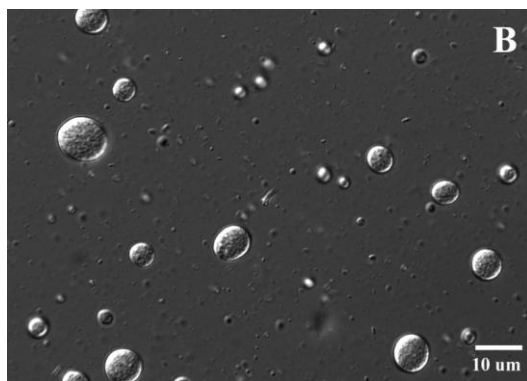


**Figure 4.3B:** Representative DIC microscopy image of hydrogel particles subjected to 100 rpm mixing treatment at pH 5

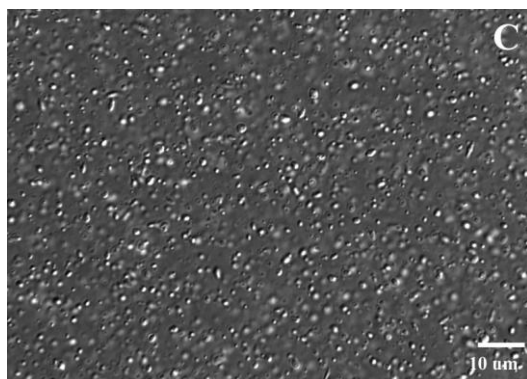


**Figure 4.3C:** Representative DIC microscopy image of hydrogel particles subjected to 1000 rpm mixing treatment at pH 5

As stated previously, mixing conditions impacted the final size of filled hydrogel particles. With the exception of D(0.9) obtained by light scattering, samples mixed at the highest speed (1000 rpm) had the smallest diameter compared to the samples that were not mixing or were mixed at 100 rpm as determined by optical microscopy and image analysis. This decline in particle diameter can be partially attributed to the low interfacial tension of water-in-water emulsions. In general, interfacial tension measurements for water-in-water emulsions are generally  $10^3$ - $10^4$  times lower than those of oil-in-water emulsions (Erni, et al., 2009; Frith, 2010). Due to the low interfacial tension of these systems, emulsification can be achieved using a low energy density (energy input per unit volume of emulsion) homogenization device such as a high speed mixer as opposed to a high energy density device such as a high pressure homogenizer (McClements, 2005; Erni, et al., 2009).

Optical microscopy results for all size classes and light scattering results for classes D(0.5) and D(0.9) showed that the size of the hydrogel particles in samples that received no mixing (0 rpm) were actually smaller than those mixed at 100 rpm. This observation suggests that shear induced coalescence may have occurred in the sample mixed at 100 rpm. Similar results were reported by Wolf, Scirocco, Frith, and Norton (2000) and Wolf, Frith, Singleton, Tassieri, and Norton (2001) as the particle size, measured by optical microscopy, of phase separated mixtures of gellan and carrageenan subjected to constant shear stress (0.1 to 10 Pa) during gelation were larger than samples gelled under quiescent conditions( Wolf, et al., 2000; Wolf, et al., 2001).

Particle size measurements obtained by static light scattering were different from those obtained by optical microscopy and image analysis especially at the highest particle

class (D(0.9)). This discrepancy could be attributed to the way particle size is calculated for these two methods. For image analysis, the equivalent surface area was used to calculate particle diameter, that is the surface area was measured and the diameter of a theoretical sphere with this surface area was calculated. In the case of static light scattering, the volume of the particle is used to determine the diameter of a theoretical sphere with this volume (Malvern Instruments, 2007). A further concern associated with determining particle size by static light scattering is selecting the correct optical model for data analysis. Since the dispersed phase of this system consisted of both emulsified oil droplets as well as dispersed phase from the W/W emulsion, it is not possible to measure the refractive index of this phase. For this reason, we used the Fraunhofer approximation of Mie theory as this model does not require knowledge of the refractive index of the particle. Unfortunately, the assumptions of this approximation may result in errors in determining the size of particles below 50  $\mu\text{m}$  (Malvern Instruments, 2010). Overall, particle size measurements performed by static light scattering did show that the high speed mixing decreased the proportion of large hydrogel particles.

Images obtained by DIC microscopy highlight the substantial difference in particle size between samples mixed at 1000 rpm and samples mixed at either 100 rpm or not mixed. The formation of smaller particles under more intense mixing conditions suggests that the interfacial tension between the dispersed and continuous phases of this water-in-water emulsion is relatively low. As a result of this low interfacial tension, significant deformation of the dispersed phase of a water-in-water emulsion can occur with the application of mild shear (Wolf, et al., 2000; Wolf, et al., 2001; Erni, et al., 2009; Frith, 2010). Several studies conducted on the effects of shear on phase separated

biopolymer systems have noted the formation of long strings or threads of dispersed phase upon exposure to shear (Wolf, et al., 2000; Wolf, et al., 2001; Wolf & Frith, 2003). No strings or threads were observed in this system. This observation suggests that the higher viscosity ratio (viscosity of dispersed phase relative to viscosity of continuous phase) of this system ( $>1$ ) favors the formation of ellipsoidal particles as opposed to systems where viscosity ratios are lower ( $\sim 0.01$ ) and string formation is favored (Wolf, et al., 2000). The viscosity ratio is also related to the capillary number,  $Ca$ , defined as follows:

$$Ca = \frac{n_c \dot{\gamma} r}{\sigma} \quad (4.4)$$

where  $n_c$  = viscosity of continuous phase,  $\dot{\gamma}$  = shear rate,  $r$  = radius of the particle, and  $\sigma$  = interfacial tension.

The critical capillary number can be defined as shear conditions where a droplet will either deform (below the critical capillary number) or breakup (above the critical capillary number). According to calculations performed by Grace (1982), the critical capillary number will decrease as the viscosity ratio increases from 0.01 to 1. Since our system has a viscosity ratio close to 1, its corresponding lower critical capillary number would favor droplet breakup as opposed to droplet formation, limiting string formation (Grace, 1982; Capron, Costeux, & Djabourov, 2001). It is also possible that string-like structures were formed during shearing, but these structures relaxed into spheroid-like shapes once shearing was stopped.

#### 4.4.2 Influence of pH on the Stability of Cross-Linked and Control (Not Cross-Linked) Filled Hydrogel Particles

In this set of experiments, the stability of filled hydrogel particles was evaluated against changes in pH. Both control (not cross-linked) particles and particles cross-linked with the enzyme transglutaminase were evaluated. The average particle size ( $D_{3,2}$ ) of the particles at pH 5 (the initial pH of the system) was  $2.61 \pm 0.09 \mu\text{m}$  with transglutaminase and  $2.77 \pm 0.13 \mu\text{m}$  without transglutaminase. The pH of all samples was then adjusted to pH 2-8. Analysis of the particle size of both cross-linked and control particles showed little change in average particle size ( $D_{3,2}$ ) from pH 2-5 with the exception of a slight increase in particle size at pH 2 (Figure 4.4). Significant changes in average particle size measurements were seen at higher pH values (pH 6-8) (Figure 4.4). In case of control particles, there was an initial increase in particle size at pH 6 followed

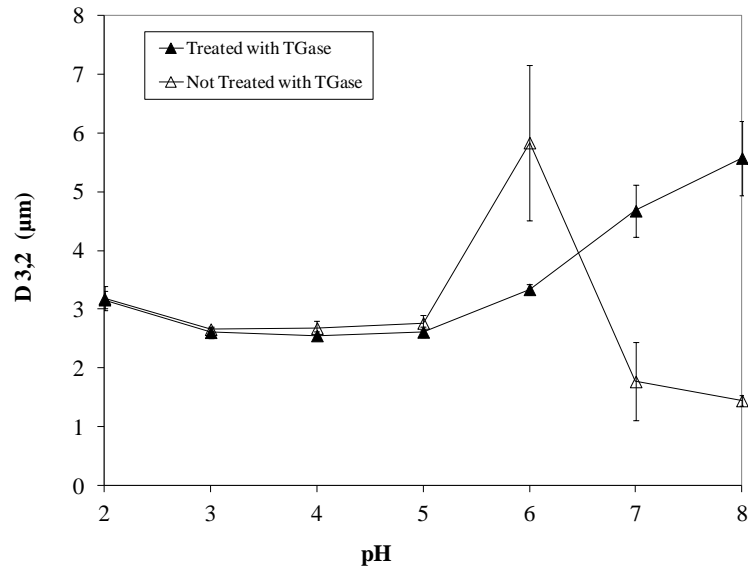


**Figure 4.4:** Particle diameter ( $D_{3,2}$  ( $\mu\text{m}$ )) determined by static light scattering versus pH for filled hydrogel particles treated with TGase and filled hydrogel particles not treated with TGase

by a substantial decline in the average diameter of these particles at pH 7 and pH 8. In contrast, the average particle diameter of cross-linked filled hydrogel particles gradually increased as the pH increased from pH 6 to 8.

To confirm results obtained by static light scattering, the particle size of cross-linked and control filled hydrogel particles adjusted to pH 3 and pH 5 as well as cross-linked particles at pH 7 was determined by light microscopy and image analysis. Control filled hydrogel particles were not measured at pH 7 as preliminary experiments confirmed that the droplets seen in this sample were not stable filled hydrogel particles but rather a water-in-water emulsion undergoing phase separation. Results from image analysis agreed with the trend seen in the static light scattering data (Figure 4.5). At both pH 3 and pH 5, the average particle size of cross-linked and control particles is nearly identical while at pH 7 the particle size of the cross-linked particles increased slightly. For simplicity, only the parameter equiv. D(0.5) is shown; however similar trends were noted for the parameters equiv. D(0.1) and equiv. D(0.9).

In addition to measuring particle size, diluted samples at each pH interval were examined by DIC microscopy. The samples were diluted in buffer at the same pH examined so that only stable hydrogel particles and not the dispersed phase of a system undergoing phase separation would be shown in these images. Microscopy images of cross-linked and control filled hydrogel particles at pH 5 showed the presence of filled hydrogel particles varying in size from  $\sim 1\text{-}4\ \mu\text{m}$  (Figure 4.6A, Figure 4.6B). When the pH of the control sample was increased from pH 5 to pH 7, the particles disappear and only small droplets of emulsified oil can be seen (Figure 4.6C). This image can be directly compared to Figure 4.6D, a microscopy image of cross-linked filled hydrogel

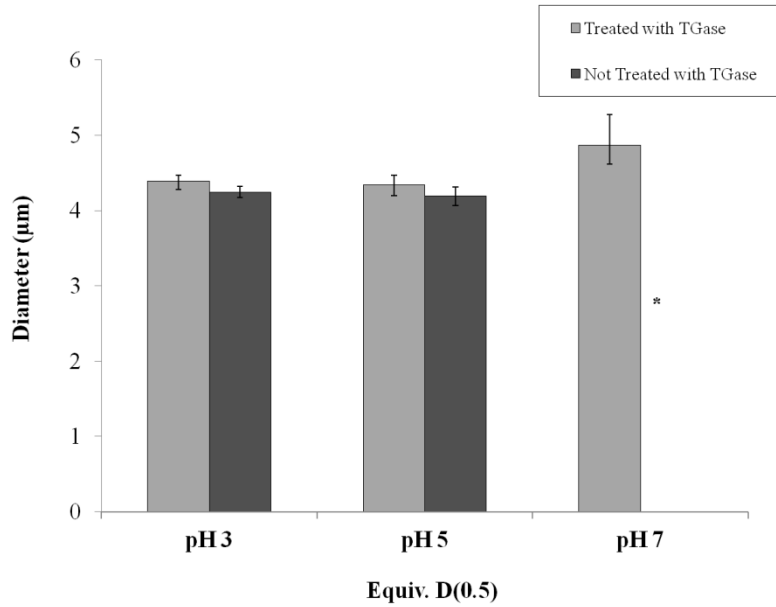


**Figure 4.5:** Particle diameter (Equiv. D(0.5)) for filled hydrogel particles treated and not treated with TGase at pH 3, pH5, and pH 7

particles at pH 7. Unlike the control sample at pH 7, filled hydrogel particles are clearly visible at pH 7. Zeta potential measurements were taken for both cross-linked and control particles at each pH interval. Results revealed that the magnitude of the zeta potential of both cross-linked and control particles increased sharply from pH 2 to pH 4 as the particles became more negatively charged followed by slight increases in negative charge from pH 5 to pH 8 (Figure 4.7). There was little difference between the zeta potential measurements of cross-linked and control particles.

The stability of filled hydrogel particles formed in this study was strongly influenced by changes in pH. From pH 2 to pH 5, both control and cross-linked particles remained stable. This observation suggests that pectin from the continuous phase was able to form a complex with the caseinate-rich dispersed phase in this pH range. Based on the zeta potential measurements, the electrical charge present on these particles decreases

as the pH decreases from pH 5 to pH 2, yet particle stability is maintained. This observation suggests that steric forces may play a large role in particle stability at low pH. At pH 5, caseinate is close to its isoelectric point of 4.6 (Kinsella, 1984) which would suggest that it has at least some positive patches on its surface. Since pectin is a polyelectrolyte, its apparent dissociation constant will depend on solution conditions with a  $pK_a$  value typically in the range from pH 3.5-4.5 (CP Kelco, 2005; Endress, Mattes, & Norz, 2006). Thus at pH 5, partially positive caseinate should interact with the negatively charged pectin and aid in the stabilization of the filled hydrogel particles. The fact that the hydrogel particles were negatively charged at pH 5 also suggests that pectin formed an anionic coating around the surface of the caseinate-rich filled hydrogel particles.

Previous work conducted by Rediguieri et al (2007) on a similar phase separated system of pectin and caseinate also suggested that pectin complexes with caseinate at low pH. In these experiments, the concentration of both pectin and caseinate were measured in upper and lower phases following phase separation as a function of pH. As the pH was decreased from pH 5 to pH 3, the relative concentration of pectin in the lower dispersed phase (caseinate-rich) steadily increased while the relative concentration of pectin in the upper continuous phase declined, indicating the formation of pectin-caseinate complexes (Rediguieri, et al., 2007).

Unlike the behavior at low pH, there is a clear distinction between the stability of cross-linked and control filled hydrogel particles above pH 5. Under these conditions, both caseinate and pectin are negatively charged, and thus, there is a tendency for these polymers to repel each other rather than complex. This agrees with previous observations

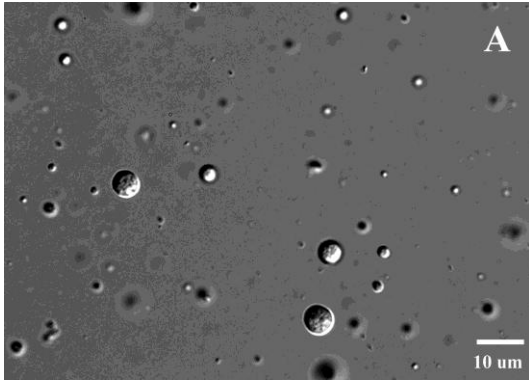


**Figure 4.6A:** Representative DIC microscopy image of filled hydrogel particles not treated with TGase at pH 5 previously diluted by a factor of 10 in pH 5 adjusted buffer

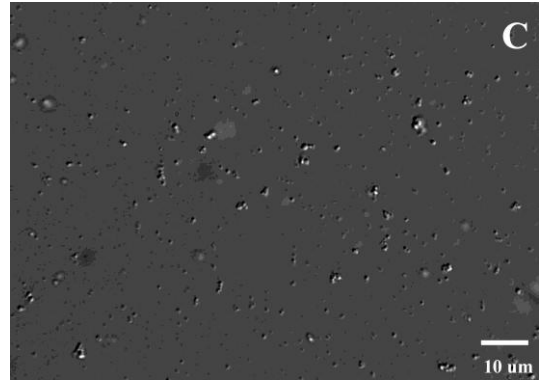


**Figure 4.6C:** Representative DIC microscopy image of filled hydrogel particles not treated with TGase at pH 7 previously diluted by a factor of 10 in pH 7 buffer

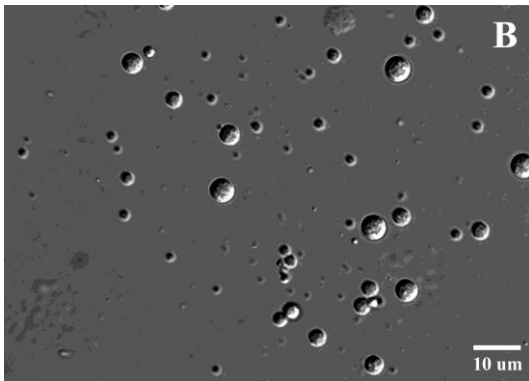


**Figure 4.6B:** Representative DIC microscopy image of filled hydrogel particles treated with TGase at pH 5 previously diluted by a factor of 10 in pH 5 adjusted buffer

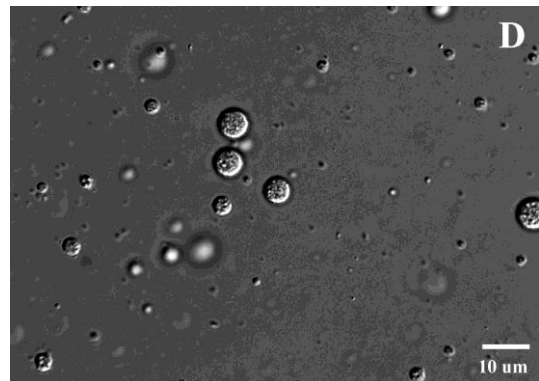


**Figure 4.6D:** Representative DIC microscopy image of filled hydrogel particles treated with TGase at pH 7 previously diluted by a factor of 10 in pH 7 buffer

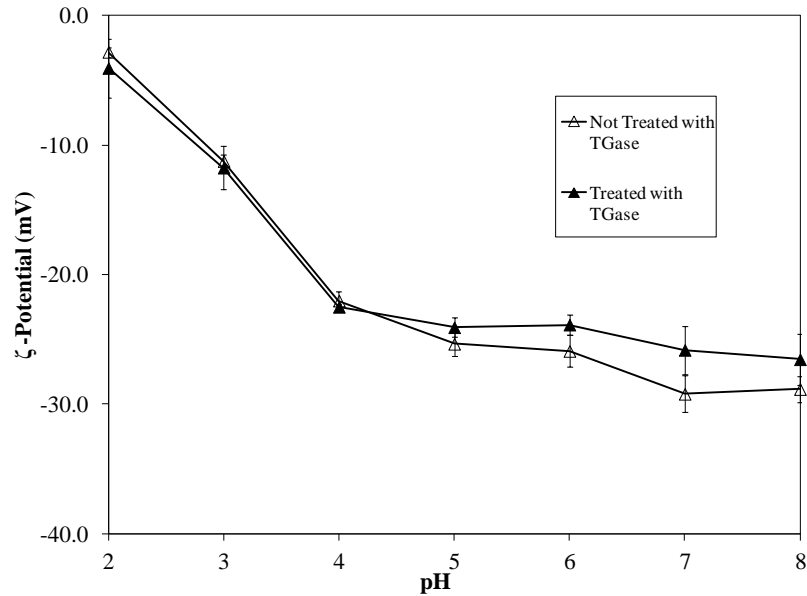


**Figure 4.7:** Zeta potential versus pH for filled hydrogel particles treated and not treated with TGase

that report electrostatic complexes between anionic polysaccharides and proteins are reversible and tend to dissociate above the isoelectric point of the protein (Ye, 2008). In the case of the control particles, particle size data measured by static light scattering revealed a substantial decline in particle size following dilution at pH 7 and pH 8. Microscopy also confirmed the absence of filled hydrogel particles following dilution with pH adjusted buffer. It is interesting to note the difference in the particle size obtained by microscopy compared to static light scattering at higher pH (6-8). Based on light scattering data, D 3,2 is calculated to be over 1  $\mu\text{m}$  at pH 7-8 for particles not cross-linked with transglutaminase. Images obtained by microscopy, however, show the presence of much smaller droplets with a diameter of  $\sim 0.2 \mu\text{m}$ . It is well known that the Fraunhofer approximation is particularly inaccurate for determining particle size when

the size of the particles is below 2  $\mu\text{m}$  (Malvern Instruments, 2010). This fact may explain the observed discrepancy between these two methods.

The addition of transglutaminase as a protein cross-linking agent substantially improved the stability of filled hydrogel particles from pH 6 to pH 8. Transglutaminase is an enzyme that is capable of forming intra- and inter-molecular cross-links in proteins by catalyzing the acyl-transfer of the  $\gamma$ -carboxy amide group on glutamine and the  $\epsilon$ -amino group on lysine. Since caseinate has a relatively large number of exposed lysine and glutamine residues available for cross-linking, it is an excellent substrate for cross-linking by transglutaminase (DeJong & Koppelman, 2002). In essence, transglutaminase was able to trap the structure of these filled hydrogel particles at pH 5. This entrapment prevented the loss of structure despite the electrostatic repulsion between pectin and caseinate molecules at high pH. Interestingly, there was an appreciable increase in the diameter of the cross-linked hydrogel particles when the pH was increased from 5 to 8 (Figure 4.4). This effect can be attributed to the swelling of hydrogel particles due to electrostatic repulsion between negatively charged biopolymer molecules (both pectin and caseinate) within the gel matrix.

#### **4.4.3 Influence of Sodium Chloride on the Stability of Filled Hydrogel Particles**

Since sodium chloride is a common ingredient in foods, it was important to evaluate the effects of increasing levels of sodium chloride on the stability of both cross-linked and control filled hydrogel particles. There was little difference in the particle size for both the control and cross-linked particles at all salt concentrations (0-500 mM sodium chloride) (data not shown). Zeta potential measurements showed a decrease in the electrical charge on the particles with increasing concentrations of sodium chloride up to

200 mM sodium chloride (Figure 4.8). As mentioned previously, zeta potential measurements could not be measured on particles with sodium chloride concentrations above 200 mM.

The decline in zeta potential had no impact on particle size, indicating that particles were stable even at high levels of sodium chloride. Salts are known to screen electrostatic interactions, which potentially have a number of effects on hydrogel particle properties. First, salt addition will decrease the electrostatic attraction between oppositely charged groups (anionic - cationic) within the hydrogel particles, which could lead to particle dissociation or swelling by weakening cross-links. Second, salt addition will reduce the electrostatic repulsion between similarly charged groups (anionic-anionic or cationic-cationic) within the hydrogel particles, which could lead to particle shrinkage since biopolymer molecules can pack closer together. Nevertheless, we did not observe any significant changes upon addition of salt (0 to 500 mM NaCl), which suggests that the levels used were insufficient to induce these effects or that particle shrinkage and swelling were balanced. Finally, salt addition will also screen the electrostatic repulsion between the hydrogel particles themselves, which could lead to particle aggregation. We did not observe appreciable particle aggregation upon salt addition in this study, which may have occurred for a number of reasons: (i) the continuous phase was so viscous that the rate of particle movement was slow; (ii) the salt concentrations were not sufficiently high; (iii) the hydrogel particles were stabilized by other repulsive interactions, e.g., steric repulsion. In several studies conducted on the stabilization of acidified milk drinks using high methoxy pectin, steric stabilization has been proposed as the mechanism in which

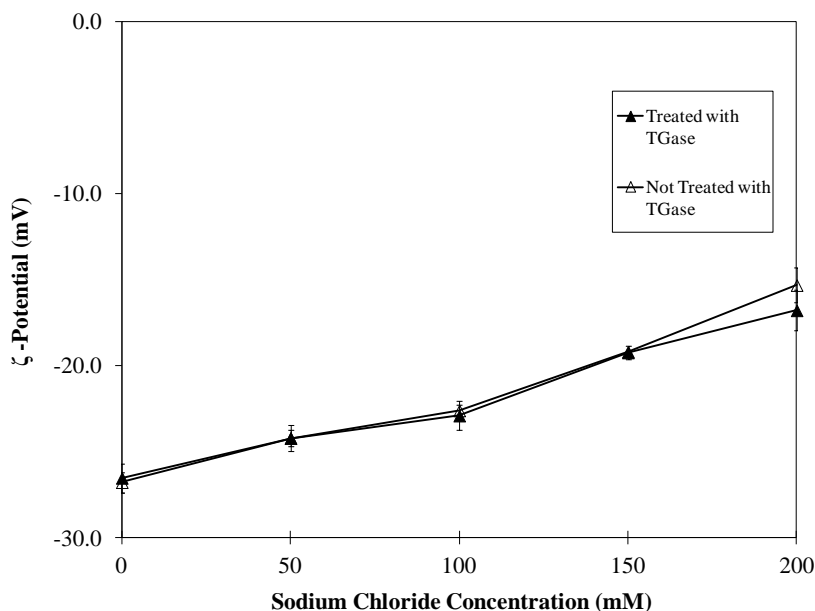


**Figure 4.8:** Zeta potential versus sodium chloride concentration for filled hydrogel particles treated and not treated with TGase

pectin prevents milk protein flocculation and subsequent separation (Leskauskaite, Liutkevichius, & Valantinaite, 1998; Tromp, de Kruij, van Eijk, & Rolin, 2004; Jensen, Rolin, & Ipsen, 2010). The structure of pectin is such that it consists of both charged and uncharged regions. As the pH is lowered, negatively charged regions of pectin adsorb onto positive regions present on the surface of casein micelles while uncharged regions of pectin protrude out into solution. Thus, these uncharged regions confer steric stabilization to casein micelles at low pH. Although the caseinate present in our system is not in its original micellar form, it is still reasonable to assume that steric stabilization from pectin plays a major role in stabilizing our system.

#### 4.4.4 Influence of Calcium Chloride on the Stability of Filled Hydrogel Particle

Since most Americans do not meet their daily requirements for calcium intake, fortifying foods and beverages with the essential mineral calcium may be important for optimal health and disease prevention (Miller, Jarvis, & McBean, 2001). To assess the stability of cross-linked and control filled hydrogel particles to calcium ions, filled hydrogel particles were exposed to increasing levels of calcium chloride (0- 8 mM), stored overnight, and analyzed the following day. Figure 4.9 shows the change in average particle diameter (D 3,2) versus the concentration of calcium chloride present in the system. From 0 to 4 mM calcium chloride, the average particle diameter was relatively small ( $\sim 3 \mu\text{m}$ ). Above 4 mM calcium chloride, the average particle size increases dramatically to between 10-50  $\mu\text{m}$  for both cross-linked and not cross-linked particles. As the concentration of calcium increased, the system changed from a viscous liquid to a semi-solid gel. As seen in Figure 4.10, concentrations of calcium chloride at or above 4 mM resulted in the formation of a gelled sample that did not flow under normal gravitational forces. Sample evaluation by optical microscopy revealed that individual particle integrity was maintained at the highest level of calcium addition (data not shown).

In terms of zeta potential measurements versus calcium concentrations, the electrical charge on these particles decreased the most when calcium was first introduced into the system (0 to 2 mM calcium chloride) (Figure 4.11). At higher levels of calcium,

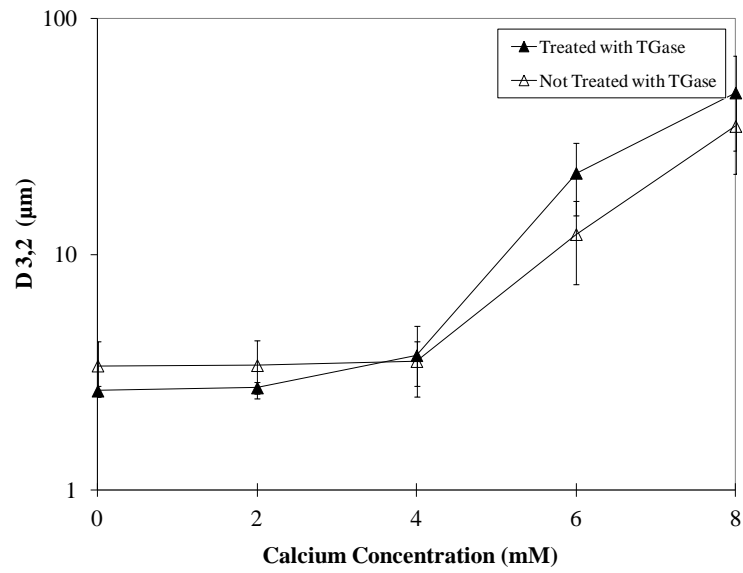


**Figure 4.9:** Particle size (D 3,2) ( $\mu\text{m}$ ) versus calcium chloride concentration for filled hydrogel particles treated and not treated with TGase

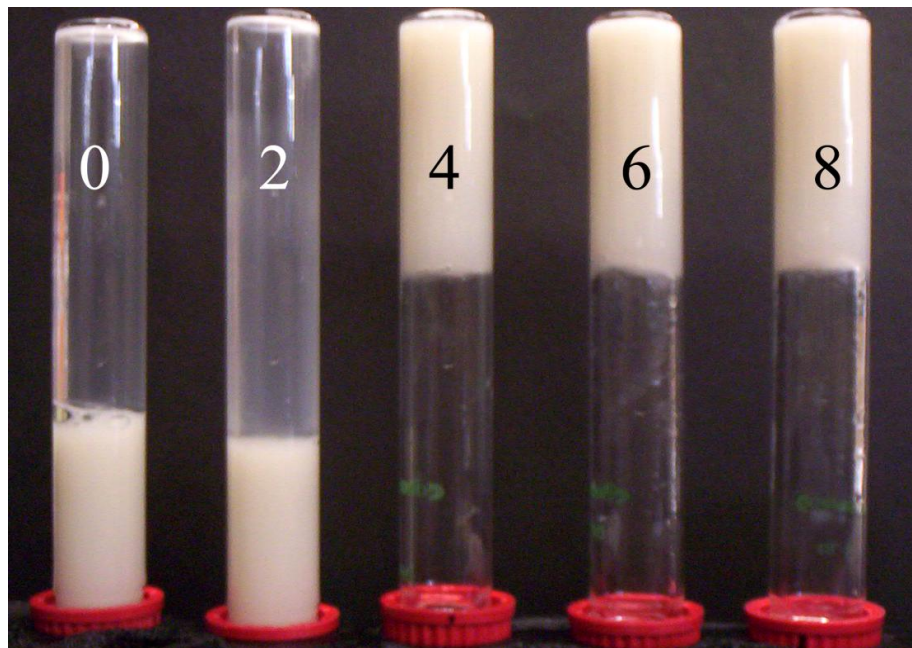


**Figure 4.10:** Photograph of filled hydrogel particles with increasing concentrations of calcium chloride (0-8 mM)

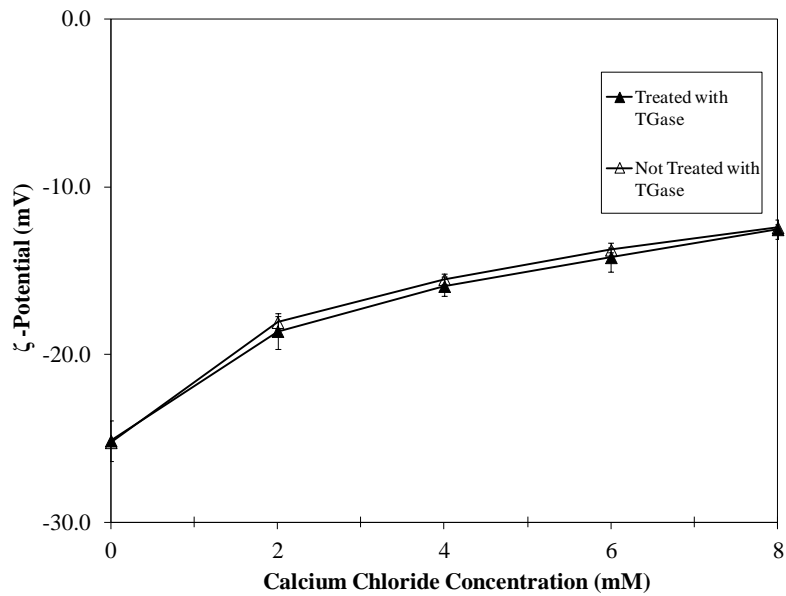


**Figure 4.11:** Zeta potential versus calcium chloride concentration for filled hydrogel particles treated and not treated with TGase

the electrical charge continued to decline but much less so than when calcium was first added. The increase in average particle size at calcium concentrations above 4 mM calcium chloride suggests that significant particle aggregation has occurred. Analysis of samples containing higher levels of calcium (8 mM calcium chloride) by optical microscopy, however, showed no evidence of aggregation or loss of individual particle integrity. Furthermore, it was noted that samples containing 4-8 mM calcium chloride formed a semi-solid gel that was difficult to disperse prior to particle size analysis by static light scattering. Based on these observations, the large particle size at 6 and 8 mM of calcium chloride can be attributed to gel fragments formed during the dispersion of these samples as opposed to hydrogel flocculation or coalescence.

The addition of low concentrations (below 0.10 M) of calcium chloride have been shown to increase the apparent viscosity of concentrated (14% w/w) solution of sodium caseinate. This increase has been attributed to a competition for water between the calcium salt and sodium caseinate (Carr, Munro, & Campanella, 2002). Furthermore, polyvalent ions such as calcium are believed to form cross-links with both carboxyl and ester phosphate groups present on caseinate (Morr, 1982). Both of these factors would contribute to the gelation of the filled hydrogel particle suspension. The difference in the behavior of these particles to calcium ions as opposed to sodium ions can be explained by the binding affinity of caseinate to these two ions. Electrochemical studies conducted on the addition of calcium chloride to concentrated dispersions of sodium caseinate have shown that sodium ions rapidly exchange for calcium ions, indicating that caseinate has a much higher affinity for binding calcium than sodium. This higher binding affinity may explain why the addition of calcium had such a dramatic impact on these particles while there was negligible impact to these particles upon the addition of sodium (Clark, Lips, & Hart, 1989). In addition, calcium is a multivalent ion that can induce biopolymer aggregation through charge neutralization and ion bridging effects.

#### **4.4.5 Influence of Heating on the Stability of Filled Hydrogel Particles**

The purpose of this set of experiments was to evaluate the effect of thermal treatments on the stability of both cross-linked and control filled hydrogel particles. Following fabrication, filled hydrogel particles were heated for 20 minutes at temperatures from 40°C-90°C followed by rapid cooling in a 25°C water bath. All

samples were then stored overnight prior to analysis the following day. Results showed that thermal treatments had no impact on the particle size or zeta potential of either cross-linked or control filled hydrogel particles (data not shown).

#### **4.5 Conclusions**

There were two main objectives of this work, first to evaluate how different mixing conditions influenced the formation of filled hydrogel particles and second to determine how these particles behave when exposed to external stresses. In terms of the first objective, this study clearly demonstrated that mixing conditions during particle formation have a significant impact on the size of filled hydrogel particles. Under low or no mixing conditions, average particle diameters were significantly larger compared to particles formed under more intense mixing.

In an effort to improve particle stability, the enzyme transglutaminase was used as a cross-linking agent following particle formation. Both cross-linked and not cross-linked particles were assessed for their stability to heating, salts (sodium chloride and calcium chloride), and changes in pH. Cross-linking had a significant impact on particle integrity under neutral and slightly alkaline conditions (pH 6-8) as cross-linked particles retained their structure at higher pH while particles that were not cross-linked disintegrated. This difference can be attributed to the formation of inter- and intra-molecular protein cross-links as a result of treatment with transglutaminase. Under acidic conditions (pH 2-5), both cross-linked and not cross-linked particles were stable. Furthermore, both cross-linked and not cross-linked particles were stable to heat as well as the addition of sodium

chloride. The addition of low levels of calcium (4-8 mM) to either particle type resulted in the formation of a strong macroscopic gel. This behavior was attributed to the strong binding affinity of calcium ions to caseinate.

The potential benefits of using the enzyme transglutaminase as a cross-linking agent for filled hydrogel particles merits further investigation. An optimization study to determine the appropriate enzyme concentration and incubation conditions for cross-linking would be beneficial. This study also revealed that the size of filled hydrogel particles can be altered using different mixing conditions. Thus, it would be interesting to investigate whether or not these differences in size influence particle characteristics such as viscosity and optical properties.

Results from this research clearly demonstrate both the versatility and robustness of filled hydrogel particles as a delivery system for lipophilic bioactive compounds. By adjusting conditions such as shear, one can manipulate the size of filled hydrogel particles, and this difference may have a profound impact on the final delivery system. Following formation and cross-linking, we were also able to demonstrate the excellent stability of this system to common external stresses. The challenge is to continue to improve on this current system such that the process of forming and stabilizing these particles is both economical and practical.

## CHAPTER 5

### INHIBITION OF LIPID OXIDATION BY ENCAPSULATION OF EMULSION DROPLETS WITHIN HYDROGEL MICROSPHERES

#### 5.1 Abstract

The purpose of this study was to assess whether the oxidation of polyunsaturated lipids could be inhibited by encapsulating them within protein-rich hydrogel microspheres (size range 1 – 100  $\mu\text{m}$ ). Filled hydrogel microspheres were fabricated as follows: (i) high methoxy pectin, sodium caseinate, and casein-coated lipid droplets were mixed at pH 7, (ii) the mixture was acidified (pH 5), (iii) casein was cross-linked using transglutaminase, (iv) the pH was adjusted to pH 7. Samples were stored in the dark at 55°C and were monitored for lipid hydroperoxide formation and headspace propanal. Oxidation of fish oil (1% vol/vol) in the microspheres was compared with that in oil-in-water emulsions stabilized by either sodium caseinate or Tween 20. Emulsions stabilized by Tween 20 oxidized faster than either microspheres or emulsions stabilized by casein, while microspheres and the casein stabilized emulsion showed similar oxidation rates. Results highlight the natural antioxidant properties of food proteins.

#### 5.2 Introduction

Lipid oxidation is a major concern of the food industry because it leads to changes in the perceived quality and nutritional value of many foods, particularly those containing unsaturated fats (Belitz, et al., 2009a). Although some degree of lipid oxidation can be beneficial in producing desirable flavors in foods such as fried foods (Choe & Min, 2007), lipid oxidation is usually associated with unfavorable changes including the

development of off-flavors, a reduction in the nutritional properties of lipids, and the creation of harmful free radicals (Jacobsen, 1999). Although there are many factors that can either promote or retard lipid oxidation, fatty acid composition is a significant factor in determining oxidative stability with unsaturated lipids oxidizing at a faster rate than lipids that are more saturated (McClements & Decker, 2000; Choe & Min, 2006).

There is substantial evidence that the consumption of foods rich in polyunsaturated omega-3 fatty acids can reduce the risk of chronic diseases such as heart disease, arthritis, and some types of cancer (Ruxton, et al., 2007; Riediger, et al., 2009; Yashodhara, et al., 2009). Enriching foods with lipids rich in omega-3 fatty acids would be one strategy to improve the nutritional profile of lipid based foods. Unfortunately, the high level of unsaturated fatty acids in these lipids make them highly susceptible to oxidative deterioration and to the production of objectionable off-flavors such as metallic, fishy, and rancid aromas (Jacobsen, et al., 2008). Strategies such as reducing oxygen levels, altering interfacial properties, or adding a metal chelator could be used to control lipid oxidation in these omega-3 enriched foods (McClements & Decker, 2000; Waraho, et al., 2011).

Research has shown that food proteins can inhibit lipid oxidation in food emulsions (McClements & Decker, 2000; Hu, McClements, & Decker, 2003; Faraji, et al., 2004; Elias, McClements, & Decker, 2005; Elias, Kellerby, & Decker, 2008; Waraho, et al., 2011). A wide range of mechanisms are associated with the antioxidant properties of proteins including inactivation of reactive oxygen species, free radical scavenging, metal chelation, hydroperoxide reduction, enzymatic removal of oxidants, and creation of a physical barrier between reactants (Elias, et al., 2008). Sodium caseinate is a

commercial ingredient usually manufactured through acid coagulation of casein from milk followed by solubilization in lye and spray drying (Belitz, Grosch, & Schieberle, 2009b). It consists of four main protein fractions:  $\alpha_{s1}$ -casein,  $\alpha_{s2}$ -casein,  $\beta$ -casein, and  $\kappa$ -casein, present in solution as small aggregates of approximately 10-12 nm (Farrer, & Lips, 1999). Caseinates are surface-active molecules that are widely used in the food industry as emulsifiers because of their ability to adsorb to oil droplet surfaces during homogenization and then stabilize the droplets against aggregation during storage. In oil-in-water emulsions, casein has proven to be highly effective at preventing lipid oxidation (Hu, et al., 2003; Faraji, et al., 2004; Haahr & Jacobsen, 2008; Mora-Gutierrez, Attaie, & Farrell, 2010; Ries, Ye, Haisman, & Singh, 2010). The antioxidant properties of casein have been attributed to its ability to scavenge free radicals (Díaz and Decker, 2004; Rival, Boeriu, & Wichers, 2001) and to chelate transition metals as the phosphorylated serine residues present on casein are known to form complexes with metal cations (Díaz, Dunn, McClements, & Decker, 2003; Faraji, et al., 2004).

A hydrogel can broadly be defined as a water-swollen matrix formed by cross-linked hydrophilic polymers (Chen, et al., 2006). For application in foods, hydrogels are usually fabricated from natural polymers (proteins and polysaccharides) rather than synthetic polymers. Filled hydrogel microspheres consist of oil droplets embedded within a spherical hydrogel particle that has dimensions in the micrometer range, *i.e.*, 1 to 100  $\mu\text{m}$ . Typically, these particles are formed from biopolymers that are capable of both phase separation and hydrogel particle formation (Burey, et al., 2008; McClements, 2010a). In this study, filled hydrogel microspheres were fabricated from a phase separated mixture of high methoxy pectin and sodium caseinate. Previous work

confirmed that emulsified oil droplets added to this phase separated system preferentially partition into the protein-rich dispersed phase (Matalanis, et al., 2010). When this system is sheared an oil-in-water-in-water (O/W/W) emulsion is formed that consists of oil droplets trapped within a casein-rich particle that is dispersed within a pectin-rich phase (Matalanis, et al., 2010). To stabilize this system, the enzyme transglutaminase was used to cross-link the casein present in the dispersed phase to form protein-rich filled hydrogel microspheres (Figure 5.1).

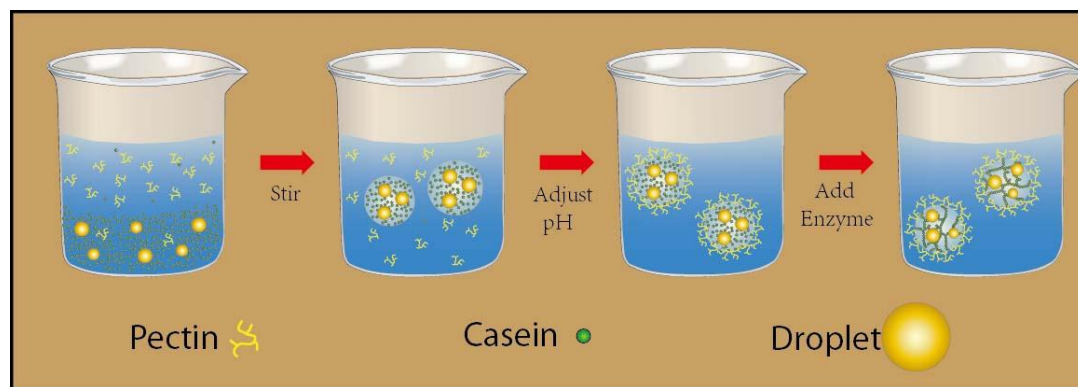


**Figure 5.1:** Formation of filled hydrogel microspheres by a multiple step process:

(i) droplets, casein and pectin are mixed together under conditions where phase separation occurs – droplets partition into the lower casein-rich phase (pH 7); (ii) the mixture is stirred leading to the formation of a O/W/W emulsion – the oil droplets are trapped within the casein phase, which forms the dispersed water phase; (iii) acid is added to reduce the pH to 5, which promotes the adsorption of pectin molecules around the filled hydrogel microspheres; (iv) the casein within the microspheres is covalent cross-linked by adding an enzyme (transglutaminase)

Because of the high concentration of antioxidant casein in the immediately vicinity of the emulsified oil droplets, we hypothesized that filled hydrogel microspheres would have enhanced oxidative stability over conventional oil-in-water emulsions. Thus,

the objective of this study was to compare the oxidative stability of filled hydrogel microspheres to conventional oil-in-water emulsions stabilized by either sodium caseinate or a synthetic emulsifier (Tween 20).

## **5.3 Materials and Methods**

### **5.3.1 Materials**

Commercial sodium caseinate was kindly donated by American Casein Company (Burlington, NJ) and was used without further purification. The percentage of protein and moisture for this material were 91.3% and 5.3% respectively as provided by the manufacturer. A commercial high methoxy pectin (Genu Pectin (Citrus), USP/100) was kindly donated by CP Kelco (Lille Skensved, Denmark) and was used without further purification. The composition of this material as provided by the manufacturer was 6.9% moisture, 89.0% galacturonic acid and 8.6% methoxy groups, which corresponds to a degree of esterification (DE) of approximately 62%.

Refined fish oil (ROPUFA® '30' n-3 EPA Oil) was kindly donated by DSM Nutritional Products (Parsippany, NJ). According to the manufacturer, this oil contains a minimum of 30% n-3 polyunsaturated fatty acids and is stabilized by ascorbyl palmitate, dl- $\alpha$ -tocopherol, and lecithin. The initial peroxide value of this oil prior to oxidation was measured and was found to be 0.37 mmol hydroperoxide/ per kg oil. Fish oil containing antioxidants was used in this study to more closely mimic oil used in commercial products, and to prevent oxidation during preparation of the delivery systems. The enzyme transglutaminase (Activa® TI) was kindly donated by Ajinomoto Food

Ingredients (Chicago, Illinois). According to the manufacturer, the activity of this enzyme preparation is 100 units of activity per gram of powdered preparation. All other chemicals used in this research were purchased from Sigma-Aldrich (St Louis, MO). Double distilled water was used to make all solutions.

### **5.3.2 Methods**

#### **5.3.2.1 Solution Preparation**

Sodium caseinate stock solutions (6% w/w, dry weight basis) and pectin stock solutions (6% w/w, dry weight basis) were prepared in buffer solutions containing an antimicrobial to prevent microbial growth (0.04% sodium azide, 10 mM phosphate buffer, pH 7). Stock solutions were mixed for 30 min using a mechanical stirrer (speed 7, Stedfast Stirrer Model SL 1200, Thermo Fisher Scientific, Waltham, MA). Initially, the sodium caseinate stock solution had a pH of ~6.8 and the pectin stock solution had a pH of ~3.8, and so both solutions were adjusted to pH 7.0 by adding sodium hydroxide (4 M) solution. The stock solutions were then centrifuged for 2 hours at 10,000 g to sediment and remove any insoluble matter.

#### **5.3.2.2 Emulsion Preparation**

Fish oil-in-water emulsions (20% oil vol/vol) stabilized with either 1.87% (w/w) sodium caseinate or 1.87% (w/w) Tween 20 were formed from fish oil, sodium caseinate or Tween 20, and buffer solution (0.04% sodium azide, 10 mM phosphate buffer, pH 7). For all emulsions, the ratio of oil to emulsifier was maintained at 10:1 by weight. Fish oil

previously frozen in a -40°C freezer was quickly defrosted under cold running water prior to emulsion formation. A coarse emulsion was formed first by blending this mixture at medium speed for 2 minutes with a high speed blender (Tissue Tearor Model 985370-395, Biospec Products Inc., Bartlesville, OK). The coarse emulsion was then homogenized with a high pressure homogenizer (Microfluidizer Model 110 L, Microfluidics, Newton, MA) for 3 passes at a chamber pressure of 11,000 psi. To prevent oil degradation, ice was used to cool the interaction chamber and the surrounding metal piping. For both the casein stabilized emulsion and the Tween 20 stabilized emulsion, representative aliquots of each emulsion were diluted with 10 mM phosphate buffer pH 7 to a final oil concentration of 1% oil (v/v). Sodium azide was added to each diluted emulsion such that the concentration of sodium azide remained at 0.04% (w/w).

### **5.3.2.3 Formation of Filled Hydrogel Microspheres**

Equal weights of 6% w/w sodium caseinate and 6% w/w pectin stock solutions were mixed together, the pH was checked and adjusted to pH 7 if necessary with 4 M sodium hydroxide, and the mixture was then stirred for 30 min at speed 7 (Stedfast Stirrer Model SL 1200, Thermo Fisher Scientific, Waltham, MA). Following stirring, this mixture was transferred to 500 ml centrifuge bottles and centrifuged at 10,000 g for 2 hours at 20 °C. Preliminary experiments confirmed that 2 hours of centrifugation was sufficient for complete phase separation. Following centrifugation, the samples were allowed to settle until distinct upper and lower phases were visible. The upper and lower phases were then carefully separated.

Filled hydrogel microspheres were formed from a mixture of 5% (vol/vol) casein-rich phase, 90% (vol/vol) pectin-rich phase, and 5% (vol/vol) of a 20% (vol/vol) fish oil-

in-water emulsion. Thus, the final mixture contained 1% (vol/vol) fish oil. This mixture was then stirred with an overhead stirrer (Stedfast Stirrer Model SL 1200, Thermo Fisher Scientific, Waltham, MA) at 300 rpm for 30 minutes to ensure homogeneity. During mixing, the pH of the mixture was measured and adjusted to pH 7 with 4 M sodium hydroxide if necessary. After this initial premixing, the system was acidified by adding one drop of 1 M citric acid every 10 seconds as the mixture was stirred at 300 rpm until it reached pH 5.

Following the formation of an O/W/W emulsion, the enzyme transglutaminase was used to cross-link the casein present within the aqueous dispersed phase. To aid in the dispersion of transglutaminase, 1 gram of powdered Activa® TI was dissolved in 10 ml of 10 mM phosphate buffer adjusted to pH 5 and stirred for several minutes before adding this solution to the mixture of filled hydrogel microspheres. The mixture of filled hydrogel microspheres was then transferred to a 40 °C water bath, and the transglutaminase solution was added at a level of 10 Units of enzyme activity/ per gram of protein using an overhead stirrer at a speed of 300 rpm for agitation. This mixture was then incubated with constant agitation at 300 rpm for 2 hours. To inactivate transglutaminase, the mixture was heated in a 85 °C water bath for 5 minutes with constant agitation at 300 rpm. The mixture was then immediately cooled on ice until the temperature of the mixture reached room temperature (~20 min).

Following cooling, the pH of this sample was adjusted from pH 5 to 7 using 1 M sodium hydroxide. This pH adjustment was carried out because we wanted to compare the oxidation of lipids in filled hydrogel microspheres with that in conventional casein-stabilized emulsions, but casein-stabilized emulsions are highly susceptible to

flocculation at pH 5 (Surh, et al., 2006). Preliminary studies showed that the thermal treatments associated with enzyme incubation and inactivation had no influence on the rate of lipid oxidation. Oil recovery experiments indicated that all of the fish oil added to the system was present in the final delivery systems.

#### **5.3.2.4 Sample Preparation and Storage Conditions**

For the lipid oxidation experiments, 1.5 mL of each sample was weighed into 10 mL headspace vials, which were capped tightly and stored in the dark at 55 °C for 17 days. All samples were rocked constantly using a Labquake® Shaker (Barnstead/Thermolyne, Dubuque, IA). Oxidation experiments were performed in duplicate.

#### **5.3.2.5 Evaluation of Physical Properties of Emulsions and Filled Hydrogel Microspheres**

The particle size distribution (PSD) of all samples was measured by static light scattering using a commercial instrument (Mastersizer 2000) with a small volume sample dispersion unit (Hydro 2000 SM) (Malvern, Worcestershire, UK). For emulsion samples, a refractive index of 1.472 and absorption of 0 were used for the dispersed phase (oil), while for the hydrogel microspheres the Fraunhofer approximation was used for the dispersed phase (hydrogel). For both emulsion and hydrogel samples, the optical properties of the dispersant were set to those of water: refractive index = 1.33; absorption = 0. All samples were diluted in 10 mM phosphate buffer adjusted to pH 7, and the stirrer speed for the small volume sample dispersion unit was set to 1250 rpm. Since the filled hydrogel microspheres were difficult to disperse inside the dispersion unit, filled

hydrogel microspheres were pre-diluted at a ratio of 1 part sample:1 part buffer prior to measuring. Each sample was measured in duplicate. The parameter  $D_{3,2}$  often referred to as the average volume mean diameter was used to assess particle size. A definition of this parameter can be found on page 56.

The  $\zeta$ -potential of all samples was measured by laser doppler electrophoresis (Zetamaster, Malvern, Worcestershire, UK). Prior to measuring, samples were diluted with 10 mM phosphate buffer pH 7. Initial experiments conducted across several dilution factors confirmed that a dilution factor of 1:1000 resulted in satisfactory count rates. Previous experiments confirmed that the  $\zeta$ -potential for all samples was negative which allowed for the use of a lower modulation frequency of 250 Hz. Five  $\zeta$ -potential measurements were taken per sample injected, and each sample was measured in duplicate for a total of ten  $\zeta$ -potential readings per sample.

#### **5.3.2.6 Determination of Lipid Oxidation**

In this study, the lipid hydroperoxide concentration was used as a measure of the primary products of oxidation, while the propanal concentration was used as a measure of the secondary products of oxidation. Lipid hydroperoxides were measured using a method adapted from Nuchi, McClements, & Decker (2001). Initial lipid extraction experiments revealed that the extraction medium (isooctane/2-propanol 3:1 vol/vol) used in this method resulted in poor lipid recovery (~30% of theoretical value) for filled hydrogel microspheres. An alternate extraction procedure using chloroform:methanol, 2:1 vol/vol resulted in satisfactory lipid recovery (~100% of theoretical value). Chloroform:methanol (2:1, v/v) (Iverson, Lang, & Cooper, 2001) has been shown to be a

superior solvent for lipid extraction from biological tissue when compared to less toxic alkane:alcohol mixtures such as isooctane:2-propanol or hexane:2-propanol. Studies have shown that mixtures of chloroform:methanol tend to extract more of the polar lipids from biological tissues than alkane/alcohol mixtures (Tanamati, Oliveira, Visentainer, Matsushita, & de Souza, 2005; Aryee & Simpson, 2009). According to Christie (1993), an ideal solvent for lipid extraction must have sufficient polarity such that it can extract lipids from biological tissues and from biomacromolecules such as proteins and polysaccharides. Thus, the superior performance of chloroform:methanol over isooctane:2-propanol could be attributed to its greater polarity. Thus for lipid extraction, 1 mL of emulsion or filled hydrogel microspheres was vigorously vortexed three times with 7.5 mL of chloroform: methanol (2:1 vol/vol) followed by centrifugation for 5 minutes at 1300 g.

Following centrifugation, 0.2 mL of the chloroform/methanol extract (lower layer) was carefully removed and mixed with 2.8 mL of methanol/1-butanol (2:1 vol/vol). Depending on the concentration of hydroperoxides, the chloroform/methanol extract was diluted with solvent such that the final absorbance of the reacted sample remained below 1.0. This mixture (3.0 mL) was then reacted with 15  $\mu$ L of 3.94 M ammonium thiocyanate and 15  $\mu$ L of ferrous iron solution (prepared by reacting 0.132 M barium chloride and 0.144 M ferrous sulfate). The mixture was vortexed and allowed to react for 20 minutes at room temperature in the dark before the absorbance of the sample was measured at 510 nm using a spectrophotometer. The concentration of hydroperoxides was determined based on a standard curve of cumene hydroperoxide (0-20  $\mu$ M).

The above method has been used in our laboratory to measure hydroperoxide formation in conventional oil-in-water emulsion systems. To confirm that this method was suitable for filled hydrogel microspheres, an initial experiment was conducted using a casein stabilized 20% (vol/vol) hexadecane (a nonoxidizing lipid source) oil-in-water emulsion to which a known quantity of cumene hydroperoxide was added. This emulsion was then either diluted in buffer to 1% (vol/vol) hexadecane or incorporated into filled hydrogel microspheres at a final concentration of 1% (vol/vol) hexadecane. Recovery of hydroperoxides from filled hydrogel microspheres was relatively high ( $\approx 85\%$  relative to the recovery of hydroperoxides in casein-stabilized emulsions), and so this method was deemed suitable for filled hydrogel microspheres.

Propanal concentrations were measured using a Shimadzu 17A gas chromatograph equipped with an AOC-5000 autosampler (Shimadzu, Kyoto, Japan). Each sample consisted of 1.5 mL of sample per 10 mL GC vial, and all vials were sealed with aluminum screw caps with PTFE/silicone septa. Each vial was preheated at 45°C for 15 minutes prior to injection. Volatiles were absorbed onto a 50/30  $\mu\text{m}$  DVB/Carboxen/PDMS solid-phase microextraction (SPME) fiber needle from Supelco (Bellefonte, PA) for 2 minutes followed by desorption at the injector port (250 °C) for 3 minutes. The injection port was operated in split mode, and the split ratio was set at 5:1. Volatiles were separated using a Supelco 30 m  $\times$  0.32 mm Equity DB-1 column at 70 °C for 10 minutes with helium as a carrier gas at a flow rate of 14.0 mL/min. Detection of volatiles involved a flame ionization detector set at 250 °C. The concentration of propanal was determined based on the peak areas for a standard curve of authentic propanal.

## 5.4 Results & Discussion

### 5.4.1 Evaluation of Physical Properties of Emulsions and Filled Hydrogel Microspheres

Since the physical properties of emulsions can have a major impact on lipid oxidation, it is important to measure particle characteristics such as size and charge. The particle size distributions of all three samples from this study (1% fish oil in Tween 20-stabilized emulsions, casein-stabilized emulsions, or filled hydrogel microspheres) are shown in Figure 5.2. The mean particle diameters ( $d_{32}$  and  $d_{43}$ ) calculated from the particle size distributions are shown in Table 5.1. As would be expected, the conventional oil-in-water emulsions contained smaller particles than the filled hydrogel microspheres. Emulsions stabilized by Tween 20 and casein had fairly similar particle

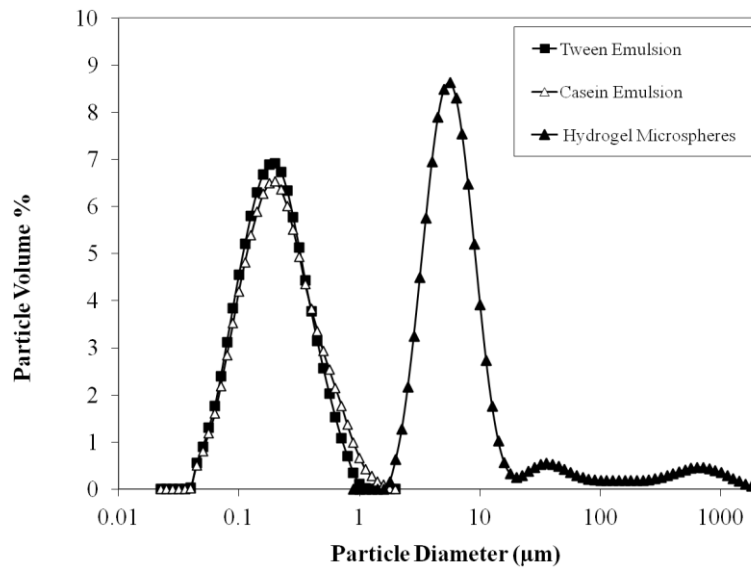


**Figure 5.2:** Particle size distribution of casein stabilized emulsion, Tween stabilized emulsion, and filled hydrogel microspheres

**Table 5.1:** Particle size diameter and zeta potential of tween stabilized emulsion, casein stabilized emulsion, and cross-linked filled hydrogel particles (Results shown are of samples from the first oxidation study. Similar results were observed for replicate study.)

<b>Sample</b>	<b>D 3,2 (µm)</b>	<b>D 4,3 (µm)</b>	<b>Zeta Potential</b>
<b>Tween Emulsion</b>	0.15	0.22	-28.5
<b>Casein Emulsion</b>	0.16	0.25	-39.4
<b>Filled Hydrogel Microspheres</b>	5.36	47.39	-29.2

size distributions and mean particle diameters, which suggests that their particle size was mainly determined by the homogenization conditions, rather than emulsifier type. The large size of the hydrogel microspheres can be attributed to the fact that they were formed using relatively mild shearing conditions, rather than intense homogenization conditions

The overall scattering pattern of filled hydrogel particles will be the result of light scattered from the hydrogel particles themselves as well as from the lipid droplets trapped within them. For this reason, we also used optical microscopy to examine the microstructure of the filled hydrogel microsphere suspensions. The microscopy images of the microspheres, in combination with previous confocal microscopy images of similar samples, suggested that the majority of the oil droplets were encapsulated within the hydrogel microspheres (Figure 5.3).

Electrical charge ( $\zeta$ -potential) measurements of the particles in the emulsions and microsphere suspensions indicated that they were all negative at pH 7 (Table 5.1). The casein stabilized-emulsion had a larger charge (more negative) than either the filled hydrogel microspheres or the Tween 20 stabilized-emulsion. The electrical charge on protein stabilized emulsions is strongly dependent on the pH of the system compared to

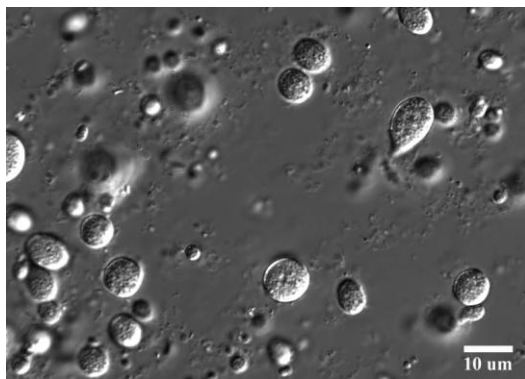


**Figure 5.3:** Microstructure of filled hydrogel microspheres determined by optical microscopy with differential interference contrast (DIC).

the isoelectric point (pI) of the adsorbed proteins (McClements, 2005). The negative charge on the droplets in the casein-stabilized emulsion can therefore be attributed to the fact that the pH was above the pI of casein ( $\approx 4.6$ ) (Kinsella, 1984). Although Tween 20 is a nonionic surfactant, previous studies have shown that emulsions containing this emulsifier are negatively charged at higher pH (Hsu & Nacu, 2003), which has been attributed to preferential adsorption of anionic species to the droplet surfaces (such as hydroxyl ions or free fatty acids). The electrical charge on filled hydrogel microspheres was less negative than that of the casein stabilized emulsion, which may be because the microspheres are comprised of a mixture of casein and pectin.

#### **5.4.2 Lipid Oxidation in Filled Hydrogel Microspheres and Emulsions**

The purpose of this set of experiments was to compare the oxidative stability of filled hydrogel microspheres to that of conventional oil-in-water emulsion systems emulsified with either a synthetic nonionic surfactant (Tween 20) or a protein (sodium caseinate). In particular, we wanted to establish whether embedding the lipid droplets

within a hydrogel matrix containing high concentrations of antioxidant protein (casein) would be more effective at inhibiting lipid oxidation than simply having a thin layer of casein molecules around each oil droplet surface. The formation of hydroperoxides during storage at 55 °C was monitored for samples containing 1% fish oil in Tween 20 emulsions, casein emulsions, or filled hydrogel microspheres (Figure 5.4). The hydroperoxide concentration in the Tween 20 emulsions increased sharply after 3 days of storage, and then declined after further storage, which can be attributed to conversion of these primary oxidation products to secondary oxidation products. The casein emulsion and the filled hydrogel microspheres showed modest increases in hydroperoxide levels from 0 to 12 days storage, and then the hydroperoxide levels decreased. To account for

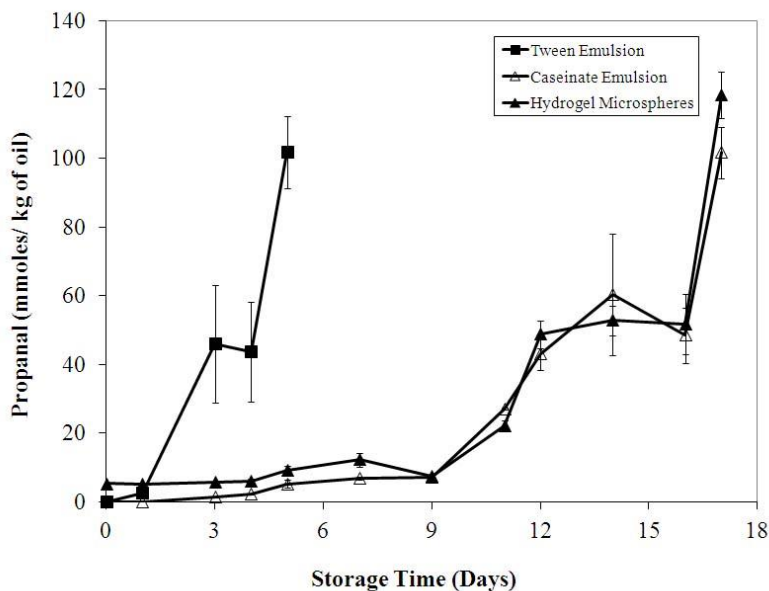


**Figure 5.4:** Concentration of primary reaction products (hydroperoxides) formed during storage at 55 °C detected in casein stabilized emulsions, Tween stabilized emulsions, and filled hydrogel microspheres.

the lower recovery of hydroperoxides from hydrogel microspheres compared to the recovery from conventional emulsions, peroxide values for hydrogel samples were increased by 15% as determined previously (see section 5.3.2.6) . Nevertheless, even accounting for differences in recovery the amount of peroxides produced was still higher from the casein emulsions than from the filled hydrogel microspheres. Both filled hydrogel microspheres and casein emulsion samples exhibited similar trends in terms of the onset, peak, and decline of hydroperoxides. The formation of propanal, a secondary product of lipid oxidation, followed a trend similar to that of peroxide formation (Figure 5.5). Propanal levels increased sharply for the Tween 20 emulsion after 3 days of storage while propanal levels only increased appreciably for the casein emulsions and filled hydrogel microspheres after 9 days storage.

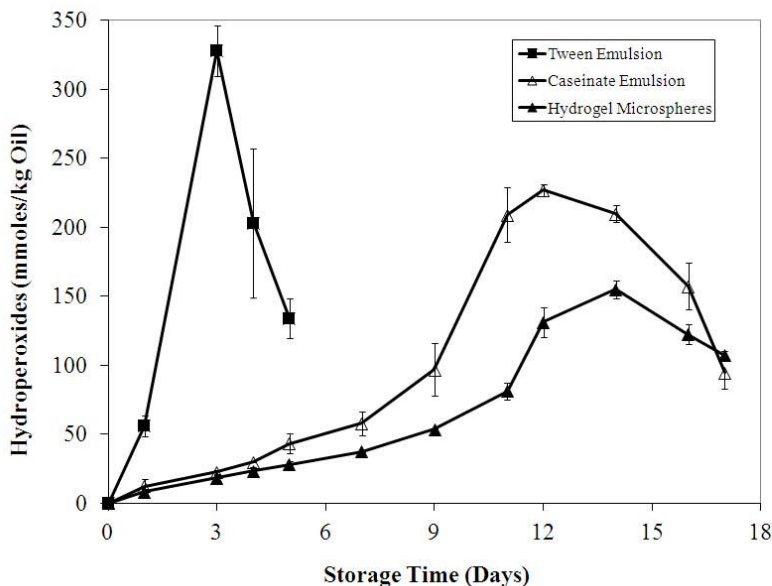


**Figure 5.5:** Concentration of secondary reaction products (propanal) formed during storage at 55 °C detected in casein stabilized emulsions, Tween stabilized emulsions, and filled hydrogel microspheres

Based on our results, it is clear that the Tween 20 emulsion oxidized faster than either the casein emulsion or the filled hydrogel microspheres. Food proteins such as casein are known to have antioxidant properties including scavenging free radicals and chelating pro-oxidant metals like iron (Elias, et al., 2008). In particular, casein contains phosphoserine residues that are capable of binding transition metals (Rival, et al., 2001; Díaz, Dunn, McClements, & Decker, 2003). Thus, it would make sense that the system not containing protein (i.e. the Tween 20 stabilized emulsion) would oxidize significantly faster than systems that did contain protein. However, it is not clear what is the predominant antioxidant mechanism of the casein in the two protein stabilized emulsions. In both emulsions it be expected that any protein not absorbed to the emulsion droplet surface or entrapped in microspheres would partition into the continuous phase. This aqueous phase protein could bind transition metals and inhibit them from interacting with the lipids in the emulsion droplets (Faraji, et al., 2004). However, in the microspheres, there would be a greater amount of protein near the emulsion droplet and thus the casein's ability to scavenge free radicals could be more important. Although both casein stabilized emulsions had similar oxidative stability, the mechanisms by which lipid oxidation was inhibited could be different.

The fast rate of oxidation for the Tween 20 emulsion could be attributed in part to the negative droplet charge of this emulsion at pH 7. Previous work conducted on lipid oxidation of a Tween 20 stabilized fish oil emulsion showed that oxidation rates were substantially faster at pH 7 compared to pH 3. This difference was attributed to the strong association between positively charged iron, a strong promoter of lipid oxidation, and negatively charged oil droplets at neutral pH (Mancuso, McClements, & Decker, 1999).

There was little difference between the oxidation rates of the casein emulsion and the filled hydrogel microspheres. The concentration of casein present in the filled hydrogel microsphere suspensions (~2.7%) was substantially greater than the level present in the casein emulsions (~0.09%). Moreover, the design of filled hydrogel microspheres is such that emulsified oil preferentially partitions into the casein rich dispersed phase of the water-in-water emulsion, creating a high protein environment to surround and protect the emulsified oil. Several studies conducted on the oxidation of oil-in-water emulsions stabilized with casein have shown that the rate of lipid oxidation tends to decrease with increasing levels of casein (Hu, et al., 2003; Faraji, et al., 2004; Ries, et al., 2010; Kargar, Spyropoulos, & Norton, 2011). In the oxidation study conducted by Ries et al (2010), a wide range of casein concentrations (0.5-10%) were examined for their influence on the oxidation rate of a linoleic acid emulsion. In general, the extent of lipid oxidation decreased as the concentration of protein in the system increased, but this effect became less dramatic as the protein concentration was increased. Thus, it is possible that the difference in protein concentration between the filled hydrogel microspheres and the casein stabilized emulsion was not large enough to see a large difference in the oxidation rate of these two samples. In other words, there was sufficient antioxidant casein in both systems to effectively inhibit lipid oxidation.

## **5.5 Conclusions**

This study was designed to determine whether incorporating polyunsaturated lipid droplets within hydrogel microspheres containing an antioxidant protein (casein) could be used to effectively inhibit oxidation. We therefore compared the oxidative stability of fish oil incorporated into filled hydrogel microspheres, oil-in-water emulsions stabilized by a

nonionic surfactant (Tween 20), and oil-in-water emulsions stabilized by a protein (casein). Our results showed that filled hydrogel microspheres had superior oxidative stability compared to Tween 20 stabilized emulsions, but there was little difference between the oxidative stability of filled hydrogel microspheres and casein stabilized emulsions. We attribute the improved stability of both the filled hydrogel microspheres and the casein stabilized emulsions to the presence of casein as this protein is known to have good antioxidant properties.

Although there was not a significant benefit to using filled hydrogel microspheres over conventional protein-stabilized emulsions in terms of oxidative stability, there may be other reasons to justify the fabrication of these microspheres. Casein-stabilized emulsions are prone to droplet flocculation at pH values around their isoelectric point, whereas we have shown that filled hydrogel microspheres are more stable to aggregation under these conditions. In addition, filled hydrogel microspheres may prove useful for controlling the release of encapsulated components in the mouth, stomach or small intestine, which may be useful in the development of some functional foods. In summary, this study clearly demonstrates that food proteins (casein) can be highly effective at preventing lipid oxidation of emulsified lipids. The challenge is to design systems where the natural antioxidant properties of proteins can be used to their fullest potential to prevent lipid oxidation in real food matrices.

## CHAPTER 6

### INFLUENCE OF LIPID DROPLET ENCAPSULATION WITHIN BIOPOLYMER HYDROGEL MICROSPHERES ON THEIR DIGESTION: AN *IN VITRO* STUDY

#### 6.1 Abstract

The objective of this study was to determine the influence of encapsulation of protein-coated lipid droplets within biopolymer hydrogel microspheres on their digestibility by lipase. We therefore compared the *in vitro* lipid digestion of non-encapsulated (“emulsions”) and encapsulated (“filled microspheres”) casein-coated lipid droplets. Filled microspheres were fabricated from a phase separated mixture of pectin and sodium caseinate along with emulsified oil to form an oil-in-water-in-water (O/W/W) emulsion. The microspheres were then acidified, cross-linked with transglutaminase, and washed to remove excess pectin. Filled hydrogel microspheres were stable to simulated mouth conditions but formed large flocs under simulated gastric conditions. The casein stabilized emulsion showed modest droplet flocculation under simulated mouth conditions and showed significant flocculation and coalescence under simulated gastric conditions. The structure of both microspheres and emulsions was completely destroyed following *in vitro* digestion. Digestion profiles revealed similar rates of lipid digestion for both microspheres and emulsions. Results confirm that filled hydrogel microspheres are a suitable delivery system for lipophilic bioactives.

## 6.2 Introduction

Chronic disease prevention is an important public health issue for developed countries. Factors such as an aging population and increasing health care costs highlight the need for chronic disease prevention in the developed world. Nutritional therapies such as functional foods and dietary supplements represent one approach towards the prevention of chronic disease (Heurtault, et al., 2003; Eussen, et al., 2011). Although there are many definitions of functional foods, one common theme is that functional foods may provide health benefits “beyond basic nutrition”(Henry, 2010). These health benefits are usually associated with the incorporation of one or more bioactive compounds (Eussen, et al., 2011). Most bioactive compounds fall under one of three classifications, namely lipids, proteins, or carbohydrates. Of these three categories, lipophilic bioactives pose several challenges regarding their incorporation into foods. In particular, these hydrophobic compounds are difficult to incorporate into aqueous foods, and they are often highly susceptible to oxidative deterioration (McClements, et al., 2009b; de Vos, Faas, Spasojevic, & Sikkema, 2010). Thus, there is a great need to develop food grade delivery systems that can be used to encapsulate and protect lipophilic bioactives.

Emulsion-based delivery systems are excellent candidates for delivering lipophilic bioactives (McClements, et al., 2007; McClements, 2010a; Sagalowicz & Leser, 2010). One category of emulsion-based delivery system that may be particularly suitable for certain applications is filled hydrogel microspheres. These particles consist of emulsified oil droplets trapped inside a hydrogel particle matrix that is then dispersed within an aqueous medium. Filled hydrogel microspheres can be fabricated using a multistep

process. First, an oil-in-water emulsion is formed using a water-soluble emulsifier. Second, this emulsion is mixed with a biopolymer solution that is capable of phase separating into an oil-in-water-in-water (O/W/W) dispersion. Third, the environmental conditions are altered to promote hydrogel particle formation (McClements, et al., 2007; McClements, 2010a). In our system, filled hydrogel microspheres were fabricated from a phase separated mixture of high methoxy pectin and sodium caseinate. When this system is sheared an O/W/W emulsion is formed that consists of oil droplets trapped within a casein-rich particle that is dispersed within a pectin-rich phase (Matalanis, et al., 2010). To stabilize this system, this mixture is first acidified to promote the adsorption of pectin onto the surface of the casein-rich microspheres through electrostatic attraction. The enzyme transglutaminase is then used to cross-link the casein present within these microspheres, and the continuous pectin-rich phase is removed by washing.

Lipid bioavailability can be defined as the fraction of ingested lipid that ends up in systemic circulation (Versantvoort, Kamp, & Rompelberg, 2004). One of the major factors that determines the overall bioavailability of a lipid is its *bioaccessibility* or the fraction of a component that is released into the gastrointestinal tract (McClements, et al., 2009b; McClements & Li, 2010). Evaluating the bioaccessibility of a new lipid based delivery system is critical as bioactive compounds must be released in the correct location of the body, such as the small intestine or the colon for maximum adsorption and bioactivity. To assess the bioaccessibility of the lipid encapsulated in our filled hydrogel microspheres, we subjected our delivery system to a simulated gastrointestinal tract consisting of conditions designed to simulate the mouth, stomach, and small intestine. For comparison purposes, we also characterized the behavior of a conventional protein

stabilized emulsion using the same gastrointestinal model. Thus, the objective of this work was to compare the *in vitro* lipid digestion of non-encapsulated and encapsulated protein-coated lipid droplets so as to determine the potential biological behavior of filled hydrogel microspheres.

## **6.3 Materials and Methods**

### **6.3.1 Materials**

Commercial sodium caseinate was kindly donated by American Casein Company (Burlington, NJ) and was used without further purification. The percentage of protein and moisture in this material were 92% and 4.5% as reported by the manufacturer. High methoxy pectin (Genu Pectin (Citrus), USP/100) was kindly donated by CP Kelco (Lille Skensved, Denmark). The composition of this material as provided by the manufacturer was 6.9% moisture. Corn oil (Mazola, ACH Food Companies, Memphis, TN) was purchased at a local supermarket. The enzyme transglutaminase (Activa® TI) was kindly donated by Ajinomoto Food Ingredients (Chicago, Illinois). According to the manufacturer, the activity of this enzyme preparation is 100 units of activity per gram of powdered preparation. The non-polar dye Bodipy 493/503 was purchased from Invitrogen (Carlsbad, CA). Lipase from porcine pancreas, type II (L3126), bile extract (porcine, B8613), and porcine gastric mucin Type II were purchased from Sigma-Aldrich (St. Louis, MO). All other chemicals used in this research were purchased from Sigma-Aldrich (St Louis, MO). Double distilled water was used to make all solutions.

### **6.3.2 Methods**

This study was designed to simulate the digestion of filled hydrogel microspheres using a mouth, stomach, and small intestine model. A conventional sodium caseinate stabilized oil-in-water emulsion (same oil level as filled hydrogel microspheres ) was also included in this study for comparison purposes.

#### **6.3.2.1 Formation and Characterization of Phase Separated Biopolymer Mixtures**

Previous work confirmed that an equal weight mixture of 6% pectin and 6% caseinate (final concentration 3% pectin, 3% caseinate) at pH 7 will phase separate into an upper phase rich in pectin and a lower phase rich in caseinate. The relative location of these two layers can be attributed to a difference in density, with the upper phase having a lower density (~1.02 g/ml) than the lower phase (~1.04 g/ml). Thus, a sodium caseinate stock solution (6% w/w, dry weight basis) and a pectin stock solution (6% w/w, dry weight basis) were prepared in buffer solutions containing an antimicrobial to prevent microbial growth (0.04% sodium azide, 10 mM phosphate buffer, pH 7) using a mechanical stirrer (Stedfast Stirrer Model SL 1200, Thermo Fisher Scientific, Waltham, MA). Both solutions were then adjusted to pH 7.0 by adding 4 M sodium hydroxide. Equal weights of 6% w/w sodium caseinate and 6% w/w pectin stock solutions were weighed out, the pH was checked and adjusted to pH 7 if necessary, and the mixture was then stirred together (Stedfast Stirrer Model SL 1200, Thermo Fisher Scientific, Waltham, MA). Following stirring, this mixture was transferred into centrifuge bottles and centrifuged at 10,000 g for 2 hours at 20 °C. Longer centrifugation times did not change the height of the phase separated layers, indicating that 2 hours of centrifugation

was sufficient for complete phase separation. Following centrifugation, the upper and lower phases were carefully separated and stored for further analysis.

The concentration of protein in the upper and lower phases was determined by the Bradford protein assay (Bradford, 1976). A standard curve of absorbance *versus* concentration of sodium caseinate was constructed to determine the casein content of the two phases. The concentration of carbohydrate in the upper and lower phases was determined using the phenol-sulfuric acid method (DuBois, et al., 1956). A standard curve of absorbance *versus* concentration of pectin was constructed to determine the pectin content of the two phases. Once the concentration of sodium caseinate and pectin were determined for the upper and lower phases, large quantities of either phase were easily made. Thus, the upper phase was prepared by making a solution containing 4.03% (w/w) pectin and 0.22% (w/w) sodium caseinate in 10 mM phosphate buffer with 0.04% (w/w) sodium azide while the lower phase was prepared by making a solution containing 0.52% (w/w) pectin and 14.2 % (w/w) sodium caseinate in 10 mM phosphate buffer with 0.04% (w/w) sodium azide. Following dispersion, the pH of each phase was then adjusted to pH 7 with 4 M sodium hydroxide.

### **6.3.2.2 Emulsion Preparation**

An oil-in-water emulsion (20.74 % oil w/w) stabilized with 2.07% (w/w) sodium caseinate was formed from corn oil, sodium caseinate, and buffer solution (0.04% sodium azide, 10 mM phosphate buffer, pH 7). A coarse emulsion was formed first by blending this mixture at a speed of 20,000 rpm for 2 minutes with a high speed blender (Tissue Tearor Model 985370-395, Biospec Products Inc., Bartlesville, OK). The coarse emulsion was then homogenized with a high pressure homogenizer (Microfluidizer

Model 110 L, Microfluidics, Newton, MA) for 3 passes at a chamber pressure of 11,000 psi. Emulsions formed by this method had an average volume-weighted mean diameter ( $D_{4,3}$ ) of 0.37  $\mu\text{m}$  and an average surface-weighted mean diameter ( $D_{3,2}$ ) of 0.32  $\mu\text{m}$  as measured by static light scattering (Mastersizer 2000, Malvern, Worcestershire, UK).

For comparison purposes, a casein stabilized emulsion with the same oil percentage as the filled hydrogel microspheres was prepared. This emulsion was formed by diluting the emulsion prepared previously using 10 mM phosphate buffer. Sodium azide was added to this diluted emulsion such that the concentration of sodium azide remained at 0.04% (w/w). Analysis of the oil content of filled hydrogel microspheres revealed that some oil was lost during the process of forming these particles. For this reason, a sodium caseinate emulsion diluted to 2.5% (wt/wt) oil was prepared (the average oil content of the filled hydrogel microspheres as determined by fat extraction and analysis - see section 6.3.2.4).

### **6.3.2.3 Formation of Filled Hydrogel Microspheres**

A water-in-water (W/W) emulsion is formed when proportions of the isolated upper and lower phases described in section 6.3.2.1 are mixed together. When the proportion of upper phase is much greater (above ~80% vol/vol) than the proportion of lower phase, the lower phase will form the dispersed phase of the W/W emulsion, and the upper phase will form the continuous phase. The addition of emulsified oil to this W/W emulsion resulted in the emulsified oil droplets partitioning into the dispersed phase.

Filled hydrogel microspheres were formed from a mixture of 5% (vol/vol) lower phase, 90% (vol/vol) continuous phase and 5% (vol/vol) of a 20.74% (w/w) corn oil-in-water emulsion. Thus, the final mixture contained 1% (w/w) corn oil. This mixture was

then stirred with an overhead stirrer at 300 rpm, and the pH was measured and adjusted to pH 7.0 with 4M sodium hydroxide if necessary. One drop of 1 M citric acid was then added every 10 seconds under constant stirring at 300 rpm until the mixture reached pH 5. The microspheres were then cross-linked by adding a solution of transglutaminase (0.1 g transglutaminase/ml of 10 mM phosphate buffer pH 5) at a level of 10 Units of enzyme activity/ per gram of protein and incubating the mixture at 40°C for 2 hrs with constant agitation at 300 rpm. To inactivate transglutaminase, the mixture was heated in a 85 °C water bath for 5 minutes with constant agitation at 300 rpm. The mixture was then cooled on ice for 20 mins. Following cooling, the particles were washed at a ratio of 1 part particles to 4 parts of 10 mM phosphate buffer (pH 5) and then centrifuged at 10,000 g for 10 minutes. The washing solution (along with a majority of the continuous phase) was decanted, and the washed particles were resuspended in 10 mM phosphate buffer pH 7 with 0.04% sodium azide such that the final weight of particles and buffer was ¼ the initial weight of particles. This level of reconstitution was designed to achieve an initial oil level of 4% w/w in these particles. The particles were then adjusted to pH 7 using 4M sodium hydroxide. The level of oil in these particles was then determined experimentally (see section 6.3.2.4).

#### **6.3.2.4 Fat Extraction and Analysis of Filled Hydrogel Microspheres and Emulsion**

The level of oil in both the reconstituted filled hydrogel microspheres and the conventional caseinate stabilized O/W emulsion was determined by lipid extraction using chloroform:methanol, 2:1 vol/vol (Iverson, et al., 2001). Briefly, 1 gram of emulsion or filled hydrogel microspheres was vigorously vortexed three times with 7.5 mL of chloroform: methanol (2:1 vol/vol) followed by centrifugation for 30 minutes at ~2400 g.

Following centrifugation, 2 ml of the lower solvent phase was removed, and the solvent was evaporated under a stream of nitrogen. The amount of extracted oil was then determined gravimetrically. Previous experiments confirmed that oil recovery rates from filled hydrogel microspheres were ~100% of theoretical values.

### **6.3.2.5 Simulated Gastrointestinal Digestion Model**

*Simulated Mouth Conditions:* Artificial saliva was prepared according to the procedure described by Sarkar, Goh, & Singh (2009a). The level of porcine gastric mucin Type II used was 30 g/L. Equal weights of either emulsion or reconstituted filled hydrogel microspheres and artificial saliva were mixed together, and the pH was adjusted to pH 6.8. This mixture was then stirred for 5 mins.

*Simulated Gastric Conditions:* Simulated gastric fluid was prepared from a solution consisting of 2 g of sodium chloride, 7 ml of concentrated hydrochloric acid, and 3.2 g of pepsin diluted to 1 liter of solution with double distilled water. The pH of this solution was then checked and adjusted to pH 1.2 if necessary. Equal weights of the mixture obtained following simulated mouth conditions and simulated gastric fluids were mixed together, and the pH of this mixture was adjusted to pH 2.5. This mixture was then transferred to a conical flask and allowed to incubate at 37°C in an incubator shaker at 100 rev/min for 2 hrs.

*In Vitro Digestion of Lipids:* An *in vitro* digestion model described by Hu, Li, Decker & McClements (2010) was used with modifications to simulate lipid digestion in the small intestine. Briefly, a 60 g sample of the mixture obtained following simulated gastric conditions was weighed, and this mixture was transferred to a 37°C water bath. To this mixture, 2 ml of a 750 mM calcium chloride solution along with 8 ml of a bile

extract solution (46.9 mg bile/ml 10 mM phosphate buffer pH 7) were added under stirring (stirrer speed 4), and the pH was adjusted to 7. Lastly 5 ml of a lipase solution (24 mg lipase/ml 10 mM phosphate buffer pH 7) was added under stirring, and an autotitration unit (Metrohm USA, Inc.) controlled by a software program (Tiamo 1.2.1 software, Metrohm GA, Switzerland) was used to titrate the free fatty acids released during lipid digestion with 0.2 M standardized sodium hydroxide such that the pH of this system was held constant at pH 7.0. Thus, the final composition of this digestion system (75 ml total sample) contained 20 mM calcium chloride, 5mg/ml bile extract, and 1.6 mg/ml lipase. The percentage of free fatty acids (%FFA) released was calculated using the following equation:

$$\%FFA=100\times\frac{V_{NaOH}\times m_{NaOH}\times M_{lipid}}{w_{lipid}\times 2} \quad (6.1)$$

where  $V_{NaOH}$  is the volume of titrant in liters,  $m_{NaOH}$  is the molarity of sodium hydroxide,  $M_{lipid}$  is the molecular weight of corn oil taken to be 872 g/mol , and  $w_{lipid}$  is the weight of oil in the digestion system in grams. Blanks (samples without oil) were run, and the volume of titrant used for these samples was subtracted from the corresponding samples that contained oil.

#### **6.3.2.6 Evaluation of the Physical Properties of Emulsions and Filled Hydrogel Microspheres During Digestion**

In an effort to understand how simulated digestion conditions impact the physical properties of filled hydrogel microspheres and emulsions , samples of filled hydrogel

microspheres were evaluated for their size, charge, and microstructure before digestion as well as after simulated mouth conditions, after simulated gastric conditions, and after *in vitro* lipid digestion. The particle size of all samples was measured by static light scattering using a commercial instrument (Mastersizer 2000) with a small volume sample dispersion unit (Hydro 2000 SM) (Malvern, Worcestershire, UK). For emulsion samples, a refractive index of 1.472 and absorption of 0 were used for the dispersed phase (oil). For the hydrogel microspheres, the Fraunhofer approximation was used, which does not depend on particle refractive index. For both emulsion and hydrogel samples, the optical properties of the dispersant were set to those of water (refractive index = 1.33; absorption = 0). All samples were diluted in 10 mM phosphate buffer adjusted to the pH of the sample, and the stirrer speed for the dispersion unit was set to 1250 rpm. The parameter  $D_{3,2}$  often referred to as the average volume mean diameter was used to assess particle size. A definition of this parameter can be found on page 56.

The  $\zeta$ -potential of all samples was measured by laser doppler electrophoresis (Zetamaster, Malvern, Worcestershire, UK). Prior to measuring, samples were diluted with 10 mM phosphate buffer adjusted to the pH of the sample. Initial experiments conducted across several dilution factors confirmed that a dilution factor of 1:1000 resulted in satisfactory count rates. Previous experiments confirmed that the  $\zeta$ -potential for all samples was negative which allowed for the use of a lower modulation frequency of 250 Hz. Five  $\zeta$ -potential measurements were taken per sample injected.

To observe the structural changes that occurred during digestion, confocal microscopy images were taken of all samples. To observe the oil phase, the hydrophobic dye Bodipy 493 (0.1 mg/mL) was added to corn oil, and this mixture was covered and

stirred overnight. This dyed oil was then used to form a microfluidized emulsion as described in section 6.3.2.2. For the filled hydrogel microspheres, Rhodamine B was used to visualize the protein present in these particles. Rhodamine B was first dissolved in double distilled water at a concentration of 0.05% w/v. This solution was then added at a concentration of 5  $\mu\text{L/g}$  of mixture into the mixture of 5% (vol/vol) lower phase, 90% (vol/vol) continuous phase, and 5% (vol/vol) of a 20.74% (w/w) corn oil-in-water emulsion dyed with Bodipy 493. This mixture was then acidified, cross-linked, washed, and reconstituted as described in section 6.3.2.3. Fixed slides of all samples were magnified using a microscope (Nikon D-Eclipse C1 80i, Nikon, Melville, NY) with an oil immersion objective lens (60 $\times$ , 1.40 NA). An air cooled argon ion laser Model IMA1010 BOS (Melles Griot, Carlsbad, CA) was used to excite Bodipy 493 at 488 nm. Emission spectra for Bodipy 493 were detected in the 515 nm channel equipped with a narrow pass filter (HQ 515/30m). Rhodamine B was excited with a 543 nm Melles Griot helium-neon laser Model 05-LGP-193 (Melles Griot, Carlsbad, CA) and detected in the 605 nm channel (HQ 605LP/75m). The pinhole size was set at 33.3  $\mu\text{m}$ . All images were taken and processed using the instruments software program (EZ- CS1 version 3.8, Nikon, Melville, NY). In addition to microscopy, photographs were taken of samples prior to digestion and during the digestion process. To visualize the oil fraction in these samples, Nile Red (0.1 mg/ml) was first dissolved in heated corn oil and allowed to stir overnight. This dyed oil was then used to form a microfluidized emulsion as described in section 6.3.2.2. The dyed emulsion was then used to form the filled hydrogel microspheres as well as for the emulsion sample. All samples were photographed following overnight storage at room temperature.

### **6.3.2.7 Statistical Analysis**

All experiments were carried out in at least duplicate using freshly prepared samples. In vitro digestion profiles were performed in triplicate on freshly prepared samples. One-way ANOVA tests were used to test significance of parameter means.

## **6.4 Results and Discussion**

### **6.4.1 Characterization of Emulsions and Filled Hydrogel Microspheres During Digestion**

The purpose of this set of experiments was to gain a better understanding of the physical changes that occur during simulated digestion of filled hydrogel microspheres. For comparison, a standard protein-stabilized emulsion was also examined. Thus, filled hydrogel microspheres and emulsion samples were subjected to simulated mouth (pH 6.8), stomach (pH 2.5), and intestine (pH 7) conditions to simulate lipid digestion. The particle size, charge, microstructure, and macrostructure were measured initially and after each step of the digestion model.

#### **6.4.1.1 Particle Size and Electrical Charge**

*Initial:* As expected, the initial particle diameter of the filled hydrogel microspheres ( $D_{3,2} = 3.5 \mu\text{m}$ ) was appreciably larger than the emulsion sample ( $D_{3,2} = 0.2 \mu\text{m}$ ) (Figure 6.1). The initial electrical charge ( $\zeta$ -potential) was negative for both the filled hydrogel and emulsion samples (Figure 6.2). The electrical charge was more

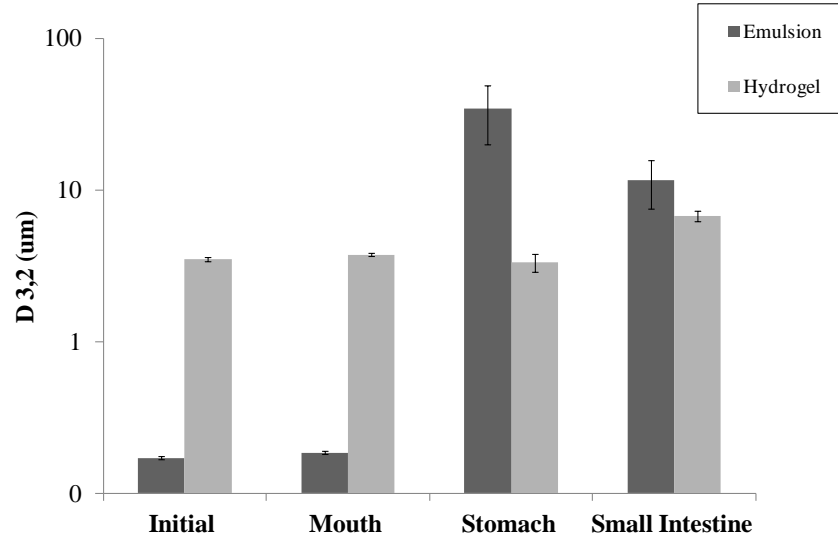


**Figure 6.1:** Particle size (D 3,2) (um) for emulsion and hydrogel samples prior to digestion and following simulated digestion in the mouth, stomach, and small intestine.

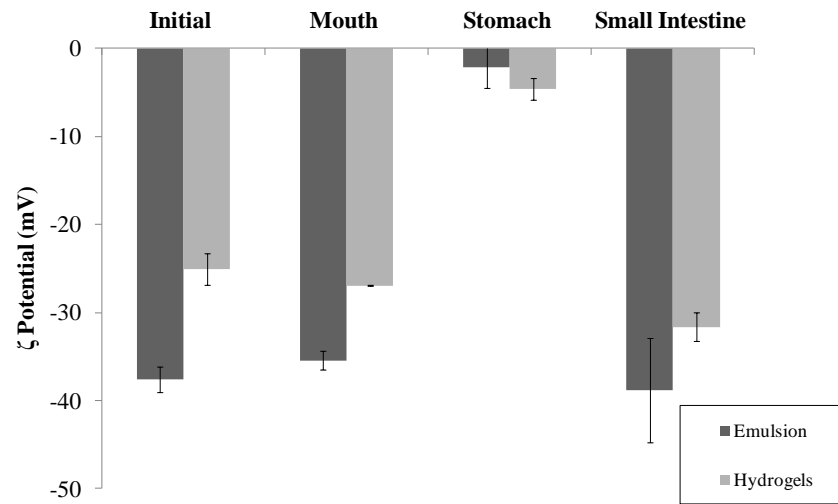


**Figure 6.2:** Zeta potential measurements for emulsion and hydrogel microspheres prior to digestion and following simulated digestion in the mouth, stomach, and small intestine

negative on the emulsion droplets than on the hydrogel microspheres. This difference could be because the hydrogel sample contained both pectin and casein while the emulsion sample contained only casein.

*Oral Conditions:* Following exposure to simulated oral conditions, both samples showed little difference in particle size diameter. Since the pH of the mouth (pH 6.8) was quite similar to the pH of the initial samples (pH 7), there was almost no change in the electrical charge for either sample (Figure 6.2).

*Stomach Conditions:* The particle size of the filled hydrogel microspheres showed little change following exposure to simulated stomach conditions (pH 2.5) ( $D_{3,2} = 3.3 \mu\text{m}$ ). By comparison, the particle size of the emulsion sample increased dramatically ( $D_{3,2} = 34.3 \mu\text{m}$ ) following exposure to simulated stomach conditions (Figure 6.1). Casein stabilized emulsions are known to be unstable at pH values close to their isoelectric point of 4.6. This instability can be attributed to a large reduction in the electrostatic repulsion between droplets which allows for extensive droplet flocculation (Dickinson, 1997b; McClements, 2004). Although the pH of the stomach is far away from the pI of casein, the process of reducing the pH caused the sample to pass through its pI, resulting in droplet flocculation. Similar results were reported by Surh et al. (2006) for casein stabilized emulsions. Electrical charge measurements showed a dramatic reduction in the negative charge present on both samples (Figure 6.2). For the emulsion sample, the lack of a strong electrostatic repulsion between droplets ultimately resulted in droplet aggregation.

*Small Intestine Conditions:* Following exposure to simulated small intestine conditions (pH 7), the average particle size of the filled hydrogel microspheres increased

substantially to  $D_{3,2} = 6.8 \mu\text{m}$ , indicating further particle instability. The particle size of the emulsion sample actually decreased to  $D_{3,2} = 11.6 \mu\text{m}$  although it remained somewhat greater than that of the filled hydrogel microspheres sample (Figure 6.1). This decrease could be attributed to the change in the electrical charge on these droplets from almost zero at pH 2.5 to highly negative at pH 7. Under these conditions, negatively charged droplets would tend to repel each other causing disruption of flocs, thereby resulting in a lower particle size. Electrical charge measurements showed that both samples were highly negatively charged (Figure 6.2). This change is likely due to both the change in pH of the system as well as the addition of anionic species including free fatty acids and bile salts.

#### **6.4.1.2 Microstructure**

*Initial:* Confocal microscopy images of filled hydrogel microspheres prior to digestion showed the presence of green-stained oil droplets trapped within red-stained protein-rich microspheres (Figure 6.3A). By comparison, microscopy images of the emulsion sample revealed a large number of small ( $<1 \mu\text{m}$ ) oil droplets distributed throughout the sample (Figure 6.4A).

*Oral Conditions:* Exposure to simulated mouth conditions appeared to have little impact on the microstructure of the filled hydrogel microspheres beyond a simple dilution effect (Figure 6.3B). On the other hand, some droplet flocculation was observed in the emulsion sample (Figure 6.4B). One of major components of artificial saliva is mucin (Vingerhoeds, Blijdenstein, Zoet, & van Aken, 2005; Sarkar, et al., 2009a), which is known to be negatively charged at neutral pH (Bansil & Truner, 2006; Sarkar, et al., 2009a). Casein is also negatively charged at this pH, and therefore droplet flocculation

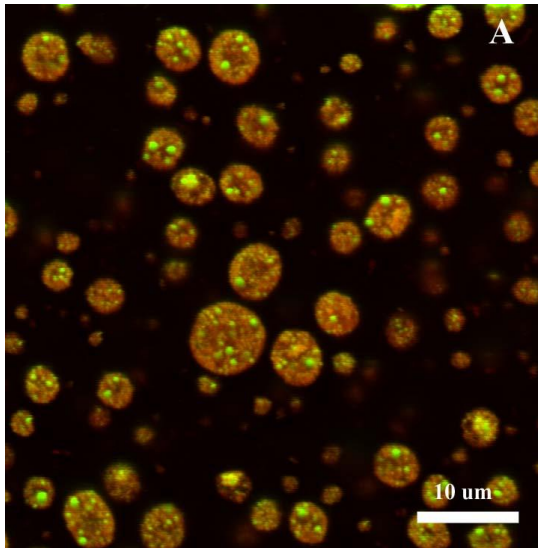


**Figure 6.3A:** Confocal micrograph of filled hydrogel microspheres prior to digestion at pH 7, oil is shown in green and protein is shown in red

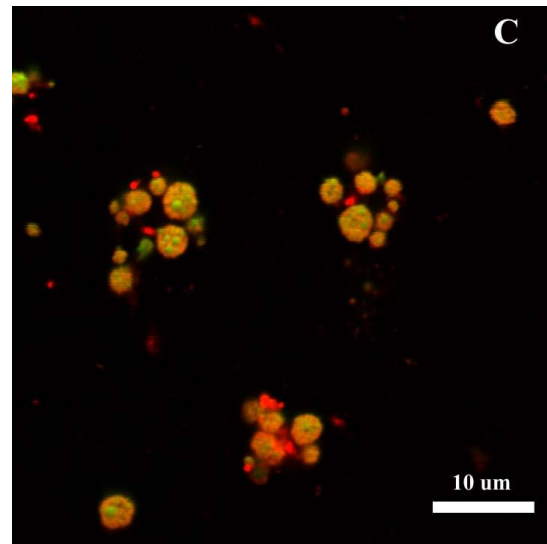


**Figure 6.3C:** Confocal micrograph of filled hydrogel microspheres following simulated gastric conditions at pH 2.5, oil is shown in green and protein is shown in red

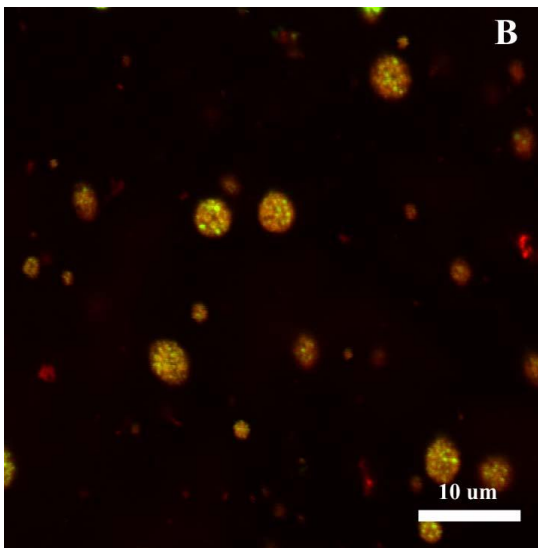


**Figure 6.3B:** Confocal micrograph of filled hydrogel microspheres following simulated mouth conditions at pH 6.8, oil is shown in green and protein is shown in red

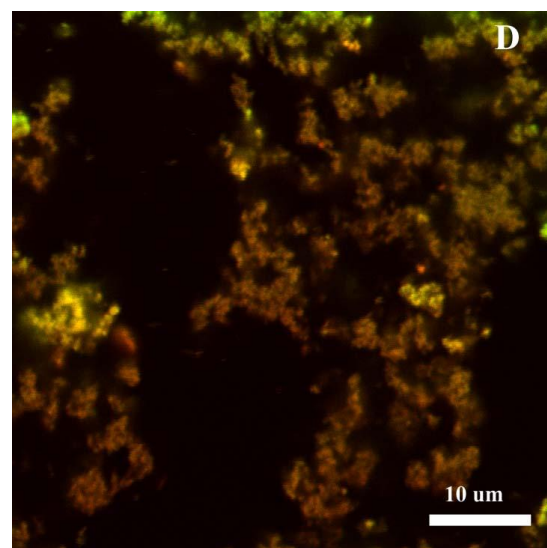


**Figure 6.3D:** Confocal micrograph of filled hydrogel microspheres following in vitro lipid digestion at pH 7, oil is shown in green and protein is shown in red

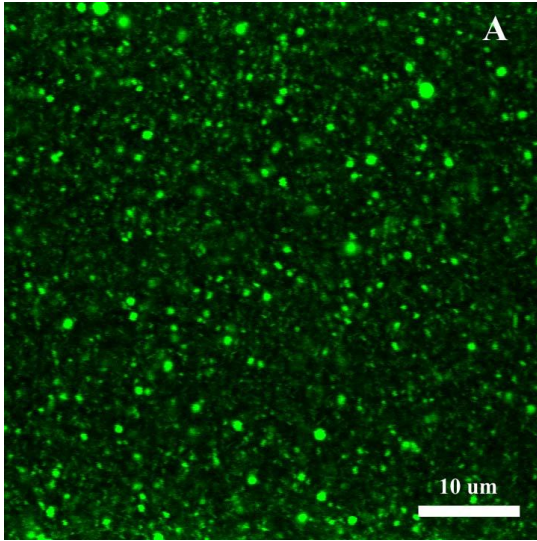


**Figure 6.4A:** Confocal micrograph of casein stabilized emulsion prior to digestion at pH 7, oil is shown in green

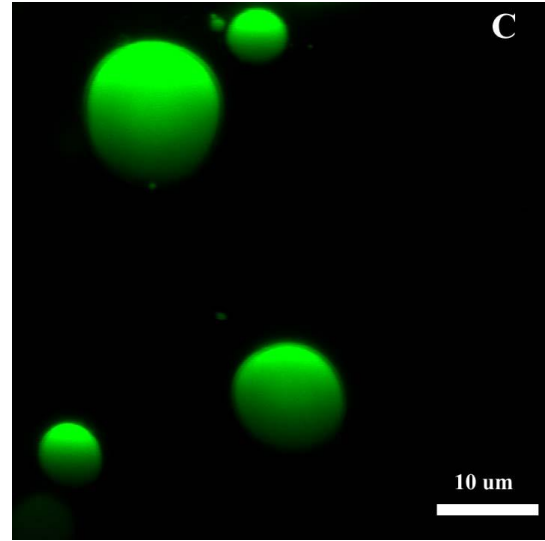


**Figure 6.4C:** Confocal micrograph of casein stabilized emulsion following simulated mouth conditions at pH 6.8, oil is shown in green

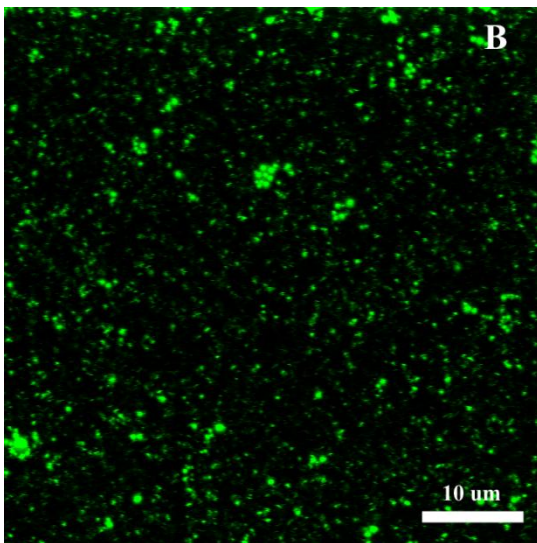


**Figure 6.4B:** Confocal micrograph of casein stabilized emulsion following simulated gastric conditions at pH 2.5, oil is shown in green

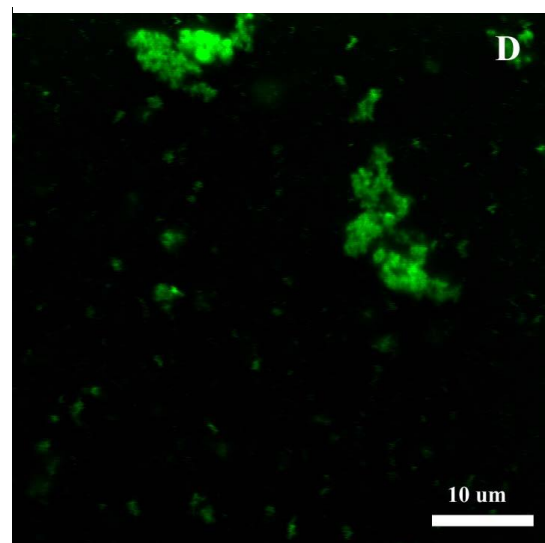


**Figure 6.4D:** Confocal micrograph of casein stabilized emulsion following in vitro lipid digestion at pH 7, oil is shown in green

due to electrostatic bridging between mucin and casein would be unlikely. The exclusion of nonadsorbing colloidal particles from the surface of emulsion droplets results in an osmotic pressure gradient which may promote depletion flocculation in emulsions (Dickinson, 2003; McClements, 2005). Mucin is also known to bind to proteins and therefore may have promoted flocculation by linking proteins on different droplets. Several other studies involving the interaction between protein-stabilized emulsions and artificial saliva at neutral pH have shown that depletion flocculation tends to occur in these systems (Vingerhoeds, et al., 2005; Silletti, Vingerhoeds, Norde, & van Aken, 2007; Sarkar, et al., 2009a).

*Gastric Conditions:* Figure 6.3C depicts the filled hydrogel microspheres sample following exposure and incubation to simulated gastric fluids (pH 2.5). Clusters of intact microspheres are clearly visible in this sample, which suggests that the particles were stable to disintegration but that they were prone to flocculation. Previous work on this system showed that filled hydrogel microspheres were stable to droplet flocculation at low pH (pH 2-3) in the absence of pepsin, despite the lack of a significant particle charge. This observation suggests that steric forces play a large role in particle stability at low pH. Thus, it is possible that pepsin present in the simulated gastric fluid partially digested some of the protein surrounding these microspheres. This would result in a loss in steric repulsion between individual microspheres, resulting in the formation of clusters of microspheres. Emulsion flocculation has been noted in a number of *in vitro* digestion studies following simulated gastric digestion, and a loss in steric repulsion has been

suggested as a possible explanation for the observed flocculation (Sarkar, Goh, Singh, & Singh, 2009b; Macierzanka, Sancho, Mills, Rigby, & Mackie, 2009; Golding, et al., 2011).

By comparison, confocal images of the sodium caseinate emulsion following simulated gastric digestion revealed the presence of large ( $>10\ \mu\text{m}$ ) oil droplets indicating that the initial structure of the emulsion was lost in this sample (Figure 6.4C). As suggested by Golding and Wooster (2010), protein-stabilized emulsions tend to flocculate upon exposure to the acidic conditions used to simulate gastric digestion as the protein passes through its isoelectric point. Coalescence of the flocculated emulsion then begins to take place as the protein present on the droplet surface is digested by pepsin (Golding Wooster, 2010).

*Small Intestine Conditions:* As shown in Figure 6.3D, the structure of filled hydrogel microspheres was completely lost following *in vitro* digestion (pH 7). The absence of lipid droplets in this sample indicates that the encapsulated droplets were readily released from these microspheres and that nearly all of the lipid droplets were digested by pancreatic lipase. The structure of the casein stabilized emulsion sample following *in vitro* digestion is shown in Figure 6.4D. Recent studies conducted in our laboratory using a similar *in vitro* digestion system for protein-stabilized emulsions showed that a relatively large number of undigested lipid droplets remained intact following *in vitro* lipid digestion (Sandra, Decker, & McClements, 2008; Hur, Decker, & McClements, 2009). Our results, however, show that our emulsion sample was completely or nearly completely digested after 2 hours. This result is in agreement with

Li and McClements (2011) as no lipid droplets were observed for a conventional protein ( $\beta$ -lactoglobulin) stabilized emulsion following *in vitro* lipid digestion.

#### **6.4.1.3 Macrostructure**

In this set of experiments, both samples were prepared using oil dyed with Nile Red. Changes to the distribution of the oil in these samples was then monitored during the digestion process. As shown in Figure 6.5A, there was little change to the overall appearance of the filled hydrogel microsphere system until after the small intestinal stage (sample IV). According to Dahan and Hoffman (2006), the upper clear yellow layer in sample IV consists of lipid digestion products solubilized by bile salts in mixed micelles and vesicles. The lower layer of sample IV most likely consists of insoluble material including calcium soaps of free fatty acids and undigested protein and pectin. As for the emulsion sample, little change can be seen between the initial emulsion and the emulsion after experiencing simulated mouth conditions (Figure 6.5B, sample II). Exposure to simulated gastric conditions resulted in significant creaming of emulsified oil (sample III) which confirms the instability of this emulsion to the acidic conditions of simulated gastric fluid. Following *in vitro* digestion, the emulsion (sample IV) consisted of two layers, a large turbid upper phase and a small lower opaque layer.

#### **6.4.2 In Vitro Lipid Digestion of Emulsion and Filled Hydrogel Microspheres**

Since filled hydrogel microspheres are a new type of delivery system for lipophilic bioactives, it is important to assess the digestibility of any lipids encapsulated

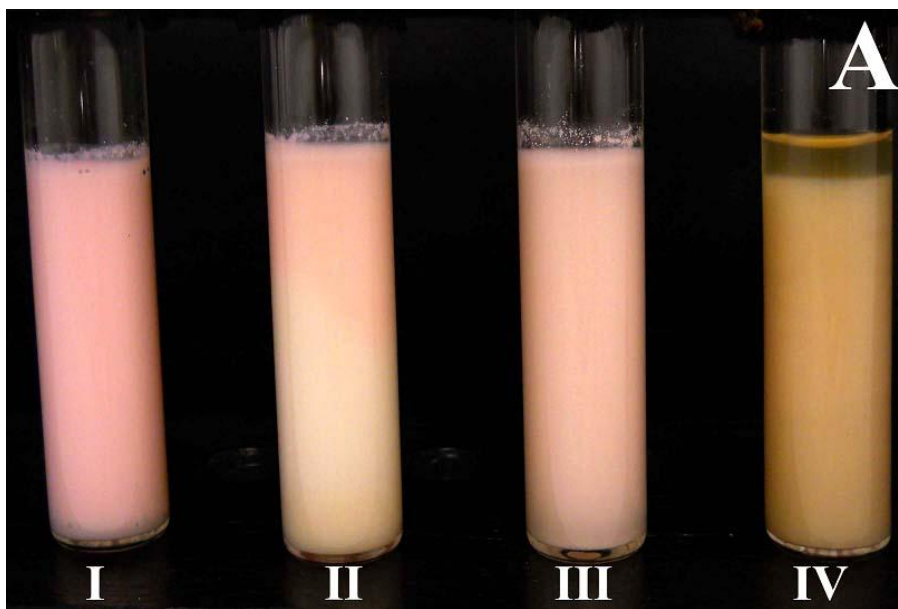


**Figure 6.5A:** Photograph of filled hydrogel microspheres prior to digestion (I), following simulated mouth conditions (II), following simulated gastric conditions (III), and following in vitro lipid digestion (IV), oil dyed in red

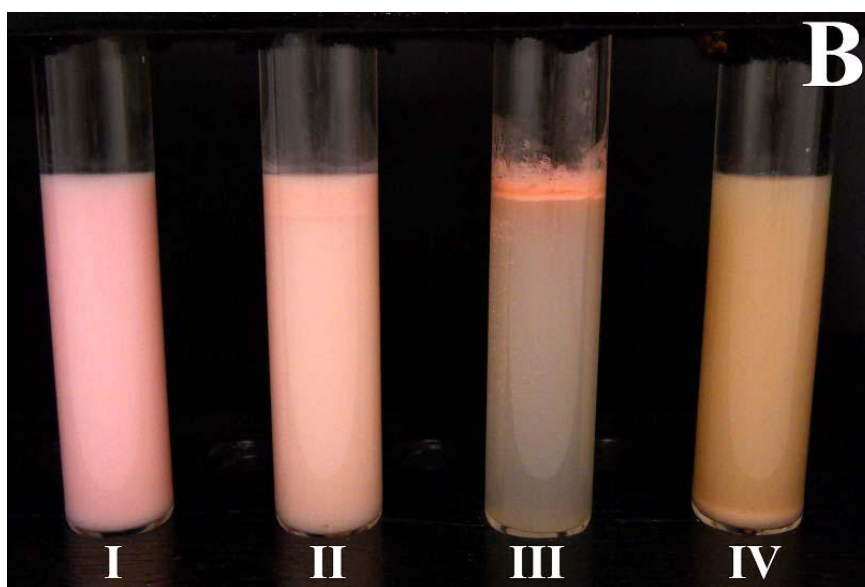


**Figure 6.5B:** Photograph of emulsion sample prior to digestion (I), following simulated mouth conditions (II), following simulated gastric conditions (III), and following in vitro lipid digestion (IV), oil dyed in red

within them. Thus, the objective of this set of experiments was to compare the *in vitro* digestibility of lipid droplets in filled hydrogel microspheres with those in a conventional emulsion at the same oil content.

Figure 6.6 shows the percentage of free fatty acids (% FFA) released from the emulsion and filled hydrogel microsphere samples over the course of a two hour digestion period. Based on these profiles, both the filled hydrogel microspheres as well as the protein stabilized emulsion were digested at similar rates, and the lipid present in these samples was completely digested within two hours of *in vitro* digestion. In addition to comparing these two samples, we also wanted to determine the influence of the addition of pepsin to our simulated gastric fluid on the *in vitro* digestion of our microspheres. Initial results showed little difference in the *in vitro* lipid digestibility of our microspheres with or without pepsin (data not shown).

In an effort to confirm this observation statistically, a mathematical *in vitro* digestion model developed by Li and McClements (2010) was applied to our experimental data, and the parameter  $k$  ( $\mu\text{mol sec}^{-1} \text{m}^{-2}$ ) which is related to the rate of digestion was calculated using the solver function in Excel. Average values for  $k$  were quite similar for both filled hydrogel microspheres ( $k=0.16 \text{ umol sec}^{-1} \text{ m}^{-2}$ ) and emulsion ( $k=0.17 \text{ umol sec}^{-1} \text{ m}^{-2}$ ), and a one-way ANOVA test confirmed that there was no significant difference for the digestion rate ( $k$ ) between these two samples. It is interesting to note that digestion profiles for these samples were quite similar despite their structural differences following simulated gastric conditions. As previously

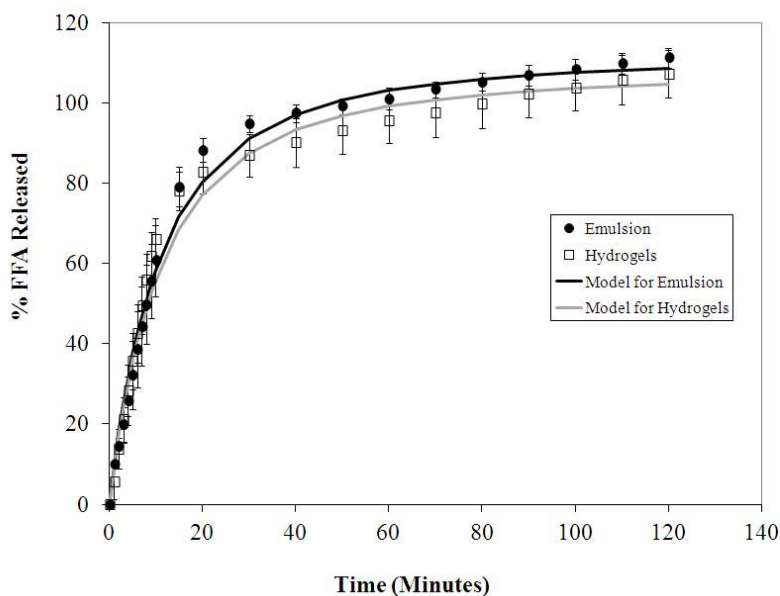


**Figure 6.6:** % Free fatty acids (FFA) released versus time (minutes) for filled hydrogel microsphere and emulsion samples during in vitro lipid digestion at pH 7

discussed in section 6.4.1.2, flocs consisting of individual filled hydrogel microspheres could be seen while the structure of the protein stabilized emulsion was completely lost following simulated gastric conditions. Our results agree with several other *in vivo* studies which found that emulsions that were stable in the stomach were digested in the small intestine at similar rates as emulsions that were unstable in the stomach (Marciani, et al., 2007; Marciani, et al., 2009; Golding, et al., 2011).

## 6.5 Conclusions

This study was designed to compare the lipid digestion of emulsified oil encapsulated within protein-rich filled hydrogel microspheres to that of a conventional protein stabilized O/W emulsion using an *in vitro* gastrointestinal model. Furthermore,

this work was designed to evaluate particle characteristics such as size, charge, and structure during the digestion process. According to our *in vitro* digestion model, this study shows that lipids encapsulated inside hydrogel microspheres were digested at the same rate as those in conventional emulsions. One important characteristic for any lipophilic delivery system is bioaccessibility or the fraction of the lipophilic bioactive that is released by a food matrix into the digestive juices (McClements & Li, 2010). This work confirms that the oil encapsulated inside filled hydrogel microspheres should be highly accessible to the human body, and thus, this system would be a good candidate for delivering lipophilic bioactives to the small intestine for digestion and adsorption.

## CHAPTER 7

### HYDROGEL MICROSPHERES FOR ENCAPSULATION OF LIPOPHILIC COMPONENTS: OPTIMIZATION OF FABRICATION & PERFORMANCE

#### 7.1 Abstract

Filled hydrogel microspheres consisting of small oil droplets trapped within biopolymer matrices are useful for encapsulating and delivering lipophilic bioactive agents. The aim of this study was to improve the current method of microsphere fabrication by increasing lipid loading capacity and microsphere yields, reducing the number of processing steps involved in fabrication, and creating microspheres that resist gravitational separation during storage. Filled hydrogel microspheres were fabricated from a phase separated mixture of pectin, caseinate, and emulsified oil to form an oil-in-water-in-water (O/W<sub>1</sub>/W<sub>2</sub>) emulsion. This system was then acidified and the resulting microspheres were cross-linked with transglutaminase. The order in which the biopolymer phases (W<sub>1</sub> and W<sub>2</sub>) and oil droplets (O) were mixed together did not impact the lipid loading capacity. Decreasing the proportion of the continuous biopolymer phase (W<sub>2</sub>) used in the preparation procedure increased microsphere yields; however too low proportions (60-70%) caused excessive foaming and protein coagulation. Alternative methods of fabricating filled hydrogel particles using free oil (rather than emulsified oil) proved unsuccessful, resulting in the formation of large non-encapsulated oil droplets ( $d \sim 10 \mu\text{m}$ ). Hydrogel microspheres with high stability to gravitational separation could be produced by controlling the amount of oil contained within these microspheres, since this led to density matching of the particle to the surrounding aqueous phase.

## 7.2 Introduction

A number of food and beverage products can be classified as oil-in-water (O/W) emulsions, including milk, dressings, mayonnaise, sauces, and ice cream (McClements, 2005). Recently, O/W emulsions have been used to encapsulate and deliver lipophilic bioactive components in functional foods and beverages (Yin, Chu, Kobayashi, & Nakajima, 2009; Li, Le Maux, Xiao, & McClements, 2009; Hatanaka, et al., 2010; Gudipati, Sandra, McClements, & Decker, 2010; Ozaki, et al., 2010). There has also been great interest in extending the functional performance of emulsion-based systems using structural design principles (McClements, et al., 2009b; Lesmes & McClements, 2009; McClements, 2010a). This interest in structural design has led to the development of various types of structured-emulsions, such as multilayer ( $O_M/W$ ), water-in-oil-in-water ( $W/O/W$ ), water-in-water ( $W/W$ ), and oil-in-water-in-water ( $O/W/W$ ) emulsions (McClements, et al., 2007; McClements, 2010a; Sagalowicz & Leser, 2010). These more complex structures have the potential to provide certain benefits over conventional O/W emulsions, such as reduced fat contents, enhanced stability, or targeted delivery in the body (McClements, et al., 2007; Palzer, 2009; McClements, et al., 2009b; de Vos, Faas, Spasojevic, & Sikkema, 2010; McClements, 2010a; Eussen, et al., 2011).

Filled hydrogel microspheres are an example of a  $O/W_1/W_2$  type of structured emulsion (Matalanis, et al., 2010; Matalanis & McClements, 2012). These systems consist of oil droplets (O) trapped within a hydrogel matrix ( $W_1$ ) that is dispersed within an aqueous medium ( $W_2$ ). The general scheme for forming these microspheres involves creating an O/W emulsion using a water-soluble surfactant, adding this emulsion to a solution of one or more biopolymers, and then adjusting the environmental conditions of

the system to form and stabilize the microspheres (McClements, 2010a). Typically, the diameter of the microspheres produced using this method range from 1 to 100  $\mu\text{m}$ .

One technique for fabricating filled hydrogel microspheres involves the use of a segregated mixture of biopolymers (McClements, et al., 2007; McClements, 2010a). The segregation of a mixture of two biopolymers (often a protein and a polysaccharide) tends to occur when relatively strong repulsive forces act between them as these forces cause them to separate into two phases. Each of these phases is rich in one of the biopolymers and depleted in the other (Grinberg & Tolstoguzov et al., 1997; de Kruif & Tuinier, 2001). When these phases are mixed together, a water-in-water emulsion ( $W_1/W_2$ ) is formed. Usually, the phase that represents the larger volume fraction will form the continuous phase of the W/W emulsion while the phase that represents the smaller volume fraction will form the dispersed phase (Norton & Frith, 2001; Frith, 2010). To form filled hydrogel microspheres using a mixture of segregated biopolymers, oil droplets must be incorporated into the dispersed phase of a W/W emulsion so as to form the desired O/W/W structure. Oil droplets can be incorporated either by mixing an O/W emulsion directly with the phase separated system, or by mixing the emulsified droplets with the dispersed phase and then adding the continuous phase (McClements, 2010a).

In our previous work, we fabricated microspheres from a segregated mixture of high methoxy pectin and sodium caseinate at pH 7 (Matalanis, et al., 2010; Matalanis & McClements, 2012). Upon mixing, this system formed a W/W emulsion with the dispersed phase being rich in casein and depleted in pectin and the continuous phase being rich in pectin and depleted in casein. When casein-coated oil droplets were incorporated into this system they preferentially moved into the dispersed (casein-rich)

phase, and the resulting O/W/W structure was trapped by acidifying the mixture (Matalanis, et al., 2010). To further stabilize these microspheres, an enzyme (transglutaminase) was used to cross-link the casein molecules present within the microspheres (Matalanis & McClements, 2012).

From a practical perspective, the method currently used to fabricate filled hydrogel microspheres has several disadvantages. Firstly, the amount of oil encapsulated within the hydrogel particles is relatively low (~1-3% of the overall system). Secondly, the current method is a multi-step process that requires a substantial amount of time. Third, the microspheres formed are relatively large and therefore prone to gravitational separation (sedimentation) during storage. Thus, the purpose of this study is to improve the current procedure for preparing filled hydrogel microspheres by addressing each of these issues, which may increase the commercial viability of this method in the food industry.

## **7.3 Materials and Methods**

### **7.3.1 Materials**

Commercial sodium caseinate was kindly donated by American Casein Company (Burlington, NJ) and was used without further purification. The percentage of protein and moisture in this material as reported by the manufacturer were 92% and 4.5%, respectively. High methoxy pectin (Genu Pectin (Citrus), USP/100) was kindly donated by CP Kelco (Lille Skensved, Denmark). The composition of this material as provided by the manufacturer was 6.9% moisture. Corn oil (Mazola, ACH Food Companies,

Memphis, TN) was purchased at a local supermarket. The enzyme transglutaminase (Activa® TI) was kindly donated by Ajinomoto Food Ingredients (Chicago, Illinois). According to the manufacturer, the activity of this enzyme is 100 units per gram of powdered preparation. The non-polar dye Bodipy 493/503 was purchased from Invitrogen (Carlsbad, CA). All other chemicals used in this research were purchased from Sigma-Aldrich (St Louis, MO). Double distilled water was used to make all solutions.

### **7.3.2 Methods**

The purpose of this study was to improve the current published method for fabricating filled hydrogel microspheres based on phase separation of biopolymer mixtures (Matalanis & McClements, 2012). More specifically, this study focused on the following three issues associated with microsphere fabrication: (i) increase the quantity of microspheres and the oil loading of each individual microsphere; (ii) reduce the number of processing steps associated with microsphere fabrication; (iii) produce density matched microspheres that will not sediment or cream in low viscosity liquids.

#### **7.3.2.1 Formation and Characterization of Phase Separated Biopolymer Mixtures**

Previous work confirmed that an equal weight mixture of 6% pectin and 6% caseinate (final concentration 3% pectin, 3% caseinate) at pH 7 will phase separate into an upper phase rich in pectin and a lower phase rich in caseinate. The relative location of these two layers can be attributed to a difference in density, with the upper phase having a lower density (~1.02 g/ml) than the lower phase (~1.04 g/ml). Thus, a sodium caseinate stock solution (6% w/w, dry weight basis) and a pectin stock solution (6% w/w, dry weight basis) were prepared in buffer solutions containing an antimicrobial to prevent

microbial growth (0.04% sodium azide, 10 mM phosphate buffer, pH 7) using a mechanical stirrer (Stedfast Stirrer Model SL 1200, Thermo Fisher Scientific, Waltham, MA). Both solutions were then adjusted to pH 7.0 by adding 4 M sodium hydroxide. Equal weights of 6% w/w sodium caseinate and 6% w/w pectin stock solutions were weighed out, the pH was checked and adjusted to pH 7 if necessary, and the mixture was then stirred together (Stedfast Stirrer Model SL 1200, Thermo Fisher Scientific, Waltham, MA). Following stirring, this mixture was transferred into centrifuge bottles and centrifuged at 10,000 g for 2 hours at 20 °C. Longer centrifugation times did not change the height of the phase separated layers, indicating that 2 hours of centrifugation was sufficient for complete phase separation. Following centrifugation, the upper and lower phases were carefully separated and stored for further analysis.

The concentration of protein in the upper and lower phases was determined by the Bradford protein assay (Bradford, 1976). A standard curve of absorbance *versus* concentration of sodium caseinate was constructed to determine the casein content of the two phases. The concentration of carbohydrate in the upper and lower phases was determined using the phenol-sulfuric acid method (DuBois, et al., 1956). A standard curve of absorbance *versus* concentration of pectin was constructed to determine the pectin content of the two phases. Once the concentration of sodium caseinate and pectin were determined for the upper and lower phases, large quantities of either phase were easily made. Thus, the upper phase was prepared by making a solution containing 4.03% (w/w) pectin and 0.22% (w/w) sodium caseinate in 10 mM phosphate buffer with 0.04% (w/w) sodium azide while the lower phase was prepared by making a solution containing 0.52% (w/w) pectin and 14.2 % (w/w) sodium caseinate in 10 mM phosphate buffer with

0.04% (w/w) sodium azide. Following dispersion, the pH of each phase was then adjusted to pH 7 with 4 M sodium hydroxide.

### **7.3.2.2 Emulsion Preparation**

To create an initial protein stabilized oil-in-water (O/W) emulsion, 30 % corn oil, 3% (w/w) sodium caseinate, and a buffer solution (0.04% sodium azide, 10 mM phosphate buffer, pH 7) were blended at a speed of 20,000 rpm for 2 minutes with a high speed blender (Tissue Tearor Model 985370-395, Biospec Products Inc., Bartlesville, OK) to form a coarse emulsion. This coarse emulsion was then homogenized with a high pressure homogenizer (Microfluidizer Model 110 L, Microfluidics, Newton, MA) for 3 passes at a chamber pressure of 11,000 psi to form a fine emulsion with a surface-weighted mean diameter ( $d_{32}$ ) of 0.17  $\mu\text{m}$  as measured by static light scattering (Mastersizer 2000, Malvern, Worcestershire, UK).

### **7.3.2.3 Influence of Order of Addition on Lipid Loading Capacity**

In this set of experiments, filled hydrogel microspheres were formed from a mixture of 5% (vol/vol) lower phase, 90% (vol/vol) upper phase and 5% (vol/vol) of a 30% (w/w) corn oil-in-water emulsion. All solutions were mixed using a mechanical stirrer (Stedfast Stirrer Model SL 1200, Thermo Fisher Scientific, Waltham, MA). The following three mixing procedures were compared in this study:

- **Treatment A:** The lower phase was first mixed with the O/W emulsion for five minutes at 300 rpm. The upper phase was then added, and this mixture was mixed for an additional five minutes at 300 rpm.

- **Treatment B:** The lower phase, O/W emulsion, and upper phases were mixed together simultaneously for five minutes at 300 rpm.
- **Treatment C:** The upper phase was first mixed with the O/W emulsion for five minutes at 300 rpm. The lower phase was then added, and this mixture was then mixed for an additional five minutes at 300 rpm.

Following mixing, each sample was then stirred with an overhead stirrer at 300 rpm, and the pH was measured and adjusted to pH 7.0 with 4M sodium hydroxide if necessary. One drop of 1 M citric acid was then added every 10 seconds under constant stirring at 300 rpm until the mixture reached pH 5. The microspheres formed by phase separation were then cross-linked by adding a solution of transglutaminase (0.1 g transglutaminase/ ml of 10 mM phosphate buffer pH 5) at a level of 10 Units of enzyme activity/ per gram of protein and incubating the mixture at 40°C for 2 hrs with constant agitation at 300 rpm. To inactivate transglutaminase, the mixture was heated in a 85 °C water bath for 5 mins with constant agitation at 300 rpm. The mixture was then cooled on ice for 20 mins. Following cooling, the particles were washed at a ratio of 1 part particle suspension to 4 parts of buffer solution (10 mM phosphate, pH 5) and then centrifuged at 10,000 g for 10 minutes. The washing solution (along with a majority of the continuous phase) was then decanted.

Next, the washed microspheres were analyzed for oil and moisture content. The oil content of the washed particles was determined as described below (section 7.3.2.4). Moisture content was determined using a digital moisture analyzer (MX-50, A&D Company, Limited, San Jose, CA) set at 100°C until a constant weight was achieved.

The loading capacity (LC) of each sample was then calculated using the following expression:

$$LC = \frac{L}{D} \times 100 \quad (7.1)$$

where  $L$  = the mass of lipid in 1 g of washed particles and  $D$  = the dry mass of 1 g of washed particles.

#### **7.3.2.4 Fat Extraction and Analysis of Filled Hydrogel Microspheres**

The level of oil in the washed filled hydrogel microspheres was determined by lipid extraction using chloroform:methanol, 2:1 vol/vol (Iverson, et al., 2001). Briefly, 1 gram of filled hydrogel microspheres was vigorously vortexed three times with 7.5 mL of chloroform: methanol (2:1 vol/vol) followed by centrifugation for 30 minutes at ~2400 g. Following centrifugation, 2 ml of the lower solvent phase was removed, and the solvent was evaporated under a stream of nitrogen. The amount of extracted oil was then determined gravimetrically. Previous experiments confirmed that oil recovery rates from filled hydrogel microspheres were ~100% of theoretical values.

#### **7.3.2.5 Simplification of Fabrication Method**

In an attempt to simplify the process of fabricating filled hydrogel particles, several methods that involved using “free oil” (oil that was not previously emulsified) were compared to a method that involved using emulsified oil. For all methods, the final

concentration of oil, pectin, and casein were kept the same. Thus, the following methods were compared:

- **Emulsion Method:** For this method, a “particle phase” was formed by dispersing sodium caseinate and high methoxy pectin at the same concentration as in the lower phase into a 30% oil-in-water emulsion. Concentrations of casein and pectin were based on the buffer weight of the emulsion as opposed to the total weight of the emulsion (buffer + oil). This phase was then mixed with upper phase at a ratio of 10% (vol/vol) “particle phase” and 90% (vol/vol) upper phase. The pH of the mixture was then adjusted to pH 7 using 4 M sodium hydroxide.
- **Free Oil - Simple Mixture Method:** In this method, sodium caseinate, high methoxy pectin, and corn oil were dispersed into buffer (10 mM phosphate buffer pH 7, 0.04% azide) at their final concentrations (*i.e.* at the same concentration as a mixture of 90% (vol/vol) upper phase, 5% (vol/vol) lower phase, and 5% (vol/vol) emulsified oil). Thus, 1.33% (wt/wt) sodium caseinate, 3.66% (wt/wt) high methoxy pectin, and 2.69% (wt/wt) corn oil were dispersed in buffer, and the pH of the mixture was adjusted to pH 7 using 4 M sodium hydroxide.
- **Free Oil – Complex Mixture Method:** In this method, a “particle phase” was formed by dispersing sodium caseinate and high methoxy pectin at the same concentration as in the lower phase along with free oil in buffer (10 mM phosphate buffer pH 7, 0.04% azide). This phase was then mixed with upper phase at a ratio of 10% (vol/vol) “particle phase” and 90%

(vol/vol) upper phase. The pH of the mixture was then adjusted to pH 7 using 4 M sodium hydroxide

Following formation, each sample was acidified to pH 5, cross-linked with the enzyme transglutaminase, and heat inactivated as described in section 7.3.2.3 with the exception that particles were not washed in buffer. Microspheres were then examined for their microstructure and particle size (section 7.3.2.6).

### **7.3.2.6 Evaluation of Physical Characteristics of Filled Hydrogel Microspheres**

The particle size of all samples was measured by static light scattering using a commercial instrument (Mastersizer 2000) with a small volume sample dispersion unit (Hydro 2000 SM) (Malvern, Worcestershire, UK). For emulsion samples, a refractive index of 1.472 and absorption of 0 were used for the dispersed phase (oil) and the scattering patterns were analyzed by Mie theory. For hydrogel microspheres, the Fraunhofer approximation was used, which does not depend on particle refractive index. For both emulsion and hydrogel samples, the optical properties of the dispersant were set to those of water (refractive index = 1.33; absorption = 0). All samples were diluted in 10 mM phosphate buffer adjusted to the pH of the sample, and the stirrer speed for the dispersion unit was set to 1250 rpm. The parameter  $D_{3,2}$  often referred to as the average volume mean diameter was used to assess particle size. A definition of this parameter can be found on page 56.

The  $\zeta$ -potential of all samples was measured by laser Doppler electrophoresis (Zetamaster, Malvern, Worcestershire, UK). Prior to measuring, samples were diluted with 10 mM phosphate buffer adjusted to the pH of the sample. Initial experiments

conducted across several dilution factors confirmed that a dilution factor of 1:1000 resulted in appropriate instrument count rates. Previous experiments confirmed that the  $\zeta$ -potential for all samples was negative which allowed for the use of a lower modulation frequency of 250 Hz. Five  $\zeta$ -potential measurements were taken per sample injected.

To examine the microstructure of various samples, confocal and DIC (differential interference contrast) microscopy images were taken. For DIC images, samples were viewed with a microscope (Nikon D-Eclipse C1 80i, Nikon, Melville, NY) using an oil immersion objective lens (60 $\times$ , 1.40 NA) along with a 2x camera zoom. For confocal microscopy, samples were dyed prior to particle formation. To observe the oil phase, the hydrophobic dye Bodipy 493 (0.05 mg/mL) was added to corn oil, and this mixture was covered and stirred overnight. This dyed oil was then used to form an emulsion as described in section 7.3.2.2 . For the filled hydrogel microspheres, Rhodamine B was used to stain the protein present in these microspheres. Rhodamine B was first dissolved in double distilled water at a concentration of 0.05% w/v. This solution was then added at a concentration of 5  $\mu$ L/g of sample into the mixture of “particle phase” and upper phase. This mixture was then acidified and cross-linked as described in section 7.3.2.3.

Samples were magnified using a microscope (Nikon D-Eclipse C1 80i, Nikon, Melville, NY) with an oil immersion objective lens (60 $\times$ , 1.40 NA). An air cooled argon ion laser Model IMA1010 BOS (Melles Griot, Carlsbad, CA) was used to excite Bodipy 493 at 488 nm. Emission spectra for Bodipy 493 were detected in the 515 nm channel equipped with a narrow pass filter (HQ 515/30m). Rhodamine B was excited with a 543 nm Melles Griot helium-neon laser Model 05-LGP-193 (Melles Griot, Carlsbad, CA) and detected in the 605 nm channel (HQ 605LP/75m). The pinhole size was set at 33.3  $\mu$ m.

All images were taken and processed using the instrument's software program (EZ- CS1 version 3.8, Nikon, Melville, NY).

### **7.3.2.7 Influence of Volume Ratio on Filled Hydrogel Microsphere Formation**

In order to understand how the volume proportions of upper phase and “particle phase” impact particle yield, the volume ratio of “particle phase” and upper phase was varied from 1% (vol/vol) “particle phase”/99% (vol/vol) upper phase to 40% (vol/vol) “particle phase”/60% (vol/vol) upper phase. Following formation, each sample was acidified to pH 5, cross-linked with transglutaminase, and heat inactivated as described in section 7.3.2.3 with the exception that particles were not washed with buffer.

### **7.3.2.8 Fabrication of Density Matched Filled Hydrogel Microspheres**

In an effort to fabricate filled hydrogel microspheres that will not cream or sediment in low viscosity liquids, microspheres with increasing concentrations of oil (0%, 9.1%, 18.2%, and 27.3% (w/w)) were fabricated. Initially, a concentrated “particle phase” was prepared by dissolving caseinate and pectin in a 30% corn O/W emulsion to give the same biopolymer concentrations as determined in the lower phase of the phase separated system (based on the weight of buffer in the emulsion), and then adjusting to pH 7. The concentrated “particle phase” was then mixed with different portions of lower phase that did not contain emulsified oil to form a series of “particle phases” with different oil contents. For the samples containing 0% oil, the particle phase consisted of only lower phase without emulsified oil. A mixed system was then prepared by mixing 10% (vol/vol) “particle phase” with 90% (vol/vol) upper phase. This mixture was then

acidified and cross-linked as described in section 7.3.2.3 with the exception that the particles were not washed.

Fabricated microspheres were evaluated for size, charge, microstructure, lightness ( $L^*$ ), and apparent viscosity. Lightness was measured using a colorimeter (Color Flex EZ, Hunter Lab, Reston, VA). The apparent viscosity of particle suspensions and individual biopolymer phases was measured using a dynamic shear rheometer (Kinexus rheometer, Malvern, Worcestershire, UK). A cup and bob geometry consisting of a bob with a diameter of 25 mm and a cup with a diameter of 27.5 mm was used to conduct a shear rate ramp from 0.1 to 100  $s^{-1}$  for all samples. A power model was fitted to the viscosity data to generate the flow index ( $n$ ) and consistency index ( $k$ ).

To evaluate the stability of these microspheres to sedimentation or creaming, particles were diluted at a ratio of 1 part microspheres to 99 parts 10 mM phosphate buffer pH 7 adjusted to pH 5 with 0.04% sodium azide, and 6 g of each diluted suspension was weighed out into individual glass test tubes. The initial suspensions were scanned using a laser vertical profiling system (Turbiscan Classic MA 2000, Formulacion, Wynnewood PA). Samples were stored at room temperature and rescanned after 1 and 7 days. Photographs were also taken of all samples both initially and after 1 and 7 days of storage. In an effort to reduce the time required to assess particle stability, 6 g of each diluted suspension was transferred into glass centrifuge test tubes. All samples were scanned initially, centrifuged for 1 hr at  $150 \times g$ , and then rescanned. Photographs were taken of all samples before and after centrifugation. In the case of laser vertical profiling, transmission (T%) and back-scattering (B%) profiles as a function of sample height were collected and analyzed using the instruments software program (Turbisoft

version 1.21). The change in the height of the transmission zone following storage or centrifugation was used to calculate the Sediment Index defined as follows:

$$\text{Sedimentation Index} = \frac{C}{S} \times 100 \quad (7.2)$$

where  $C$  = height of the transparent transmission zone (in mm) following storage or centrifugation and  $S$  = is the total height of the sample (in mm).

#### **7.3.2.9 Statistical Analysis**

All experiments were carried out in triplicate using freshly prepared samples.

### **7.4 Results and Discussion**

#### **7.4.1 Influence of Order of Addition on Lipid Loading Capacity**

An important criterion to consider when developing a delivery system for bioactive components is the system's loading capacity, defined as the mass of encapsulated material per unit mass of carrier material. In general, the loading capacity of a delivery system should be as high as possible to allow for the most effective and economic delivery of bioactive components (McClements, et al., 2009a). In this study, the loading capacity of filled hydrogel microspheres relies on the partitioning of oil droplets into the dispersed (casein-rich) biopolymer phase of a W/W system. Consequently, the method used to introduce the oil droplets into the system may impact its lipid loading capacity. Thus, the objective of this set of experiments was to determine

whether the order in which various phases were mixed together influenced lipid loading capacity.

Three different mixing treatments (A, B, and C) were studied to determine their influence on the lipid loading capacity. In treatment A, the emulsion was first mixed with the lower phase (caseinate-rich) and then the upper phase (pectin-rich) was added. In treatment B, all three phases (upper, lower, and emulsion) were mixed together simultaneously. In treatment C, the emulsion phase was first mixed with the upper phase and then the lower phase was added. We found little difference in the lipid loading capacity among the three treatments studied:  $LC = 67\% \pm 2\%$  for A,  $65\% \pm 2\%$  for B, and  $69\% \pm 4\%$  for C. This result shows that mixing order had little impact on the final lipid content of the microspheres. Previous research conducted on the partitioning of emulsified oil droplets in a phase separated system of 3% sodium caseinate and 3% pectin at pH 7 showed that oil droplets rapidly partitioned into the casein-rich phase after gentle mixing (Matalanis, et al., 2010). Based on these findings, one can conclude that the partitioning of emulsified oil into the casein-rich phase of the phase separated systems occurred rapidly. Consequently, the initial location of the oil droplets in the system did not have a major impact on the loading capacity of these microspheres.

#### **7.4.2 Simplification of Fabrication Method**

The current “emulsion” method for fabricating filled hydrogel microspheres requires a number of steps including: preparing both upper and lower phases; preparing an oil-in-water emulsion; mixing the upper, lower, and emulsion phases to form an O/W/W emulsion; acidifying the O/W/W emulsion; and lastly, cross-linking these microspheres with enzyme. To reduce the number of steps associated with microsphere

fabrication, two alternative methods were compared with the “emulsion” method. The final compositions of the three systems studied were the same, but the method used to prepare each system was different. In the “free oil - simple mixture” method, free oil, caseinate, and pectin were directly dispersed into buffer solution and then mixed together. In the “free oil – complex mixture” method, free oil was initially dispersed into the lower phase, and then this mixture was mixed with the upper phase.

An examination of the microstructure of the samples created by both of the “free oil” methods revealed that neither of them created filled hydrogel microspheres (Figures 7.1A,7.1B). Instead, they resulted in the formation of casein-rich particles (~1-2  $\mu\text{m}$ ) and

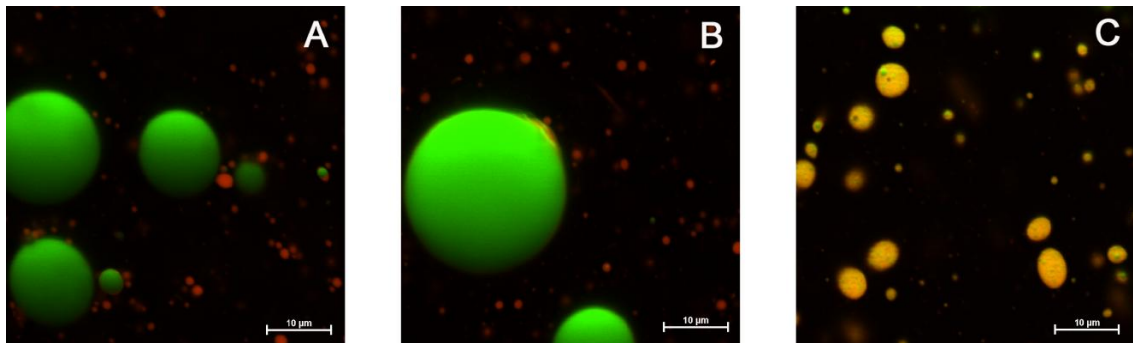


**Figure 7.1:** Confocal micrograph images of structures formed from oil, caseinate, and pectin (pH 5) using three different methods: A. the “simple mixture” method where all the components are directly mixed together; B. the “free oil method” – free oil is dispersed into the lower phase first, and then this phase is mixed with the upper phase; and C. the “emulsion” method –biopolymers are mixed with a pre-fabricated emulsion. Oil is dyed in green while protein is dyed in red, scale bar is 10  $\mu\text{m}$

large oil droplets (~10  $\mu\text{m}$ ). In contrast, the “emulsion” method produced filled hydrogel microspheres consisting of small oil droplets trapped within protein-rich particles (Figure 7.1C). A comparison of the particle size distribution of samples fabricated by the three methods further highlights the difference in their microstructures (Figure 7.2). A large

proportion of the particles in the samples fabricated using the “free oil” methods had diameters between 10 and 100  $\mu\text{m}$ , which correspond to the large oil droplets observed in the microscopy images. In contrast, the majority of particles in the sample fabricated using the “emulsion” method had diameters of 10  $\mu\text{m}$  or less, which suggests that this sample consisted of relatively small filled hydrogel microspheres. The presence of a small proportion of larger particles (10-100  $\mu\text{m}$ ) in the sample fabricated by the “emulsion” method can likely be attributed to the formation of some protein aggregates during cross-linking by transglutaminase (see section 7.4.3).

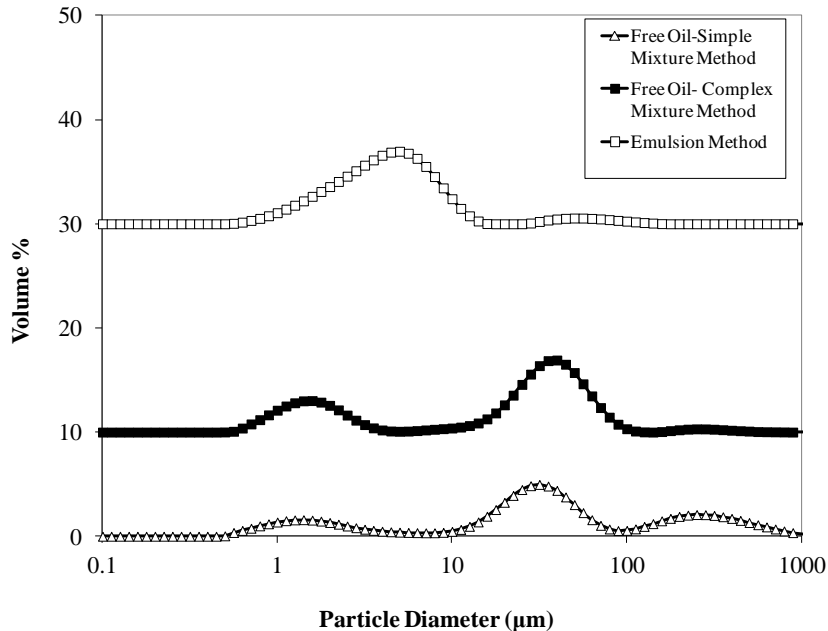


**Figure 7.2:** Particle size distribution of particles formed by the Free Oil-Simple Method., the Free Oil-Complex Method, and the Emulsion Method

The inability of either “free oil” method to form filled hydrogel microspheres maybe the result of the significantly lower interfacial tension of water-in-water emulsions

( $10^3$ - $10^4$  lower) compared to oil-in-water emulsions (Frith, 2010). Because of the low interfacial tension of water-in-water emulsions, modest shearing can cause significant droplet deformation and ultimately droplet breakup (Erni, et al., 2009). Since the interfacial tension of an oil-in-water emulsion is much greater, mild shearing will not cause substantial droplet breakup, and thus, the smaller droplets formed from the water-in-water emulsion would be unable to encapsulate the much larger oil droplets present in the system. It should be noted that although the emulsifier of the O/W emulsion used to fabricate these microspheres by the “emulsion” method is casein, the same biopolymer as the dispersed phase, other emulsifier may be used in this method. Preliminary experiments using the emulsifier Tween 20 instead of casein showed that the emulsified oil in this system preferentially migrated to the dispersed casein-rich phase. These experimental results agree with the explanation in our previous publication (Matalanis et al, 2010) that the migration of oil into the dispersed casein-rich phase is driven by a biopolymer depletion mechanism.

#### **7.4.3 Influence of Volume Ratio on Filled Hydrogel Microsphere Formation and Microstructure**

An important property of a phase separated biopolymer system is the relative volume fraction of each phase. For a two phase system, the phase that represents the larger fraction by volume will typically form the continuous phase while the phase that represents the smaller fraction by volume will form the dispersed phase (Norton & Frith, 2001; Frith, 2010). In our study, we wanted the protein-rich phase to form the dispersed

phase because this phase can be enzymatically cross-linked. Thus, it was important that the volume fraction of the casein-rich phase was less than that of the pectin-rich phase. Considering both the above restrictions as well as the desire to increase particle yields, we sought to maximize the quantity of microspheres fabricated by the emulsion method. To address this issue, we examined the influence of the volume fraction of the biopolymer disperse phase (“particle phase”) on the formation of filled hydrogel microspheres.

Optical micrographs of the structure of filled hydrogel microspheres formed by mixing different ratios of “particle phase”(oil droplets + lower phase) and continuous phase (upper phase) are shown in Figures 7.3A and 7.3B. A few isolated spherical particles were observed in the system prepared by mixing 1% “particle phase” and 99% disperse phase (Figure 7.3A). On the other hand, a large number of closely packed elongated spheroid particles were observed in the system prepared by mixing 40% disperse phase with 60% continuous phase (Figure 7.3B). Unfortunately, several problems occurred during the preparation of microspheres containing high proportions of “particle phase”. Most notably, excessive foam formation was observed in systems made with high (30-40% vol/vol) proportions of “particle phase”. In an effort to remove this foam, these samples were centrifuged at 1,000 g for 10 min, which resulted in a thick

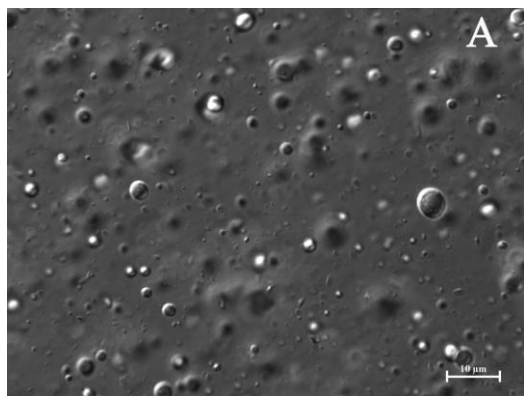


**Figure 7.3A:** Optical micrographs of filled hydrogel particles formed from 1% (vol/vol) particle phase (oil droplets + lower phase) and 99% (vol/vol) upper phase

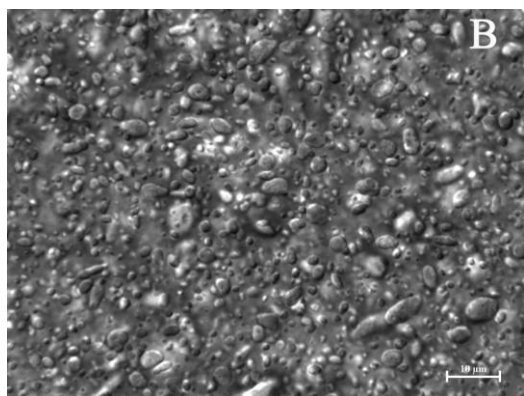


**Figure 7.3B:** Optical micrographs of filled hydrogel particles formed from 40% (vol/vol) particle phase (oil droplets + lower phase) and 60% (vol/vol) upper phase



**Figure 7.4:** Photograph and micrograph of filled hydrogel particles formed from 30% (vol/vol) lower phase and emulsion and 70% (vol/vol) upper phase after centrifugation at 1,000 g for ten minutes. Note coagulated protein on surface of mixture, and coagulated protein (left) and free particles (right) in micrograph

layer of what appeared to be coagulated protein on their surfaces (Figure 7.4). Analysis of the microstructure of this surface layer revealed the formation of large aggregates along with some individual microspheres (Figure 7.4).

The rate at which the particles in an emulsion will aggregate depends on the collision frequency and the fraction of collisions that lead to aggregation. In particular, the collision frequency is dependent on the total number of particles encountered in a given time and volume (McClements, 2005). By increasing the number of microspheres in the system, the collision frequency and aggregation rate will increase. To prevent an excessive amount of aggregation during microsphere fabrication, the proportion of

particle phase was reduced to 10% (vol/vol). At this ratio, some aggregation was still observed after microsphere formation, but it was much less than at higher particle phase concentrations.

#### **7.4.4 Fabrication of Density Matched Filled Hydrogel Microspheres**

Gravitational separation is a common instability mechanism for colloidal-based delivery systems intended for use in foods and beverages (Jones & McClements, 2010; Matalanis, Jones, & McClements, 2011). This form of instability occurs when the density of the particle differs from that of the surrounding liquid. If the particles are less dense than the surrounding liquid, they tend to move upwards (creaming), whereas if they are more dense they tend to move downwards (sedimentation). The speed at which particles move depends on their size, with larger particles moving more rapidly than smaller ones. Filled hydrogel microspheres are relatively large ( $d > 1 \mu\text{m}$ ), and thus, these microspheres are prone to gravitational separation. The instability of these microspheres to gravitational forces would limit their use in products that have low viscosity continuous phases such as beverages. We therefore examined the possibility of retarding or preventing the gravitational separation of the filled hydrogel microspheres by varying the amount of oil they contained which in turn impacts the density of these microspheres.

#### 7.4.4.1 Structural and Physicochemical Properties

Initially, we characterized the structural and physicochemical properties of filled hydrogel microsphere suspensions containing different oil contents. Confocal fluorescence micrographs of the filled hydrogel microspheres are shown in Figures 7.5A-7.5D. A fluorescent dye was used to stain the oil phase green while the protein was dyed with the red dye Rhodamine B. As the amount of oil droplets in the hydrogel microspheres increased there was a decrease in their redness and increase in their yellowness/greenness.

The confocal micrographs also indicated that the size of the hydrogel microspheres increased as the oil content increased (Figures 7.5A-7.5D), which was supported by light scattering measurements (Figure 7.6). The presence of oil droplets within the lower phase may have made particle disruption more difficult when the upper and lower phases were blended together, thereby leading to larger hydrogel microspheres being formed. Droplet disruption under shear flow conditions depends on the ratio of the dispersed phase and continuous phase viscosities, *i.e.*,  $\eta_D/\eta_C$  (Grace, 1982). We therefore measured the apparent viscosities of the dispersed and continuous phases and used this data to calculate the viscosity ratio for each system at a fixed shear rate similar to that used during the mixing stage, *i.e.*,  $100 \text{ s}^{-1}$ . There was an appreciable increase in the viscosity ratio as the concentration of oil in the dispersed phase increased (Table 7.1). The incorporation of oil droplets into the disperse phase may therefore have inhibited droplet disruption due to this increase in viscosity ratio, leading to larger hydrogel microspheres being formed.

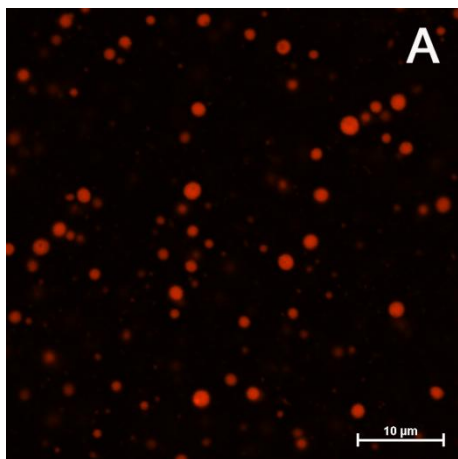


**Figure 7.5A:** Confocal micrographs of filled hydrogel particles containing 0% (w/w) oil. The protein appears red, and the scale bars represent 10  $\mu\text{m}$

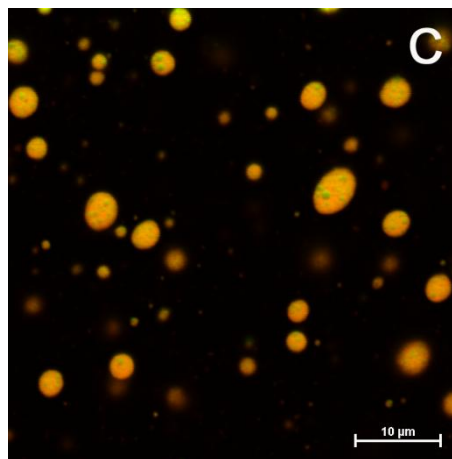


**Figure 7.5C:** Confocal micrographs of filled hydrogel particles containing 18.2% (w/w) oil. The oil appears in green while the protein appears red, and the scale bars represent 10  $\mu\text{m}$

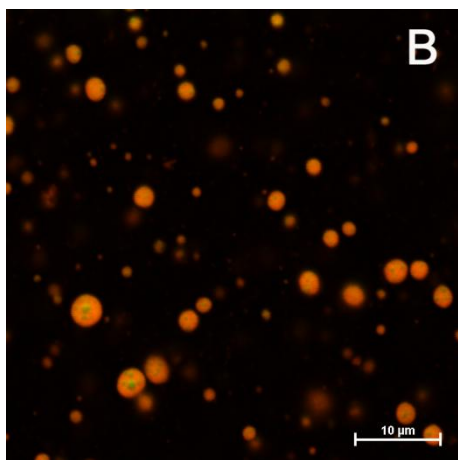


**Figure 7.5B:** Confocal micrographs of filled hydrogel particles containing 9.1% (w/w) oil. The oil appears in green while the protein appears red, and the scale bars represent 10  $\mu\text{m}$

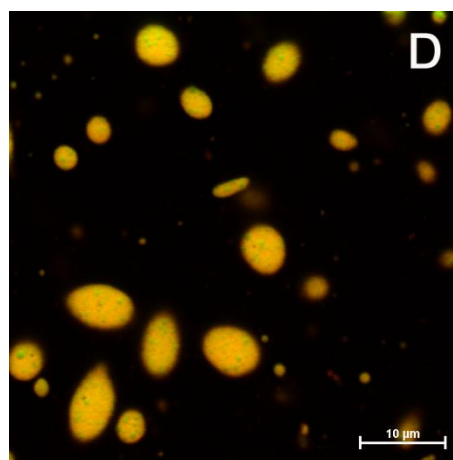


**Figure 7.5D:** Confocal micrographs of filled hydrogel particles containing 27.3% (w/w) oil. The oil appears in green while the protein appears red, and the scale bars represent 10  $\mu\text{m}$

The overall apparent shear viscosity, optical properties (lightness), and electrical characteristics ( $\zeta$ -potential) of filled hydrogel microsphere suspensions with different oil contents was also measured (Table 7.2). These suspensions were prepared by blending 10% “particle phase” (lower phase + oil droplets) with 90% continuous phase (upper phase). There was little difference in the apparent viscosities of suspensions containing different oil contents, which suggests that the filled hydrogel microspheres had similar effects on the flow profiles of the suspensions.

There was a slight increase in the overall lightness ( $L^*$ ) of the suspensions as the oil droplet concentration within the microspheres increased, with the  $L^*$  value increasing from around 75 to 81% as the oil content within the microspheres increased from 0 to 27.3% (Table 7.2). This effect may have been due to an increase in the refractive index of the microspheres due to the presence of oil. The overall refractive index of the filled hydrogel phase depends on its composition and the refractive indices of the different components within it (Jones & McClements, 2010; Matalanis et al., 2011). To a first approximation, the overall particle refractive index ( $n_p$ ) is given by the sum of contributions from the water (W), biopolymer (B), and oil (O) components:

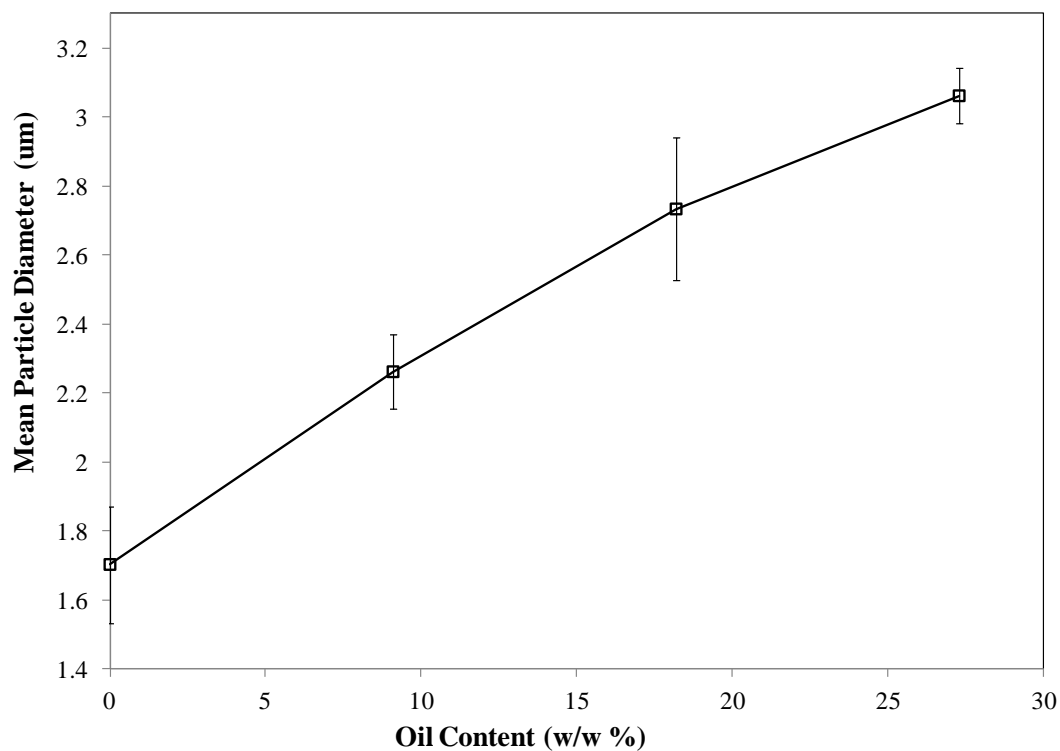


**Figure 7.6:** Mean particle diameter ( $D_{32}$ ) for filled hydrogel particles fabricated with increasing concentrations of emulsified oil in the disperse phase

**Table 7.1:** Apparent viscosity for continuous and dispersed phase and viscosity ratio for microsphere with increasing oil levels (0-27.3% oil)

Sample	Apparent Viscosity of Dispersed Phase@ Shear Rate $100.1 \text{ s}^{-1}$ (Pa·s)	Apparent Viscosity of Dispersed Phase@ Shear Rate $100.1 \text{ s}^{-1}$ (Pa·s)	Viscosity Ratio ( $\eta_{\text{apparent (dispersed phase)}} / \eta_{\text{apparent (continuous phase)}}$ )
0% oil	1.13	0.31	3.70
9.1% oil	2.63	0.31	8.58
18.2% oil	4.43	0.31	14.45
27.3% oil	6.34	0.31	20.72

**Table 7.2:** Apparent Viscosity,  $n$ ,  $K$ , zeta potential, and LAB readings for particles with increasing oil levels (0-27.3% oil)

Sample	Apparent Viscosity @ Shear Rate $1 \text{ s}^{-1}$	$n$	$K$	Zeta Potential	$L^*$ Value
0% oil	0.44 Pa·s	0.98	0.43 Pa s <sup>n</sup>	-26.6 ± 0.3	75.1 ± 1.3
9.1% oil	0.48 Pa·s	0.97	0.48 Pa s <sup>n</sup>	-27.3 ± 1.4	77.4 ± 0.9
18.2% oil	0.42 Pa·s	0.98	0.42 Pa s <sup>n</sup>	-26.2 ± 0.3	78.2 ± 0.6
27.3% oil	0.45 Pa·s	0.98	0.45 Pa s <sup>n</sup>	-27.8 ± 0.6	80.9 ± 0.3

$n_p = (1 - \phi_B - \phi_O)n_W + \phi_B n_B + \phi_O n_O$ , where  $n$  is the refractive index and  $\phi$  is the fraction of the specified component present. The refractive index of water is around 1.33, whereas those of oil and biopolymer are around 1.47. An increase in the total amount of oil + biopolymer present would therefore lead to an increase in the overall refractive index of biopolymer present would therefore lead to an increase in the overall refractive index of the microspheres. There was an appreciable increase in the sum of oil and biopolymer present within the microspheres with increasing oil content (Table 7.3), which could be due to some light scattering by the oil droplets within the microspheres, as well as by the microspheres themselves.

The presence of different amounts of oil droplets within the filled hydrogel microspheres had little effect on their overall electrical characteristics, with all samples being negatively charged. Previous studies have shown that this kind of hydrogel microsphere is negatively charged at pH 5, which was attributed to the presence of anionic pectin molecules onto the surfaces (Matalanis & McClements, et al., 2012)

**Table 7.3:** Physical properties associated with calculating creaming velocity ( $U$ ) for filled hydrogel particles with increasing concentrations of oil (0-27.3% w/w)

Oil Content % (w/w)	Biopolymer Content % (w/w)	Oil-to-Biopolymer Ratio	Diameter ( $\mu\text{m}$ )	$\rho_p$	Creaming Velocity ( $\text{kg/m}^3$ ) (mm/day)
0%	14.7	0	1.70	1039	-5.4
9.1%	13.4	0.68	2.26	1027	-6.6
18.2%	12.0	1.51	2.74	1015	-5.4
27.3%	10.7	2.55	3.06	1003	-1.5

#### 7.4.4.2 Stability to Gravitational Separation

The creaming or sedimentation rate of non-interacting rigid spherical particles suspended in a dilute Newtonian liquid (water) can be modeled by the following equation:

$$U = -\frac{2gr^2(\rho_P - \rho_W)}{9\eta_W} \quad (7.3)$$

In this equation,  $U$  is the creaming velocity (positive  $U$  for creaming; negative  $U$  for sedimentation),  $g$  is the acceleration due to gravity,  $r$  is the radius of the particle,  $\rho$  is the density,  $\eta$  is the shear viscosity, and the subscripts  $W$  and  $P$  refer to water and particles, respectively. The density of filled hydrogel microspheres depends on their composition, and can be approximately modeled using the following equation:

$$\rho_P = \phi_B \rho_B + \phi_O \rho_O + (1 - \phi_B - \phi_O) \rho_W \quad (7.4)$$

Here the subscripts *B*, *W*, and *O* refer to the biopolymer, water and oil phases, respectively,  $\rho$  is the density of each phase, and  $\phi$  is the volume fraction of each phase (Jones & McClements, 2010; Matalanis, et al., 2011). Gravitational separation can be inhibited when the density of the particle ( $\rho_{\text{Particle}}$ ) equals the density of the surrounding fluid ( $\rho_W$ ). The particle composition required to meet this criteria can be established by rearranging Equation 4:

$$\phi_O = -\frac{\phi_B(\rho_B - \rho_W)}{(\rho_O - \rho_W)} = -\frac{\phi_B \Delta\rho_B}{\Delta\rho_O} \quad (7.5)$$

We measured the density of the lower biopolymer phase, which contained 14.7% biopolymer (casein + pectin), to be  $1039 \text{ kg m}^{-3}$ . Assuming a linear relationship between solution density and biopolymer concentration we estimated the effective density of the biopolymer molecules (i.e. the density of a 100% biopolymer solution) to be  $\rho_B = 1265 \text{ kg m}^{-3}$ . The density of the aqueous and oil phases was  $\rho_W = 1000 \text{ kg m}^{-3}$  and  $\rho_O = 918 \text{ kg m}^{-3}$ , respectively. Consequently the density contrasts for the oil and biopolymer that appear in the above are:  $\Delta\rho_O \approx -82 \text{ kg m}^{-3}$  and  $\Delta\rho_B \approx +265 \text{ kg m}^{-3}$ , respectively.

Consequently, if the dispersed phase composition is controlled so that  $\phi_O \approx 3.2 \times \phi_B$ , then the particles should be density matched to the surrounding continuous phase which should prevent gravitational separation.

We therefore prepared a series of filled hydrogel microspheres with different particle phase compositions by mixing different ratios of lower phase with oil phase. The lower phase had a constant biopolymer concentration (casein + pectin = 14.7%). Consequently, the final compositions of the disperse phase (lower phase + oil phase) were 0 to 27.3% oil and 14.7 to 10.7% biopolymer, which corresponded to  $\phi_O/\phi_B \approx 0$  to 2.6 (Table 7.3). Consequently, one would expect the system with the highest oil content to have the best stability against gravitational separation. The stability of the microspheres to gravitational separation was then predicted according to the Stokes equation using the values for particle size, density, and continuous phase viscosity listed in Table 7.3. These predictions suggested that the microspheres containing the highest oil content should be relatively stable to gravitational separation while microspheres with lower oil contents should undergo appreciable sedimentation due to their relatively high densities compared to water.

A series of filled hydrogel microsphere suspensions containing different oil contents were prepared and then diluted with buffer solution. Dilution was carried out since the original samples were too viscous to exhibit appreciable creaming, presumably due to the relatively high concentration of pectin in the continuous phase. Photographs of the samples were then taken after 0 and 7 days storage at room temperature (Figure 7.7). Prior to storage, all samples had a uniformly cloudy appearance. After 7 days of storage the samples containing 0 to 18.2% oil in the dispersed phase were almost completely transparent with a thin white sediment visible at the bottom of the tubes, while the samples containing 27.3% oil remained cloudy throughout. A direct comparison of the % transmission results obtained by laser vertical profiling of diluted samples containing

either 0% or 27.3% oil after 7 days storage is shown in Figure 7.8. From these profiles, it is clear that microspheres containing 0% oil were highly prone to sedimentation during storage while those containing 27.3% oil were not. The susceptibility of the various

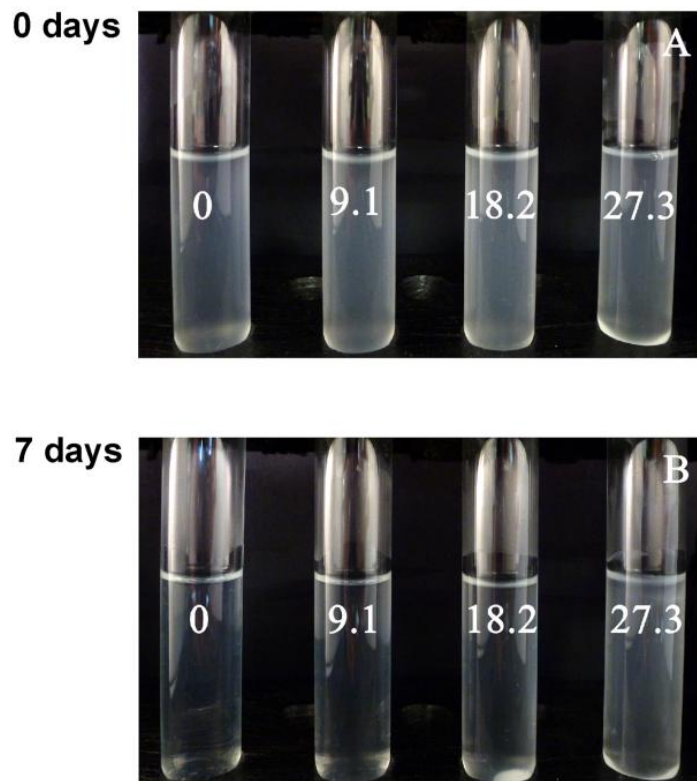


**Figure 7.7:** Photographs of filled hydrogel particles with increasing oil content (0, 9.1, 18.2, and 27.3% oil) diluted 1:100 in buffer at pH 5 after 0 (A) and 7 (B) days storage at ambient temperature

microsphere suspensions to settling was characterized by calculating the sedimentation indices from the laser profiling measurements (Figure 7.9). The experimentally determined sedimentation indices were compared with predicted values calculated using Stokes equation and the parameters in Table 7.1 (Figure 7.9). There was good qualitative

agreement between the predicted and measured values for suspensions containing different oil contents. With the exception of the sample containing 27.3% oil, all samples were predicted to undergo almost complete sedimentation after 7 days storage. The experimental sedimentation indices were greater than the predicted values for the samples with relatively low oil contents, which may have been due to some change in the internal

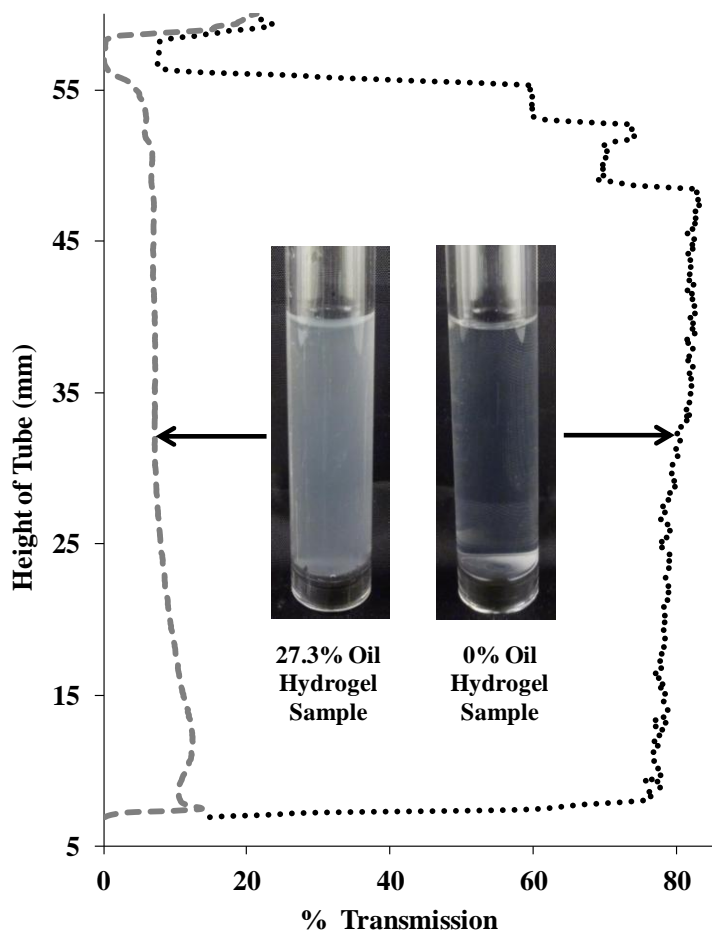


**Figure 7.8:** Comparison of vertical laser profiles of % transmission versus sample height for filled hydrogel particles diluted 1:100 in buffer (pH 5) containing 0% oil and 27.3% oil after 7 days of storage at room temperature

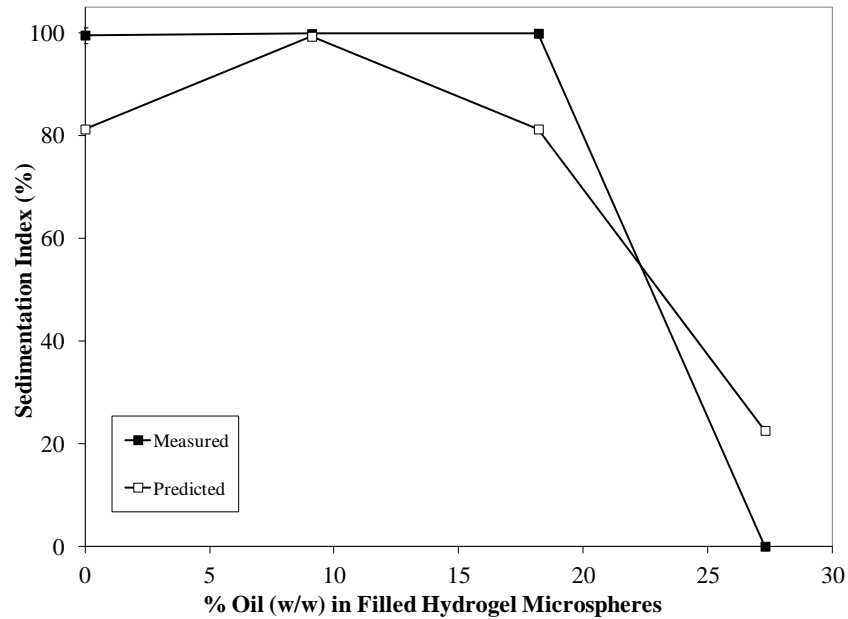


**Figure 7.9:** Predicted and experimental sedimentation indices versus oil content of filled hydrogel particles diluted 1:100 in buffer at pH 5 after 7 days of storage at room temperature

composition (and therefore density) of the microspheres or due to changes in the particle size. The predicted sedimentation index for the sample containing 27.3% oil was actually appreciably higher than the experimental value (where no sedimentation was observed). This may have been due to differences in the internal composition of the microspheres after initial preparation. In the predictions it is assumed that the microspheres have the same composition as the mixture prepared by combining the lower biopolymer phase and the oil droplets together. In reality, there may be changes in the composition and structure of this mixture during the preparation procedure, *e.g.*, due to changes in pH or dilution.

From an industrial perspective, it is often desirable to predict the susceptibility of a given sample to gravitational separation using an accelerated test. Creaming or

sedimentation of colloidal dispersions can be accelerated using centrifugation. We therefore examined the influence of centrifugation on the stability of the microspheres to sedimentation. Diluted microspheres (1:100) were scanned using laser profiling, subjected to centrifugation ( $150 \times g$  for 1 hour), and then rescanned. The sedimentation index was then calculated from the laser profiling data for systems with different oil contents within the microspheres. The sedimentation index measurements indicated that microspheres containing 0 to 18.2% oil all moved to the bottom of the tubes after centrifugation, while those containing 27.3% oil remained suspended in solution (Figure 7.10). Thus, the centrifugation and gravitational separation results both indicate that the stability of the microspheres to settling can be greatly enhanced by matching their density to the surrounding aqueous phase by incorporating sufficient oil droplets. These results also confirm that mild centrifugation is a good accelerated test for establishing the stability of the microspheres to settling.

## **7.5 Conclusions**

The overall goal of this work was to improve the current method of fabricating filled hydrogel microspheres using phase separated biopolymer solutions. More specifically, we sought to increase the lipid loading capacity and yield of the microspheres, to simplify the current method of making microspheres, and to fabricate density matched microspheres. Our results showed that the order in which different phases of biopolymers and emulsified oil were added did not impact the lipid content of these microspheres. The microsphere yield could be increased by increasing the volume fraction of the dispersed phase, however using too much dispersed phase resulted in substantial foaming and coagulation.

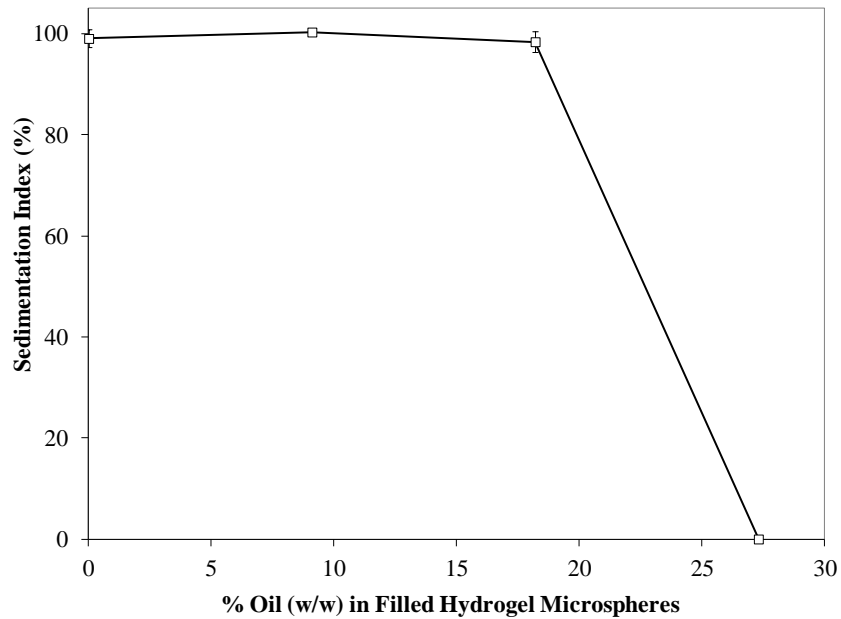


**Figure 7.10:** Sedimentation index versus oil content of filled hydrogel particles diluted 1:100 in buffer at pH 5 after centrifugation at  $150 \times g$  for 1 hour

We attempted to use free oil in place of emulsified oil to reduce the number of processing steps associated with fabricating hydrogel microspheres. However, samples made with free oil did not form the desired filled hydrogel structure. Instead, these samples consisted of a mixture of protein-rich particles and large non-encapsulated oil droplets, rather than filled hydrogel microspheres. Lastly, we have shown that filled hydrogel microspheres with different densities can be created by adjusting the percentage of oil within the disperse phase. At the highest level of oil examined, we were able to form microspheres with a density equal to that of water. A dilute suspension of these density matched microspheres did not cream or sediment during storage (one week at room temperature) nor upon mild centrifugation ( $150x g$  for 1 hour).

Although progress has been made in improving this method for fabricating filled hydrogel particles, there is still significant room for improvement, particularly in the area of increasing lipid loading capacity and particle yields. One potential area for future work would be to examine different emulsifiers for the initial O/W emulsion including other biopolymers as well as synthetic emulsifiers to determine their impact on lipid loading capacity and particle yields. Another area for future research would be to identify other combinations of biopolymers (*e.g.*, proteins and polysaccharides) that phase separate and create microspheres with higher lipid contents or increased yields.

## CHAPTER 8

### CONCLUSIONS

The overall goal of this work was to create a food grade delivery system for lipophilic bioactives known as filled hydrogel particles consisting of lipid droplets encapsulated within protein-rich biopolymer particles. Results showed that it was possible to fabricate filled hydrogel particles using a method that involved first segregation and then aggregation of a mixture of biopolymers. In this case, a segregated mixture of high methoxy pectin and sodium caseinate at pH 7 was mixed with emulsified oil to form an oil-in-water-in-water emulsion ( $O/W_1/W_2$ ) where  $W_1$  (the dispersed phase) was rich in casein and depleted in pectin while  $W_2$  (the continuous phase) was rich in pectin and depleted in casein. Based on experiments involving the behavior of emulsified oil in either casein-rich dispersed phase or pectin-rich continuous phase, it was found that the preferential migration of emulsified oil into the casein-rich dispersed phase is due to a reduction in the unfavorable osmotic pressure in this phase. This reduction in osmotic pressure can be attributed to biopolymer depletion.

Following formation, this structured  $O/W_1/W_2$  emulsion was stabilized by acidification to pH 5 which resulted in a portion of the pectin present in the continuous phase to complex on the surface of the casein-rich filled hydrogel particles. To further stabilize these particles, the enzyme transglutaminase was used to cross-link the protein present in these particles. Cross-linking particles with transglutaminase substantially improved their stability at high pH (pH 7-8) as the integrity of cross-linked particles at neutral pH was maintained while particles that were not cross-linked disintegrated at this

pH. Both cross-linked and not cross-linked particles were stable at lower pH (pH 2-5) as well as at high concentrations of sodium chloride (0-500 mM). As for particle stability following the addition of calcium chloride (0-8 mM), both cross-linked and not cross-linked particles formed a strong macroscopic gel at a concentration above 4 mM calcium chloride.

A number of factors associated with the fabrication process were investigated to either improve upon the initial method of particle fabrication or to modify particle characteristics. The following highlights the factors examined and their impact on the fabrication process:

- **Mixing Speed:** The speed at which a mixture of high methoxy pectin, sodium caseinate, and emulsified oil was mixed at during acidification from pH 7 to pH 5 had an impact on the size of filled hydrogel particles. The particle size of samples mixed at high speeds was significantly smaller compared to samples mixed at slower speeds.
- **Emulsified Oil Versus Free Oil:** Replacing emulsified oil with free oil in the mixture for particle fabrication resulted in the formation of large free (not encapsulated) oil droplets and small protein-rich particles. Thus, it was imperative for this method that emulsified oil be used for fabricating these particles.
- **Density Matching:** By controlling the level of oil, biopolymer, and water present in these particles, it was possible to fabricate particles that resisted gravitational separation during storage in a low viscosity liquid.

This enhanced stability was attributed to the equal density of the particle to that of the continuous phase.

Since filled hydrogel particles represent a new type of emulsion-based delivery system for lipid-based bioactives, it was important to assess the oxidative stability of the lipids encapsulated within these particles. For this reason, a comparative oxidation study using commercial fish oil was conducted on filled hydrogel particles, on a casein-stabilized O/W emulsion, and on a Tween 20-stabilized O/W emulsion. Oxidation results showed that emulsions stabilized by Tween 20 oxidized faster than either filled hydrogel particles or emulsions stabilized by casein, while filled hydrogel particles and casein-stabilized emulsions showed similar oxidation rates. Although the oxidative stability of filled hydrogel particles was not superior to that of a conventional casein-stabilized O/W emulsion, these results do highlight the antioxidant properties of food proteins in foods containing lipids.

In addition to evaluating oxidative stability, it was also important to assess the digestibility of the lipid encapsulated in these particles. Using an *in vitro* gastrointestinal model, both filled hydrogel particles and a casein stabilized O/W emulsion were examined for their stability (particle size and charge) to simulated mouth, stomach, and small intestine conditions as well as their susceptibility to digestion by lipase under simulated small intestine conditions. Filled hydrogel particles were stable to simulated mouth conditions, formed large flocs under simulated gastric conditions, and completely disintegrated following simulated small intestine conditions. As for lipid digestion, filled hydrogel particles were digested at similar rates when compared to a casein stabilized O/W emulsion. These results confirmed that the lipid present in filled hydrogel particles

is highly accessible for digestion and absorption in the body and that this delivery system would be appropriate for delivering lipid based bioactives in foods.

One opportunity for future work on this delivery system would be to improve the yield and lipid loading capacity of filled hydrogel particles. One potential strategy for increasing lipid loading capacity would be to examine emulsions with different droplet diameters as droplet size is known to influence depletion flocculation with larger droplets having a lower critical flocculation concentration (CFC) than smaller droplets (McClements, 2000). Emulsifier type would be another area to investigate for its impact on loading capacity. In this work, high concentrations of dispersed (particle) phase resulted in not only increased particle yields but also excessive protein coagulation and foam formation. Using a different O/W emulsion with a different particle size or emulsifier might help to prevent coagulation and foaming which would ultimately allow for higher particle yields. Another area for investigation would be to examine other protein/polysaccharide combinations at concentrations where they exhibit incompatibility to determine if these systems could be used to form filled hydrogel particles with superior properties compared to the current system.

In summary, filled hydrogel particles are a novel emulsion based delivery system for foods and beverages. Besides delivering bioactive compounds, these particles have the potential for use in foods to create novel textures or to reduce fat content. The challenge remains in improving the current method of particle fabrication to maximize yields and loading capacity while minimizing the time and effort required to manufacture this delivery system.

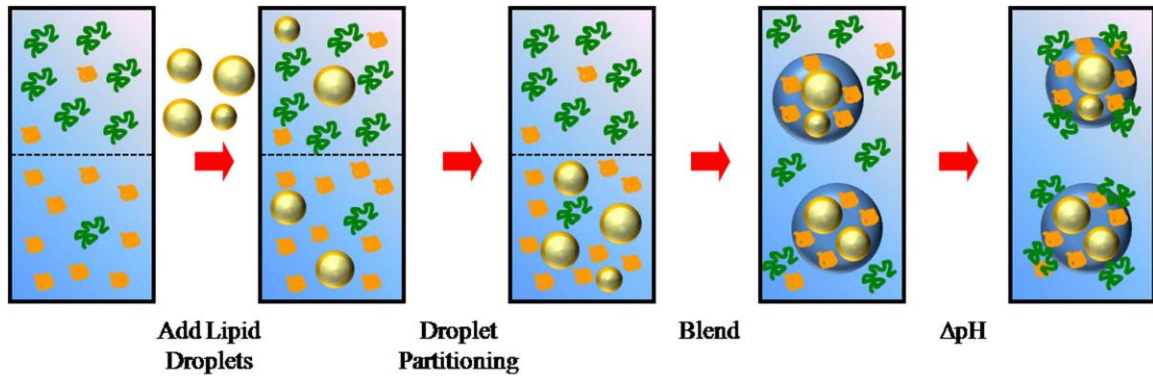
## APPENDIX

### PARTITIONING OF EMULSION DROPLETS IN PHASE SEPARATED BIOPOLYMER MIXTURES

One of the most important steps in the formation of filled hydrogel particles is to promote the movement of the lipid droplets into the biopolymer phase that will eventually form the disperse phase. In this section, we consider the free energy changes determining the partitioning of lipid droplets between two phase-separated biopolymer phases. Consider a system that consists of monodisperse lipid droplets dispersed within a container that contains two phase-separated biopolymer phases (Figure A.1). For simplicity, we assume that each biopolymer phase contains only one kind of monodisperse biopolymer molecule (A or B), that can be defined by its number concentration ( $n_A$  or  $n_B$ ), its molecular weight ( $M_A$  or  $M_B$ ) and its radius of gyration ( $r_{g,A}$  or  $r_{g,B}$ ). The effective molar volume occupied by each biopolymer molecule is therefore given by  $V_{mA} = 4\pi r_{gA}^3/3$  or  $V_{mB} = 4\pi r_{gB}^3/3$ . The overall volume fraction occupied by each biopolymer phases is  $\Phi_A$  and  $\Phi_B$ , where ( $\Phi_A + \Phi_B = 1$ ). The lipid droplets can be defined by their number concentration ( $n_D$ ) and radius ( $r_D$ ).

The distribution of lipid droplets between the two biopolymer phases can be described by the following equation:

$$\frac{\phi_U}{\phi_L} = \exp\left(\frac{\Delta G}{kT}\right) \quad (\text{A.1})$$



**A1.1:** Schematic drawing depicting the formation of filled hydrogel particles by sequential segregative and aggregative phase separation of pectin and casein

where  $\phi_U$  and  $\phi_L$  are the volume fractions of the lipid droplets in the upper and lower biopolymer phases, respectively.  $\Delta G$  is the free energy required to transfer a lipid droplet from the lower to upper biopolymer phases,  $k$  is Boltzman's constant, and  $T$  is the absolute temperature. If  $\Delta G = 0$ , then  $\phi_U = \phi_L$ , and the droplets are homogenously distributed through the system; if  $\Delta G > 0$ , then  $\phi_U < \phi_L$ , and the droplets accumulate in the lower phase, and if  $\Delta G < 0$ , then  $\phi_U > \phi_L$ , and the droplets accumulate in the upper phase.

The overall free energy can be divided into a number of contributions: (i) the *transfer free energy* ( $\Delta G_{\text{transfer}}$ ) required to introduce lipid droplets into a biopolymer phase, with the phase with the lowest transfer energy being the one that the droplets favor; (ii) the *mixing free energy* associated with entropy of mixing effects ( $\Delta G_{\text{mixing}}$ ), which favors a random distribution of lipid droplets throughout the volume; (iii) the *gravitational free energy* ( $\Delta G_{\text{gravity}}$ ), which favors the accumulation of lipid droplets in the upper phase because oil has a lower density than water (or biopolymer-rich phases):

$$\Delta G = \Delta G_{transfer} + \Delta G_{mixing} + \Delta G_{gravity} \quad (\text{A.2})$$

An analysis of the entropy of mixing associated with having all the lipid droplets accumulating in the lower phase rather than in the upper phase leads to (Atkins, 2006):

$$\Delta G_{mixing} = -n_D k_B T \ln \left( \frac{\phi_U}{\phi_L} \right) \quad (\text{A.3})$$

An analysis of the gravitational free energy associated with having all the lipid droplets accumulating in the lower phase rather than in the upper phase leads to:

$$\Delta G_{gravity} = \frac{n_D 4\pi r_D^3 g}{3} \frac{h}{2} \left( \rho_{Lipid} - \frac{1}{2} \langle \rho_U + \rho_L \rangle \right) \quad (\text{A.4})$$

Here,  $g$  is the gravitational constant,  $h$  is the height of the overall system, and  $\rho_U$ ,  $\rho_L$  and  $\rho_{lipid}$  are the densities of the upper phase, lower phase and lipid, respectively

An analysis of the transfer free energy associated with moving all of the lipid droplets from the upper phase to the lower phase leads to:

$$\Delta G_{transfer} = \frac{4\pi r_D^3}{3} \left[ \left( \left( 1 + \frac{\delta_B}{r_D} \right)^3 - 1 \right) \Pi_B - \left( \left( 1 + \frac{\delta_A}{r_D} \right)^3 - 1 \right) \Pi_A \right] \quad (\text{A.5})$$

Here  $\delta$  is the radius of gyration of the biopolymer molecule (the thickness of the depletion zone),  $r_D$  is the droplet radius, and the subscripts A and B refer to the different

biopolymers in the upper and lower phases, respectively.  $\Pi$  is the osmotic pressure associated with the biopolymers in each phase:

$$\Pi_A = n_A kT \left( 1 + \frac{n_A 4\pi r_{g,A}^3}{3} \right) \quad \Pi_B = n_B kT \left( 1 + \frac{n_B 4\pi r_{g,B}^3}{3} \right) \quad (\text{A.6})$$

Here  $n_A$  and  $n_B$  are the number concentrations (number per unit volume) of the biopolymer molecules in the upper and lower phases. In practice, both biopolymers are present in both phases and can therefore contribute to the osmotic stress. Therefore the sum of osmotic stresses from both biopolymers should be used. The magnitudes of the different free energy contributions were calculated for lipid droplets with a radius of 200 nm, using the above equations, the data in Table 3.1, and literature values for the radius of gyration and molecular weight of casein aggregates ( $r_g = 10$  nm ; MW = 875 kDa) (O'Connell, Grinberg, & de Kruijff, 2003) and of pectin molecules ( $r_g = 20$  nm ; MW = 120 kDa) (Fishman, Chau, Kolpak, & Brady, 2001). The calculated values of the free energy contributions were  $\Delta G_{\text{transfer}} = -65 \text{ J m}^{-3}$ ,  $\Delta G_{\text{mixing}} = +0.0019 \text{ J m}^{-3}$ , and  $\Delta G_{\text{gravity}} = -0.59 \text{ J m}^{-3}$ . These calculations clearly show that the transfer free energy associated with the depletion interaction (which strongly favors movement into the protein-rich lower phase) is much stronger than either the mixing or gravitational forces.

## BIBLIOGRAPHY

- Arora, S., Ali, J., Ahuja, A., Khar, R., & Baboota, S. (2005). Floating drug delivery systems: A review. *AAPS PharmSciTech*, 6(3), E372-E390.
- Aryee, A. N. A. & Simpson, B. K. (2009). Comparative studies on the yield and quality of solvent-extracted oil from salmon skin. *Journal of Food Engineering*, 92(3), 353-358.
- Bansil, R. & Turner, B. S. (2006). Mucin structure, aggregation, physiological functions and biomedical applications. *Current Opinion in Colloid & Interface Science*, 11(2-3), 164-170.
- Belitz, H., Grosch, W., & Schieberle, P. (2009a). Lipids. In H. Belitz, W. Grosch, & P. Schieberle, *Food Chemistry 4<sup>th</sup> Edition* (pp. 158-247). New York, NY: Springer.
- Belitz, H. D., Grosch, W., & Schieberle, P. (2009b). Milk and dairy products. In H. Belitz, W. Grosch, & P. Schieberle, *Food Chemistry 4<sup>th</sup> Edition* (pp. 498-545). New York, NY: Springer.
- Bradford, M. M. (1976). A rapid and sensitive method for the quantitation of microgram quantities of protein utilizing the principle of protein-dye binding. *Analytical Biochemistry*, 72(1-2), 248-254.
- Braga, A. L. M., Menossi, M., & Cunha, R. L. (2006). The effect of the glucono- $\delta$ -lactone/caseinate ratio on sodium caseinate gelation. *International Dairy Journal*, 16(5), 389-398.
- Burey, P., Bhandari, B. R., Howes, T., & Gidley, M. J. (2008). Hydrocolloid gel particles: Formation, characterization, and application. *Critical Reviews in Food Science and Nutrition*, 48(5), 361-377.
- Capron, I., Costeux, S., & Djabourov, M. (2001). Water in water emulsions: phase separation and rheology of biopolymer solutions. *Rheologica Acta*, 40(5), 441-456.
- Carey, M. C., Small, D. M., & Bliss, C. M. (1983). Lipid digestion and absorption. *Annual Review of Physiology*, 45(1), 651-677.
- Carr, A. J., Munro, P. A., & Campanella, O. H. (2002). Effect of added monovalent or divalent cations on the rheology of sodium caseinate solutions. *International Dairy Journal*, 12(6), 487-492.

- Chaiyasit, W., Elias, R. J., McClements, D. J., & Decker, E. A. (2007). Role of physical structures in bulk oils on lipid oxidation. *Critical Reviews in Food Science & Nutrition*, 47(3), 299-317.
- Chen, J. (2009). Food oral processing—A review. *Food Hydrocolloids*, 23(1), 1-25.
- Chen, J. S., Dickinson, E., & Edwards, M. (1999). Rheology of acid-induced sodium caseinate stabilized emulsion gels. *Journal of Texture Studies*, 30(4), 377-396.
- Chen, B., McClements, D. J., & Decker, E. A. (2011). Minor components in food oils: a critical review of their roles on lipid oxidation chemistry in bulk oils and emulsions. *Critical Reviews in Food Science and Nutrition*, 51(10), 901-916.
- Chen, L., Remondetto, G. E., & Subirade, M. (2006). Food protein-based materials as nutraceutical delivery systems. *Trends in Food Science & Technology*, 17(5), 272-283.
- Choe, E. & Min, D. B. (2006). Mechanisms and factors for edible oil oxidation. *Comprehensive Reviews in Food Science and Food Safety*, 5(4), 169-186.
- Choe, E. & Min, D. B. (2007). Chemistry of deep-fat frying oils. *Journal of Food Science*, 72(5), R77-R86.
- Choe, E. & Min, D. B. (2009). Mechanisms of antioxidants in the oxidation of foods. *Comprehensive Reviews in Food Science and Food Safety*, 8(4), 345-358.
- Clark, A. H., Lips, A., & Hart, P. M. (1989). Electrochemical approach to studies of binding and electrostatic interaction in concentrated food dispersions. In R. D. Bee, P. Richmond, & J. Mingins (Eds.), *Food colloids* (Vol. 75) (154-171). Cambridge: The Royal Society of Chemistry.
- Cooper, C. L., Dubin, P. L., Kayitmazer, A. B., & Turksen, S. (2005). Polyelectrolyte-protein complexes. *Current Opinion in Colloid & Interface Science*, 10(1-2), 52-78.
- Coupland, J. N. & McClements, D. J. (1996). Lipid oxidation in food emulsions. *Trends in Food Science & Technology*, 7(3), 83-91.
- CP Kelco. (2005). GENU® pectin book. CP Kelco, Atlanta, GA, 1-29.

- Dahan, A. & Hoffman, A. (2006). Use of a dynamic in vitro lipolysis model to rationalize oral formulation development for poor water soluble drugs: correlation with in vivo data and the relationship to intra-enterocyte processes in rats. *Pharmaceutical Research*, 23(9), 2165-2174.
- Dahan, A. & Hoffman, A. (2008). Rationalizing the selection of oral lipid based drug delivery systems by an in vitro dynamic lipolysis model for improved oral bioavailability of poorly water soluble drugs. *Journal of Controlled Release*, 129(1), 1-10.
- de Kruif, C. G. & Tuinier, R. (2001). Polysaccharide protein interactions. *Food Hydrocolloids*, 15(4-6), 555-563.
- de Kruif, C. G., Weinbreck, F., & de Vries, R. (2004). Complex coacervation of proteins and anionic polysaccharides. *Current Opinion in Colloid & Interface Science*, 9(5), 340-349.
- de Vos, P., Faas, M. M., Spasojevic, M., & Sikkema, J. (2010). Encapsulation for preservation of functionality and targeted delivery of bioactive food components. *International Dairy Journal*, 20(4), 292-302.
- Dea, I. C. M. (1989). Industrial polysaccharides. *Pure and Applied Chemistry*, 61(7), 1315-1322.
- Decker, E. A. (1998). Strategies for manipulating the prooxidative/antioxidative balance of foods to maximize oxidative stability. *Trends in Food Science & Technology*, 9(6), 241-248.
- DeJong, G. A. H. & Koppelman, S. J. (2002). Transglutaminase catalyzed reactions: impact on food applications. *Journal of Food Science*, 67(8), 2798-2806.
- Díaz, M., Dunn, C. M., McClements, D. J., & Decker, E. A. (2003). Use of caseinophosphopeptides as natural antioxidants in oil-in-water emulsions. *Journal of Agricultural and Food Chemistry*, 51(8), 2365-2370.
- Díaz, M. & Decker, E. A. (2004). Antioxidant mechanisms of caseinophosphopeptides and casein hydrolysates and their application in ground beef. *Journal of Agricultural and Food Chemistry*, 52(26), 8208-8213.
- Dickinson, E. (1997a). Enzymic crosslinking as a tool for food colloid rheology control and interfacial stabilization. *Trends in Food Science & Technology*, 8(10), 334-339.

- Dickinson, E. (1997b). Properties of emulsions stabilized with milk proteins: Overview of some recent developments. *Journal of Dairy Science*, 80(10), 2607-2619.
- Dickinson, E. (1998). Stability and rheological implications of electrostatic milk protein–polysaccharide interactions. *Trends in Food Science & Technology*, 9(10), 347-354.
- Dickinson, E. (2003). Hydrocolloids at interfaces and the influence on the properties of dispersed systems. *Food Hydrocolloids*, 17(1), 25-39.
- Dickinson, E., Semenova, M. G., Antipova, A. S., & Pelan, E. G. (1998). Effect of high-methoxy pectin on properties of casein-stabilized emulsions. *Food Hydrocolloids*, 12(4), 425-432.
- Dongowski, G. (1997). Effect of pH on the in vitro interactions between bile acids and pectin. *Zeitschrift Für Lebensmitteluntersuchung Und -Forschung A*, 205(3), 185-192.
- Dube, M., Schäfer, C., Neidhart, S., & Carle, R. (2007). Texturisation and modification of vegetable proteins for food applications using microbial transglutaminase. *European Food Research and Technology*, 225(2), 287-299.
- DuBois, M., Gilles, K. A., Hamilton, J. K., Rebers, P. A., & Smith, F. (1956). Colorimetric method for determination of sugars and related substances. *Analytical Chemistry*, 28(3), 350-356.
- Einhorn-Stoll, U., Salazar, T., Jaafar, B., & Kunzek, H. (2001). Thermodynamic compatibility of sodium caseinate with different pectins. Influence of the milieu conditions and pectin modifications. *Nahrung/Food*, 45(5), 332-337.
- Elias, R. J., Kellerby, S. S., & Decker, E. A. (2008). Antioxidant Activity of Proteins and Peptides. *Critical Reviews in Food Science and Nutrition*, 48(5), 430.
- Elias, R. J., McClements, D. J., & Decker, E. A. (2005). Antioxidant activity of cysteine, tryptophan, and methionine residues in continuous phase  $\beta$ -Lactoglobulin in Oil-in-Water Emulsions. *Journal of Agricultural and Food Chemistry*, 53(26), 10248-10253.
- Endress, H., Mattes, F., & Norz, K. (2006). Pectins. In Y. H. Hui (Ed.), *Handbook of Food Science, Technology, and Engineering Volume 3* Boca Raton, FL USA: CRC Press.

- Erni, P., Cramer, C., Marti, I., Windhab, E. J., & Fischer, P. (2009). Continuous flow structuring of anisotropic biopolymer particles. *Advances in Colloid and Interface Science*, 150(1), 16-26.
- Eussen, S. R. B. M., Verhagen, H., Klungel, O. H., Garssen, J., van Loveren, H., van Kranen, H. J., & Rompelberg, C. J. M. (2011). Functional foods and dietary supplements: Products at the interface between pharma and nutrition. *European Journal of Pharmacology*, 668, Supplement 1(0), S2-S9.
- Faraji, H., McClements, D. J., & Decker, E. A. (2004). Role of continuous phase protein on the oxidative stability of fish oil-in-water emulsions. *Journal of Agricultural and Food Chemistry*, 52(14), 4558-4564.
- Farrer, D. & Lips, A. (1999). On the self-assembly of sodium caseinate. *International Dairy Journal*, 9(3-6), 281-286.
- Fishman, M. L., Chau, H. K., Kolpak, F., & Brady, J. (2001). Solvent effects on the molecular properties of pectins. *Journal of Agricultural and Food Chemistry*, 49(9), 4494-4501.
- Frankel, E.N. (1980). Lipid oxidation. *Progress in Lipid Research*, 19(1-2), 1-22.
- Frith, W. J. (2010). Mixed biopolymer aqueous solutions – phase behaviour and rheology. *Advances in Colloid and Interface Science*, 161(1-2), 48-60.
- Gaaloul, S., Corredig, M., & Turgeon, S. L. (2009). Rheological study of the effect of shearing process and  $\kappa$ -carrageenan concentration on the formation of whey protein microgels at pH 7. *Journal of Food Engineering*, 95(2), 254-263.
- Gargouri, Y., Julien, R., Bois, A. G., Verger, R., & Sarda, L. (1983). Studies on the detergent inhibition of pancreatic lipase activity. *Journal of Lipid Research*, 24(10), 1336-1342.
- Genovese, D. B., Lozano, J. E., & Rao, M. A. (2007). The rheology of colloidal and noncolloidal food dispersions. *Journal of Food Science*, 72(2), R11-R20.
- Gibbs, B. F. & Kermasha, S. (1999). Encapsulation in the food industry: a review. *International Journal of Food Sciences & Nutrition*, 50(3), 213.
- Golding, M. & Wooster, T. J. (2010). The influence of emulsion structure and stability on lipid digestion. *Current Opinion in Colloid & Interface Science*, 15(1-2), 90-101.

- Golding, M., Wooster, T. J., Day, L., Xu, M., Lundin, L., Keogh, J., & Clifton, P. (2011). Impact of gastric structuring on the lipolysis of emulsified lipids. *Soft Matter*, 7(7), 3513-3523.
- Grace, H. P. (1982). Dispersion phenomena in high viscosity immiscible fluid systems and application of static mixers as dispersion devices in such systems. *Chemical Engineering Communications*, 14(3-6), 225-277.
- Grinberg, V. Y. & Tolstoguzov, V. B. (1997). Thermodynamic incompatibility of proteins and polysaccharides in solutions. *Food Hydrocolloids*, 11(2), 145-158.
- Gudipati, V., Sandra, S., McClements, D. J., & Decker, E. A. (2010). Oxidative stability and in vitro digestibility of fish oil-in-water emulsions containing multilayered membranes. *Journal of Agricultural and Food Chemistry*, 58(13), 8093-8099.
- Ha, C. R. & Iuchi, I. (2003). Transglutaminase. In J. R. Whitaker, A. G. J. Voragen, & D. W. S. Wong (Eds.), *Handbook of Food Enzymology* (637-655). New York, NY: Dekker.
- Haahr, A. & Jacobsen, C. (2008). Emulsifier type, metal chelation and pH affect oxidative stability of n-3-enriched emulsions. *European Journal of Lipid Science and Technology*, 110(10), 949-961.
- Hao, J. & Heng, P. W. S. (2003). Buccal delivery systems. *Drug Development and Industrial Pharmacy*, 29(8), 821-832.
- Hatanaka, J., Chikamori, H., Sato, H., Uchida, S., Debari, K., Onoue, S., & Yamada, S. (2010). Physicochemical and pharmacological characterization of  $\alpha$ -tocopherol-loaded nano-emulsion system. *International Journal of Pharmaceutics*, 396(1), 188-193.
- Henry, C. J. (2010). Functional foods. *European Journal of Clinical Nutrition*, 64(7), 657-659.
- Heurtault, B., Saulnier, P., Pech, B., Proust, J., & Benoit, J. (2003). Physico-chemical stability of colloidal lipid particles. *Biomaterials*, 24(23), 4283-4300.
- Hsu, J. & Nacu, A. (2003). Behavior of soybean oil-in-water emulsion stabilized by nonionic surfactant. *Journal of Colloid and Interface Science*, 259(2), 374-381.

- Hu, M., McClements, D. J., & Decker, E. A. (2003). Lipid oxidation in corn oil-in-water emulsions stabilized by casein, whey protein isolate, and soy protein isolate. *Journal of Agricultural and Food Chemistry*, 51(6), 1696-1700.
- Hu, M., Li, Y., Decker, E. A., & McClements, D. J. (2010). Role of calcium and calcium-binding agents on the lipase digestibility of emulsified lipids using an in vitro digestion model. *Food Hydrocolloids*, 24(8), 719-725.
- Hur, S. J., Decker, E. A., & McClements, D. J. (2009). Influence of initial emulsifier type on microstructural changes occurring in emulsified lipids during in vitro digestion. *Food Chemistry*, 114(1), 253-262.
- Ivanova, M. G., Panaiotov, I., Bois, A., Gargouri, Y., & Verger, R. (1990). Inhibition of pancreatic lipase by ovalbumin and  $\beta$ -lactoglobulin A at the air/water interface. *Journal of Colloid and Interface Science*, 136(2), 363-374.
- Iverson, S., Lang, S., & Cooper, M. (2001). Comparison of the bligh and dyer and folch methods for total lipid determination in a broad range of marine tissue. *Lipids*, 36(11), 1283-1287.
- Jacobsen, C. (1999). Sensory impact of lipid oxidation in complex food systems. *Lipid / Fett*, 101(12), 484-492.
- Jacobsen, C., Let, M. B., Nielsen, N. S., & Meyer, A. S. (2008). Antioxidant strategies for preventing oxidative flavour deterioration of foods enriched with n-3 polyunsaturated lipids: a comparative evaluation. *Trends in Food Science & Technology*, 19(2), 76-93.
- Jensen, S., Rolin, C., & Ipsen, R. (2010). Stabilisation of acidified skimmed milk with HM pectin. *Food Hydrocolloids*, 24(4), 291-299.
- Jones, O. G. & McClements, D. J. (2010). Functional biopolymer particles: design, fabrication, and applications. *Comprehensive Reviews in Food Science and Food Safety*, 9(4), 374-397.
- Kargar, M., Spyropoulos, F., & Norton, I. T. (2011). The effect of interfacial microstructure on the lipid oxidation stability of oil-in-water emulsions. *Journal of Colloid and Interface Science*, 357(2), 527-533.
- Kellerby, S. S., McClements, D. J., & Decker, E. A. (2006). Role of proteins in oil-in-water emulsions on the stability of lipid hydroperoxides. *Journal of Agricultural and Food Chemistry*, 54(20), 7879-7884.

- Kim, H., Decker, E. A., & McClements, D.J. (2006). Preparation of multiple emulsions based on thermodynamic incompatibility of heat-denatured whey protein and pectin solutions. *Food Hydrocolloids*, 20(5), 586-595.
- Kinsella, J.E. (1984). Milk-proteins - physicochemical and functional-properties. *Critical Reviews in Food Science and Nutrition*, 21(3), 197.
- Kong, F. & Singh, R. (2009). Modes of Disintegration of Solid Foods in Simulated Gastric Environment. *Food Biophysics*, 4(3), 180-190.
- Koseki, M., Kitabatake, N., Doi, E., Yasuno, T., Ogino, S., Kazama, M., & Doguchi, M. (1987). Binding of Taurocholate by pectin in the presence of calcium ions. *Journal of Food Science*, 52(6), 1744-1745.
- Leskauskaitė, D., Liutkevichius, A., & Valantinaite, A. (1998). Influence of the level of pectin on the process of protein stabilization in an acidified milk system. *Milchwissenschaft*, 53(3), 149-152.
- Lesmes, U. & McClements, D. J. (2009). Structure–function relationships to guide rational design and fabrication of particulate food delivery systems. *Trends in Food Science & Technology*, 20(10), 448-457.
- Li, Y., Le Maux, S., Xiao, H., & McClements, D. J. (2009). Emulsion-based delivery systems for tributyrin, a potential colon cancer preventative agent. *Journal of Agricultural and Food Chemistry*, 57(19), 9243-9249.
- Li, Y. & McClements, D. J. (2010). New Mathematical Model for Interpreting pH-Stat Digestion Profiles: Impact of Lipid Droplet Characteristics on in Vitro Digestibility. *Journal of Agricultural and Food Chemistry*, 58(13), 8085-8092.
- Li, Y., Hu, M., Du, Y., Xiao, H., & McClements, D. J. (2011). Control of lipase digestibility of emulsified lipids by encapsulation within calcium alginate beads. *Food Hydrocolloids*, 25(1), 122-130.
- Li, Y. & McClements, D. J. (2011b). Controlling lipid digestion by encapsulation of protein-stabilized lipid droplets within alginate–chitosan complex coacervates. *Food Hydrocolloids*, 25(5), 1025-1033.
- Lian, G., Malone, M. E., Homan, J. E., & Norton, I. T. (2004). A mathematical model of volatile release in mouth from the dispersion of gelled emulsion particles. *Journal of Controlled Release*, 98(1), 139-155.

- Liu, J., Corredig, M., & Alexander, M. (2007). A diffusing wave spectroscopy study of the dynamics of interactions between high methoxyl pectin and sodium caseinate emulsions during acidification. *Colloids and Surfaces B: Biointerfaces*, 59(2), 164-170.
- Macierzanka, A., Sancho, A. I., Mills, E. N. C., Rigby, N. M., & Mackie, A. R. (2009). Emulsification alters simulated gastrointestinal proteolysis of  $\beta$ -casein and  $\beta$ -lactoglobulin. *Soft Matter*, 5(3), 538-550.
- Madene, A., Jacquot, M., Scher, J., & Desobry, S. (2006). Flavour encapsulation and controlled release – a review. *International Journal of Food Science & Technology*, 41(1), 1-21.
- Malone, M. E. & Appelqvist, I. A. M. (2003). Gelled emulsion particles for the controlled release of lipophilic volatiles during eating. *Journal of Controlled Release*, 90(2), 227-241.
- Malvern Instruments. (2010). Mie theory: The first 100 years. MRK1304-02, 1.
- Malvern Instruments. (2007). *Mastersizer 2000 User Manual*. (1.0 ed.). Worcestershire, UK: Malvern Instruments.
- Mancuso, J. R., McClements, D. J., & Decker, E. A. (1999). The effects of surfactant type, pH, and chelators on the oxidation of salmon oil-in-water emulsions. *Journal of Agricultural and Food Chemistry*, 47(10), 4112-4116.
- Marciani, L., Faulks, R., Wickham, M. S. J., Bush, D., Pick, B., Wright, J., Cox, E. F., Fillery-Travis, A., Gowland, P. A., & Spiller, R. C. (2009). Effect of intragastric acid stability of fat emulsions on gastric emptying, plasma lipid profile and postprandial satiety. *British Journal of Nutrition*, 101(06), 919-928.
- Marciani, L., Wickham, M., Singh, G., Bush, D., Pick, B., Cox, E., Fillery-Travis, A., Faulks, R., Marsden, C., & Gowland, P. A. (2007). Enhancement of intragastric acid stability of a fat emulsion meal delays gastric emptying and increases cholecystokinin release and gallbladder contraction. *American Journal of Physiology-Gastrointestinal and Liver Physiology*, 292(6), G1607.
- Marozienne, A. & de Kruif, C. G. (2000). Interaction of pectin and casein micelles. *Food Hydrocolloids*, 14(4), 391-394.
- Marti, I., Höfler, O., Fischer, P., & Windhab, E. J. (2005). Rheology of concentrated suspensions containing mixtures of spheres and fibres. *Rheologica Acta*, 44(5), 502-512.

- Matalanis, A., Jones, O. G., & McClements, D. J. (2011). Structured biopolymer-based delivery systems for encapsulation, protection, and release of lipophilic compounds. *Food Hydrocolloids*, 25(8), 1865-1880.
- Matalanis, A., Lesmes, U., Decker, E. A., & McClements, D. J. (2010). Fabrication and characterization of filled hydrogel particles based on sequential segregative and aggregative biopolymer phase separation. *Food Hydrocolloids*, 24(8), 689-701.
- Matalanis, A. & McClements, D. (2012). Factors influencing the formation and stability of filled hydrogel particles fabricated by protein/polysaccharide phase separation and enzymatic cross-linking. *Food Biophysics*, 7(1), 72-83.
- McClements, D. J. (2000). Comments on viscosity enhancement and depletion flocculation by polysaccharides. *Food Hydrocolloids*, 14(2), 173-177.
- McClements, D.J. (2002). Colloidal basis of emulsion color. *Current Opinion in Colloid & Interface Science*, 7(5-6), 451-455.
- McClements, D.J. (2004). Protein-stabilized emulsions. *Current Opinion in Colloid & Interface Science*, 9(5), 305-313.
- McClements, D. J. (2005). *Food Emulsions: Principles, Practice, and Techniques*. (2nd ed ed.). Boca Raton: CRC Press.
- McClements, D. J. (2010a). Emulsion Design to Improve the Delivery of Functional Lipophilic Components. *Annual Review of Food Science and Technology - (New in 2010)*, 1(1), 241-269.
- McClements, D. J. (2010b). Design of Nano-Laminated Coatings to Control Bioavailability of Lipophilic Food Components. *Journal of Food Science*, 75(1), R30-R42.
- McClements, D. J. & Decker, E. A. (2000). Lipid oxidation in oil-in-water emulsions: Impact of molecular environment on chemical reactions in heterogeneous food systems. *Journal of Food Science*, 65(8), 1270-1282.
- McClements, D., Decker, E., Park, Y., & Weiss, J. (2008). Designing Food Structure to Control Stability, Digestion, Release and Absorption of Lipophilic Food Components. *Food Biophysics*, 3(2), 219-228.
- McClements, D. J., Decker, E. A., & Park, Y. (2009a). Controlling Lipid Bioavailability through Physicochemical and Structural Approaches. *Critical Reviews in Food Science and Nutrition*, 49(1), 48-67.

- McClements, D. J., Decker, E. A., Park, Y., & Weiss, J. (2009b). Structural Design Principles for Delivery of Bioactive Components in Nutraceuticals and Functional Foods. *Critical Reviews in Food Science and Nutrition*, 49(6), 577-606.
- McClements, D. J., Decker, E. A., & Weiss, J. (2007). Emulsion-Based Delivery Systems for Lipophilic Bioactive Components. *Journal of Food Science*, 72(8), R109-R124.
- McClements, D. J. & Li, Y. (2010). Structured emulsion-based delivery systems: Controlling the digestion and release of lipophilic food components. *Advances in Colloid and Interface Science*, 159(2), 213-228.
- Mewis, J., Yang, H., Van Puyvelde, P., Moldenaers, P., & Walker, L. M. (1998). Small-angle light scattering study of droplet break-up in emulsions and polymer blends. *Chemical Engineering Science*, 53(12), 2231-2239.
- Miller, G. D., Jarvis, J. K., & McBean, L. D. (2001). The Importance of Meeting Calcium Needs with Foods. *Journal of the American College of Nutrition*, 20(2), 168S-185.
- Miller, J. D., Yalamanchili, M. R., & Kellar, J. J. (1992). Surface charge of alkali halide particles as determined by laser-Doppler electrophoresis. *Langmuir*, 8(5), 1464-1469.
- Mora-Gutierrez, A., Attaie, R., & Farrell, H. M. (2010). Lipid Oxidation in Algae Oil-in-Water Emulsions Stabilized by Bovine and Caprine Caseins. *Journal of Agricultural and Food Chemistry*, 58(8), 5131-5139.
- Morr, C. V. (1982). Functional properties of milk proteins and their use as food ingredients. *Developments in Dairy Chemistry*, 1, 375-399.
- Morris, V. J. (2007). Gels. In P. Belton (Ed.), *The Chemical Physics of Food* (151-191). Oxford, UK: Blackwell Publishing.
- Mozafari, M. R., Flanagan, J., Matia-Merino, L., Awati, A., Omri, A., Suntres, Z. E., & Singh, H. (2006). Recent trends in the lipid-based nanoencapsulation of antioxidants and their role in foods. *Journal of the Science of Food and Agriculture*, 86(13), 2038-2045.
- Norton, I. T. & Frith, W. J. (2001). Microstructure design in mixed biopolymer composites. *Food Hydrocolloids*, 15(4-6), 543-553.
- Oakenfull, D. & Glicksman, M. (1987). Gelling agents. *CRC Critical Reviews in Food Science and Nutrition*, 26(1), 1-25.

- O'Connell, J. E., Grinberg, V. Y., & de Kruif, C. G. (2003). Association behavior of  $\beta$ -casein. *Journal of Colloid and Interface Science*, 258(1), 33-39.
- Ozaki, A., Muromachi, A., Sumi, M., Sakai, Y., Morishita, K., & Okamoto, T. (2010). Emulsification of Coenzyme Q 10 Using Gum Arabic Increases Bioavailability in Rats and Human and Improves Food-Processing Suitability. *Journal of Nutritional Science and Vitaminology*, 56(1), 41-47.
- Palzer, S. (2009). Food structures for nutrition, health and wellness. *Trends in Food Science & Technology*, 20(5), 194-200.
- Pedersen, H. C. A. & Jorgensen, B. B. (1991). Influence of Pectin on the Stability of Casein Solutions Studied in Dependence of Varying Ph and Salt Concentration. *Food Hydrocolloids*, 5(4), 323-328.
- Pereyra, R., Schmidt, K. A., & Wicker, L. (1997). Interaction and stabilization of acidified casein dispersions with low and high methoxyl pectins. *Journal of Agricultural and Food Chemistry*, 45(9), 3448-3451.
- Porter, C. J. H., Trevaskis, N. L., & Charman, W. N. (2007). Lipids and lipid-based formulations: optimizing the oral delivery of lipophilic drugs. *Nat Rev Drug Discov*, 6(3), 231-248.
- Pothakamury, U. R. & Barbosa-Cánovas, G. V. (1995). Fundamental aspects of controlled release in foods. *Trends in Food Science & Technology*, 6(12), 397-406.
- Rediguieri, C. F., de Freitas, O., Lettinga, M. P., & Tuinier, R. (2007). Thermodynamic incompatibility and complex formation in pectin/caseinate mixtures. *Biomacromolecules*, 8(11), 3345-3354.
- Reis, C. P., Neufeld, R. J., Vilela, S., Ribeiro, A. J., & Veiga, F. (2006). Review and current status of emulsion/dispersion technology using an internal gelation process for the design of alginate particles. *Journal of Microencapsulation*, 23(3), 245-257.
- Reis, P., Raab, T., Chuat, J., Leser, M., Miller, R., Watzke, H., & Holmberg, K. (2008). Influence of surfactants on lipase fat digestion in a model gastrointestinal system. *Food Biophysics*, 3(4), 370-381.
- Renard, D., van de Velde, F., & Visschers, R. W. (2006). The gap between food gel structure, texture and perception. *Food Hydrocolloids*, 20(4), 423-431.
- Riediger, N. D., Othman, R. A., Suh, M., & Moghadasian, M. H. (2009). A systemic review of the roles of n-3 fatty acids in health and disease. *Journal of the American Dietetic Association*, 109(4), 668-679.

- Ries, D., Ye, A., Haisman, D., & Singh, H. (2010). Antioxidant properties of caseins and whey proteins in model oil-in-water emulsions. *International Dairy Journal*, 20(2), 72-78.
- Rival, S. G., Boeriu, C. G., & Wichers, H. J. (2001). Caseins and casein hydrolysates. 2. Antioxidative properties and relevance to lipoxygenase inhibition. *Journal of Agricultural and Food Chemistry*, 49(1), 295-302.
- Ruis, H. G. M., Venema, P., & van der Linden, E. (2007). Relation between pH-induced stickiness and gelation behaviour of sodium caseinate aggregates as determined by light scattering and rheology. *Food Hydrocolloids*, 21(4), 545-554.
- Ruxton, C., Reed, S., Simpson, M., Millington, K., & Ruxton, C. (2007). The health benefits of omega-3 polyunsaturated fatty acids: a review of the evidence. Commentary. *Journal of Human Nutrition and Dietetics*, 20(3), 275-287.
- Sagalowicz, L. & Leser, M. E. (2010). Delivery systems for liquid food products. *Current Opinion in Colloid & Interface Science*, 15(1-2), 61-72.
- Sandra, S., Decker, E. A., & McClements, D. J. (2008). Effect of interfacial protein cross-linking on the in vitro digestibility of emulsified corn oil by pancreatic lipase. *Journal of Agricultural and Food Chemistry*, 56(16), 7488-7494.
- Sarkar, A., Goh, K. K. T., & Singh, H. (2009a). Colloidal stability and interactions of milk-protein-stabilized emulsions in an artificial saliva. *Food Hydrocolloids*, 23(5), 1270-1278.
- Sarkar, A., Goh, K. K. T., Singh, R. P., & Singh, H. (2009b). Behaviour of an oil-in-water emulsion stabilized by  $\beta$ -lactoglobulin in an in vitro gastric model. *Food Hydrocolloids*, 23(6), 1563-1569.
- Siepmann, J., & Siepmann, F. (2008). Mathematical modeling of drug delivery. *International Journal of Pharmaceutics* 364(2):328-343.
- Sila, D. N., Van Buggenhout, S., Duvetter, T., Fraeye, I., Roeck, A. D., Van Loey, A., & Hendrickx, M. (2009). Pectins in processed fruits and vegetables: part ii—structure–function relationships. *Comprehensive Reviews in Food Science and Food Safety*, 8(2), 86-104.
- Silletti, E., Vingerhoeds, M. H., Norde, W., & van Aken, G. A. (2007). The role of electrostatics in saliva-induced emulsion flocculation. *Food Hydrocolloids*, 21(4), 596-606.

- Singh, H., Ye, A., & Horne, D. (2009). Structuring food emulsions in the gastrointestinal tract to modify lipid digestion. *Progress in Lipid Research*, 48(2), 92-100.
- Streubel, A., Siepmann, J., & Bodmeier, R. (2006). Drug delivery to the upper small intestine window using gastroretentive technologies. *Current Opinion in Pharmacology*, 6(5), 501-508.
- Surh, J., Decker, E. A., & McClements, D. J. (2006). Influence of pH and pectin type on properties and stability of sodium-caseinate stabilized oil-in-water emulsions. *Food Hydrocolloids*, 20(5), 607-618.
- Syrbe, A., Bauer, W. J., & Klostermeyer, H. (1998). Polymer Science Concepts in Dairy Systems--An Overview of Milk Protein and Food Hydrocolloid Interaction. *International Dairy Journal*, 8(3), 179-193.
- Tanamati, A., Oliveira, C., Visentainer, J., Matsushita, M., & de Souza, N. (2005). Comparative study of total lipids in beef using chlorinated solvent and low-toxicity solvent methods. *Journal of the American Oil Chemists' Society*, 82(6), 393-397.
- Tolstoguzov, V. (2002). Thermodynamic Aspects of Biopolymer Functionality in Biological Systems, Foods, and Beverages. *Critical Reviews in Biotechnology*, 22(2), 89-174.
- Tolstoguzov, V. (2003). Some thermodynamic considerations in food formulation. *Food Hydrocolloids*, 17(1), 1-23.
- Totosaus, A., Montejano, J. G., Salazar, J. A., & Guerrero, I. (2002). A review of physical and chemical protein-gel induction. *International Journal of Food Science & Technology*, 37(6), 589-601.
- Tromp, R. H., de Kruif, C. G., van Eijk, M., & Rolin, C. (2004). On the mechanism of stabilisation of acidified milk drinks by pectin. *Food Hydrocolloids*, 18(4), 565-572.
- Tuinier, R., Rolin, C., & de Kruif, C. G. (2002). Electrosorption of pectin onto casein micelles. *Biomacromolecules*, 3(3), 632-638.

- Turgeon, S. L., Beaulieu, M., Schmitt, C., & Sanchez, C. (2003). Protein–polysaccharide interactions: phase-ordering kinetics, thermodynamic and structural aspects. *Current Opinion in Colloid & Interface Science*, 8(4-5), 401-414.
- Van Puyvelde, P., Antonov, Y. A., & Moldenaers, P. (2003). Morphology evolution of aqueous biopolymer emulsions during a weak shear flow. *Food Hydrocolloids*, 17(3), 327-332.
- Van, d. M. & Kinget, R. (1995). Oral colon-specific drug delivery: a review. *Drug Delivery*, 2(2), 81-93.
- Versantvoort, C. H. M., Kamp, E.V. D. & Rompelberg, C.J.M. Development and applicability of an in vitro digestion model in assessing the bioaccessibility of contaminants from food., (Rijksinstituut voor Volksgezondheid en Milieu, 2004) <http://hdl.handle.net/10029/8885>. Accessed 14 November 2011.
- Vingerhoeds, M. H., Blijdenstein, T. B. J., Zoet, F. D., & van Aken, G. A. (2005). Emulsion flocculation induced by saliva and mucin. *Food Hydrocolloids*, 19(5), 915-922.
- Waraho, T., McClements, D. J., & Decker, E. A. (2011). Mechanisms of lipid oxidation in food dispersions. *Trends in Food Science & Technology*, 22(1), 3-13.
- Wickham, M., Garrood, M., Leney, J., Wilson, P. D. G., & Fillery-Travis, A. (1998). Modification of a phospholipid stabilized emulsion interface by bile salt: effect on pancreatic lipase activity. *Journal of Lipid Research*, 39(3), 623-632.
- Wildman, R. E. C. & Medeiros, D. M. (2000). Human digestion and absorption. In R. E. C. Wildman & D. M. Medeiros (Eds.), *Advanced Human Nutrition* Boca Raton, FL: CRC Press.
- Wolf, B. & Frith, W. J. (2003). String phase formation in biopolymer aqueous solution blends. *Journal of Rheology*, 47, 1151-1170.
- Wolf, B., Scirocco, R., Frith, W. J., & Norton, I. T. (2000). Shear-induced anisotropic microstructure in phase-separated biopolymer mixtures. *Food Hydrocolloids*, 14(3), 217-225.
- Wolf, B., Frith, W. J., Singleton, S., Tassieri, M., & Norton, I. T. (2001). Shear behaviour of biopolymer suspensions with spheroidal and cylindrical particles. *Rheologica Acta*, 40(3), 238-247.

- Wooster, T. J., Golding, M., & Sanguansri, P. (2008). Impact of Oil Type on Nanoemulsion Formation and Ostwald Ripening Stability. *Langmuir*, 24(22), 12758-12765.
- Wrolstad, R. E. & Smith, D. E. (2010). Color Analysis. In S. S. Nielsen (Ed.), *Food Analysis* (573-586). New York, NY: Springer.
- Yang, L., Chu, J. S., & Fix, J. A. (2002). Colon-specific drug delivery: new approaches and in vitro/in vivo evaluation. *International Journal of Pharmaceutics*, 235(1-2), 1-15.
- Yashodhara, B., Umakanth, S., Pappachan, J., Bhat, S., Kamath, R., & Choo, B. (2009). Omega-3 fatty acids: a comprehensive review of their role in health and disease. *Postgraduate Medical Journal*, 85(1000), 84-90.
- Ye, A. (2008). Complexation between milk proteins and polysaccharides via electrostatic interaction: principles and applications – a review. *International Journal of Food Science & Technology*, 43(3), 406-415.
- Yin, L. J., Chu, B. S., Kobayashi, I., & Nakajima, M. (2009). Performance of selected emulsifiers and their combinations in the preparation of  $\beta$ -carotene nanodispersions. *Food Hydrocolloids*, 23(6), 1617-1622.